Development of Lead Compounds for Trypanocidal Drugs based on Inhibitors of Parasite Glycolysis

Matthew William Nowicki

The University of Edinburgh

A thesis submitted for the degree of Doctor of Philosophy May 2005

Declaration

This thesis is submitted in part fulfilment of the requirement for the degree of Doctor of Philosophy at the University of Edinburgh. Unless otherwise stated, the work is original and has not been previously submitted, in whole or in part, for any degree at this, or any other University.

Acknowledgements

There are several people that I would like to thank who have helped and supported me during my time as a postgraduate, and I only hope that I don't leave anyone out. Firstly, I would like to thank my supervisor, Professor Nick Turner, and also Professor Sabine Flitsch, for their advice, support and encouragement over the time I have spent with their group. I am also very grateful for the help of our collaborators in the ICMB (now ISMB), especially Dr. Linda Gilmore, Professor Malcolm Walkinshaw, Dr. Lindsay Tulloch, Buabarn Poonperm and the various visitors to the lab including Jose 'Pepe' Martinez, Marcos Navaro and Bimo Tejo. Also, a big thank you goes to Dr. Veronique Hannaert for the *in vivo* assays and to Professor Paul Michels for heading and organising such a wonderful collaboration. I have to give a special thank you to Robert Smith, whose help with the ZMD I could not have done without. Likewise, I would like to thank all the technical staff in the department, in particular John Millar for the smooth running of the NMR service and for helping out when needed. I also cannot leave out all the Turner-Flitsch group members who have made my time in Edinburgh so colourful, especially Dr. Reuben Carr, Kirk Malone, Colin Dunsmore, Fraser Brown and of course, Tom Eve. Thank you also to Dr. Kevin Bailey who proof read in a time of upheaval for himself, and also my parents, Vivien and Henryk, for their grammatical expertise. Finally, thank you to the EC for funding and for making this research possible.

Abstract

The parasitic protozoa *Trypanosoma* and *Leishmania* are the cause of several highly disabling and often fatal diseases that affect millions of people in tropical and sub-tropical regions. Glycolysis and especially the glycolytic enzymes within these parasites have been identified as potential targets for anti-trypanosomatid drugs. Recent research had identified *N*-aryl-1-amino-2,5-anhydro-1-deoxy-1-D-mannitol derivatives as inhibitors of the enzyme phosphfructokinase (PFK), with IC_{50} values in the low millimolar range. Following the synthesis of two compound libraries of 2,5-anhydro-1-deoxy-D-mannitol derivatives, **37** was identified as a new inhibitor of PFK, with an IC_{50} = 0.41 mM. Due to the structural similarities between these inhibitors and the effector for pyruvate kinase (PyK), fructose-2,6-bisphosphate, the libraries were also screened against PyK; **70** was identified as a new inhibitor and lead compound, with an IC_{50} = 58 μM. Competition experiments and molecular modelling suggested that **70** does indeed compete for the effector binding site.

Lead and synthetic development led to the synthesis of a third library of δ-furanoid sugar amino amides. Approximately, a 10-fold increase in inhibition was observed for this library against PFK, the most potent inhibitor being **110** with an IC_{50} = 23 μM. Competition experiments and molecular modelling suggested that **110** competes for the fructose-6-phosphate binding site. This library also gave good inhibition against PyK. Other areas of lead modification were also investigated that could lead to further library synthesis.

In vivo testing of inhibitor **37** against trypanosomatid cells showed promising inhibitory activity, with an ED_{50} = 0.15 mM. Such a result is promising for the future development of these inhibitors as, at an early stage of development, they already exhibit anti-parasitic properties.

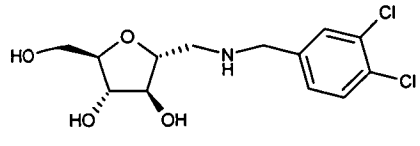

37

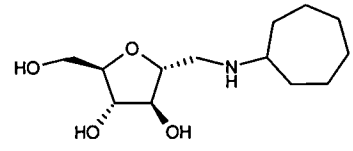

70

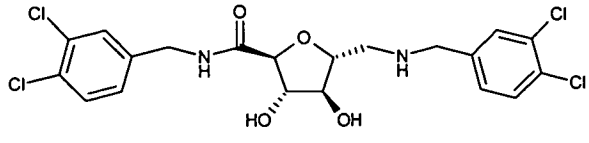

110

Abbreviations

ACD	Available chemical directory
ADME	Absorption, distribution, metabolism, excretion
ADP	Adenosine diphosphate
AMP	Adenosine monophosphate
ATP	Adenosine triphosphate
BOC	*tert*-Butoxycarbonyl
BOC_2O	Di-*tert*-butyl dicarbonate
1,3-BPGA	1,3-Bisphosphoglycerate
CV	Cone voltage
Cys	Cysteine
d	Doublet
DCM	Dichloromethane
DHAP	Dihydroxyacetone phosphate
DIPEA	*N*,*N*-Diisopropylethylamine
ED_{50}	Dose required for 50 % response in a biological system
EDCI	1-Ethyl-3-(3′-dimethylaminopropyl)carbodiimide
ESI	Electrospray ionisation mass spectrometry
FAB	Fast atom bombardment
F6P	Fructose-6-phosphate
FTIR	Fourier transform infrared
GAPDH	Glyceraldehyde-3-phosphate dehydrogenase
Gly-3-P	L-Glycerol-3-phosphate

G-3-P	Glyceraldehyde-3-phosphate
GTP	Guanidine triphosphate
HBA	Hydrogen bond acceptors
HBD	Hydrogen bond donors
HCl	Hydrochloric acid
HK	Hexokinase
HOBt	1-Hydroxybenzotriazole
HRMS	High resolution mass spectrometry
IC_{50}	Concentration required for 50 % inhibition
K_d	Dissociation constant
K_i	Inhibition constant
K_M	Michaelis constant
Lm	*Leishmania mexicana*
Lys	Lysine
m	Multiplet
$[M + H]^+$	Protonated molecular ion
$[M + Na]^+$	Sodium adduct of molecular ion
mCPBA	*meta*-Chloroperbenzoic acid
MeCN	Acetonitrile
MeOH	Methanol
$NaBH_3CN$	Sodium cyanoborohydride
NAD^+	Nicotinamide adenine dinucleotide (oxidised form)
NADH	Nicotinamide adenine dinucleotide (reduced form)
NMR	Nuclear magnetic resonance

PEP	Phosphoenolpyruvate
PFK	Phosphofructokinase
2-PGA	2-Phosphoglycerate
3-PGA	3-Phosphoglycerate
PGAM	Phosphoglycerate mutase
ppm	Parts per million
PyK	Pyruvate kinase
q	Quartet
s	Singlet
SAR	Structure-activity relationship
SHAM	Salicylhydroxamic acid
t	Triplet
Tb	*Trypanosoma brucei*
TFA	Trifluoroacetic acid
TLC	Thin layer chromatography
UTP	Uridine triphosphate

Chapter 1

Introduction

1 Introduction.

1.1 Overview.

This thesis is concerned with the development and synthesis of inhibitors of glycolysis in parasites, in particular small molecules targeted against trypanosomatidae. By way of an introduction to this topic, some aspects and general methods of drug discovery, design and development are discussed. There then follows a more detailed review about trypanosomatidae, the glycolytic pathway and the rationale for selecting the glycolytic pathway as a target for trypanocidal drugs.

1.2 Drug discovery, design and development.

1.2.1 Introduction.

Traditionally, natural products have been the main and most important source for new drugs. Compounds have been isolated from many organisms including plants, animals (toxins) and micro-organisms.[1] One of the most famous was the serendipitous discovery of the anti-bacterial drug, penicillin **1**[2] (general structure shown), and more recently the discovery of the anti-cancer compound, Taxol® **2**, isolated from the western yew *Taxus brevifolia*[3] (Figure 1.1).

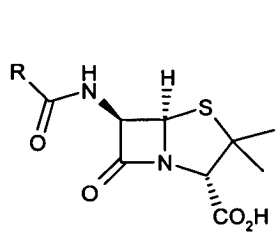

1

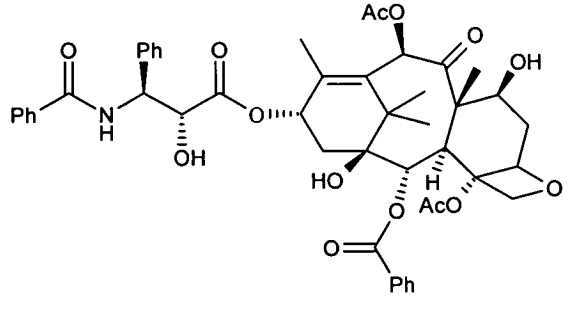

2

Figure 1.1 General structure of penicillin **1** and structure of Taxol® **2**.

Using standard medicinal chemistry procedures, these natural compounds were modified to produce drugs with improved activity, selectivity, bio-availability and ADME properties; reduced toxicity; and an altered spectrum of activity.[4-7] The greatest constraint in this process is the synthesis and evaluation of candidate compounds sequentially. This is particularly true for the β-lactam penicillin derivatives, where, over a 30 year period, thousands of compounds were synthesised and screened for anti-bacterial activity.[7] However, advances in the wide field of medicinal chemistry, in particular utilising combinatorial chemistry[7,8] and high through-put screening (HTS),[9] have radically changed the drug discovery process.

1.2.2 Target identification and lead discovery.

It is generally regarded that one of the initial steps in drug discovery is the identification of lead compounds that bind to a receptor or enzyme of interest. However, in order to do this, a therapeutic target must first be identified and validated, whether the disease concerned is infectious or non-infectious. Identification aims to find targets (normally proteins or DNA/RNA) whose regulation may lead to the inhibition or reversal of disease progression.[10] This has not always been the case; in the example of the discovery of penicillin, its anti-bacterial properties were discovered well before the target enzyme, peptidoglycan transpeptidase, was known.[1] The sequencing of the human genome and other organism genomes has led to an increase in the number of potential therapeutic targets.[10] Complementary to this advance has been the development of technologies and tools to aid in target identification and validation.[10]

Once a target or set of targets has been identified and validated as drugable, the next

step is to identify a lead compound. This can be accomplished in at least two ways; firstly, by random screening of primary compound libraries, where no specific structure or substructure is needed; secondly, by screening biased or focused compound libraries, where the individual members may bare a structural similarity to either substrates (or substrate intermediates) of the target, or of already identified lead compounds from random screening.[7] Advances in combinatorial and parallel synthetic chemistry, as well as screening techniques, has meant that compound libraries can be prepared and screened quickly and efficiently, with the goal being the discovery new lead compounds or even of new drugs.[11]

1.2.3 Library synthesis.

Combinatorial chemistry is a very powerful tool in drug discovery as it facilitates the synthesis of large, small molecule compound libraries[12] that are then screened for biological activity against a known target. It has been particularly important, not only for lead discovery, but also for lead modification. Combinatorial chemistry is defined as "the systematic and repetitive, covalent connection of a set of different 'building blocks' of varying structure to each other to yield a large array of diverse molecular entities".[11] A general example of this can be seen in Figure 1.2.

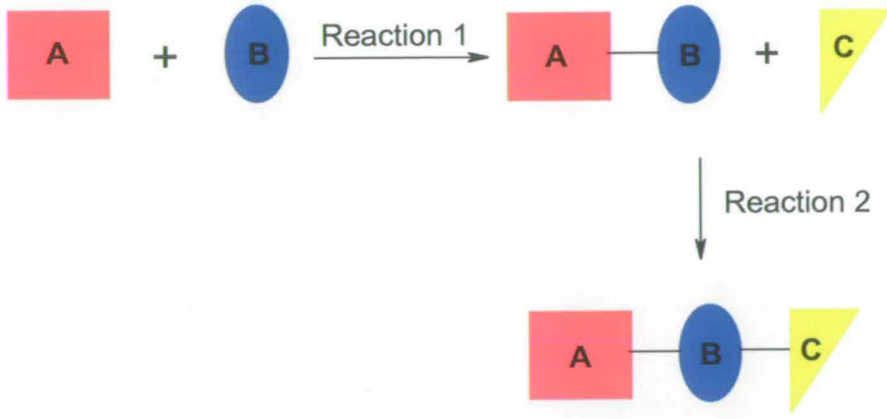

Figure 1.2 General example of the synthesis of a combinatorial compound library, based on a linear motif.

It is evident from Figure 1.2 that the route to make large number of diverse compounds is greatly facilitated by combinatorial chemistry. For example, using 10 x **A** and 10 x **B** building blocks, Reaction 1 would synthesise 100 compounds (10 x 10) of the type A-B. Introduction of 10 x **C** building blocks for Reaction 2 would generate 1000 compounds (100 x 10) of the type A-B-C. Methods such as *split synthesis* on solid phase are used for this type of combinatorial library.[13] Although this is a very basic example, it illustrates how large compound libraries can be generated based around simple, well known reactions such as peptide synthesis reactions,[11] whether on solid phase or in solution. Thousands of compounds have been synthesised and screened using combinatorial chemistry, and this increase in compound synthesis was expected to reduce the required time from finding an initial lead, to turning it in to a pre-clinical drug candidate.[14] Although some lead compounds have been identified by this approach,[15,16] it was realised that the dramatic increase in the number of compounds available for screening would not necessarily lead to good, new lead compounds. In fact, it was observed that the hit

rates were actually higher using tradition medicinal chemistry methods.[14] It is now more common to find lead discovery and lead optimisation geared towards more rational structure-based design, often marrying the fields of combinatorial and parallel synthetic chemistry, computational chemistry and X-ray crystallography.[14]

1.2.4 Lead modification.

In situations where information about the structure and residues of the drug target are known (either by NMR or X-ray crystallography), structure-based library design becomes another very useful tool in the early phases of lead modification.[14] Once an initial inhibitor has been identified, libraries can be designed based on its structure, creating a "focused library"; a diverse library of structurally similar compounds. A classical example of this is the synthesis of benzodiazepines[12] as shown in Figure 1.3. Using 3 simple building blocks, libraries of benzodiazepines were easily accessible introducing 4 elements of diversity.[12]

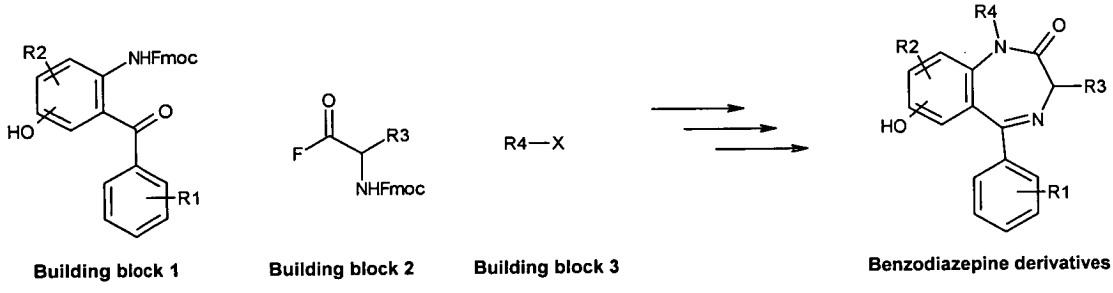

Figure 1.3 Access to benzodiazepine library from 3 simple building blocks.[12]

High throughput screening is the method usually employed to screen large libraries[9] and allows the simultaneous biological screening of each compound and relates it to a measure of inhibition of the chosen target. Therefore, this method permits a rapid

evaluation of each compound synthesised and can also result in the identification of structure-activity relationships (SARs).[1]

Most drugs tend to be structurally specific[1] and act at specific receptor sites (such as the active site of an enzyme); hence, potency and activity are very susceptible to small changes in chemical structure. Recognition of certain ligand-receptor interactions may become apparent at this stage, such as hydrogen bonding and hydrophobic interactions.[17] However, identifying specific ligand-receptor interactions and confirming structure-activity relationships is greatly enhanced using computational power, incorporating docking methods.[18] If structural information about the target is known (X-ray crystal structure), compounds of interest can be docked into the receptor site using programmes such as DOCK,[18] taking into account steric and electronic parameters to find the most probable mode of binding. Although specific ligand-receptor interactions can only be formally identified by NMR or an X-ray crystal structure of the inhibitor-target complex, docking still allows comparison between ligands and may identify reasons for trends in biological activity, allowing for the rationalisation of structure-activity relationships. In the initial stages of lead modification, this can be very useful not only for identifying potential ligand-receptor interactions and rationalising SARs, but also for further lead development.

In recent years, a major concern in the drug discovery process has been the relevance of library or inhibitor design towards obtaining good drug-like molecules. Due to the advances in combinatorial chemistry, high-throughput screening and molecular genetics, the goal in lead modification was to find more potent inhibitors without necessarily taking in to account solubility, absorption and permeability properties

that are essential for bioavailability.[19] High-throughput screening methods are such that general solvents like dimethyl sulfoxide (DMSO) are used regularly in assays. Therefore, highly insoluble compounds can be screened and activity determined, the net result being *in vitro* activity is reliably identified for compounds with very poor thermodynamic solubility properties.[19] Medicinal chemistry often relies on incorporation of lipophilic moieties during lead modification to improve *in vitro* activity.[17,19] Conversely, it has been found difficult to improve on *in vitro* potency by incorporating polar groups. Both these observations only emphasise the trend towards design of inhibitors with poor solubility in an aqueous medium. Work in this area by Lipinski *et al.*,[19] led to the discovery of set of rules, now more commonly referred to as the Lipinski Rule of 5:

> "The 'rule of 5' predicts that poor absorption or permeation is more likely when there are more than 5 H-bond donors, 10 H-bond acceptors, the molecular weight is greater than 500 and the calculated Log P (CLogP) is greater than 5."[19]

At each round of lead modification, it is generally accepted that these parameters are likely to change, so it has been suggested that this rule is taken in to account early on in lead discovery programmes. However, the rule has been violated by a number of compounds including antibiotics, antifungals, vitamins and cardiac glycosides, which is thought to be due to the presence of functional groups which may act as substrates for transporters.[19,20] Further work in this area suggest modifications are needed as compounds that are compliant with the Lipinski Rule of 5 may still exhibit poor solubility and permeability.[21-23] Such suggestions have been made by Hann and

Oprea[22] who formulated the following criteria for lead like compounds: molecular weight ≤ 460; $-4 \leq \text{LogP} \leq 4.2$; number of rotatable bonds ≤ 10; number of rings ≤ 4; number of hydrogen bond donors ≤ 5; number of hydrogen bond acceptors ≤ 9.

1.2.5 Recent methodologies in drug discovery and drug design.

Although advances in combinatorial chemistry and high throughput screening have made it possible both to synthesise and biologically evaluate large numbers of compounds, this is still a small number in comparison to the total number of compounds that could be synthesised and evaluated.[24] In section 1.2.4, the idea of computationally docking potential ligands into receptor sites was introduced. Leading on from both of these notions is the application of virtual screening.[24] This method seeks to explore the binding mode and affinity of potential ligands from commercial databases such as the Available Chemicals Database (ACD), or smaller in-house databases such as more focused virtual libraries.[25] As well as acting as a screening method to identify potential ligands, virtual screening also acts as a filter to cut down on the vast number of compounds that could be potentially synthesised at the start of a drug discovery programme, hence, streamlining the whole process that chemists and computational chemists already use.[24]

X-Ray crystallography is a useful technique that has been used to identify not only protein structures, but also ligand receptor interactions, and has been widely used for lead optimisation in drug discovery.[26] Due to the importance that X-ray crystallography has on the acquisition of three-dimensional information (including binding interactions and structure-activity relationships), its function has, recently,

been broadened into a new approach for lead discovery and modification.[26] High-throughput X-ray crystallography has recently been developed and is used to screen molecular fragments and precisely define their binding sites to the target proteins. In turn, this method can be utilised as a guide for lead development and optimisation. A particular advantage is the identification of low affinity binding sites caused by small molecule fragments. Although their binding affinity may be in the millimolar range, concentrations used are much higher than conventional high-throughput methods,[26-28] and therefore, weaker binding sites and low affinity compounds can be identified that may have been missed by other screening methods.[26-28] The interactions that these fragments identify could prove to be crucial for lead identification and development, as the binding mode is specific, and the key interactions are well defined.[26]

In the method described above, the idea of screening molecular fragments was introduced and leads on to another recently developed method; fragment-based drug discovery.[29] In fragment-based approaches, low molecular weight chemical fragments (or very small molecules) are screened against a target of interest by means of an assay such as high concentration binding assays[30] or crystallography-based methods.[31] Fragments which show inhibition, or the ability to bind to the target, can be considered as building blocks of a more complex lead compound series.

There are two main methods in which fragments are converted into lead compounds. The first of these is fragment optimisation, whereby hits with micromolar (or better) affinities undergo conventional optimisation strategies (using methods such as combinatorial chemistry). An example of this can be seen in Figure 1.4 where

benzimidazole **3** was identified as a weak inhibitor of gelatinase B, and, following library design and synthesis based on this structure (and mechanistic considerations), inhibitor **4** was discovered, which showed over a 100-fold improvement in potency.[32]

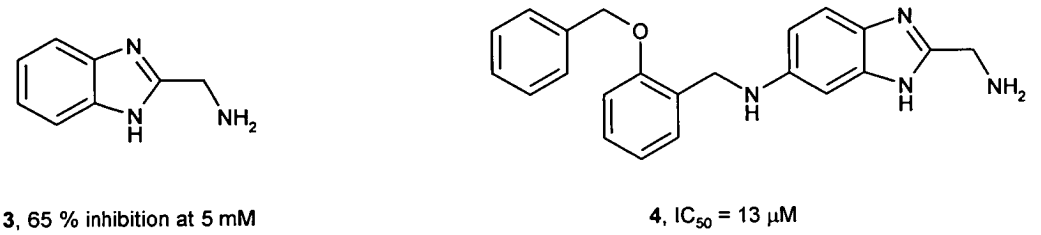

3, 65 % inhibition at 5 mM **4**, IC_{50} = 13 μM

Figure 1.4 Fragment optimisation of Gelatinase B inhibitor.[32]

The second method is fragment merging and linking.[29] The specific binding modes of fragments are preserved by linking or merging them together, usually leading to an increased affinity for the target. An illustration of this can be seen in Figure 1.5 where the linking together of fragments **5** and **6** – which were already found to be moderate inhibitors of FK506 binding protein (FKBP) – produced inhibitor **7**; a 100-fold binding enhancement over fragment **5** was observed.[33]

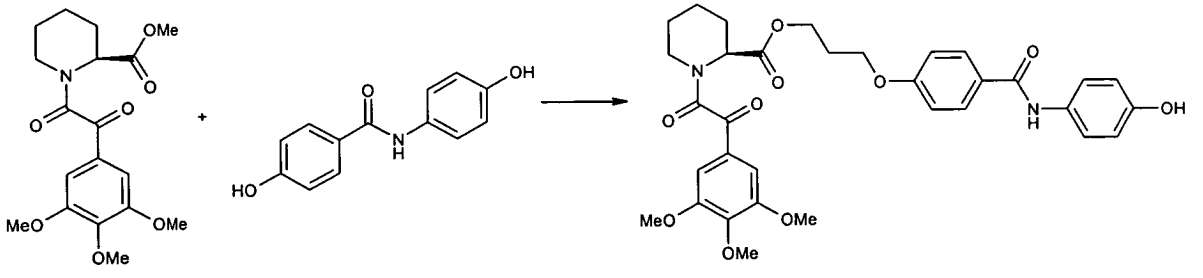

5, K_d = 2 mM **6**, K_d = 100 mM **7**, K_d = 0.019 mM

Figure 1.5 Fragment linking of FKBP inhibitors.[33]

These examples are just a few of the total number of emerging strategies. They are developed by chemists and biologists worldwide, all attempting to identify potential drug targets and their inhibitors, with the goal not only of finding new drugs, but also of understanding, more fully, the biological processes and systems by which disease occurs and its progression inhibited.

1.3 Trypanosomatids.

1.3.1 Trypanosomatid disease.

African sleeping sickness, Chagas' disease and leishmaniasis are highly disabling and sometimes fatal diseases associated with the continents of Africa and South America. The parasitic protozoa *Trypanosoma* and *Leishmania* are the cause of these diseases and belong to the order Kinetoplastida.[34,35]

Sleeping sickness in humans (African trypanosomiasis) is caused by two subspecies of *Trypanosoma brucei* (*Tb*). The usually chronic form of the disease, found in West Africa, is caused by *Tb gambiense*, and takes several years to progress to the meningoencephalitic stage; the more acute form that predominates in East Africa is caused by *Tb rhodesiense*, which only takes a few weeks to progress to this second stage.[34,36] Whilst in the blood and lymphatic system of the host, the trypanosomes proliferate before invading the central nervous system. This disease threatens over 60 million people in 36 countries of sub-Saharan Africa each day. It is estimated that between 300,000 and 500,000 people have the disease, and if left untreated, both forms of the disease are fatal at the second stage. Unfortunately the current available treatment seems to be far from satisfactory.[37] Suramin **8** and pentamidine **9**, (first administered in 1922 and 1937, respectively) are used for the early stages of the

disease.[36] Drugs used to treat the second stage (with central nervous involvement) are melarsoprol **10**, (1949) and, the only drug to become available in the recent past, eflornithine **11**, (1990, Figure 1.6).

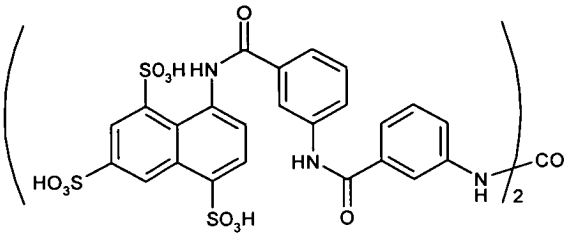

8

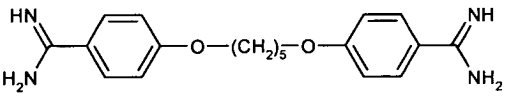

9

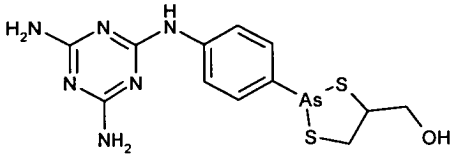

10

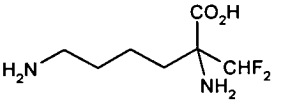

11

Figure 1.6 Structures of suramin **8**, pentamidine **9**, melarsoprol **10** and eflornithine **11**.

These drugs, however, are far from adequate. Resistance against pentamidine by *Tb gambiense* has been observed, and eflornithine is ineffective against *Tb rhodesiense*. Recently, problems in treating this disease have emerged due to the resistance of trypanosomes to melarsoprol **10**. As well as these problems, suramin **8**, pentamidine **9**, and in particular melarsoprol **10**, have serious side effects on the human host. Eflornithine **11** itself is impractical as it needs a hospital setting for administration of the drug, which is often unaffordable due to its high cost.[36]

Chagas' disease is caused by *Trypanosoma cruzi* and has a wide distribution in Central and South America. Many wild and domestic mammals can act as host for this flagellated protozoan parasite.[34] Transmission of the parasite can occur in

different ways: either the deposition of faeces on the skin (by a blood sucking reduviid bug) at the time of biting, or more directly by transfusion of infected blood or congenital transmission. Chagas' disease affects around 16 - 18 million people, and of these, about 5 – 6 million have developed incurable complications. These can appear between 10 – 20 years after the initial acute phase of the disease and include; cardiac lesions, digestive disorders and peripheral neurological disorders. Although there has been a significant improvement in the control of Chagas' disease by targeting the insect vectors, treatment is only available for the acute stages of the disease. Development of drugs is therefore needed to overcome the chronic form.[34]

The disease leishmaniasis is caused by the different species of the genus *Leishmania*. Over 20 different species are known to be pathogenic to humans and they are transmitted by the bite of the phlebotomine sandfly. Depending on the form of the disease, the leishmaniases are divided into three general clinical patterns: cutaneous, visceral and mucocutaneous. It is thought that over 367 million people are at risk from this disease in 88 countries, and that there are at least two million new cases of leishmaniasis each year. The standard treatment courses that are currently available can only be given parenterally. They are long, expensive and may cause severe adverse reactions.[34]

Although chemotherapy is not, at present, satisfactory, it still remains the major method for the control of these diseases. Vaccine development has been attempted but has proved unsuccessful, due to the fact that many of the aforementioned parasites have developed intricate mechanisms for evading their host's immune system.[38] The reason why there is a limited amount of available treatment, is simply due to the market economy; most people that are at risk from these tropical and sub-

tropical diseases are among the poorest in the world so there has been little financial incentive for pharmaceutical companies to invest in the development of new drugs.[34,38]

1.3.2 Targets for anti-trypanosomatid drugs.

In the last two decades, molecular approaches have been introduced to define potential new targets in trypanosomatidae, and to design new drugs, as the mechanisms for the currently available drugs remain largely unknown.[38,39] It appears that in trypanosomatidae, glycolysis is essential for survival in the human host:[38] the only supply of ATP for African trypanosomatidae living in the mammalian bloodstream, is the glycolytic breakdown of glucose to pyruvate. They have no Krebs cycle or mitochondrial respiratory chain that is coupled to ATP production[40] and, therefore, inhibition of glycolysis will lead to rapid death of these parasites.[41-43] Due to the fact that trypanosomatidae have a long evolutionary distance between themselves and their mammalian hosts,[44] and also because of the unusual organisation of the glycolytic pathway in these parasites,[40,45] the parasitic enzymes are endowed with distinct properties (see section 3.5). Therefore, these properties may be exploited in structure or mechanism-based design of inhibitors, so that the glycolytic pathway of the host would remain unaffected.[46]

1.3.3 The glycolytic pathway in trypanosomatidae.

In contrast to other organisms, the seven glycolytic enzymes that convert glucose to 3-phosphoglycerate, are located in peroxime-like organelles called glycosomes (see Figure 1.7).[40,45] (In other organisms, they are usually found in the cytosol).

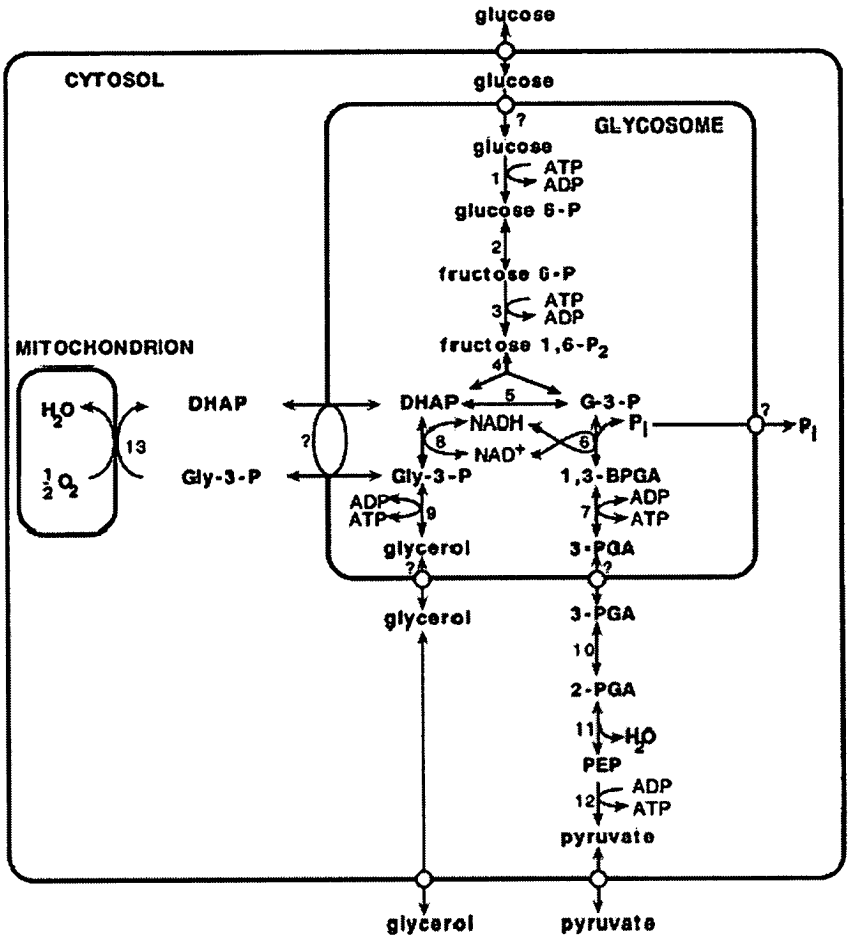

Figure 1.7[40] The stoichiometric scheme of glycolysis in blood from *T. brucei*. 1, Hexokinase; 2, glucose-6-phosphate isomerase; 3, phosphofructokinase; 4, aldolase; 5, triose-phosphate isomerase; 6, glyceraldehyde-3-phosphate dehydrogenase; 7, phosphoglycerate kinase; 8, glycerol-3-phosphate dehydrogenase; 9, glycerol kinase; 10, phosphoglycerate mutase; 11, enolase; 12, pyruvate kinase; 13, glycerol-3-phosphate oxidase. Abbreviations: 1,3-BPGA, 1,3-bisphosphoglycerate: DHAP, dihydroxyacetone phosphate; G-3-P, glyceraldehyde-3-phosphate; Gly-3-P, glycerol-3-phosphate; PEP, phospho*enol*pyruvate; 2-PGA, 2-phosphoglycerate; 3-PGA, 3-phosphoglycerate.

Net ATP synthesis occurs in the cytosol under the reaction catalysed by pyruvate kinase (PyK). This is due to the fact that the glycosomal milieu is in redox and ATP balance because of a glycosomal glycerol-3-phosphate dehydrogenase and glycerol-3-phosphate : dihydroxyacetone phosphate shuttle. This shuttle transfers electrons, eventually to allow the re-oxidation (by molecular oxygen) of NADH, produced by

glyceraldehyde-3-phosphate dehydrogenase. However, under anaerobic conditions glycerol-3-phosphate is converted to glycerol by the action of glycerol kinase, with production of ATP. Hence, the ATP and NAD^+ balance are still maintained under anaerobic conditions, but one molecule of both pyruvate and glycerol is produced, as opposed to two molecules of pyruvate. The net production of ATP is also reduced from two molecules to one.

Inhibition of any step of glycolysis in bloodstream form *T. brucei* should, in principle, stop ATP production and, therefore, cause death to the parasite. In fact, it has been shown that bloodstream form *T. brucei* dies within minutes when starved of glucose, or incubated with the plasma-membrane glucose transporter inhibitor phloretin.[47] Trypanosomatid death is also caused by inhibitors of glyceraldehyde-3-phosphate dehydrogenase, such as pentenolactone[48] or bromopyruvate,[49] and also by inhibitors of pyruvate efflux such as α-cyanocinnamic acid.[50] These inhibitors, however, cannot be used as potential drugs as they are not selective between the parasitic enzymes and the human equivalents.

A well-known method of selectively inhibiting trypanosomatid glycolysis *in vitro* is the inhibition of glycerol-3-phosphate oxidase by salicylhydroxamic acid (SHAM), whilst adding glycerol to prevent the reversal of glycerol kinase.[51] This has been found to have a trypanocidal effect in rats,[52] but the concentrations of SHAM required (1 mM) are too high. The concentration of glycerol needed (5 nM) is also toxic towards the host. Recently, however, an alternative, highly specific non-competitive inhibitor of glycerol-3-phosphate oxidase has been identified; the antibiotic ascofuranone,[53] but, as yet, no information is available about its *in vivo* efficacy.

1.4 Mechanisms of enzyme inhibition.

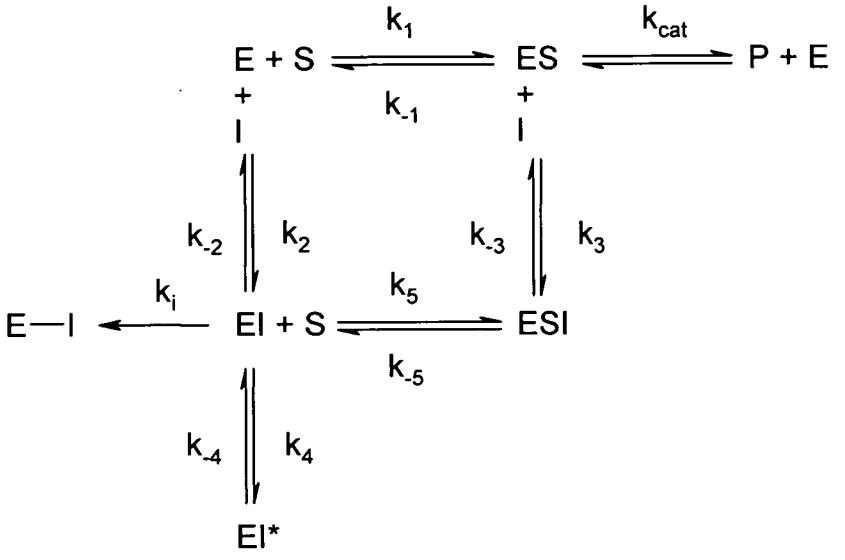

Figure 1.8 A scheme showing the mechanism of enzyme inhibition.

The scheme shown in Figure 1.8 is an illustration of the general strategy for enzyme inhibition, where E is the target enzyme, S is the substrate for the enzyme, I is the inhibitor, and P is the product formed. The scheme shows both irreversible and three types of reversible inhibition. The inhibitor, I, is a reversible competitive inhibitor if it binds to E only, and prevents S from binding. I is a reversible non-competitive inhibitor if it binds to E and ES still forms. Finally, I is an uncompetitive inhibitor if it binds to ES only. Blocking the flux of the glycolytic pathway in trypanosomatidae, through inhibition as shown in Figure 1.8, needs two requirements. Firstly, that the target enzyme has sufficient influence on the pathway to cause eventual death to the parasite if it were to be inhibited, and secondly, that the inhibitor has a high affinity for the enzyme.[36]

Figure 1.8 also shows irreversible inhibition, where the inhibitor covalently binds to

the enzyme (E-I). For example, this could be caused by the inhibitor possessing an electron acceptor site (such as a carbonyl or cyano-group), which reacts with a residue in or near the targeted binding site of the enzyme (such as the amino group on lysine).

If the inhibitor bears a structural resemblance to the transition state of an enzymatic reaction, the formation of an isomerised complex (EI*) may occur. These transition-state inhibitors are usually found to exhibit a slow-binding process, corresponding to the conformational change induced in the enzyme by the inhibitor.[1]

Inhibitor design should also try to achieve selectivity between targeted and non-targeted enzymes, thereby producing the desired effect in the parasite by targeting the parasitic enzymes, without harming the host, or interacting with the enzymes of the host. One method to achieve this would be by exploiting the differences in enzyme structure and mechanism between the target and host enzymes. Comparisons between the 3-dimensional structure of the parasite and host enzymes can reveal subtle or major differences that can be used to selectively target the parasitic enzymes by the design of specific inhibitors.[39] This has already allowed for the development of a relatively highly specific inhibitor for the trypanosomatid glycosomal enzyme, glyderaldehyde-3-phosphate dehydrogenase (Figure 1.9, inhibitor **12**).[54]

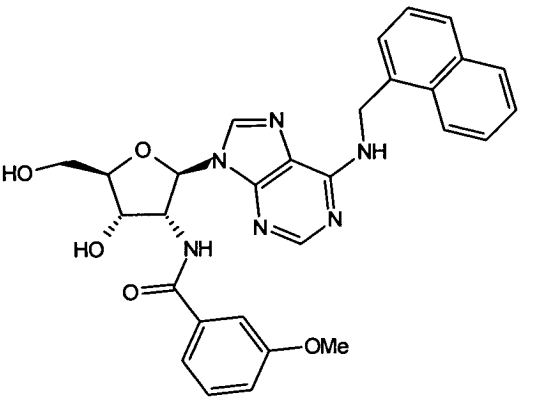

12

Figure 1.9 Selective inhibitor of trypanosomatid glyceraldehyde-3-phosphate dehydrogenase.[54]

1.5 Enzymes in the trypanosomatid glycolytic pathway.

1.5.1 Hexokinase (HK).

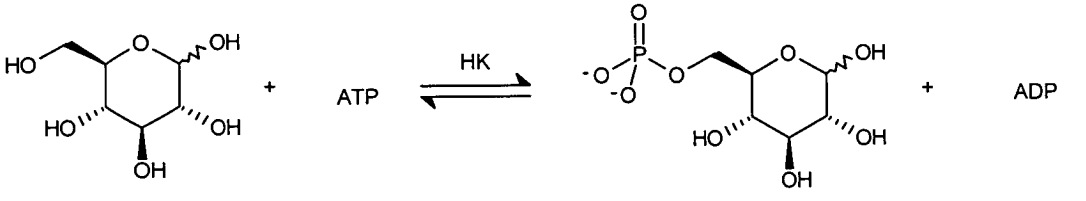

Figure 1.10 The role of hexokinase (HK).

The role of hexokinase is to catalyse the transfer of a phospho group from ATP to glucose (Figure 1.7, enzyme 1). In humans, there are four isoenzymes of hexokinase (I – IV),[55] and the trypanosomatid enzyme only has a low percentage identity with the human forms.[56] Hexokinase has a low substrate specificity, and therefore will accept a range of sugar molecules, which is also true for other hexokinases.[57] The trypanosomatid hexokinase is not regulated by its product, glucose-6-phosphate, and unlike the human isoenzymes, and it has a low specificity for ATP; indeed, it is also

able to utilise UTP and GTP.[34] Although there is no crystal structure available for the trypanosomatid hexokinase, the low sequence identity and the difference in kinetic properties from the human isoenzymes[55] potentially allows the possibility for development of selective inhibitors. In fact, this has been explored to some extent, and some *N*-acetylglucosamine derivatives were found to inhibit the enzyme. Notably, the inhibitor *N*-(*m*-bromobenzoyl)-D-glucosamine **13** (Figure 1.11) with a K_i of 3 μM (the K_M of glucose is 110 μM) has been reported.[34,58] The inhibitory activity of this compound on yeast hexokinase is 50 times poorer[59] and there are no results available for mammalian hexokinase.

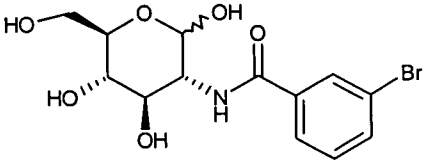

13

Figure 1.11 *N*-(*m*-Bromobenzoyl)-D-glucosamine **13**, inhibitor of trypanosomatid HK.

1.5.2 Glucose-6-phosphate isomerase (PGI).

The second glycosomal enzyme (Figure 1.7, enzyme 2) catalyses the isomerisation of glucose-6-phosphate (Glc-6-P) to fructose-6-phosphate (F6P, Figure 1.12).

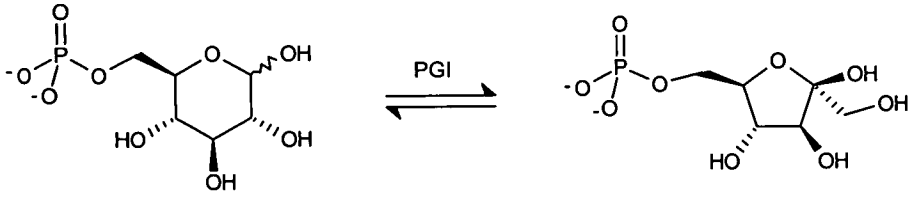

Glucose-6-phosphate Fructose-6-phosphate

Figure 1.12 The role of glucose-6-phosphate isomerase (PGI).

The percentage identity of trypanosomatid PGI with the mammalian enzyme has been shown to be 58 %.[34] No crystal structure is available for this enzyme, so its feasibility as a potential target for selective inhibitors is not yet known. It is also considered that this enzyme does not confer significant control over the glycolytic flux.[56]

1.5.3 Phosphofructokinase (PFK).

Phosphofructokinase (Figure 1.7, enzyme 3) catalyses the phosphorylation of fructose-6-phosphate (F6P) to afford fructose-1,6-bisphosphate (F1,6BP, Figure 1.13).

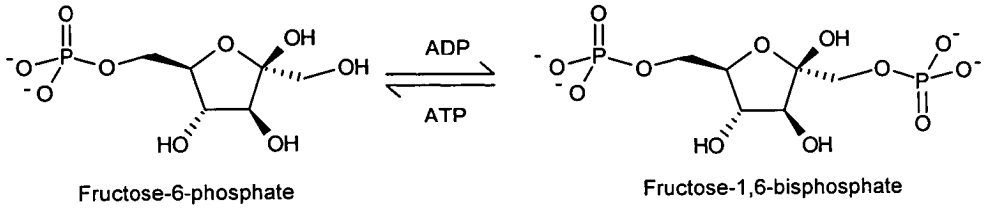

Figure 1.13 Reaction catalysed by phosphofructokinase (PFK).

The enzyme exists as a tetramer and, under physiological conditions, the reaction is irreversible. Its human counterpart consists of similar sub-units of about 85 kDa, and the regulation of this enzyme is controlled by a large number of metabolites and allosteric effectors.[34] However, the trypanosomatid enzyme has smaller sub-units of about 53 kDa,[60] and is activated only by its substrate fructose-6-phosphate, AMP and ADP.[57] It was also found that whilst the percentage identity between the phosphofructokinase of *T. brucei* and *L. donovani* is high (70 %), between these enzymes and the human enzyme it is only 20 %.[34]

Preliminary attempts to design inhibitors of trypanosomatid PFK have had promising results. Analogues of 2,5-anhydro-D-mannitol, bearing various arylamino groups at position 1 (see Figure 1.14), have shown inhibitory activity by reversibly binding at the ATP and F6P binding site.[61-63] These inhibitors and further inhibitor development are discussed further in the following chapters.

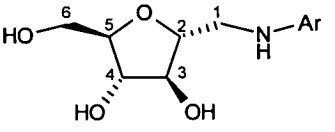

Figure 1.14 General structure of *N*-aryl-1-amino-2,5-anhydro-1-deoxy-D-mannitol that shows inhibitory activity against trypanosomatid PFK.[62]

1.5.4 Aldolase.

Aldolase (Figure 1.7, enzyme 4) catalyses the conversion of F1,6BP to dihydroxyecetone phosphate (DHAP) and D-glyceraldehyde-3-phosphate (G-3-P, Figure 1.15).

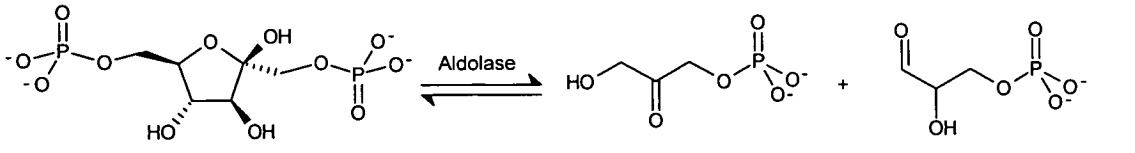

Figure 1.15 Reaction catalysed by aldolase.

The crystal structure of aldolase has been determined for both *T. brucei* and *L. mexicana* and shows a large number of charged residues.[64] Inhibitors of aldolase

have been synthesised that form a stabilised ammonium ion at the active site. They have shown significant inhibition against *T. brucei* aldolase, with virtually no effect on the mammalian forms of the enzyme.[56]

1.5.5 Triose-phosphate isomerase (TIM).

The fifth enzyme in trypanosomatid glycolysis (Figure 1.7, enzyme 5) catalyses the reversible conversion of the triose-phosphates, DHAP and G-3-P (Figure 1.16). The human form of the enzyme has been shown to have about 52 % sequence identity between the trypanosomatid forms of *T. brucei*, *T. cruzi* and *L. mexicana*.[34] The crystal structures of these enzymes show that the active site residues are reasonably well conserved, making the development of selective inhibitors more difficult.[34]

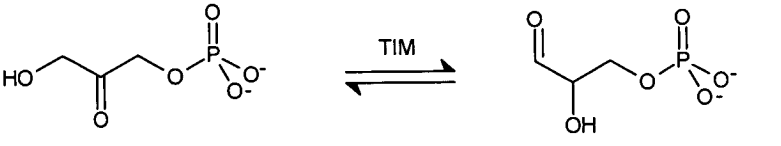

Figure 1.16 Conversion catalysed by triose-phosphate isomerase (TIM).

1.5.6 Glyceraldeyde-3-phosphate dehydrogenase (GAPDH).

Glyceraldehyde-3-phosphate dehydrogenase (Figure 1.7, enzyme 6) catalyses the phosphorylation of G-3-P to 1,3-bisphosphoglycerate (1,3-BPGA), in the presence of the cofactor, NAD^+ (Figure 1.17).

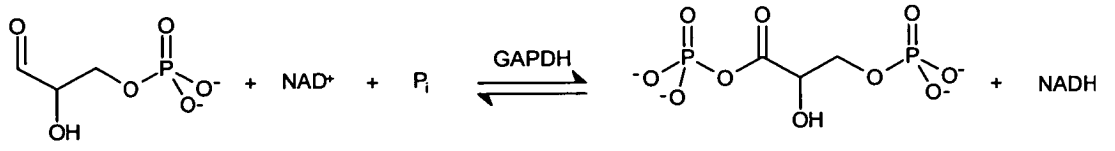

Glyceraldehyde-3-phosphate 1,3-Bisphosphoglycerate

Figure 1.17 Phosphorylation catalysed by glyceraldehyde-3-phosphate dehydrogenase GAPDH in the presence of NAD^+ and inorganic phosphate (P_i).

The trypanosomatid enzymes have a 45 – 48 % identity with the human enzyme.[34] However, a comparison of the crystal structures shows that the active site of the enzyme appears well conserved.[65] This is not the case for the NAD^+ binding site, as it appears to have a hydrophobic cleft in the adenosine binding portion of the trypanosomatid enzyme, which is not present in the human enzyme.[39] Probing of this site with adenosine derivatives has found compounds that inhibit the trypanosomatid enzyme at micromolar and sub-micromolar concerntrations, but do not affect the human enzyme.[54] Figure 1.18 shows one of these compounds (N^6-(1-naphthylmethy)-2′-deoxy-2′-(3-methoxybenzamido)-adenosine) binding at the NAD^+ binding site. It utilises the hydrophobic groove using the N^6-substituent of the purine to gain affinity, whilst gaining selectivity over the human enzyme by interactions of the 3-methoxybenzamido group in a less sterically congested region.

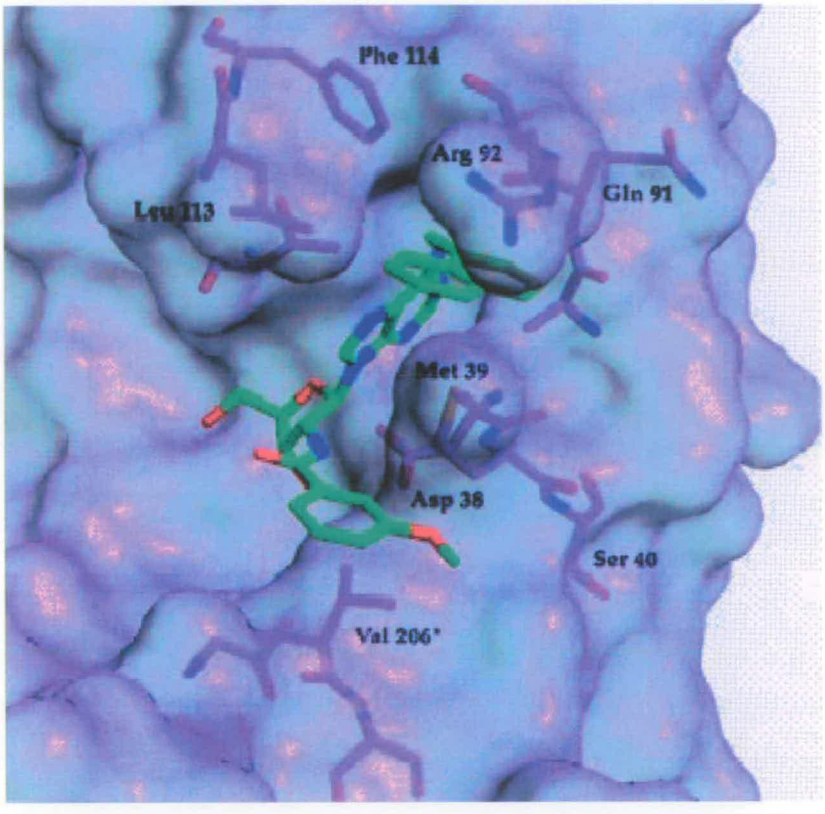

Figure 1.18 A model of *L. mexicana* GAPDH complexed with N^6-(1-naphthylmethyl)-2′-deoxy-2′-(3-methoxybenzamido)-adenosine in the NAD^+ binding pocket.[54]

1.5.7 Glycerol-3-phosphate dehydrogenase (G3PDH).

Glycerol-3-phosphate dehydrogenase (Figure 1.7, enzyme 8) catalyses the reversible conversion of DHAP and L-glycerol-3-phosphate (Gly-3-P, Figure 1.19). It has been shown that the human form of the enzyme possesses only a 28 – 30 % sequence identity with the enzymes from *T. brucei* and *L. mexicana*.[56] Coupled with the fact that the enzyme exerts significant control over glycolytic flux, this makes G3PDH a promising target for the development of selective inhibitors.[56]

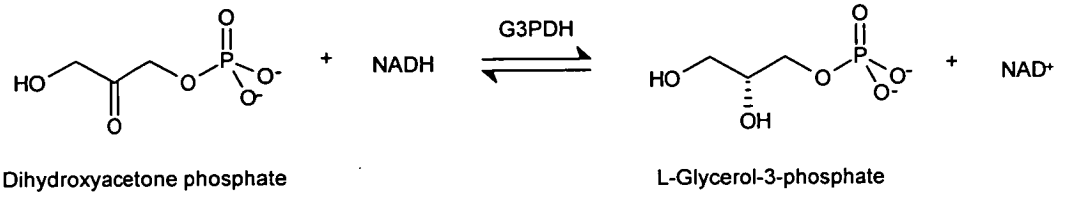

Figure 1.19 Reaction catalysed by glycerol-3-phosphate dehydrogenase (G3PDH).

1.5.8 Glycerol kinase (GK).

Glycerol kinase (Figure 1.7, enzyme 9) catalyses the ATP-dependent phosphorylation of glycerol when sugar levels are low, but catalyses the production of glycerol and ATP in anaerobic conditions[40,66] (Figure 1.20). The human form of the enzyme is only involved in glycerol phosphorylation. As it is unlikely that GK, under physiological conditions, plays an essential role in metabolism, it is also unlikely that, by itself, the enzyme is a suitable drug target.[34]

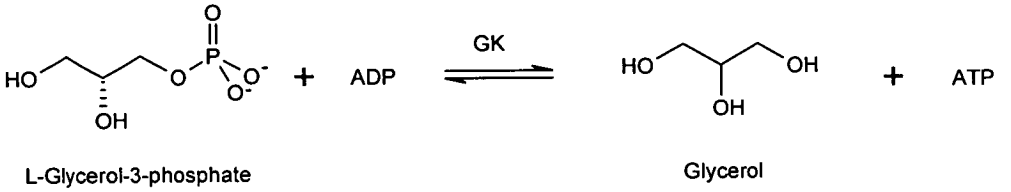

Figure 1.20 Reaction catalysed by glycerol kinase (GK).

1.5.9 Phosphoglycerate kinase (PGK).

Phosphoglycerate kinase (Figure 1.7, enzyme 7) catalyses the conversion of 1,3-BPGA to 3-phosphoglycerate (3-PGA), producing ATP (Figure 1.21).

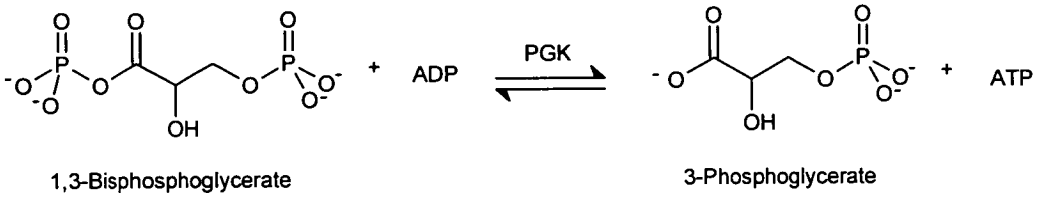

Figure 1.21 Reaction catalysed by phosphoglycerate kinase (PGK).

The percentage identity between the trypanosomatid and human enzymes is 46 %.[34] Although the active sites of the parasitic and mammalian enzymes are well conserved, there is a difference in the ADP binding pocket, which makes this enzyme an interesting target for drug development.

1.5.10 Phosphoglycerate mutase (PGAM).

Phosphoglycerate mutase (Figure 1.7, enzyme 10) catalyses the conversion of 3-PGA to 2-PGA (Figure 1.22). Two classes of enzyme have been discovered; 2,3-bisphosphoglycerate (2,3-BPGA) dependent and independent.[67] The structure and mechanisms of these enzymes are also different. Humans possess the cofactor dependent mutase, whereas trypanosomatid PGAM is cofactor independent. The trypanosomatid enzyme is completely different from the human enzyme, and modelling of its 3-dimensional structure reveals that it is more related to the family of alkaline phosphatases.[56] This difference offers an excellent opportunity for the development of selective inhibitors.

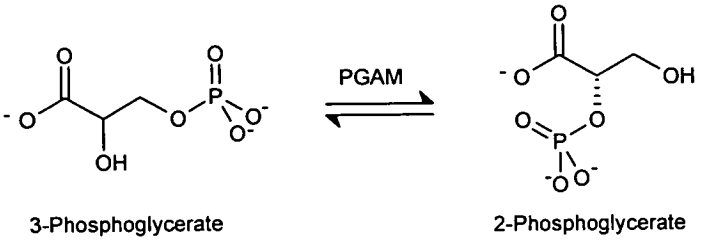

Figure 1.22 Conversion catalysed by phosphoglycerate mutase (PGAM).

1.5.11 Enolase.

Enolase (Figure 1.7, enzyme 11) catalyses the dehydration of 2-PGA to phospho*enol*pyruvate (PEP) (Figure 1.23).

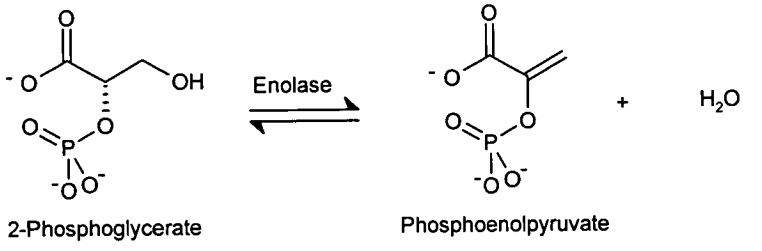

Figure 1.23 Dehydration catalysed by enolase.

Although the percentage identity between the parasitic (*T. brucei*) and the human enzyme is about 59 – 62 %, no crystal structures of either enzyme are available. Some atypical residues near the active site of the parasitic enzyme (Lys and Cys) could be exploited for the development of irreversible selective inhibitors.[34]

1.5.12 Pyruvate kinase (PyK).

Pyruvate kinase (Figure 1.7, enzyme 12) catalyses the conversion of PEP to pyruvate whilst producing ATP (Figure 1.24).

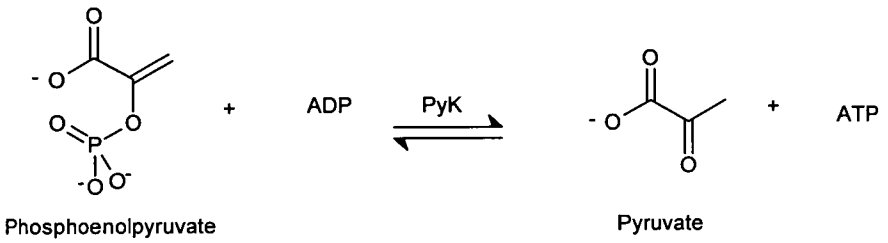

Figure 1.24 Reaction catalysed by pyruvate kinase (PyK).

Trypanosomatid PyK is allosterically regulated by fructose-2,6-bisphosphate (although fructose-1,6-bisphosphate does have a weak affinity for the effector site). This effector promotes the active R-state of the enzyme from the inactive T-state.[68] In contrast, mammals possess four isoenzymes of PyK, one of which (M1) has no allosteric regulation and the other three (M2, L and R) are regulated by fructose-1,6-bisphosphate.[67] Combined with the fact that the percentage identity between the trypanosomatid and human enzymes is 47 – 51 %, this makes PyK an excellent target for the development of selective inhibitors. Inhibitor design and synthesis for PyK is discussed in more depth in the following chapters.

1.5.13 Glycerol-3-phosphate oxidase.

Glycerol-3-phosphate oxidase (Figure 1.6, enzyme 13) is a mitochondrial enzyme. The *T. brucei* form is a complex enzyme, but as yet no sequence or structure information is available.[34]

Chapter 2

Library 1: Design, Synthesis and Evaluation

2 Library 1: Design, Synthesis and Evaluation.

2.1 Research aims.

2.1.1 Phosphofructokinase (PFK).

The overall aim of this research was to use parallel (or combinatorial) synthetic methods in order to create potential inhibitors of trypanosomal glycolysis, in particular inhibitors of the enzymes phosphofructokinase (PFK) and pyruvate kinase (PyK). The initial synthetic targets were based on work carried out by Samantha Claustre at at l'Université Paul Sabatier de Toulouse.[61-63] Inhibitors were designed as derivatives of 2,5-anhydromannitol,[62] itself being structurally analogous to fructose-6-phosphate (F6P, Figure 2.1), a substrate of the enzyme PFK. It was shown that these compounds (*N*-arylamino-2,5-anyhdro-1-deoxy-D-mannitol derivatives, Figure 2.1) inhibit *Tb* PFK by binding reversibly at both the F6P and ATP binding sites.[62]

Figure 2.1 Fructose-6-phosphate (F6P) and *N*-arylamino-2,5-anhydro-1-deoxy-D-mannitol.

In addition, it was reported that when these derivatives were phosphorylated at the 6 position, exclusive binding at the ATP binding site was observed.[62] The IC_{50} and K_d values for a selection of these compounds against *Tb* PFK can be seen in Table 2.1.

Compound	IC_{50} (mM)	K_d (μM)
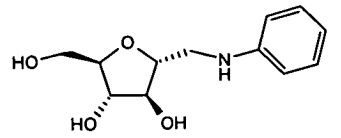 14	3	nd
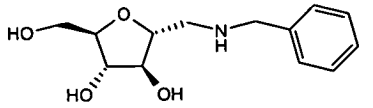 15	3	24
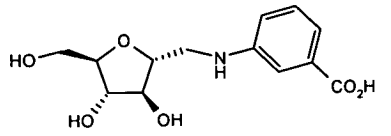 16	1.2	67
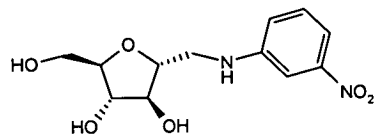 17	1.1	40
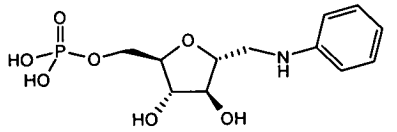 18	1.5	64
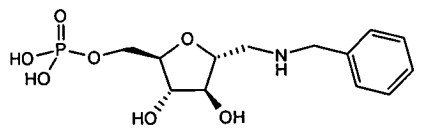 19	1.5	nd
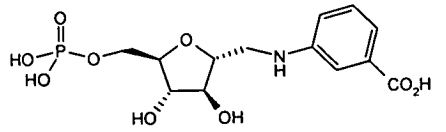 20	0.8	nd
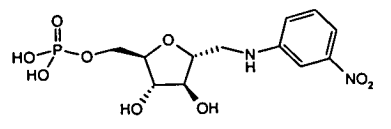 21	0.45	nd

Table 2.1 Selected IC_{50} and K_d values of *N*-arylamino-2,5-anydro-1-deoxy-D-mannitol derivatives against *Tb* PFK. Each determination was done in triplicate with SD ± 4 %.[62,63]

The presence of the phosphate group at the 6 position also led to a twofold increase in the inhibitory activity of these compounds, whilst the dissociation constants (K_ds) appeared to remain comparable. In the absence of any crystal structure of trypanosomal PFK, the specific interactions of these inhibitors with the protein are not clear. However, for the best inhibitors (3-nitrophenyl derivatives) it was thought that the nitro group formed an ionic interaction with Lys226, situated in the ATP binding site,[62] which had been determined as hydrophobic by multiple sequence alignments between *E. coli* PFK and *T. brucei* PFK, where the residues Arg81 and Arg111 in *E. coli* PFK have been replaced by proline and valine in *Tb* PFK.[60,62]

The inhibition shown by these compounds, to date the only known inhibitors of trypanosomal PFK, is relatively poor (IC_{50} values are only in the millimolar range). However, when comparing the dissociation constants (K_d) of these compounds to those of the natural substrates for *T. brucei* PFK, it was found that the values are similar (see Table 2.2).

Substrate	K_d (μM)
ATP	33 ± 2
ATP-Mg	30 ± 2
F6P	36 ± 2

Table 2.2 Dissociation constants for natural substrates of *Tb* PFK.

Therefore, the decision was made to synthesise new inhibitors based around the existing 2,5-anhydro-D-mannitol scaffold. Primarily, this would further explore substitution at the 1-position, using already known chemistry and adapting it for parallel synthesis. The idea would be to produce compounds with drug-like properties (obey Lipinski's Rule of 5[19]) of greater inhibitory activity than the previously synthesised compounds, that could lend themselves to further synthesis and development. Knowledge of the environment of the binding site of these compounds would also be attained through structure-activity relationships (SARs).

It is also interesting to note that compounds with a similar scaffold (2,5-anhydro-D-mannitol) are known to be inhibitory towards glycosidase enzymes involved in a wide range of biological processes[69,70] Inhibitors of this type are also known to be active against mycobacteria, the causative of tuberculosis (*Mycobacterium tuberculosis*);[71,72] one or more arabinosyl transferase enzymes are inhibited by these compounds, leading to increased cell wall permeability.[71]

2.1.2 Pyruvate kinase (PyK).

In contrast to PFK, no inhibitors were known for trypanosomatid PyK. However, this allosterically regulated enzyme is thought of as a good target for trypanocidal drugs due to the low sequence identity between the trypanosomal and mammalian forms of the enzyme, and due to the fact that trypanosomal PyK is regulated by fructose-2,6-bisphosphate (F2,6BP, see Figure 2.2).[68] Trypanosomatid PyK differs from mammalian PyK which is regulated by fructose-1,6-bisphosphate (F1,6BP, see Figure 2.2, discussed in introduction)[67] making the effector site an ideal target for inhibitors and inhibitor development. Although a crystal structure of *L. mexicana*

PyK has been determined, this is of the apo-enzyme and therefore is in the inactive T-state (no effector bound). Hence, the geometry of the effector site was not well known.

Advances in computational power have led to the development of programs that use structure-based or target-based approaches to screen compounds (from the Available Chemical Database or other databases) for potential ligands and inhibitors of proteins. However, with no active R-state structure of trypanosomal PyK (with effector bound), notions about the effector site have been largely based on the T-state structure and the corresponding site in the yeast enzyme in order to carry out database mining and *in silico* screening with programs such as DOCK.[18] With the outcome of this approach uncertain, an alternative strategy was produced. Due to the structural similarity between F2,6BP, F1,6BP and F6P (F1,6BP also being a substrate for PFK), the compounds synthesised for testing against PFK, would also be tested for activity against PyK. Again, with little known about the effector site for PyK, the results would hopefully provide an insight about the effector sight environment and structure, whilst also producing the first inhibitors of trypanosomal PyK. Any differences between the best inhibitors for PFK and for PyK could be exploited in further development in the hope of gaining specificity between both enzymes, as well as specificity between the trypanosomal enzymes and their mammalian counterparts.

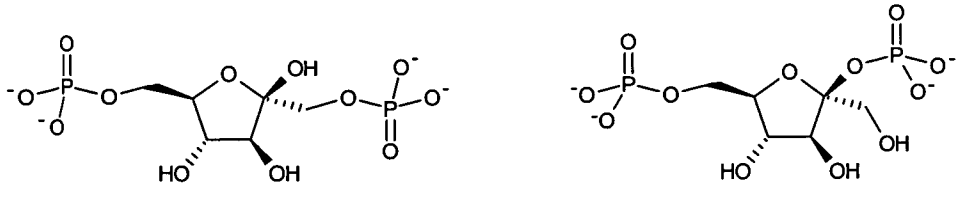

Figure 2.2 Fructose-1,6-bisphosphate (F1,6BP) and fructose-2,6-bisphosphate (F2,6BP).

2.2 Adaptation of *N*-arylamino-2,5-anhydro-1-deoxy-D-mannitol synthesis.

2.2.1 Preparative scale reactions.

As stated previously, the initial objective was to use an already known synthetic procedure and adapt it for use with parallel synthesis equipment in order to make a small library of compounds. The first step in the synthesis of these compounds is the formation of 2,5-anhydro-D-mannose **22** which forms the locked furanose scaffold. This is achieved by treatment of D-glucosamine hydrochloride with nitrous acid,[61] as shown in Figure 2.3, and is a modification of the procedure by Horton and Philips.[73]

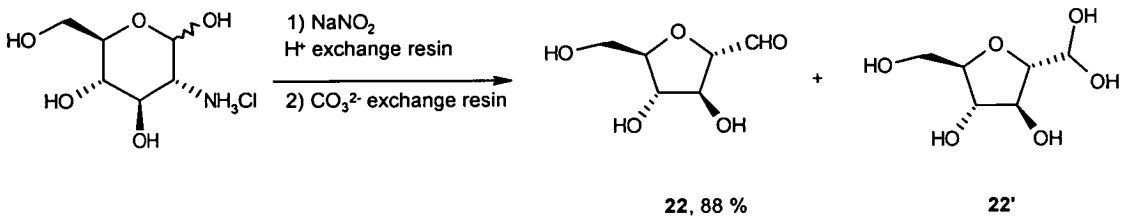

Figure 2.3 Synthesis of 2,5-anhydro-D-mannose **22**.

This stereospecific reaction can be explained by the proposed mechanism shown in Figure 2.4.[63,73] Following the formation of the diazonium ion **23**, the pyranose oxygen facilitates an intramolecular substitution reaction by rearside attack of the diazonium carbon. This results in the formation of a 3-membered cyclic intermediate **24** and the evolution of nitrogen. The 3-membered ring then breaks down in order to form 2,5-anhydro-D-mannitol **22** and it's hydrated equivalent **22'**.[63,73] This reaction occurred cleanly, in high yield (88 %) and could be scaled up in order to produce sufficient starting material for the next step of the synthesis. However, the hygroscopic nature of aldehyde **22** made it difficult to handle as a solid. It was

thought that this would provide difficulty in the practical aspects of library synthesis, so it was decided that aldehyde **22** would be handled as a methanolic solution, thus avoiding any unnecessary difficulties and errors in the weighing out of this compound, and allowing it to be dispensed automatically using the Bohdan Neptune liquid handler (see Chapter 6).

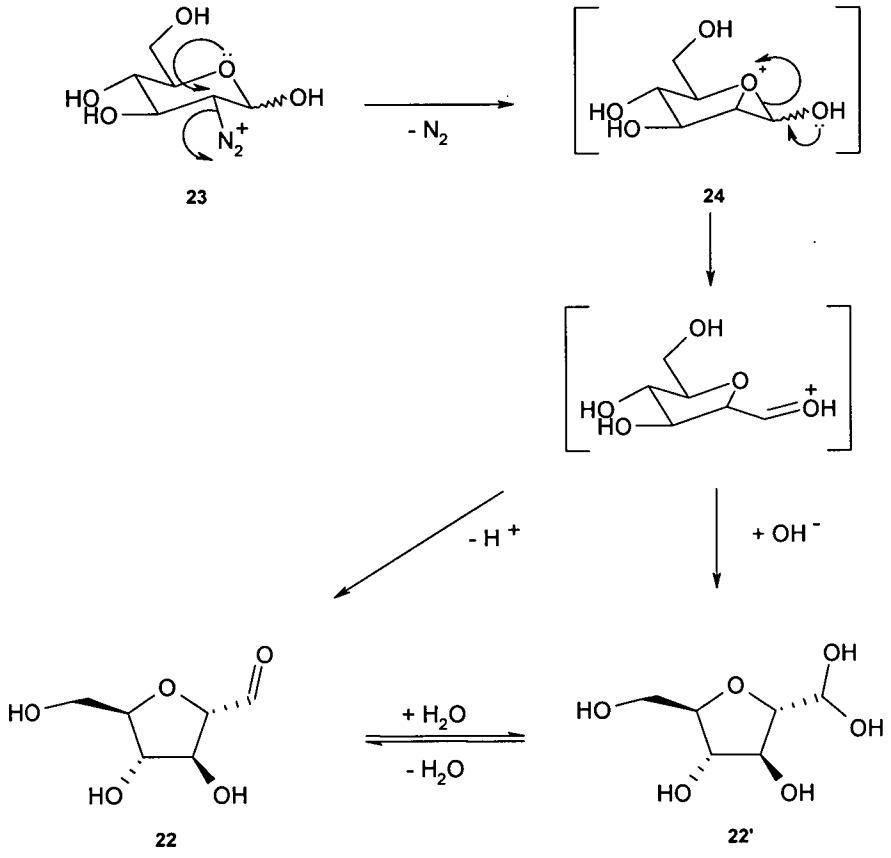

Figure 2.4 Proposed mechanism for the formation of 2,5-anhydro-D-mannitol **22**.[63,73]

The next step in the synthesis of mannitol derivatives is the reductive amination of compound **22** with an arylamine (as shown in Figure 2.5).

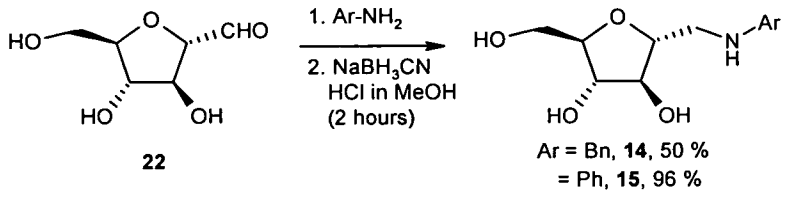

Figure 2.5 Reductive amination of aldehyde **22** with arylamines.

These reactions again followed the same procedure as set out by Claustre *et al*[61] however purification was achieved by mass directed methods using the Waters ZMD (see Chapter 6). Therefore, this method gives the advantage of not being restricted to the use of aryl amines for future synthesis; it would be possible to use amines that are poorly detected using a diode ray as used in HPLC. With the reductive amination being the reaction that would afford the target compounds, the yields were acceptable. The structures of these compounds were confirmed by comparison of ^{1}H and ^{13}C NMR spectra to those previously reported.[61,63]

2.2.2 Test library synthesis.

It is important to note that the reductive amination reactions were carried out on a preparative scale. In order to test this reaction further, it was decided to synthesise a small 4-membered library on a combinatorial scale. Before embarking on the synthesis of larger libraries, the test library would serve to check that the methods used would be suitable and robust enough for smaller, combinatorial scale reactions. The compounds that were synthesised in this test library had been previously reported[63] and are shown in Figure 2.6 along with yields.

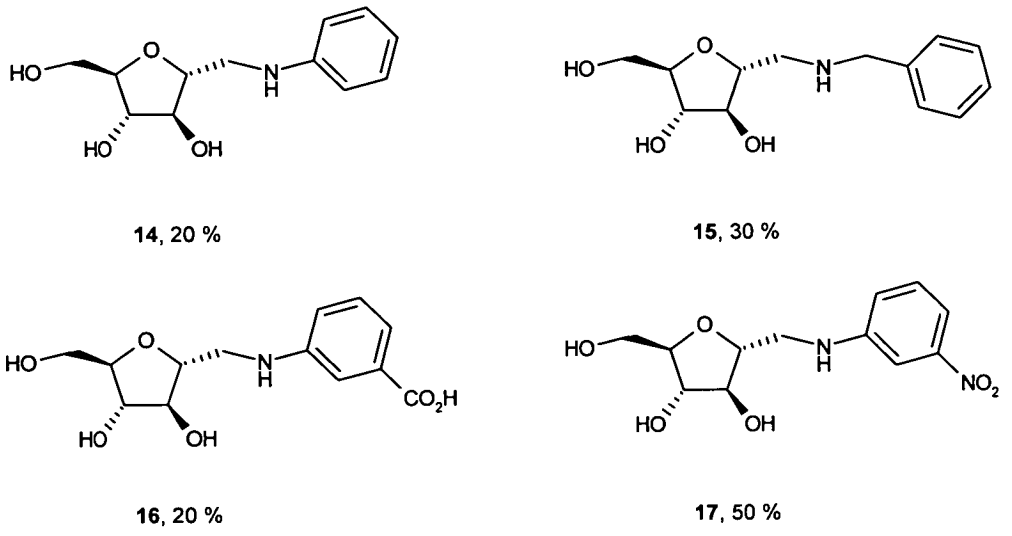

Figure 2.6 Structures and yields of test library.

Although the yields from the test library were lower than expected, enough material was produced to enable characterisation and screening against both PFK and PyK, deeming the methods suitable for synthesis of larger libraries. A possible reason for the low yields could be due to the fact that none of the reactions was monitored. Performing reactions in parallel subjects all reactions to the same general conditions. Another reason for low yield could also be loss of material during mass directed purification as again, the method used was a general method for all compounds. However, even with these problems, the overall aim of the library synthesis was achieved; to synthesise enough of each compound for characterisation of biological screening.

2.3 Library 1.

2.3.1 Library 1 design.

As mentioned previously (at the time of this library synthesis), little was actually known about the structure of substrate binding sites of trypanosomal PFK, other than that the ATP binding site may be hydrophobic in nature when comparing to other PFKs[60,62]. Therefore, the design of this library was based around current inhibitors and reaction yields as discussed in section 2.2. Table 2.1 shows screening results of current inhibitors and the effects of substitution on the aromatic ring. It is interesting to note that there is no difference in the IC_{50} values obtained for the un-substituted phenyl, **17**, and the benzyl, **15**, derivatives. Although the K_d value for **14** had not been determined, it is also interesting that the K_d value for compound **15** was comparable to those of the natural substrates for PFK. This, coupled with the fact that some inhibitors with a substituted phenyl group had already been synthesised and the effects on *Tb* PFK analysed,[61,62] led to the decision that the inhibitors synthesised in library 1 would be based around 2,5-anhydro-1-deoxy-1-(benzylamino)-D-mannitol **15**, with diversity being introduced by means of substitution of the phenyl ring. Hence, substituted benzylamine derivatives were used as the starting materials (Figure 2.7).

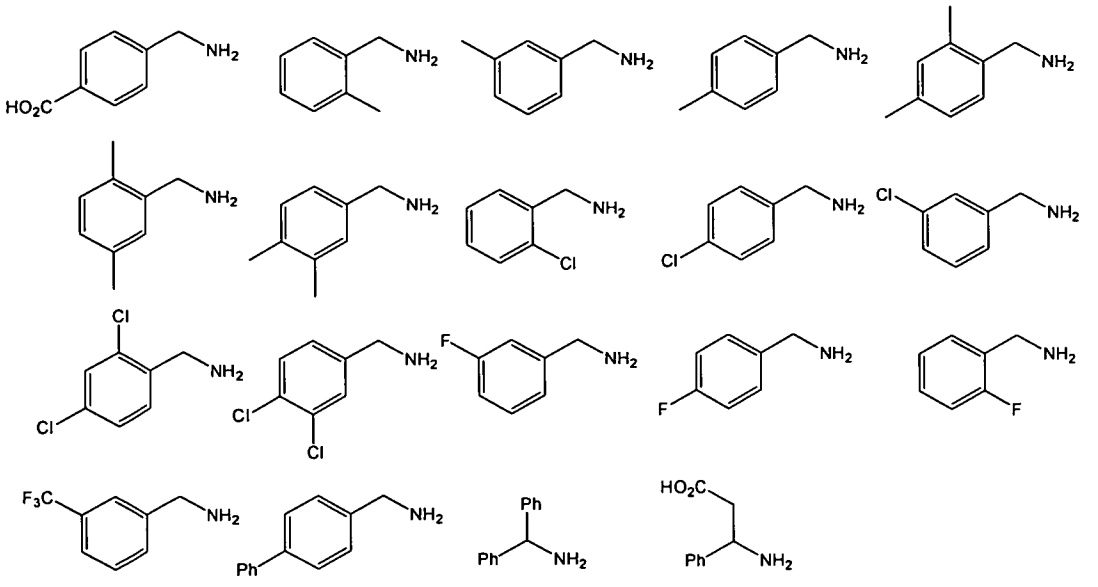

Figure 2.7 Benzylamine building blocks used in the synthesis of library 1.

The amines shown in Figure 2.7 were chosen primarily to examine the effect of mono- and di-substitutions on the phenyl ring. As well as identifying new inhibitors of *Tb* PFK, the hope would be to try to determine a pattern that relates to inhibition (based on the aromatic substitution patterns), and hence to the environment in the ligand binding site. Other benzylamine derivatives were also used in this library synthesis to increase diversity in the hope that they may show some interesting results. The library size was restricted to 19 members simply on grounds of ease of compound handling.

2.3.2 Library 1 synthesis.

Library 1 was synthesised using the schemes and methods described in section 2.2. Figure 2.8 shows the structures and yields of all compounds successfully synthesised.

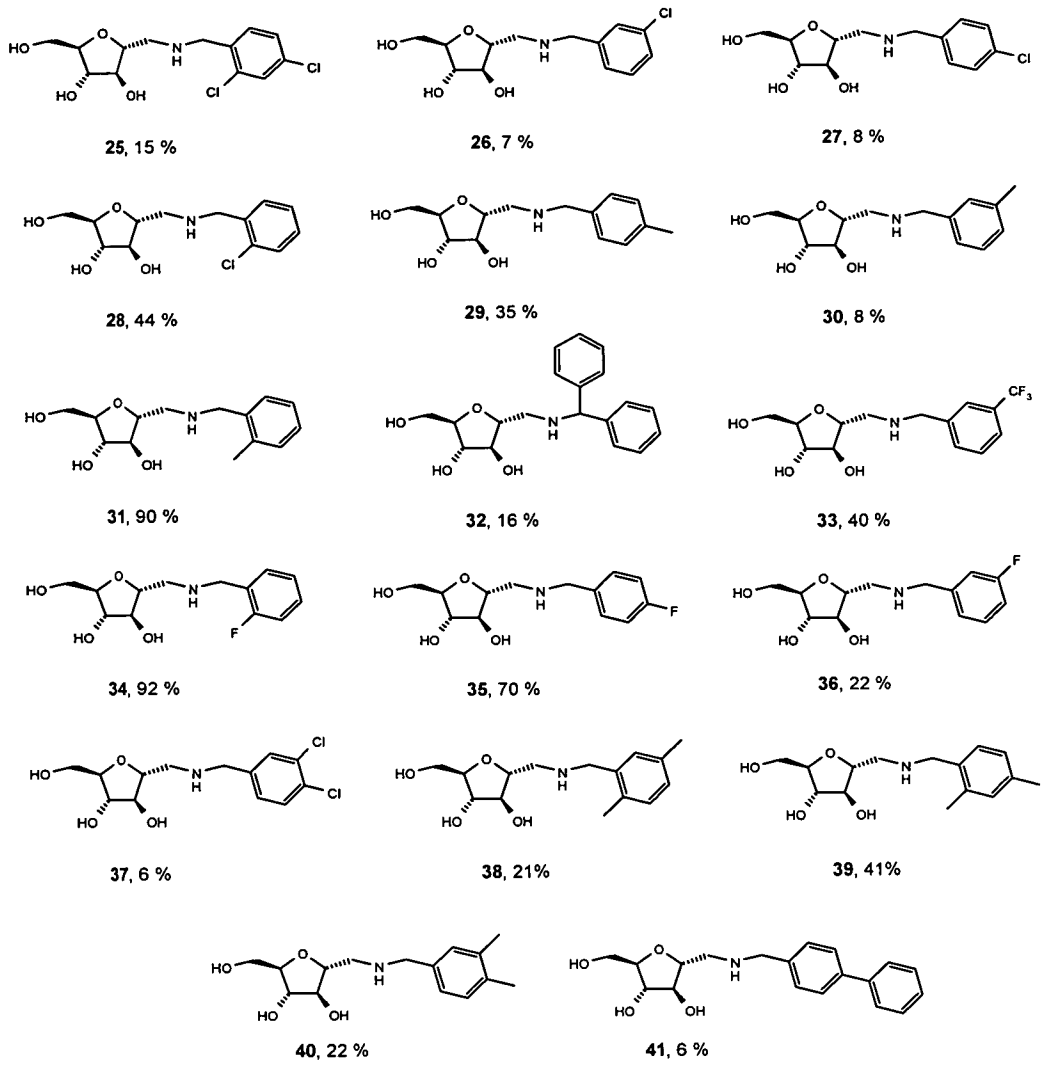

Figure 2.8 Library 1; structures and yields.

The yields for the successfully synthesised compounds ranged from 6 % to 92 %. The library was designed so that a quantitative yield would produce around 200 mg for each compound. Therefore the compounds shown in Figure 2.8 were produced in sufficient quantity for biological screening. As has already been observed in section 2.2.2 (the synthesis of the test library), some of the yields are quite low. Again, this can be attributed to the employment of a general method for all reactions. For example, those reactions with low yields may have benefited from longer reaction

times to go to completion. As well as this reason, the mass directed purification equipment (Waters ZMD) may have been a cause for the loss of yield. The reasons for this will be discussed later in Chapter 4. There were, however, two reactions in this library synthesis that were unsuccessful. These were the reactions with (4-aminomethyl)-benzoic acid and 3-amino-3-phenylpropanoic acid. On inspection of the reaction vessels, this is thought to be because neither of these compounds dissolved (or failed to dissolve fully) in the solvent, methanol. Even though the library size is quite small, 17 out of 19 compounds were synthesised, characterised and submitted for biological screening against *Tb* PFK and *Leishmania mexicana* (*Lm*) PyK. The structures of these compounds were established by comparison of ^{1}H and ^{13}C NMR spectra to those of previously reported compounds.[61,63] In particular, in the ^{1}H NMR spectra, characteristic doublet of doublet signals can be seen for the diasterotopic protons on C1 with a geminal coupling constant of around 12.5 Hz. In the ^{13}C NMR spectra, characteristic signals can be seen between δ = 76 and 86 ppm for the 4-carbon furanose scaffold (C2 – C5, see experimental). All compounds were established to have high purity by ^{13}C NMR with the baseline showing no impurities.

2.4 Biological Screening and Evaluation.

2.4.1 Initial screening method against *Tb* PFK.

The screening method for library 1 (and indeed any subsequent library) was standardised so that the procedure would be relatively rapid, adaptable to high throughput screening and could also quickly identify any potential lead compounds or good inhibitors of PFK. It was for this reason that a 5 mM screening procedure was adopted. This meant that each compound was diluted in a buffer solution (0.1

mM triethanolamine, pH 8.0), which was then tested against PFK where the final inhibitor concentration was 5 mM (0.25 μg/ml PFK, 2 mM $MgCl_2$, 2 mM F6P, 1 mM ATP, 0.3 mM NADH, 1.7 units G3PDH, 0.9 units aldolase, 1 unit TIM). The activity of the enzyme before and after incubation was measured so that the percentage remaining activity of PFK could be calculated, giving an indication of the inhibitory effect of the inhibitors. Activity was calculated by measuring the absorbance decrease caused at 340 nm by the oxidation of NADH to NAD^+ as shown by the enzyme couple in Figure 2.9. Hence, a decrease in absorbance would be proportional to the activity of *Tb* PFK, allowing for the percentage remaining activity to be determined.

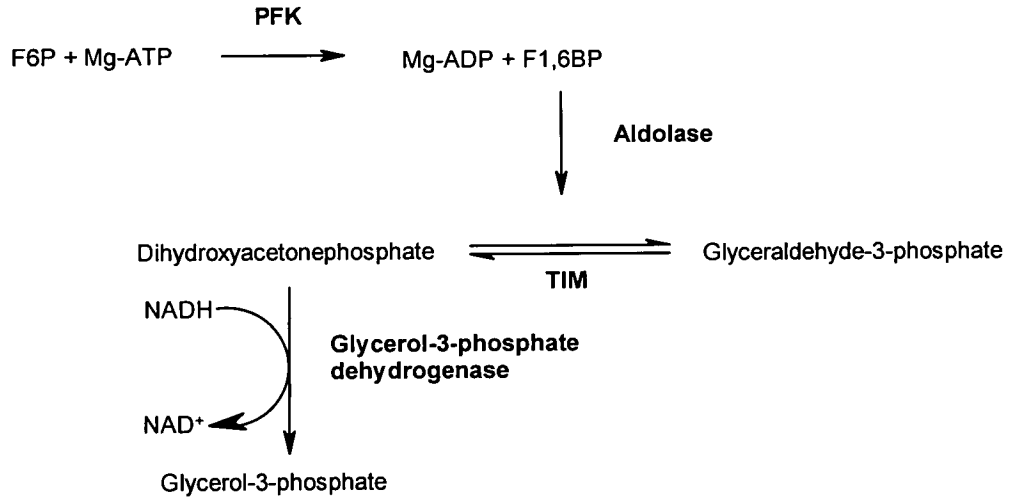

Figure 2.9 Enzyme couple used in 5 mM screen to measure the effect of compound libraries on *Tb* PFK. TIM = triose phosphate isomerase.

Any compounds that were identified as hits (showing at least 75 % inhibition at 5 mM) were then further evaluated to obtain IC_{50} values, K_d values or both.

2.4.2 Library 1 screening results against *Tb* PFK.

The results[74] of the 5 mM screen of library 1 against *Tb* PFK are shown in Table 2.3, and again are shown graphically in Figure 2.10.

Compound	Percentage (%) remaining activity
25	58.1 ± 3.4
26	85.3 ± 13.3
27	65.4 ± 12.2
28	65.2 ± 11.6
29	72.6 ± 13.9
30	61.1 ± 11.6
31	67.6 ± 4.3
32	29.8 ± 3.0
33	46.2 ± 2.9

Compound	Percentage (%) remaining activity
34	62.5 ± 11.7
35	58.6 ± 22.0
36	56.9 ± 8.7
37	4.7 ± 0.0
38	69.0 ± 13.9
39	87.3 ± 1.6
40	58.9 ± 21.8
41	75.0 ± 2.9

Table 2.3 Results of library 1 screen against *Tb* PFK.[74]

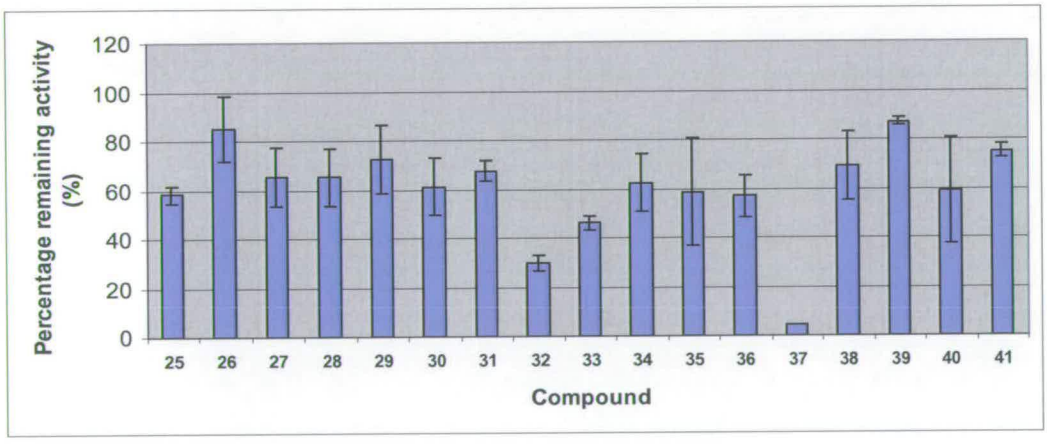

Figure 2.10 A graph showing the screening results of library 1 against *Tb* PFK.[74]

The results shown in Table 2.3 and Figure 2.10 show that all compounds tested in library 1 inhibit *Tb* PFK to some extent at 5 mM. However, it can be seen clearly from the chart in Figure 2.10 that inhibitor **37** (2,5-anhydro-1-deoxy-(3,4-

dichlorobenzylamino)-D-mannitol) has a much greater effect on the activity of PFK than any other compound, as the enzyme activity was reduced to 4.7 % of its original activity. The structure of **37** is shown in Figure 2.11 (along with the structure of the next best inhibitor in this screen, **32**, 2,5-anhydro-1-deoxy-1-(benzyhydrylamino)-D-mannitol).

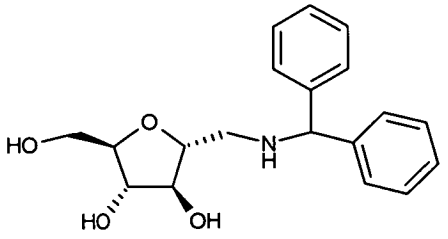

32

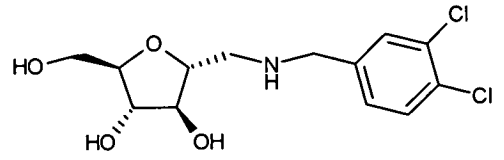

37

Figure 2.11 Structures of the best inhibitors from the library 1 screen, **32** and **37**.

Evidently, the screening results identified **37** as the best inhibitor of PFK from library 1 and hence, a potential new lead compound. Therefore, to follow on from these results, **37** was re-synthesised on a larger scale to provide a sufficient amount of the inhibitor for further testing.

Although the initial results above seem promising, they do not take into account the pKa of the secondary amine. Throughout the series of compounds, the substitution of the aromatic ring is likely to alter the aforementioned pKa value (pKa of benzylamine is 9.3. Hammet σ values for the various substiuents can give an indication of their effect on the pKa value.) The inhibitors were screened at pH 8 (7.2 for *Lm* PyK, see section 2.4.5) and deviations in pKa value from compound to compound may have an influence on the overall result as the relative amounts of

protonated inhibitor may vary in each assay, and the actual concentration of the inhibitors will also not be known accurately. It is possible to experimentally determine the pKa for each amine however, as the will become evident, trends in this library, and other libraries to follow, suggest that the pKa effect may be negligible.

2.4.3 Further compound testing and general trends.

An IC_{50} value was determined for **37** by measuring the activity of *Tb* PFK at increasing concentrations of **37** between 0.001 and 5 mM and plotting a dose-response curve.[74] These results can be seen in Figure 2.12 and Table 2.4.

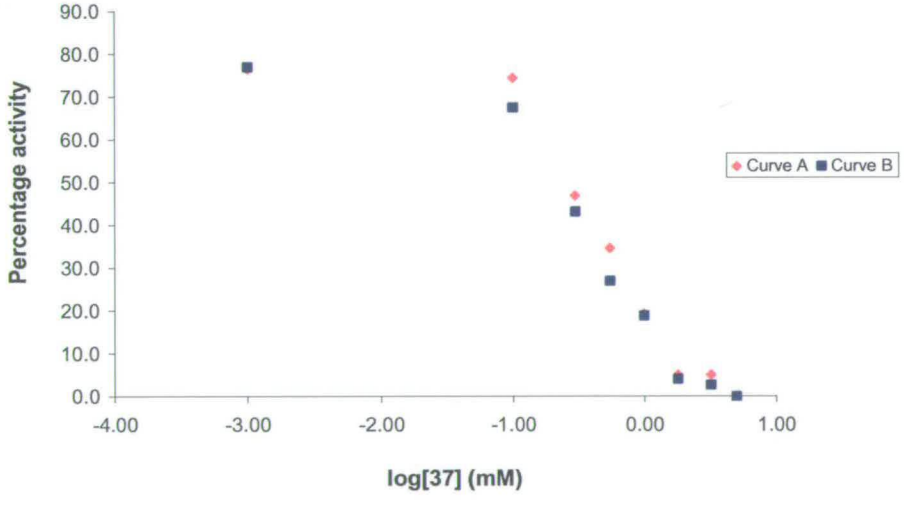

Figure 2.12 Dose-response curves for **37** against *Tb* PFK.[74]

	Curve A	Curve B	Average
IC_{50}	0.45 mM	0.37 mM	0.41 mM
R^2	0.9923	0.9951	(95 % confidence)

Table 2.4 IC_{50} values for the inhibition of *Tb* PFK by compound **37**, determined from Figure 2.12.[74]

It is now clear from Table 2.4 that the IC_{50} of **37** is 0.41 mM, making it a lead compound. This value is comparable to that of another lead compound, **21**,[62] (shown in Table 2.1) which had an IC_{50} value of 0.45 mM. It is worth noting that **21** is phosphorylated at the 6-position whereas **37** is not. The unphosphorylated derivative **17** (Table 2.1) has an IC_{50} value of 1.1 mM. As there is a twofold difference in IC_{50} values for **17** and **21**, phosphorylation of **37** may produce an inhibitor of PFK that has an even lower IC_{50} value. This, however, may only be true if **37** and the phosphorylated derivative of **37** bind in the same manner to PFK as **17** and **21** respectively. For example, inhibitor **17** has been shown to compete with ATP and shows a fully mixed-type inhibition with F6P,[62] hence will bind to both the ATP and F6P binding sites. However, inhibitor **21** has been shown only to compete with ATP,[62] hence will bind exclusively to the ATP binding site. If **37** is only competitive with either ATP or F6P – therefore already exclusively binding to one site – the effect of phosphorylation may not be as dramatic, if any improvement in inhibition is seen at all.

Fluorescence quenching of the wild type enzyme was the method used to determine the dissociation constants (K_ds) of the inhibitors, due to naturally occurring tryptophan residues in *Tb* PFK. Table 2.5 shows the K_ds of the two best inhibitors from library 1.[74] Table 2.5 also shows the K_d values for ATP and F6P, as determined by J. Martinez at the Edinburgh University, Institute of Cell and Molecular Biology.[74] It can be seen that there are slight differences between these values and those determined by S. Claustre (Table 2.2[62]) but they can be attributed to experimental differences, for example, differences in procedure, temperature and the equipment used for the experiments.

Inhibitor	K_d (μM) *Tb* PFK
ATP	16
F6P	29
32	58
37	61

Table 2.5 Dissociation constants (K_ds) of inhibitors tested against *Tb* PFK.[74]

Due to the fact that there are some discrepancies between the K_d values of ATP and F6P from both the Edinburgh and Toulouse laboratories, it is difficult to comment on the actual K_d values and draw any comparisons between the inhibitors in Table 2.5 and the original inhibitors shown in Table 2.1. However, it can be assumed that each set of results is consistent with itself, therefore allowing a comparison of the overall trend and hence, a comparison can be made between these inhibitors.

The non-phosphorylated inhibitors shown in Table 2.1 have K_d values that are similar to that of both ATP and F6P, with the exception of **11** (a twofold higher value) which has been shown not to bind at the F6P binding site.[62] The only K_d value available for the phosphorylated inhibitors is that of inhibitor **18**, which is about a twofold higher value than both those of the non-phosphorylated inhibitors, and of the natural substrates. Coupled with this apparent increase in K_d value, is a twofold reduction in the IC_{50} value. As mentioned previously, this relates to the fact that the phosphorylated inhibitors bind only at the ATP binding site exclusively, whereas the non-phosphorylated inhibitors show binding at both the ATP and F6P binding sites.[62] Relating this to **32** and **37**, they both have K_d values that are significantly higher in value than those of ATP and F6P. In the case of **37**, this also has a low IC_{50} value (comparable to that of the best phosphorylated compounds in Table 2.1). This trend in profile suggests that **32** and, in particular, **37**, resemble the profiles of the phosphorylated inhibitors. Therefore, it is conceivable that these compounds may already bind exclusively at the ATP or F6P binding sites and hence, phosphorylation of these compounds may not improve inhibition of or binding to PFK. However, there are insufficient results to be certain that this is the case; the trends only suggest that this is a possibility. Conclusive evidence would only be gained by competition experiments and crystal structures with the inhibitors bound.

Concurrent research by J. Martinez involved attempting to solve the crystal structure of *Tb* PFK. Figures 2.13 – 2.15 are of the solved structure of *Tb* PFK each figure with inhibitor **37** docked in the enzyme.[75,76] As mentioned previously, these type of compounds have the potential to bind at both the F6P and ATP binding sites.

However, for reasons discussed later in Chapter 5, **37** was docked only into the F6P binding site. The purpose here is to illustrate that it is feasible to postulate protein-ligand interactions by computational methods.

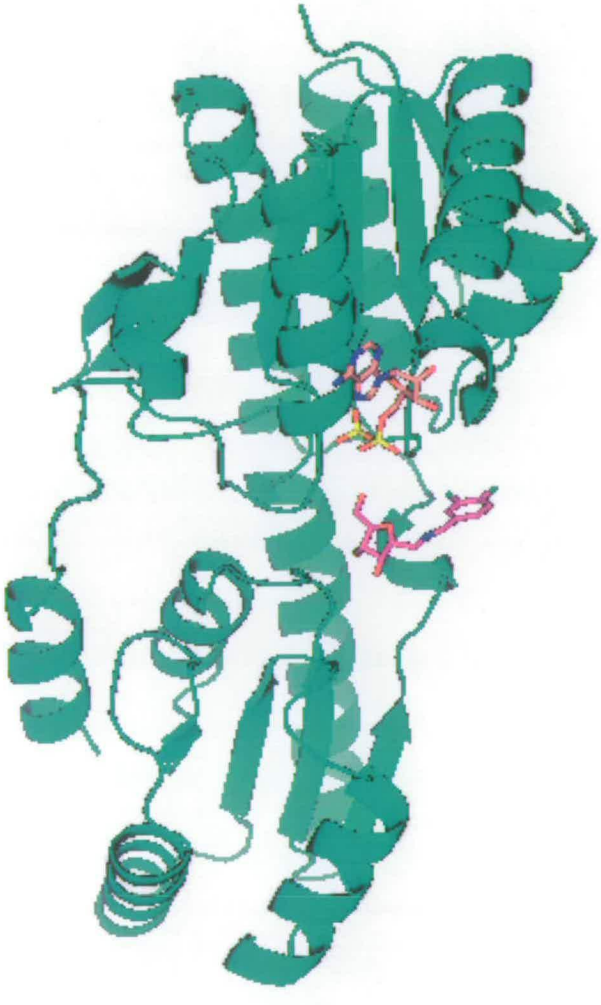

Figure 2.13 Crystal structure of *Tb* PFK with ADP (top compound) and **37** (lower compound) docked into their respective binding sites.[75,76]

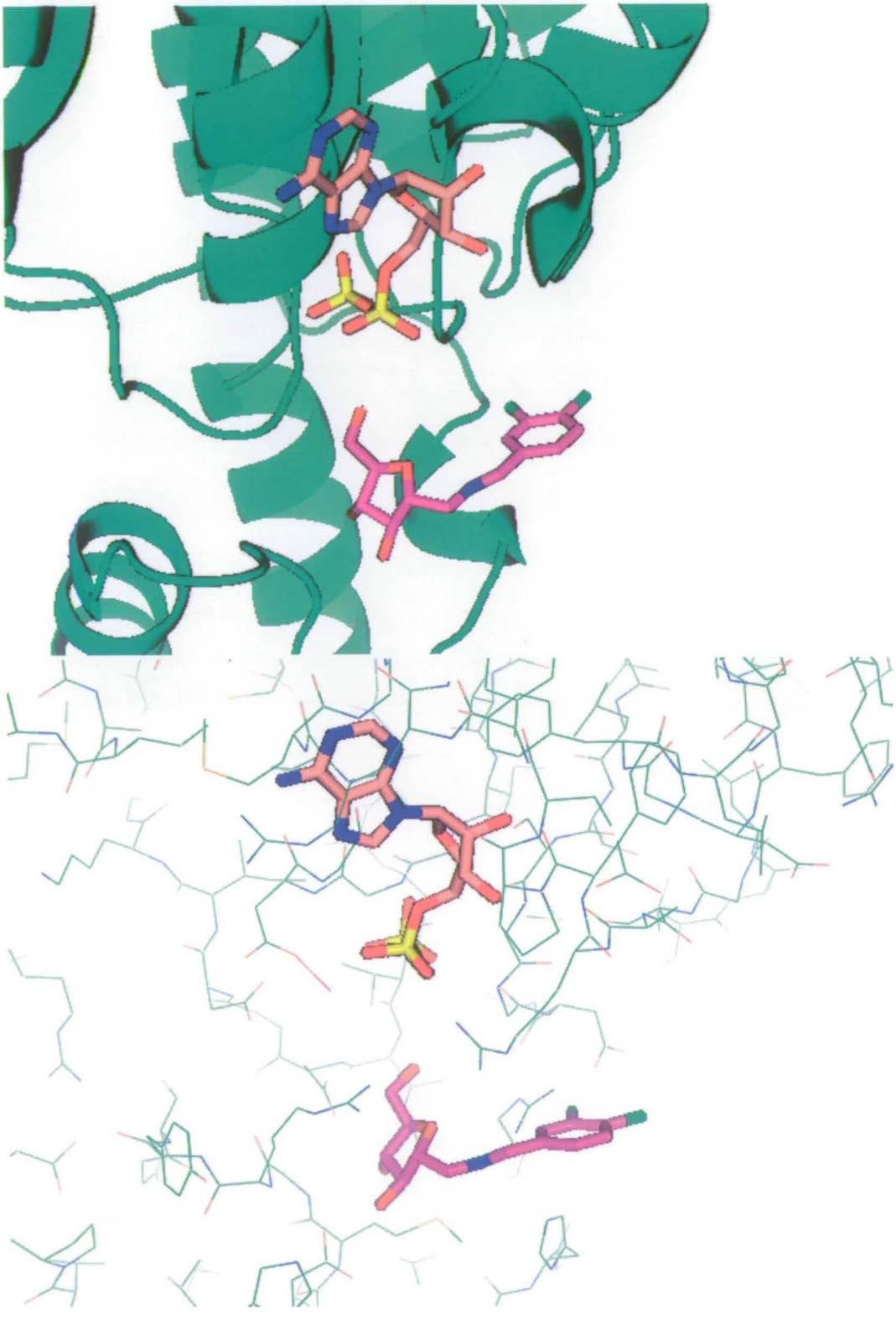

Figure 2.14 Close ups of Figure 2.13. Top diagram shows a ribbon representation. Bottom diagram shows a stick representation.[75,76]

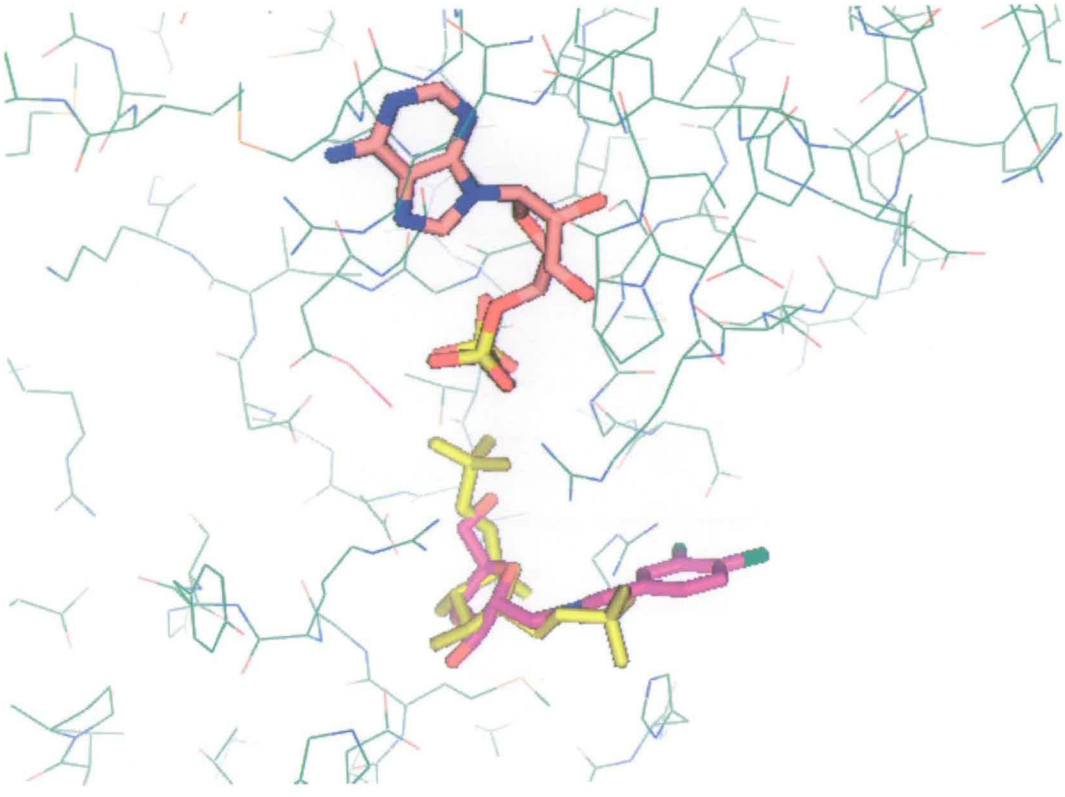

Figure 2.15 Crystal structure of *Tb* PFK showing **37** docked, overlaid with F2,6BP (yellow).[75,76]

These diagrams show the potential binding mode of compound **37** and its proximity to ADP. In particular, Figure 2.15 shows the relative positions of compound **37** and F6P. It is interesting to note that **37** has the potential to bind to *Tb* PFK in a similar manner to F6P, with the position of the furanose scaffold reasonably well conserved.

2.4.4 Inhibition trends from Library 1.

Although library 1 only consisted of 17 members, some structure-activity relationships (SARs) are evident. Firstly, there is the relationship between the various mono-substituted benzyl derivatives. Figure 2.16 displays this information, showing that, although there may only be a slight differences in value, there could be a

preference in inhibition of the order fluoro > chloro > methyl. However, this trend is probably negligible in comparison to the associated errors of the assay.

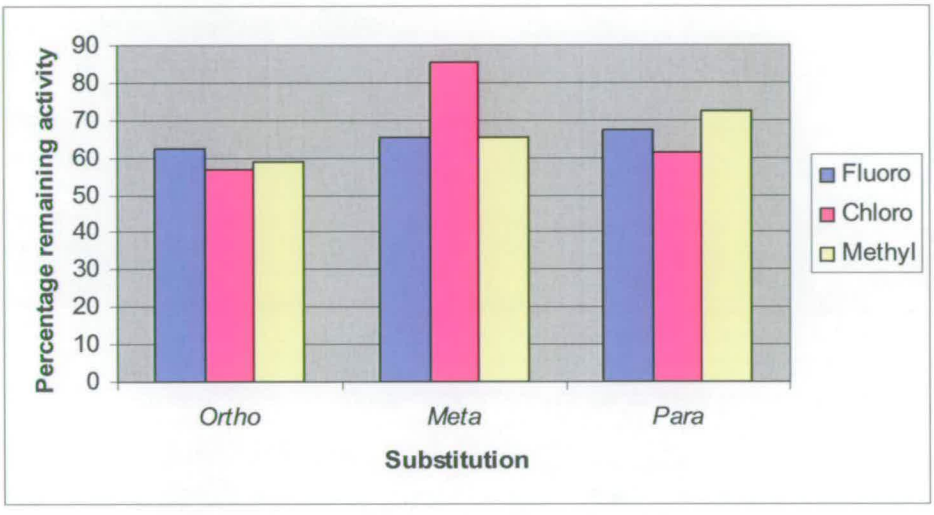

Figure 2.16 A graph showing the trends of inhibition of *Tb* PFK between mono-substituted benzyl derivatives in library 1.

More distinctive trends to result from the library 1 inhibitory screens occur with the di-substituted benzyl derivatives and are shown in Figure 2.17. This figure shows two possible SAR results. The first is that, in general, dichloro derivatives are more inhibitory than dimethyl derivatives. However, with only two results, this observation is speculative, and a further dichloro derivative would need to be tested to support this claim fully. (The *ortho – meta* dimethyl benzyl derivative did continue the general trend by only reducing the enzyme activity to 70 %).

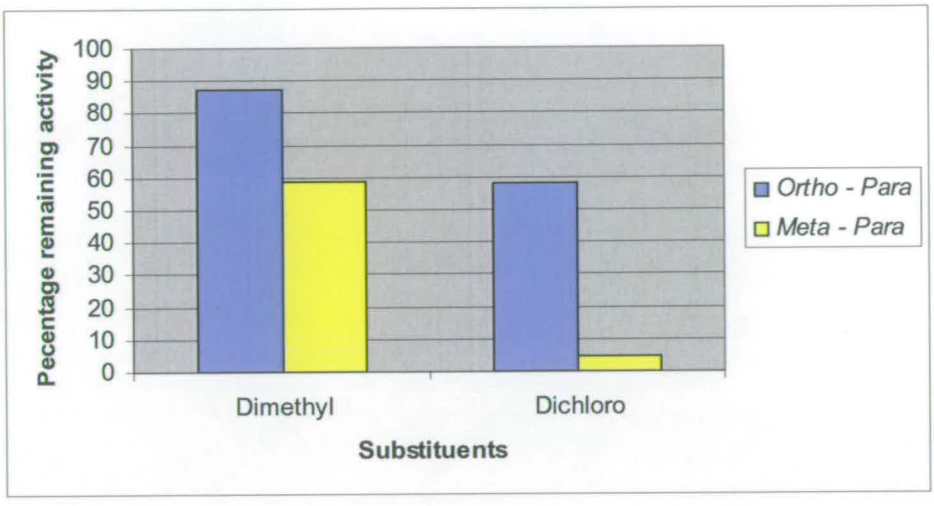

Figure 2.17 A graph showing the trends of inhibition of *Tb* PFK between di-substituted benzyl derivatives in library 1.

The second trend is that *meta – para* derivatives are more inhibitory than ortho – para derivatives. Again, this claim can only be substantiated by the results from the library 1 screen; for conclusive proof, further di-substituted derivatives would need to be synthesised and tested. However, all these trends do lead to the fact that **37** should be the best inhibitor, which is indeed the case. In the interests of improving inhibition, the only other compound that could be synthesised based on the results above would be 2,5-anhydro-1-deoxy-1-(3,4-difluorobenzylamino)-D-mannitol **42** (Figure 2.18). This compound was synthesised in a yield of 8 %, and its biological results, along with those of other non-library synthesised compounds, are discussed in Chapter 5.

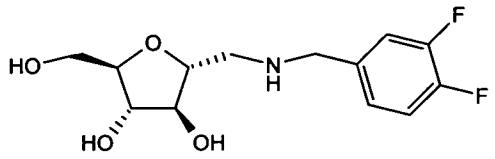

42

Figure 2.18 Structure of **42**.

Relating these trends to the structure of the ligand binding site of PFK confirmed the presence of a hydrophobic pocket. In general, hydrophobic pockets are desirable as parts of drug targets because hydrophobic groups need to be part of the potential drugs. These in turn are desirable as they improve the pharmacokinetics and the logP value of the drug, and hence allow the drug to obey one of the rules in the Lipinski Rule of 5.[19] It is also interesting to note that the compounds synthesised in library 1 fully obey the Lipinski Rule of 5 (logP results by modelling only) confirming these types of compounds as suitable leads for further drug development (see Appendix 1). The preference for *meta – para* derivatives suggest that this hydrophobic pocket may be extended slightly in this direction, in the orientation that the inhibitor is bound. It is difficult to comment further on this in the absence of a crystal structure with the inhibitor bound.

2.4.5 Initial screening method against *Lm* PyK.

A similar 5 mM screen method was adopted for initial screens against *Lm* PyK, as were done for PFK, detailed in section 2.4.1; the assay was carried out in 25 mM triethanolamine, pH 7.2 (0.4 μg/ml PyK, 3 mM $MgSO_4$, 3 mM KCl, 0.3 mM ADP, 0.42 mM NADH, 0.4 mM PEP, LDH 13.8 units). The enzyme couple used to monitor the activity of PyK is shown in Figure 2.19. Again, a decrease in absorbance

at 340 nm was measured to determine the rate of PyK and hence, the percentage remaining activity.

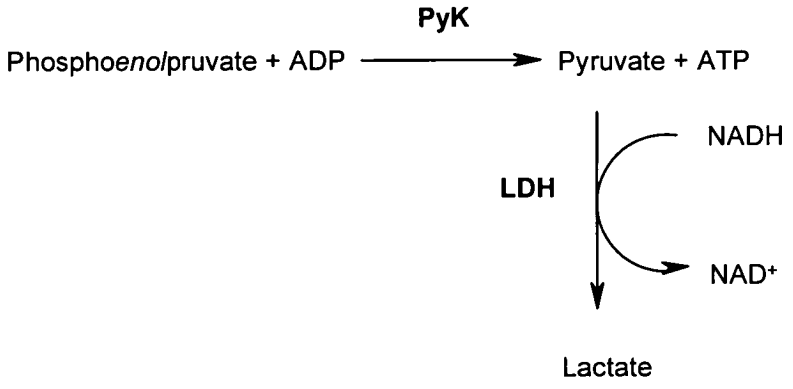

Figure 2.19 Enzyme couple used in 5 mM screen to measure the effect of compound libraries on *Lm* PyK. LDH = liver dehydrogenase.

2.4.6 Library 1 screening results against *Lm* PyK.

Results from the initial 5 mM screen against PyK are shown in Table 2.6 and graphically in Figure 2.20.[77]

Compound	Percentage (%) remaining activity
26	88
27	81
28	71
29	90
30	89
31	100
32	89

Compound	Percentage (%) remaining activity
33	105
34	42
35	107
36	100
37	43
39	103
40	85

Table 2.6 Results of library 1 screen against *Lm* PyK.[77]

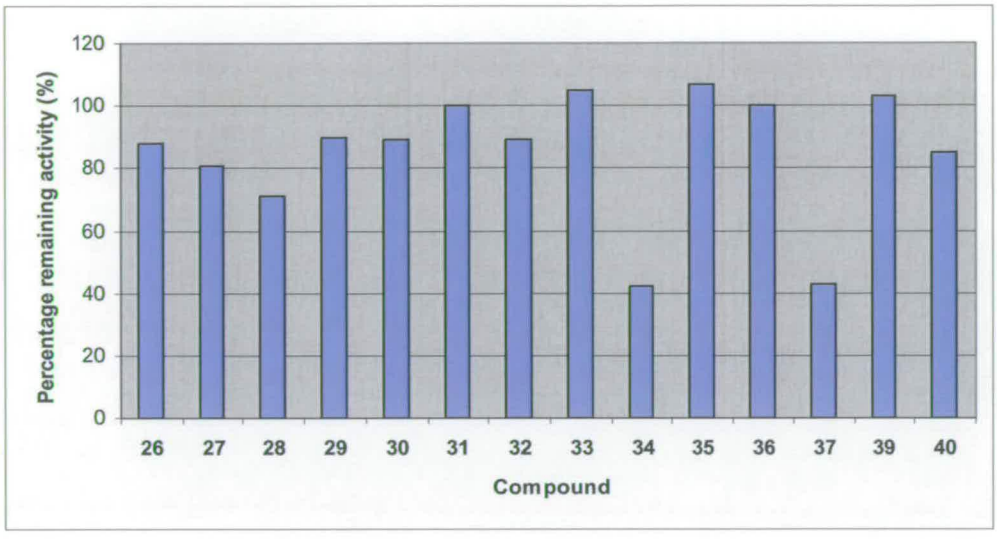

Figure 2.20 A graph showing the screening results of library 1 against *Lm* PyK.[77]

In general the results presented in Table 2.6 show that the compounds in library 1 partially inhibit or have no effect upon the activity of PyK. The two exceptions to this are **34** and **37**. These compounds inhibit PyK activity to 42 % and 43 % respectively. Although these results may seem slightly disappointing, the presence of inhibitors of PyK from library 1 show that the synthesis of further derivatives of 2,5-anhydro-1-deoxy-D-mannitol is worth pursuing. An IC_{50} value was determined for **34** by measuring the activity of *Lm* PyK at increasing concentrations of **34** between 0.001 and 5 mM (the dose-response curve for **34** can be found in the appendix). The IC_{50} value for **34** against *Lm* PyK was determined to be 1.6 mM.[78] Further library synthesis of these derivatives with a greater variation at the C-1 position was needed to help probe this enzyme further in order to find a more effective inhibitor.

2.5 Conclusion.

The library 1 screen against *Tb* PFK identified a new inhibitor and lead compound, 2,5-anhydro-1-deoxy-1-(3,4-dichlorobenzylamino)-D-mannitol **37** and its IC_{50} was determined to be 0.41 mM. Possible SAR trends show that the 3,4-dichlorobenzyl group appears to be the optimum group for greatest inhibition, and that ligand binding is likely to involve interaction with a hydrophobic pocket. However, SAR results also show that a 3,4-difluorobenzyl derivative could also prove to have significant inhibitory activity. The screening of this compound is discussed in Chapter 5.

Screens of library 1 against *Lm* PyK showed two compounds to have a moderate inhibitory effect, namely 2,5-anhydro-1-deoxy-1-(2-fluorobenzylamino)-D-mannitol **34** and 2,5-anhydro-1-deoxy-1-(3,4-dichlorobenzylamino)-D-mannitol **37**. These results show that this type of compound can inhibit PyK, but further library synthesis was needed in order to gain more effective inhibitors.

Chapter 3

Library 2: Design, Synthesis and Evaluation

3 Library 2: Design, Synthesis and Evaluation.

3.1 Library 2.

3.1.1 Library design.

Having already synthesised the first library, established a new lead compound for *Tb* PFK and shown that these compounds can also inhibit *Lm* PyK, the decision was made to synthesise a second, larger library with greater diversity. The library synthesis would use the chemistry and methods described in Chapter 2, but no restriction would be placed on the amine building blocks used. Figure 3.1 shows the 39 primary amines that were used in the synthesis of library 2. Chosen owing to their commercial availability and structural and chemical diversity, it was hoped that they would have a positive affect on inhibition. One or more of these features would hopefully gain attractive interactions with the target enzyme, resulting in inhibitors with a greater affinity for the enzyme than already existing inhibitors. These features include hydrophobic groups (linear chains, branched chains, rings), hydroxyl groups, ethereal groups, an introduction of stereocentres (to hopefully find a preference between *R* and *S* pendant side-chains), larger aromatic groups (in comparison to the benzyl derivatives in Chapter 2) and some compounds that combine two or more of these features.

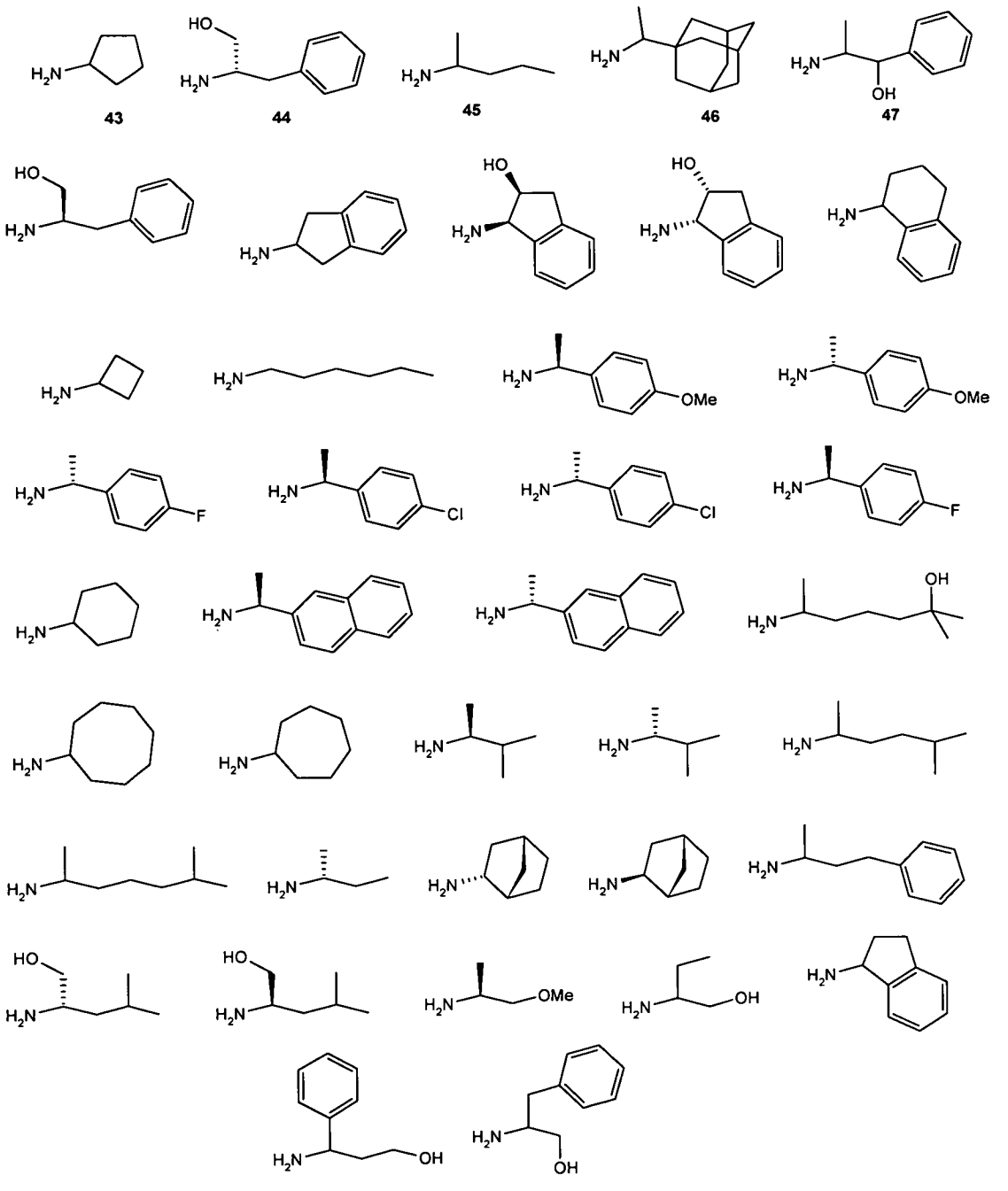

Figure 3.1 Amine building blocks used in the synthesis of library 2.

3.1.2 Test library synthesis.

In the synthesis of library 2, it was decided, as with library 1, to synthesise a small test library to ensure the chemistry and methods were still suitable now different and a wider range of amines were being used. It was decided to make a 5-membered test library using amines **43** to **47** shown in Figure 3.1; cyclopentylamine **43**, L-(-)-2-amino-3-phenyl-1-propanol **44**, 2-pentylamine **45**, 1-(1-adamantyl)-ethylamine **46** and (±)-phenylpropanolamine **47**. The structures and yields of the test library are shown in Figure 3.2. [Note: In Chapter 6, Experimental, the test library synthesis has been included in the synthesis for library 2, as the methods used were identical and the compounds synthesised would also be biologically tested using identical assays].

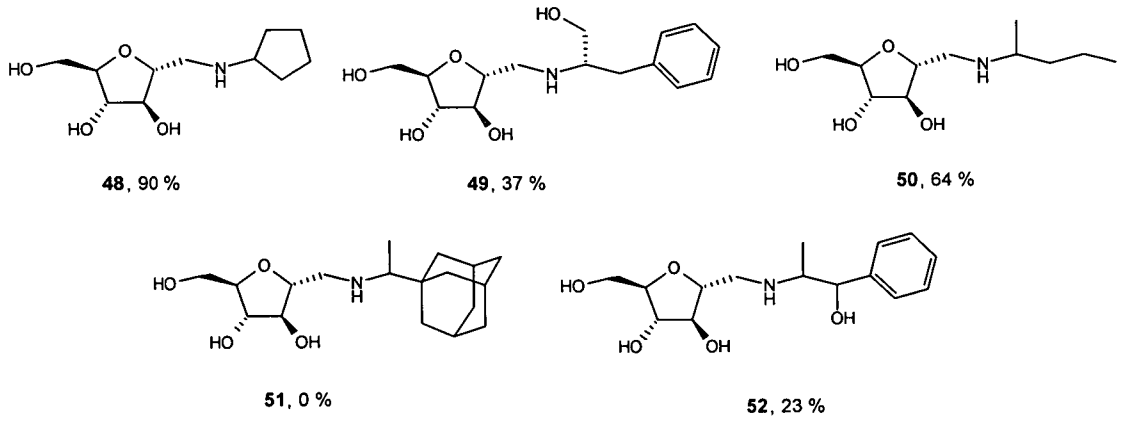

Figure 3.2 Structures and yields of test library (part of library 2).

With the exception of **51**, the test library proved successful with yields ranging from 23 % - 90 %. Although, no product was yielded for **51**, this was not a reason to alter or change the method for the synthesis of library 2 as this result could be attributed to the bulky and sterically hindered nature of the adamantyl group. The remaining compound yields were sufficient to enable characterisation and biological testing.

3.1.3 Library 2 synthesis.

Library 2 synthesis was successful, and in total 38 compounds from the 39-membered library, including the test library, were synthesised. The structures of these compounds can be seen in Figures 3.2, 3.3 and 3.4.

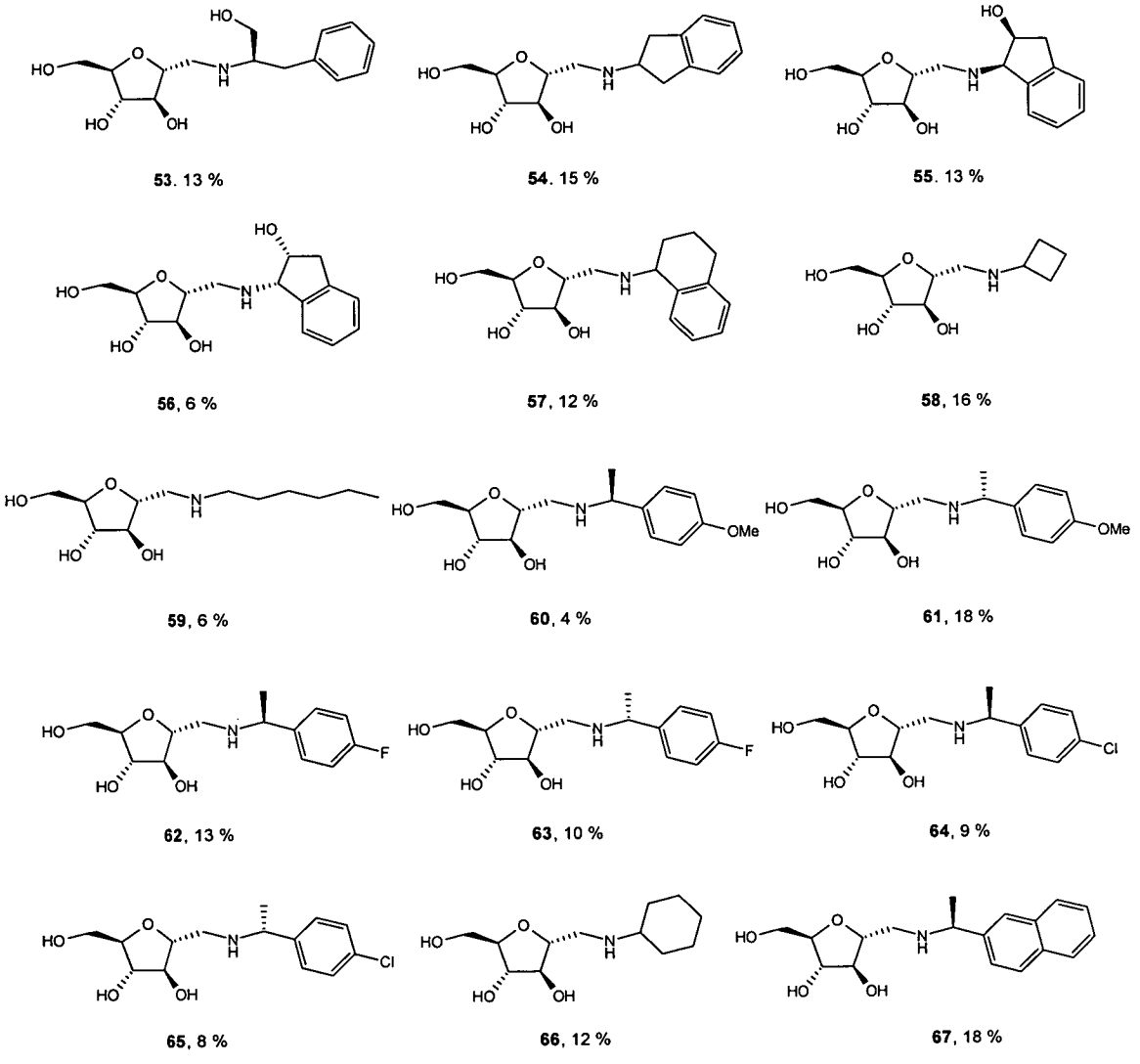

Figure 3.3 Structures and yields of 15 compounds in library 2.

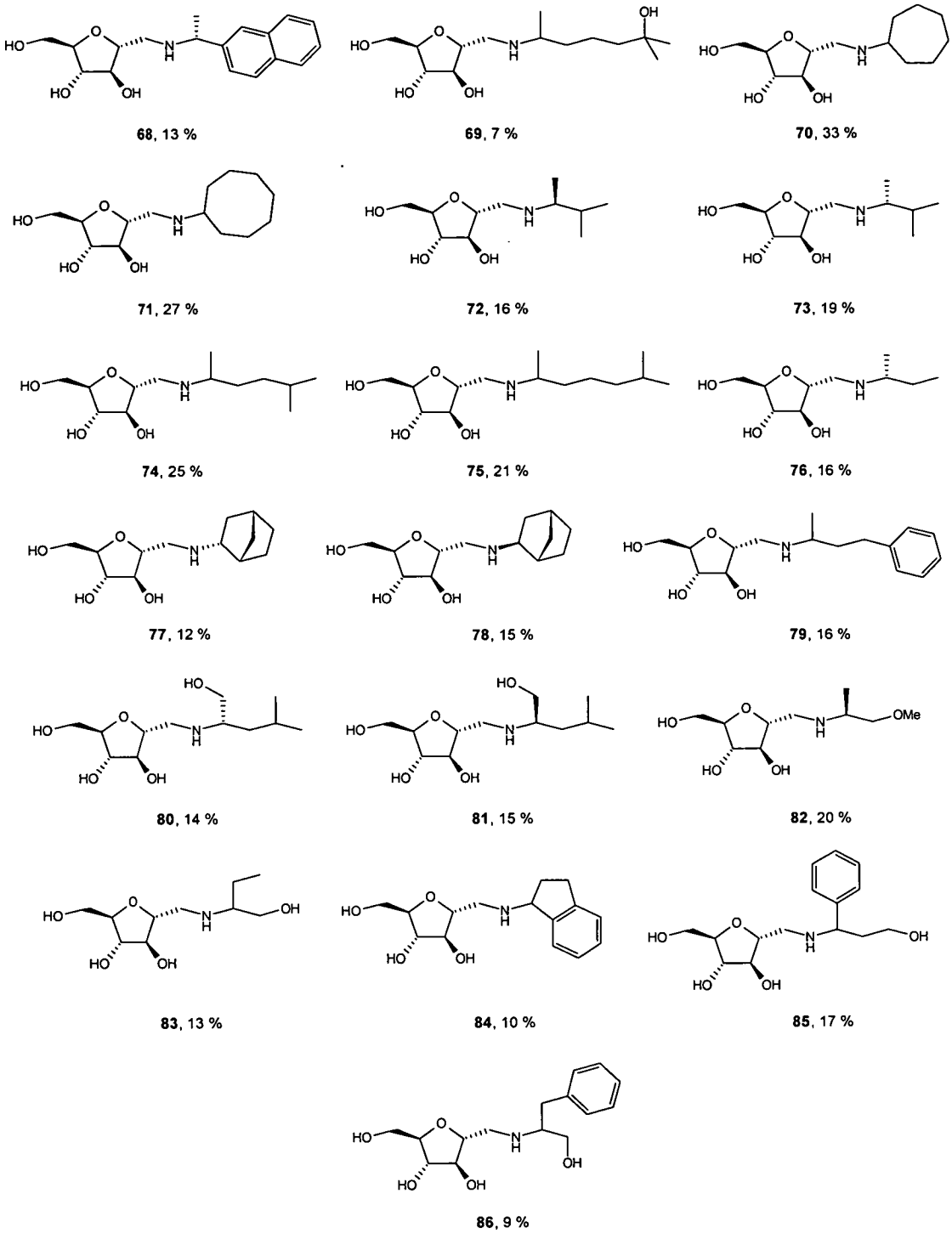

Figure 3.4 Structures and yields of the final 19 compounds in library 2.

Yields for library 2 ranged between 4 and 90 %, showing a similar spread to the yields from library 1. However, enough of each compound was synthesised to allow for characterisation and biological testing. The wide ranging yields can again be explained by the fact that a general method was employed for all reactions. Reaction monitoring did not occur, so some reactions may not have gone to completion. Once again, however, an alternative reason could be due to the mass directed purification equipment (Waters ZMD). The reasons for this will be discussed in more detail in Chapter 4. Although some of the yields may have been low, only one reaction failed; the synthesis of 2,5-anhydro-1-deoxy-1-(1-(1-adamantyl)-ethylamino)-D-mannitol **51**, as previously mentioned in section 3.1.2. Again, as for library 1, the structure for these compounds was determined by comparison of ^{1}H and ^{13}C (where available) NMR spectra with those of previousy reported compounds.[61,63]

3.2 Biological screening and evaluation.

3.2.1 Screening objectives.

Following the results from library 1, the primary objective for library 2 was hopefully to identify more potent inhibitors of *Lm* PyK. Indeed, the library was designed with this reason in mind, so screening these compounds against PyK was the main priority. However, because of the similarity between library 1 and library 2 (due to the same 2,5-anhydro-D-mannitol scaffold) the decision was made also to test these compounds against PFK, providing sufficient material was available to permit this.

3.2.2 Library 2 screening results against *Lm* PyK.

The initial screen for library 2 was the 5 mM screen using the same method as set out in section 2.4.5, and the same enzyme couple as shown in Figure 2.18 (the same procedure as for library 1). Results from this screen against a tryptophan mutant *Lm* PyK (E451W) are shown in Table 3.1, and graphically in Figure 3.5[78]. The compounds were also tested against wild type *Lm* PyK and these results are shown in Table 3.2 and graphically in Figure 3.6.[78]

Compound	Percentage (%) remaining activity	Compound	Percentage (%) remaining activity
48	52.0 ± 6.7	**68**	34.0
49	72.0 ± 10.6	**69**	125.1
50	26.3 2.1	**70**	18.6 ± 0.7
52	79.7 ±3.8	**71**	57.4 ± 4.3
53	96.7 ± 0.7	**72**	26.4 ± 4.2
54	49.3 ±10.1	**73**	85.9 ± 4.3
55	59.7 ± 0.2	**74**	114.9 ± 0.0
56	103.1 ± 11.0	**75**	80.0 ± 2.2
57	35.5 ± 1.6	**76**	28.0
58	42.6 ± 1.6	**77**	46.7 ± 0.8
59	40.1	**78**	18.7 ± 1.2
60	21.5	**79**	95.2
61	24.5	**80**	72.8 ± 6.3
62	36.0	**81**	85.8 ± 2.0
63	52.8	**82**	82.0 ± 5.6
64	58.0	**83**	89.9
65	84.2	**84**	85.8
66	83.2 ± 7.2	**85**	85.1
67	30.0	**86**	59.3

Table 3.1 Results of library 2 Screen against E451W *Lm* PyK. (Errors are shown for duplicate or triplicate assays).[78]

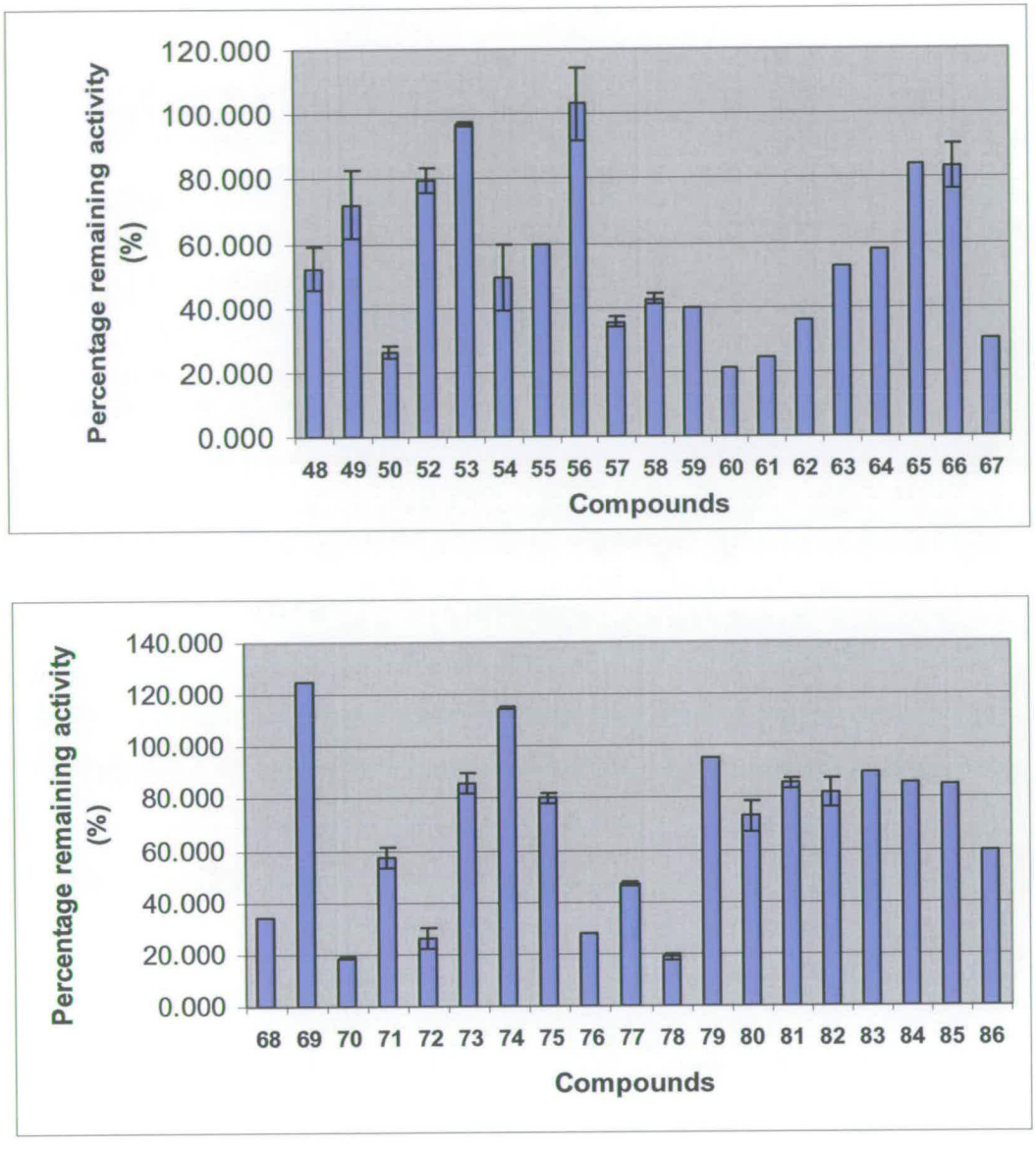

Figure 3.5 Graphs showing the results of library 2 Screen against E451W *Lm* PyK. Those results without error bars indicate a single assay result.[78]

Compound	Percentage (%) remaining activity
48	60.8
49	86.9
50	31.3
52	67.5
53	79.0
54	57.9
55	56.6
56	75.7
57	11.2
58	61.0
59	25.6
61	23.2
62	107.6
63	43.1
64	26.9
65	90.8
66	46.9
67	10.9
68	28.9

Compound	Percentage (%) remaining activity
69	101.0
70	8.0
71	28.2
72	19.2
73	90.1
74	49.7
75	48.1
76	14.1
77	45.3
78	12.9
79	90.8
80	76.6
81	101.3
82	99.2
83	96.8
84	62.6
85	89.1
86	42.9

Table 3.2 Results of library 2 screen against wild type *Lm* PyK.[78]

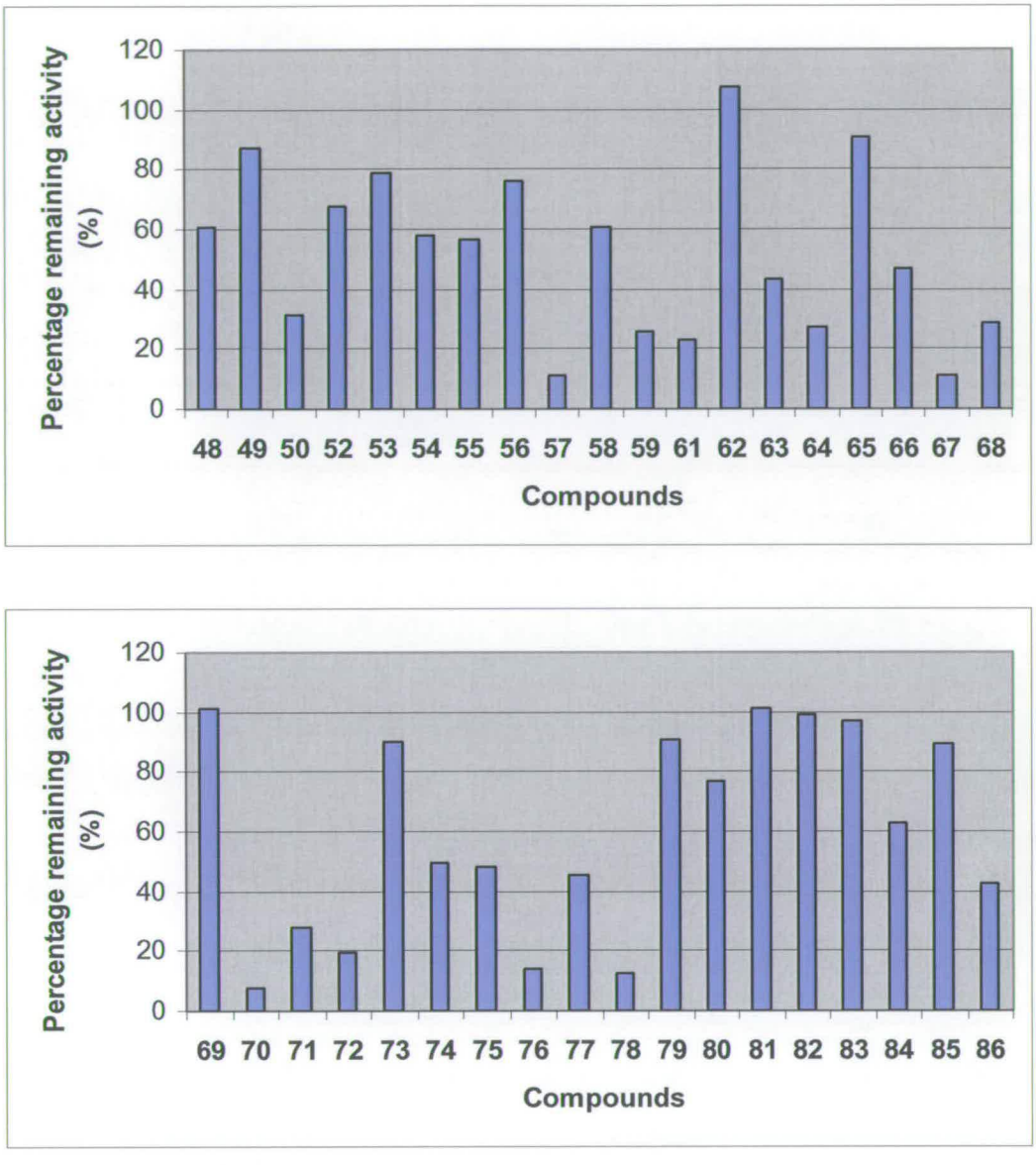

Figure 3.6 Graphs showing the results of library 2 Screen against wild type *Lm* PyK.[78]

[Note: The results against both the mutant and the wild type enzymes are shown because the screen was initially performed on the mutant. This was then repeated for the wild type enzyme; however inhibitor **60** had been consumed in the first set of assays, therefore has been omitted in Table 3.2 and Figure 3.6. A comparison between the results of the mutant and the wild type enzyme assays, however, shows a good correlation. The majority of the results are of a similar value, and all trends (discussed later) are true for both enzyme forms. All those compounds that have been identified as hits (under 36 % remaining activity) with the mutant enzyme, were also identified as hits with the wild type enzyme. However, the wild type enzyme identified two more compounds as potential hits; **61** and **71**. These did show inhibitory activity against the mutant, but insufficient to be considered a hit. It can therefore be assumed that **60** could also be considered a hit. All discussion that follows will refer to the results against wild type *Lm* PyK unless explicitly stated.]

The results presented in Table 3.2 and Figure 3.6 (combined with the results from Table 3.1) show a wide range of inhibition. Thirteen compounds (highlighted) can be identified as potential leads, with the remaining enzyme activity being under 36 %. This shows a vast improvement on library 1, the best result being that of **34** which gave remaining enzyme activity as 42 %. Indeed, the best result from library 2 was obtained by inhibitor **70** (2,5-anhydro-1-deoxy-(cycloheptylamino)-D-mannitol), which inhibited *Lm* PyK to 8.0 % of it's original activity. All thirteen compounds are shown in Figure 3.7.

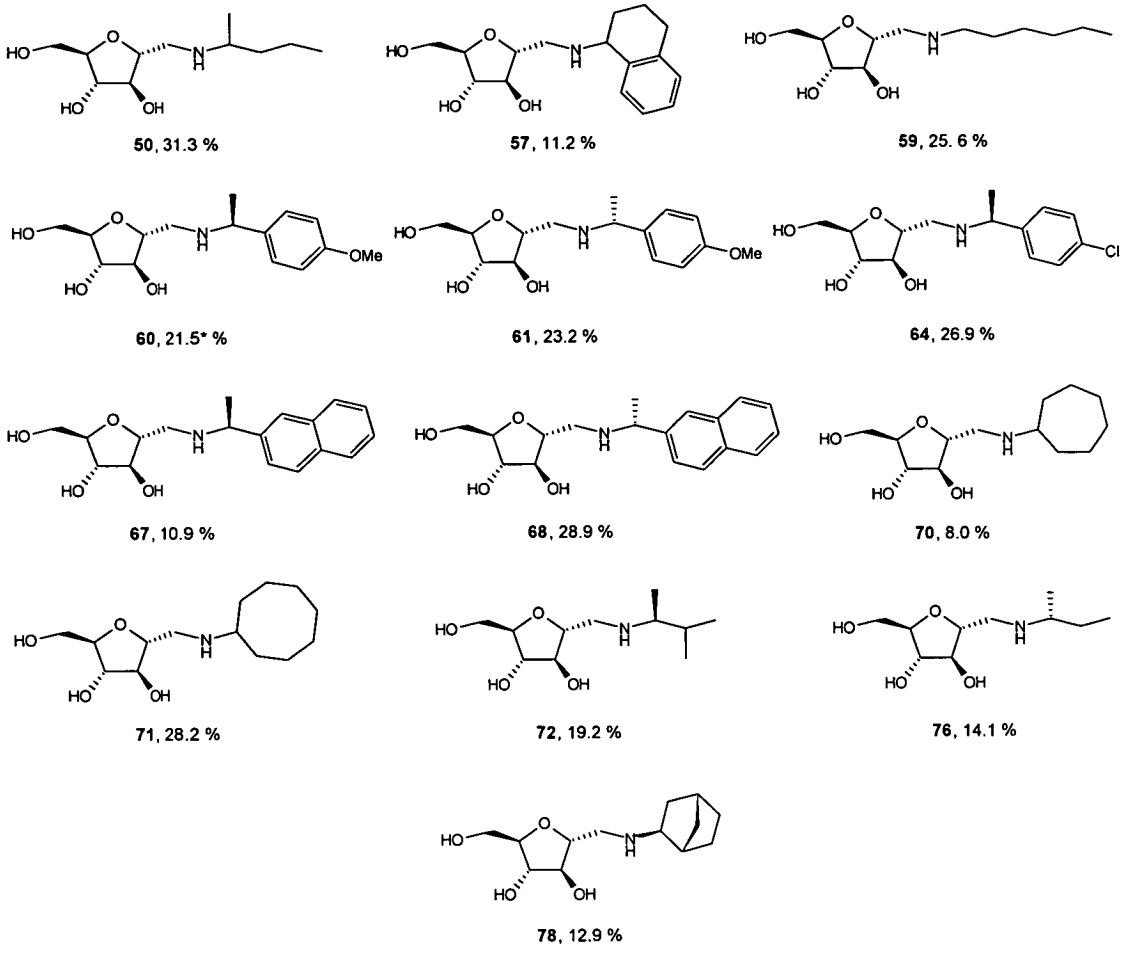

Figure 3.7 Structures of hits from the library 2 screen against *Lm* PyK, also showing percentage remaining activity from the assays. (*Result from assay against E451W *Lm* PyK).

In Figure 3.7, it becomes apparent that the majority of these inhibitors have a bulky hydrophobic group, indicating interaction with a hydrophobic pocket on PyK. It is, therefore, very likely that all these compounds will be exhibiting their inhibitory effect by binding in the same place on the enzyme. Further trends and SARs will be discussed in more detail in sections 3.2.3 and 3.2.4.

3.2.3 Further compound testing and general trends.

IC_{50} values were determined for 9 of the 13 inhibitors shown in Figure 3.7, using the same method as discussed in section 2.4.7. Table 3.3 shows the results, including IC_{50} values for both **48** and **58** as these compounds showed slight inhibitory activity (more so against the E451W mutant than the wild type enzyme). This would also act as a check to ensure there is a correlation between the initial screen and the IC_{50} values. (Dose-response curves for each compound can be found in the appendix).

Compound	IC_{50} (mM)	R^2
48	4.1	98.3
50	2.5	96.8
57	1.2	99.8
58	4.3	97.0
60	3.5	97.5
61	0.9	98.0
67	1.5	98.3
68	1.5	99.0
70	0.058	99.3
72	2.3	98.3
78	1.5	96.5

Table 3.3 IC_{50} values of hit compounds from library 2. The R^2 value gives an indication of the reliability of the IC_{50} values. This is determined from the curve of the dose-response graphs which can be found in the appendix.[78]

These results indeed do show a correlation with the initial 5 mM screen, indicating that this primary screen is a suitable method for identifying possible inhibitors and potential lead compounds. The second point to note is that there are 6 compounds

with an IC_{50} less than 1.6 mM, which is the value determined for inhibitor **34**, as discussed in Chapter 2. The most potent of these are inhibitors **61** (2,5-anhydro-1-deoxy-1-(*R*-1-(4-methoxyphenyl)ethylamino)-D-mannitol) with an IC_{50} of 0.9 mM, and **70** (2,5-anhydro-1-deoxy-1-(cycloheptylamino)-D-mannitol) with an IC_{50} of 58 μM, making the latter the new lead compound against *Lm* PyK.

The rationale for using 2,5-anhydro-1-deoxy-D-mannitol derivatives as the basis for potential inhibitor libraries was due to their structural similarity to F2,6BP, the effector for trypanosomal PyK. However, these derivatives are also structurally similar to ADP, a natural substrate for PyK. It is due to this that the inhibitors synthesised so far could well bind at either the ADP or F6P binding sites. For reasons of specificity, it is desirable to have inhibitors that bind to the F6P binding site. It was therefore necessary to try to determine where these inhibitors bound. This was done by means of competition experiments.[79] The results from these titrations show that none of the compounds significantly altered the K_M of ADP, but did reduce the V_{max} – inhibitor **70** to 15.1 % of the uninhibited maximum velocity and inhibitor **78** to 58.0 %. These results are consistent with inhibition that is non-competitive with ADP. Although the results as such cannot conclusively prove that these inhibitors bind to the effector site, they do show, however, that as the inhibitors are non-competitive with ADP, they do not exert their inhibitory effect by binding to the ADP site. Therefore they must bind elsewhere on the enzyme, and it is likely that they bind to the effector site (are competitive with F6P).

3.2.4 Inhibition trends from library 2.

Using the results obtained from the initial 5 mM screen against *Lm* PyK (both wild type and E451W mutant) it is clear that some SAR data can be obtained. The general observation that the more effective inhibitors possess a hydrophobic group has already been mentioned in section 3.2.2. The following is a more detailed look at the results of the screen and how they relate to the structure of the inhibitor and hence, the structure of the binding site.

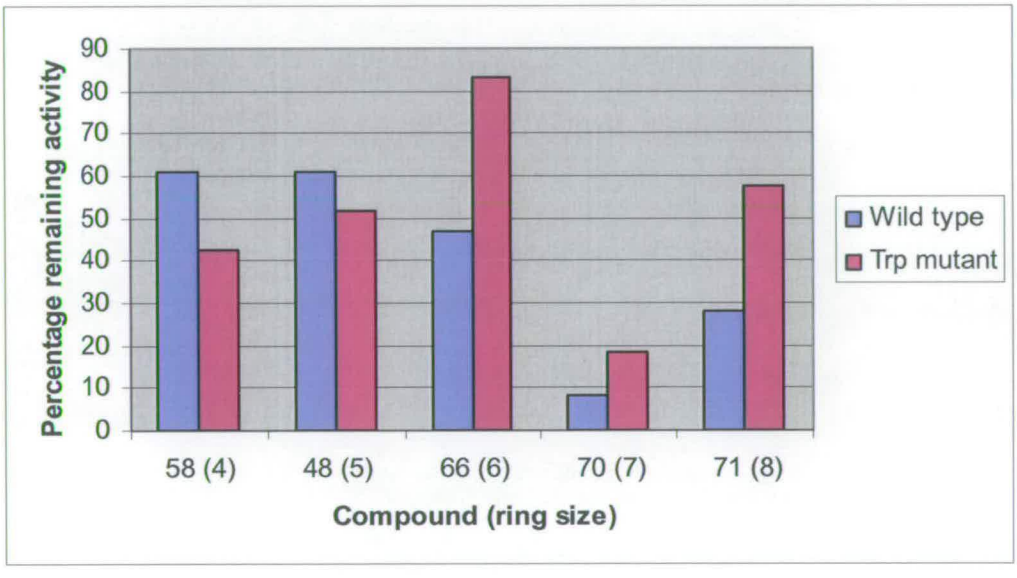

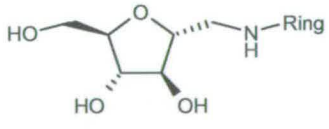

Figure 3.8 A Graph showing the effect of ring size at the 1-position upon inhibitory activity against *Lm* PyK.

Figure 3.8 shows how the ring size affects the inhibitory activity of the inhibitor. Looking at the results for the wild type enzyme, there is a clear pattern between ring size and inhibitory activity. As the ring size increases, the percentage remaining activity of the enzyme decreases, hence there is an increase in the inhibitory activity of the compound. This is true up to the point where ring size is equal to 7 (cycloheptyl). Here, the optimum ring size has been reached and hence, the cycloheptyl derivative is the most effective inhibitor for this group of compounds. As the ring size increases again, so does the percentage remaining activity of the enzyme thus the inhibitory activity of the compound decreases. This result is what would be expected of a hydrophobic cavity of a protein that was able to accommodate alkyl rings. As the ring size increases, the greater the interaction it would have with the cavity, hence greater inhibition would be observed. At a certain point (in this case at the cycloheptyl stage), the ring size would be optimum for the size of the cavity and the interactions between the two would be at the greatest (maximum inhibition). As soon as the ring size increases again, it becomes too large for the cavity and hydrophobic interactions would decrease, resulting in a fall in the level of inhibition.

The results obtained from the E451W mutant are less clear than the wild type enzyme. Overlaying the two sets of results (as seen in Figure 3.8) suggests that the overall trend may still be evident and that the result of the screen with compound **66** could be anomalous. However, it could also point to the possibility of the mutated residue having an affect on the binding of inhibitors.

Concurrent research by L. B. Tulloch at the Institute of Cell and Molecular Biology, University of Edinburgh,[80] involved using crystallographic methods in order to solve the R-state (active state) structure of *Lm* PyK. Molecular docking was carried out in

order to model inhibitor **70** in the effector site of *Lm* PyK. Initially this was carried out on the T-state structure, but this resulted in the cycloheptyl ring pointing away from the enzyme and into solvent space.[80] This result seemed highly unlikely, so the T-state structure used was unsuitable for molecular docking. However, the procedure was repeated on a modified T-state structure, where residue R404 near the effector site had been rotated to a position more commonly associated with R-state structures.[81] The result from this can be seen in Figure 3.9 (further structures can found in section 3.2.5).

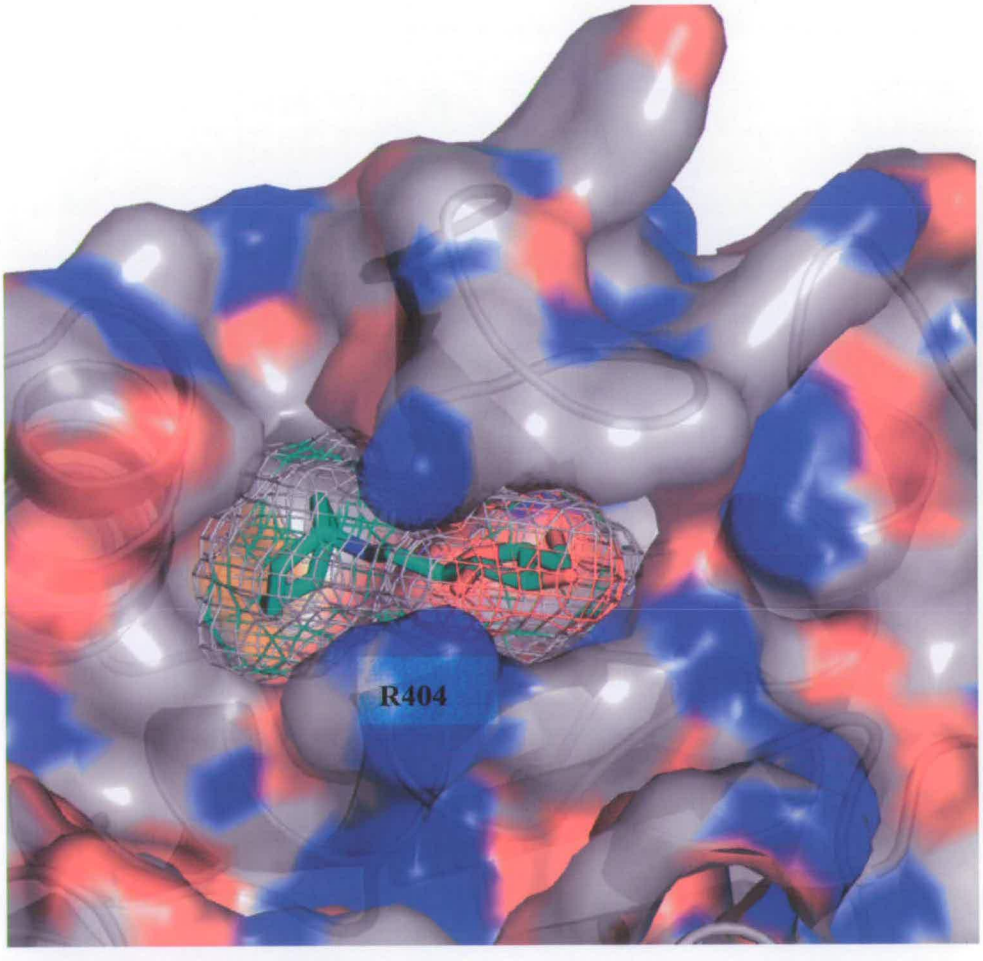

Figure 3.9 Model of **70** docked in *Lm* PyK effector site.[80] Red indicates a negative surface, blue a positive surface, and grey a hydrophobic surface.

It is evident from Figure 3.9 that this new model of the effector site for *Lm* PyK provides a more realistic result. The rotation of residue R404 has, in effect, exposed a hydrophobic pocket just next to the effector site in which the cycloheptyl group interacts; the furanose sugar scaffold binds in the effector site. A closer inspection of Figure 3.9 reveals why the 7-membered ring is optimum for binding, and hence for inhibitory activity. As already mentioned, a smaller ring size would mean fewer hydrophobic interactions with the pocket, but a larger ring size would start to make repelling interactions with the hydrophilic residues surrounding the hydrophobic pocket. This explains the result shown in Figure 3.8 where some inhibitory activity still remains when the ring size is increased to 8 (cyclooctyl). If this SAR was brought about exclusively by the size of the hydrophobic pocket, it might be expected that most or all inhibitory activity would be lost when the ring size just exceeds the optimum (8-membered as opposed to 7-membered).

The next SAR involves inhibitors that possess a chiral centre in an alpha position to the nitrogen (α-chiral). To compare these trends, compounds have been paired so that each pairing has two compounds which are diastereomers of each other, with opposite configuration at the α-chiral centre. The trends for both the wild type and mutant enzymes can be seen in Figure 3.10. Looking primarily at the results for the mutant enzyme, it is clear that there is a preference for inhibitors to possess an α-chiral centre of *S*-configuration as opposed to *R*, if an α-chiral centre is present. Although in some cases the difference in remaining enzyme activity may only be small and therefore within the error of the assays, without exception, the α-*S*-isomer of a compound pairing has the greater inhibitory activity against *Lm* PyK. It therefore

follows that the α-*S* isomer has a stronger and more favourable interaction with the effector site of *Lm* PyK. The biggest difference in inhibitory activity of a compound pair is seen with inhibitors **72** and **73**.

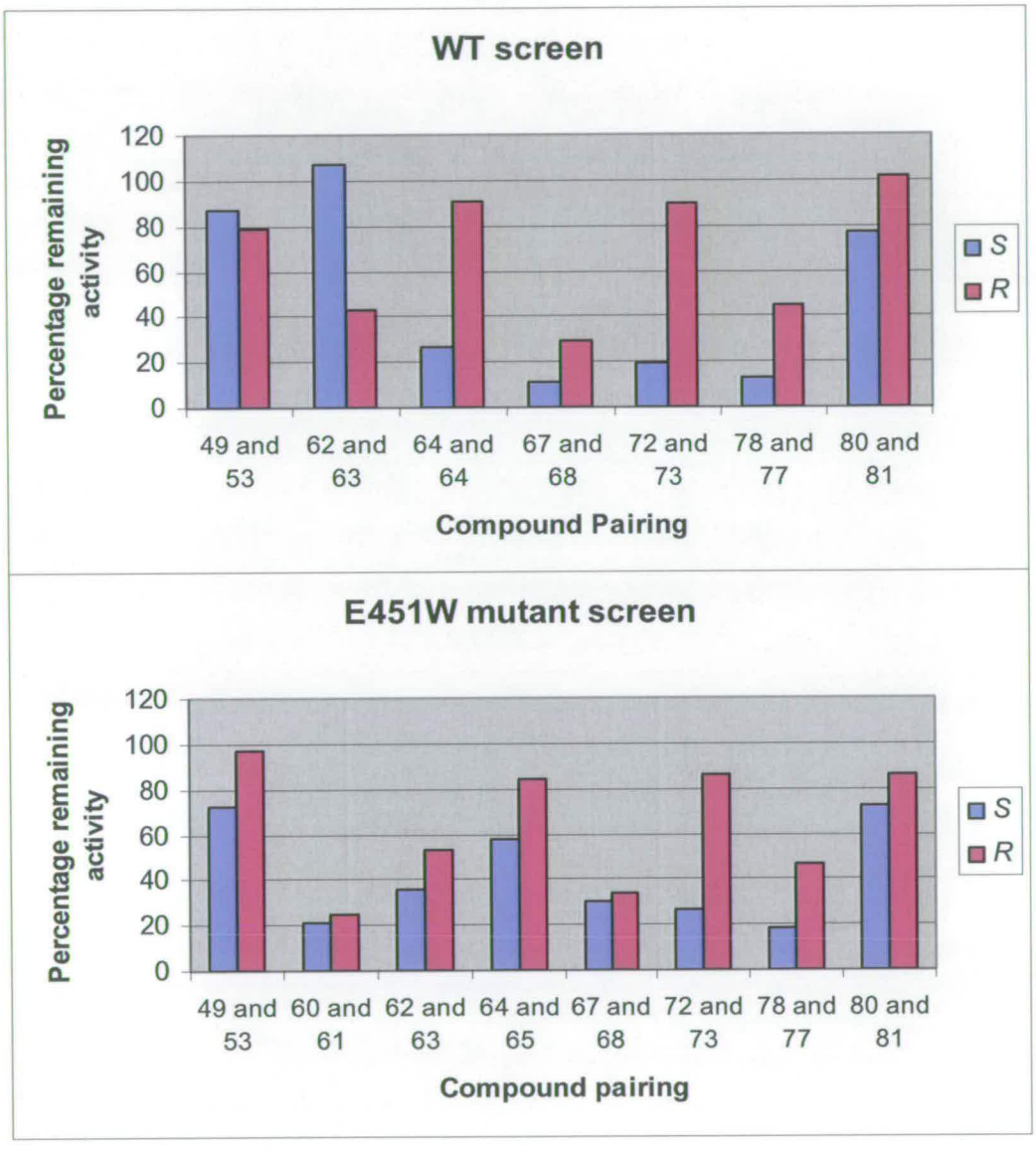

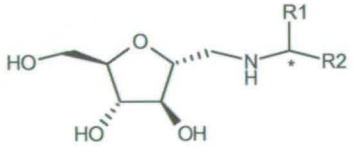

Figure 3.10 Graphs to show the influence of an α-chiral centre upon inhibitory activity against *Lm* PyK wild type (top graph) and E451W mutant (lower graph).

With regard to the results from the wild type enzyme, these again show the general trend that in a compound pairing, the α-*S*-isomer is a better inhibitor than the α-*R* isomer. However, two of the results are reversed – compound parings **49** and **53**, and **62** and **63**. It is unsure why the results from these inhibitors with the wild type enzyme differ from the results with the E451W mutant enzyme, although the difference in percentage remaining activity of the wild type enzyme when screened with both between **49** and **53** is so small that it could be due to experimental error. It is interesting to note that the biggest difference in inhibitory activity of a compound pair is again seen with **72** and **73**. These inhibitors (α-*S*- and α-*R*-2,5-anhydro-1-deoxy-1-(3-methyl-2-butylamino)-D-mannitol respectively) differ from all the other compound pairs as they possess a small, branched hydrophobic chain with no rings (aromatic or alkyl) or heteroatoms. The reason for this preference will be discussed further in section 3.2.5.

The final trend involves inhibitors that possess an alkyl chain, whether it is linear or branched. The results of this trend are shown in Figure 3.11.

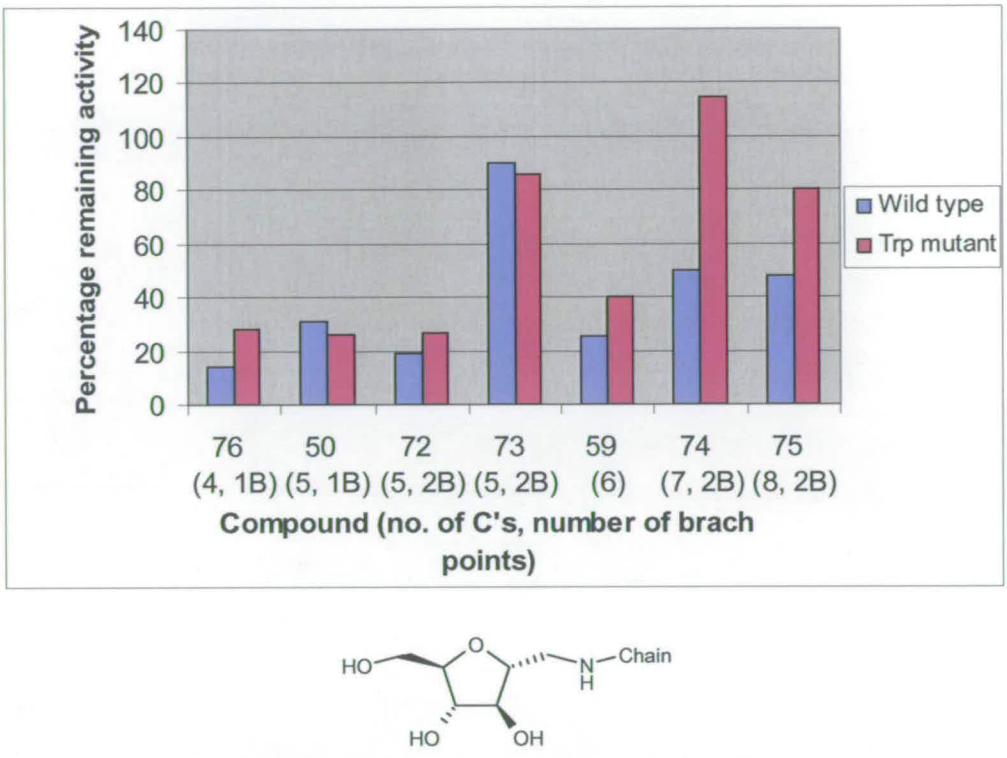

Figure 3.11 Graph to show the effect of an alkyl chain (branched or linear) at the 1-position upon inhibitory activity against *Lm* PyK.

This trend, again, generally follows what would be expected for alkyl chains interacting with a well defined hydrophobic part of the target enzyme (bearing in mind that the result for **73** is largely due to the α-chiral centre as discussed earlier). The smaller and more highly branched the chain, the stronger the interaction with the hydrophobic cavity and the more potent the inhibitor. As the chain length becomes longer, more disorder is introduced and, therefore, interactions with the hydrophobic cavity will become weaker, leading to a decrease in inhibitor potency. The same trends are seen for both the wild type and E451W mutant enzymes.

3.2.5 Molecular docking models.

It has already been seen in section 3.2.4 that molecular docking was successfully carried out on a modified T-state *Lm* PyK structure with inhibitor **70** in order to gain insight into how the lead compound interacts with the effector sight of the enzyme.[80] Further molecular docking experiments were carried out[80] on other inhibitors. The results can be seen in Figures 3.12 to 3.16.

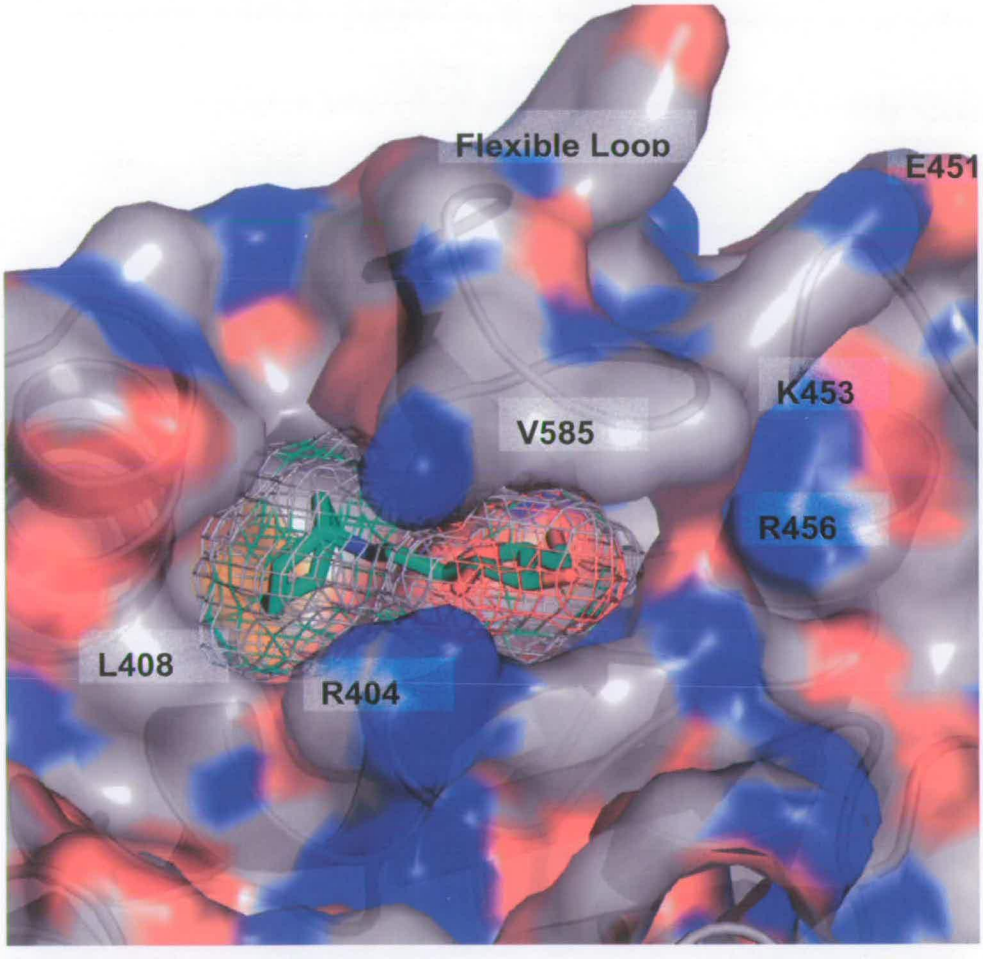

Figure 3.12 Model of **70** docked in *Lm* PyK effector site showing some surrounding residues.[80]

Returning again to the docking of **70** in the effector site of *Lm* PyK, Figure 3.12 shows this complex with some enzyme residues labelled that could make possible interactions with the inhibitor, as well as other surrounding residues. It is important to stress that this is only a model and not a crystal structure, therefore, all interactions that are mentioned are only possibilities that arise from molecular modelling. The hydrophobic cavity on the left hand side of the picture is created by a deep leucine side chain (L408). This is where the cycloheptyl group interacts. The secondary hydroxyl on C4 of the inhibitor appears to hydrogen bond to the backbone of the enzyme (at the valine residue, V585). The other secondary hydroxyl (on C3 of the inhibitor) could potentially interact with the flexible arginine residue (R404). Other potential interactions are not easily visible on this structure, but are shown on a schematic diagram in Figure 3.13. This structure also alludes to the development of these compounds at the 6-hydroxy position in order to extend the inhibitor further into the binding site.

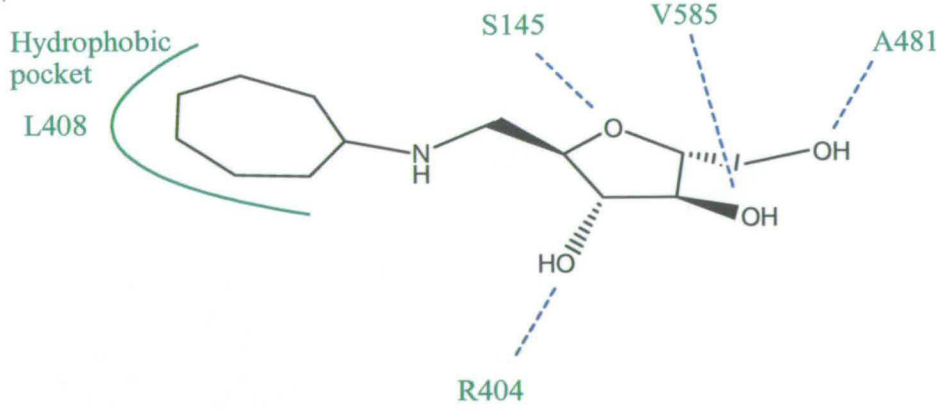

Figure 3.13 Diagram showing the potential protein-ligand interactions of inhibitor **70** in the effector site of *Lm* PyK, as determined using molecular modelling.

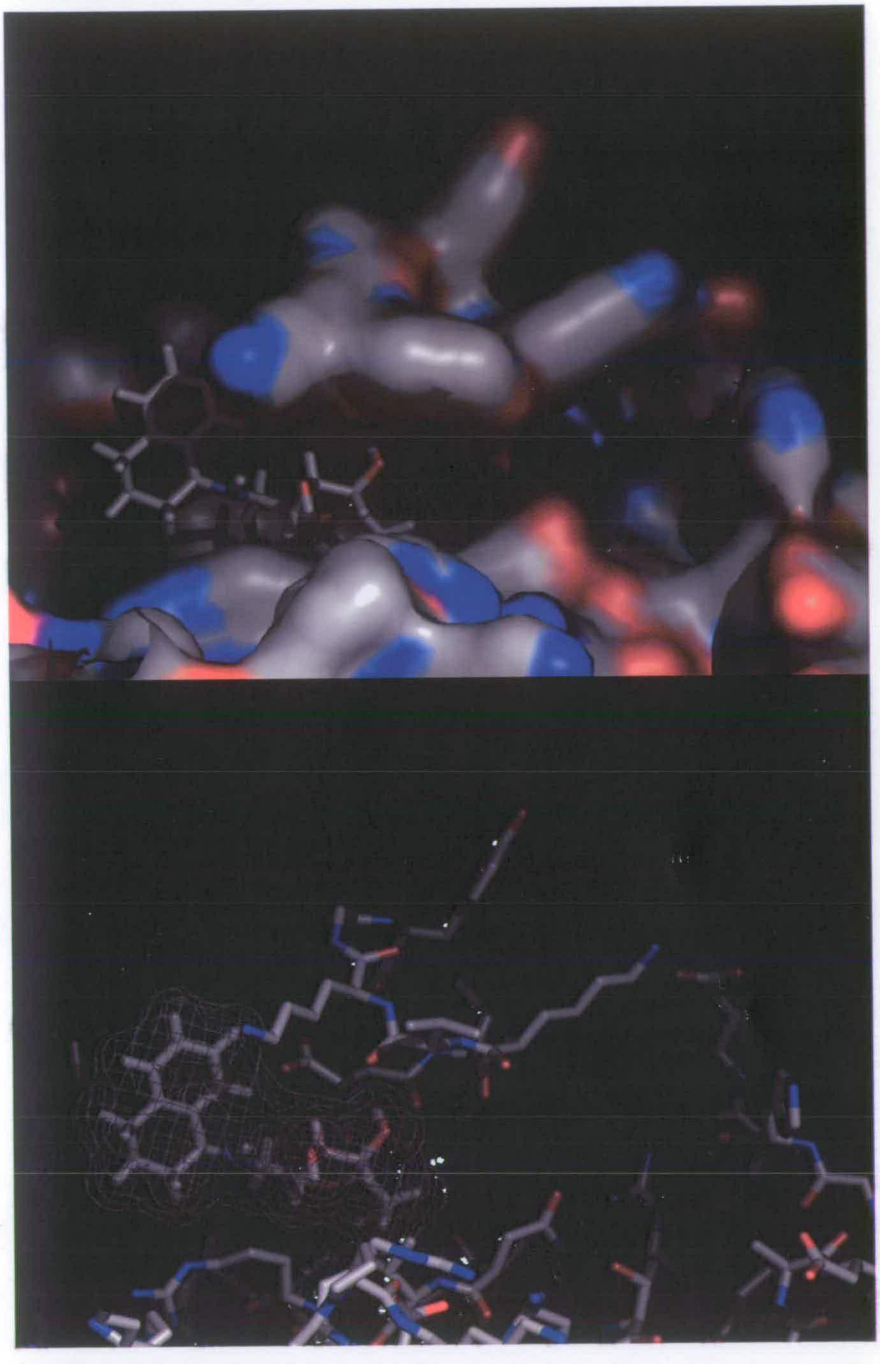

Figure 3.14 Model of inhibitor **57** docked in *Lm* PyK effector site.[80] Top picture shows the enzyme as a surface representation, bottom shows the enzyme as a stick representation.

The inhibitor with the third best IC_{50} against *Lm* PyK (1.2 mM) was **57**. Molecular docking was also carried with this inhibitor in the effector site of *Lm* PyK and the results are shown in Figure 3.14. Looking primarily at the orientation of the furanose scaffold, it is interesting to note that the same potential interactions have been identified as for inhibitor **70**. In particular, the interaction between the C4 hydroxyl group of the inhibitor and the backbone of the enzyme (at residue V585) is a lot more evident. Whilst the 1,2,3,4-tetrahydronaphthyl moiety interacts in the same place as the cycloheptyl group in inhibitor **70**, it does not appear to be sitting as deep in the hydrophobic pocket and, indeed, the aromatic portion could be repulsively interacting with the hydrophilic residues that surround the pocket. This could be a reason for why **57** is not as potent as **70**.

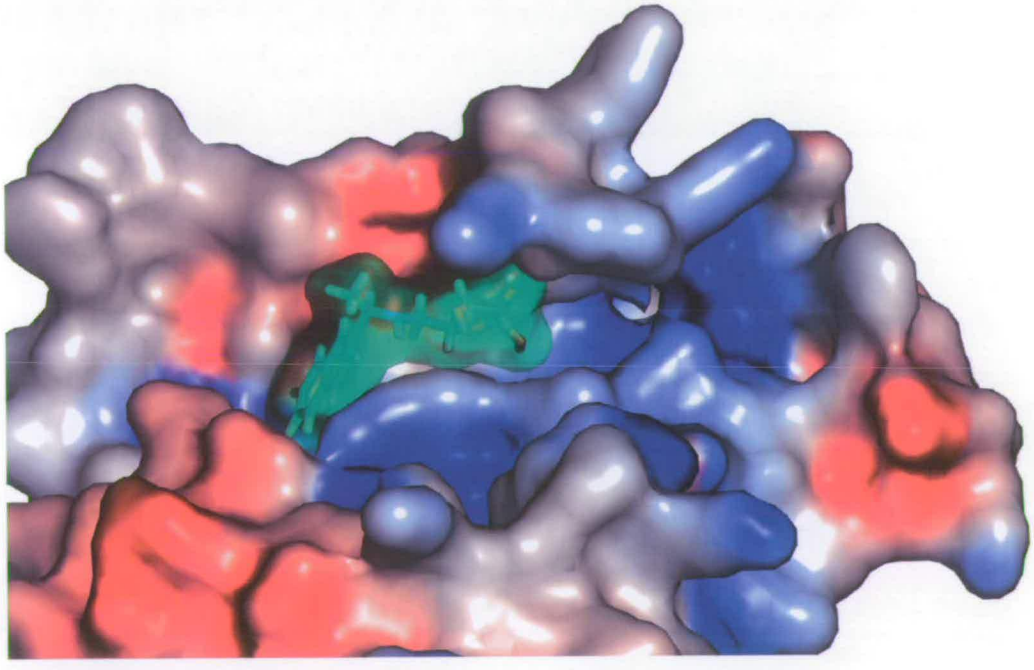

Figure 3.15 Model of **68** docked in *Lm* PyK effector site.[80]

Figure 3.15 shows **68** (another of the best six inhibitors) docked in to the effector site of *Lm* PyK. Again, it is clear that the furanose ring is making the same interactions with the enzyme as it was with inhibitors **57** and **70**, and its orientation is well conserved. It is interesting to note that the naphthyl moiety is in a different orientation to that of **57**, but in the same orientation as the cycloheptyl group in **70**. Again, the naphthyl group looks too large for the hydrophobic pocket and could be making repulsive interactions. However, this may be partly countered by the *R*-α-methyl group which could potentially make a hydrophobic interaction. It is postulated that inversion of the configuration of **68** would position the α-methyl closer to the nearby hydrophobic portion of the enzyme. Therefore, this model potentially explains the preference for the α-*S* inhibitors over the α-*R* inhibitors.

The final model shows inhibitors **72** and **73** docked in to the effector site of *Lm* PyK and is shown in Figure 3.16. As mentioned in section 3.2.4, **72** shows greater potency against *Lm* PyK than **73**, and other inhibitors with larger alkyl chains. Firstly, although this model shows that there is potential for larger alkyl chains to bind, the shape of the hydrophobic pocket is such, that smaller chains are likely to bind more effectively due to their more ordered nature. Larger chains would have to experience large conformational changes in order to bind effectively. Secondly, it is evident from a comparison between the models for **72** and **73**, why **72** is the more potent inhibitor. The α-*S*-chiral centre on **72** induces the burying of the methyl group within the hydrophobic pocket, the overall effect being that of a favourable protein-ligand interaction. The α-*R*-chiral centre on **73** brings about the exposure of the methyl group to solvent space. Hence, this mode of binding is not as favourable as with **72**

and, therefore, **72** is a more potent inhibitor. This observation is similar to that mentioned previously with inhibitor **68**, further corroborating the explanation for the increased inhibitory activity of α-*S* compounds over α-*R* compounds.

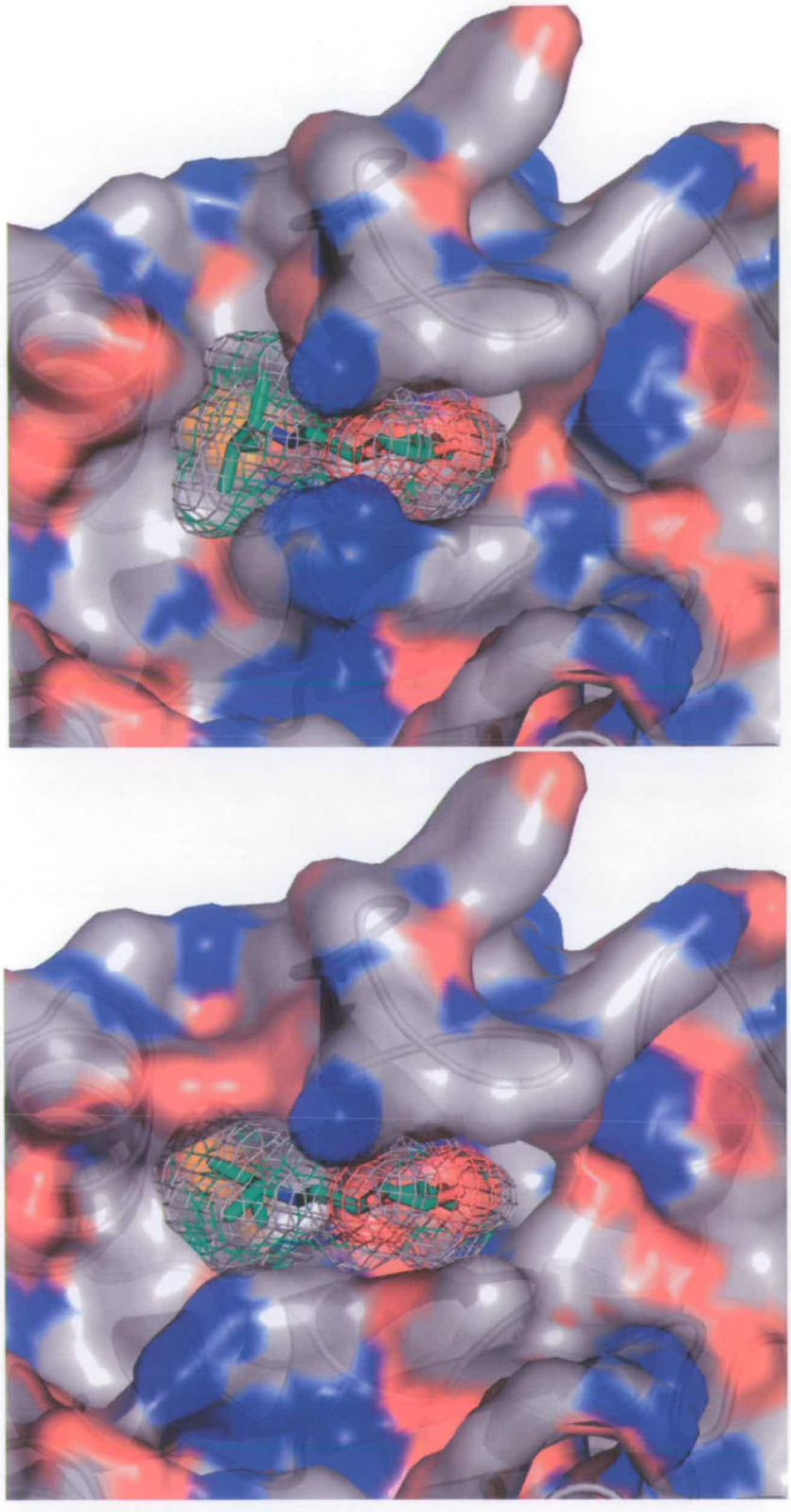

Figure 3.16 Models of **72** (top) and **73** (bottom) docked in the *Lm* PyK effector site.[80]

3.2.6 Library 2 screening results against *Tb* PFK.

As already mentioned in section 3.2.1, the remainder of any library 2 compounds from the biological evaluation against *Lm* PyK were used in a 5 mM screen against *Tb* PFK.[82] The results from the screen can be seen in Table 3.4 and Figure 3.17.

Compound	Percentage (%) remaining activity
48	87.4
49	83.8
50	70.4
52	64.0
53	77.1
54	33.2
55	57.2
56	51.9
57	61.6
58	53.9
66	69.4
68	33.2
69	58.4
70	62.9

Compound	Percentage (%) remaining activity
71	63.5
72	48.5
73	50.8
74	44.4
75	87.2
78	40.0
79	73.0
80	64.1
81	52.0
82	35.3
83	35.6
84	41.0
85	47.2
86	46.7

Table 3.4 Results of library 2 screen against *Tb* PFK.[82]

It is clear from the results shown in Table 3.4 and Figure 3.17 that the compounds in library 2 show little inhibition towards *Tb* PFK, and that none of the compounds are as good an inhibitor as **37** from library 1.

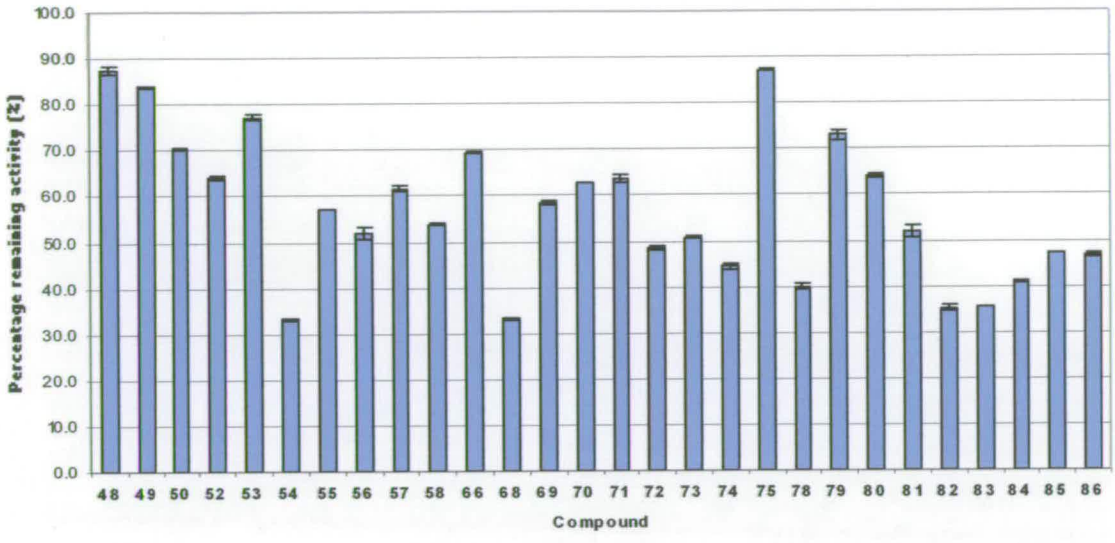

Figure 3.17 A graph showing the results of library 2 screen against *Tb* PFK.[82]

3.3 Conclusion.

Library 2 was designed and synthesised for biological testing against *Lm* PyK in order to try and identify one or more inhibitors with an IC_{50} value less than that of inhibitor **34** (1.6 mM). The initial 5 mM screen identified several potential inhibitors, and after further evaluation, six of these were found to have an IC_{50} value of 1.5 mM or less. In particular, 2,5-anhydro-1-deoxy-1-(cycloheptylamino)-D-mannitol **70**, was discovered to have an IC_{50} value of 58 μM, confirming this inhibitor as the new lead compound against *Lm* PyK. Competition experiments showed that these compounds do not compete with ADP and are therefore likely to bind to the effector site of the enzyme, as initially hoped. SAR results from the initial screen showed evidence of inhibitor interaction with a hydrophobic pocket in the effector site of *Lm* PyK, and also showed the cycloheptyl ring to be the optimum size for these hydrophobic interactions. Molecular docking again also helped to explain some of the trends seen

in the initial screen and shows the potential mode of binding of these inhibitors. It also shows potential inhibitor-protein interactions.

Library 2 was also screened against *Tb* PFK but the results did not show any improvement on the inhibitor already identified from library 1 (inhibitor **37**), or provide any new SAR information.

Chapter 4

Library 3: Design, Synthesis and Evaluation

4 Library 3: Design, Synthesis and Evaluation.

4.1 Inhibitor development.

4.1.1 Overview.

Results presented in Chapters 2 and 3 have demonstrated that library synthesis has led to the discovery of novel inhibitors for both *Tb* PFK and *Lm* PyK. In the interest of creating more potent inhibitors of the target enzymes, it was necessary to develop these newly discovered inhibitors. The following two chapters focus on this development, in particular the evolving chemistry involved in lead modification, the final library synthesised as a result of lead development, and other non-library compounds also synthesised as result of lead development.

4.1.2 Potential lead development.

Library synthesis has so far concentrated on the reductive amination reaction in order to synthesise 2,5-anhydro-1-deoxy-D-mannitol derivatives and, as already mentioned, this was successful in discovering inhibitors of both *Tb* PFK and *Lm* PyK. In order to develop these inhibitors further, it was necessary to identify possible modifications and reactions that could potentially be performed on these inhibitors. Figure 4.1 shows the modifications that could be made and also shows how the general inhibitor structure can be dissected in to separate sections; an approach that can lend itself towards combinatorial chemistry.

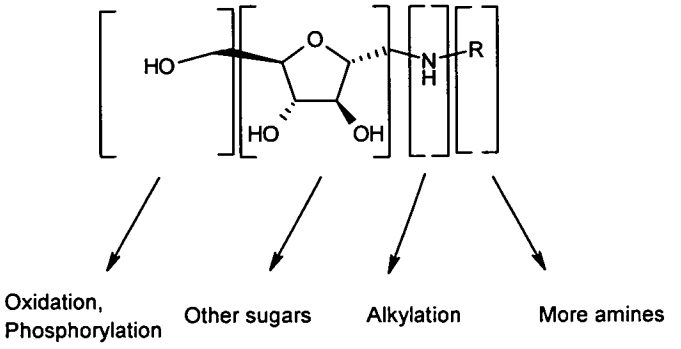

Figure 4.1 Potential modifications to general inhibitor structure.

In total, there are four sites on the general inhibitor structure where modifications can be made. First of all, there is the possibility of modifying the 6-position hydroxyl. It was thought that oxidation of this group to the acid would not only give a structurally and biologically interesting *N*-substituted sugar amino acid (SAA, see section 4.2 for a brief overview), but could also be used in amine (or amino acid) coupling reactions (see Figure 4.2), which is of particular interest as it enables the extension of these inhibitors in order to gain further binding interactions. Modelling studies suggest that this could be important for inhibition of PyK (Chapter 3). As these reactions are well known and thoroughly documented throughout the literature[13,83] it seemed an ideal basis for the design of a further library. Another modification possible at the 6-position hydroxyl is phosphorylation. It had been previously reported that phosphorylation at this position has led to an improvement of existing inhibitors of *Tb* PFK.[62] Therefore, methods to easily phosphorylate these compounds were explored and are discussed in Chapter 5.

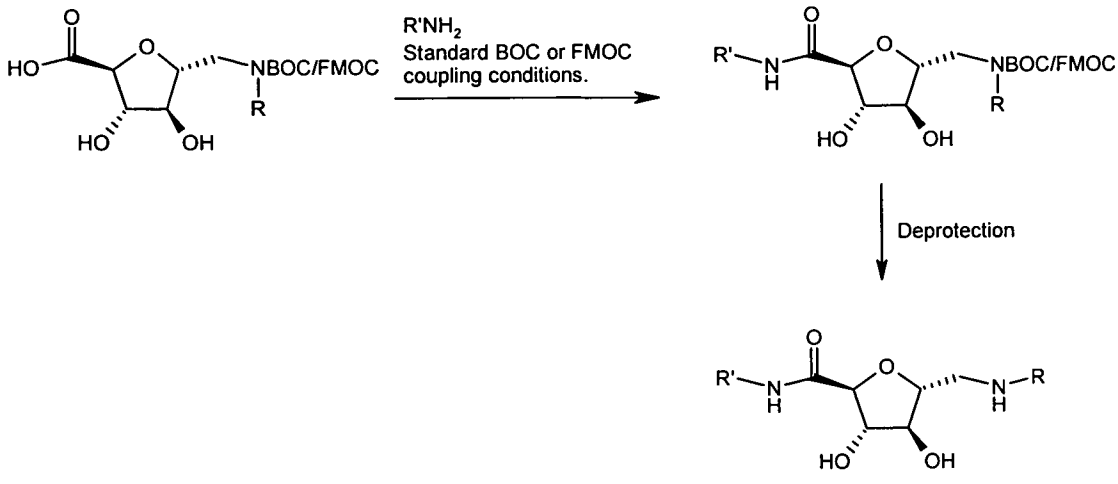

Figure 4.2 Further, possible inhibitor development of *N*-substituted sugar-amino acids to sugar amino amides.

The second possible modification that could be made is to change the stereochemistry of the furanose scaffold. This can be achieved by using alternative amino sugars as the initial starting material for the nitrous deamination reaction (as shown in Figure 2.3, Chapter 2). Again, this is discussed in more detail in Chapter 5. The next possible modification is the *N*-alkylation of the secondary amine to a tertiary amine. This, again, is also discussed in more detail in Chapter 5.

Finally, there is the possibility of using yet more primary amines to synthesise more secondary amine derivatives as shown in libraries 1 and 2. At this stage, however, it was deemed more pertinent to explore other areas of the inhibitors' structure.

4.2 Sugar amino acids (SAAs).

The synthesis of sugar amino acids (SAAs) is one method by which these inhibitors could be developed. This section is a brief introduction to both naturally occurring and synthetic SAAs. The term sugar amino acid is used to describe a class of

compounds with two immediate linkages of amino and carboxyl functionalities to a carbohydrate frame or scaffold, as shown in Figure 4.3.[84] The natural diversity that these carbohydrates offer is a powerful tool in the area of drug discovery.

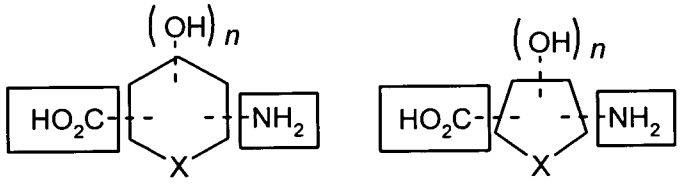

Figure 4.3 General structures of sugar amino acids.[84]

Naturally occurring SAAs are largely found as construction elements[84] such as neuraminic acid (Figure 4.4) which is often located peripherically on glycoproteins. The furanoid SAA (+)-hydantocidin exhibits herbicidal activity[85-87] whilst siastain B inhibits both β-glucuronidase and *N*-acetylneuramidase[84]. This belongs to the SAA group in which the nitrogen is within the pyranoid scaffold.[88]

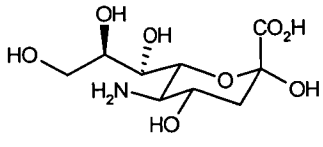

Neuraminic acid

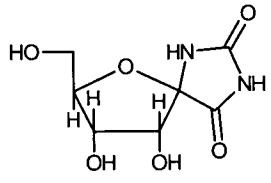

Hydantocidin

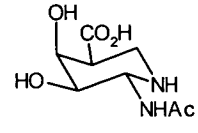

Siastatin B

Figure 4.4 Naturally occurring SAAs.

Both pyranoid and furanoid SAAs have been synthesised, not only for structural interest, but also for various biological uses, especially as mimetics.[84] Whilst there have been different methods used to synthesis δ-furanoid SAAs, none have used the approach that was proposed in section 4.12, but instead rely heavily on protection

techniques of the secondary hydroxyl groups that would lead to an extended synthesis if adopted here. A more selective approach was therefore investigated (see section 4.3.2).

4.3 Synthesis development.

4.3.1 Development of *N*-substituted-1-amino-2,5-anhydro-1-deoxy-D-mannitol synthesis.

It has already been commented upon in Chapters 2 and 3 that some of the yields from the library syntheses were poor, originally attributed to the nature of parallel synthesis where there is no reaction monitoring and all reactions are subject to the same reaction conditions. However, yields remained low when synthesising **37** and **70** on a larger scale, necessary for further inhibitor and synthesis development. Reaction monitoring by TLC (disappearance of **22**) and electrospray mass spectrometry (ESI^+) suggested that the reactions had in fact reached or approached completion, leading to the conclusion that it was not the reactions that were producing poor yields, but the purification method employed for these reactions. As mentioned in both Chapters 2 and 3, purification of these reactions was achieved by a mass-directed purification system (Waters ZMD). This works in a similar manner to a preparative HPLC system (details of sample concentration and running methods used can be found in Chapter 6). Figure 4.5 is a simple overview of how purification is achieved by this system.

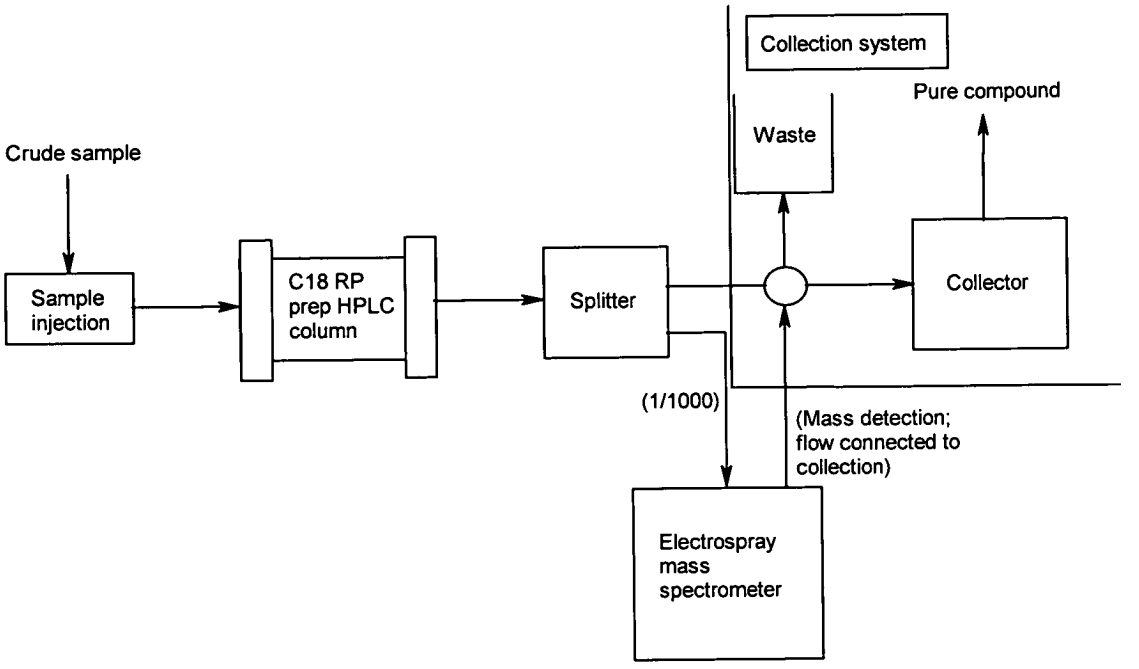

Figure 4.5 A schematic diagram showing a mass-directed purification system.

After the crude sample is injected, it is passed through a preparative scale column, which facilitates the separation of the various components in the crude sample. In the case of the reductive amination reactions, the crude product contained only the desired product and small amount of unreacted starting materials. Flow is then directed through a splitter where the majority of flow continues on to the collection system (when the system is not collecting, the flow route is directed to waste). However, a small portion of the flow (1/1000) is routed to an electrospray mass spectrometer where it is analysed. When the desired mass is detected by the mass spectrometer (pre-inputted), flow in the collection system is directed for collection. When the mass is no longer detected (or falls below a certain threshold value), the flow in the collection system is directed back to waste.

It is difficult to ascertain where the loss in yield at the purification stage was occurring, but even using a low crude sample concentration, small injection volumes and multiple injections, the percentage compound return from crude material remained low; 500 mg of crude material (using multiple injections) would yield in the range of 50 – 150 mg of pure compound (use of this method was also time consuming). Initially, the problem was thought to be due to the column, but its replacement had no effect on the overall return of isolated compound. Although this is a good, rapid system for combinatorial scale reactions (where small amounts of compounds suffice for analysis and testing), it seemed as though the persistently poor yields obtained would severely inhibit further synthetic scheme and inhibitor development. Without being able to find a reason or a cure for the low yielding performance of the mass-directed purification method, the decision was made to investigate other methods of purification, and, if necessary, adapt the reductive amination reaction accordingly.

The overall transformation of this particular reductive amination reaction is the formation of a secondary amine from a primary amine (the aldehyde in the presence of a reducing agent is effectively the alkylating agent). As the primary amine is likely to be the major impurity in the reaction, the purification technique should facilitate the separation of primary from secondary amines. Examples from the literature suggested that this indeed was eminently possible, more so with the developing field of solid phase chemistry.[89,90]

Solid phase chemistry has been used extensively in the medicinal chemistry area over recent years, not only because reactions can be carried out on a small scale and

in a combinatorial manner, but the target compounds are synthesised with high purity and little contamination, largely due to the fact that the compounds can be washed free of contaminants whilst still attached to the bead. However, attractive as this may seem, developing the reductive amination reaction on solid phase was deemed unsuitable at this point. It may have led to synthetic problems, as well as being unsuitable for preparative scale reactions due to low bead loading, both of which could have proven to be too time consuming. However, one aspect of solid phase chemistry, namely the utilisation of solid phase reagents and scavengers, could still be used without the need for moving away from solution phase chemistry. Solid phase reagents provide a technique whereby reagents can be administered to solution. Due to the fact that the reagent is supported on solid phase, there are no contaminants and no excess reagent because it can be removed from the solution by filtration after the reaction is complete. Solid phase scavenger reagents are used as a means of removing, from solution, any unwanted side products or unreacted starting material, leaving only the desired compound in solution which can be isolated, simply, by solvent removal. Adaptation of this technique to the reductive amination reaction would involve retaining aldehyde **22** and the primary amine in solution and supplying the reducing agent by means of solid support. Purification would be achieved by using a solid supported scavenging reagent to selectively remove any unreacted or excess primary amine. Work previously done in this area[91-93] had discovered that by using an excess of the primary amine, reduction of the preformed imine could be achieved by solid supported borohydride. The excess unreacted primary amine could be removed by scavenging with a solid supported aldehyde.[91] However, it was also conceivable that solid supported cyanoborohydride could be

used as the reducing agent.[92]

Each of the methods mentioned above was tested in order to ascertain, primarily, whether this technique could be used successfully in the synthesis of *N*-substituted-2,5-anhydro-1-deoxy-1-D-mannitol derivatives, and if so which gives the best results. Figure 4.6 together with Table 4.1 show the synthetic scheme, the reagents used and the results for each method.

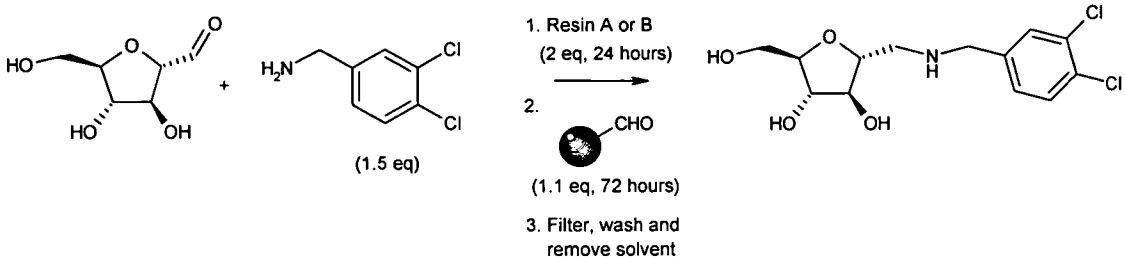

Figure 4.6 Potential new methods for synthesis of *N*-substituted-1-amino-2,5-anhydro-1-deoxy-D-mannitol derivatives. Resin A = solid supported cyanoborohydride; Resin B = solid supported borohydride. Scavenger resin = 4-benzoxybenzaldehyde polystyrene.

	Yield	Comment
Resin A	75 %	Mainly primary amine starting material (as determined by ESI^+ and ^1H NMR).
Resin B	83 %	Product only (as determined by ESI^+ and ^1H NMR).

Table 4.1 Results of using different resins in the synthesis of *N*-substituted-1-amino-2,5-anhydro-1-deoxy-D-mannitol derivatives, as shown in Figure 4.4.

The reactions were carried out in solid phase cartridges and shaking was done on the Bohdan MiniBlock synthesiser. The primary amine and aldehyde starting materials were shaken in methanol for 2 hours before addition of the reducing agent. The results in Table 4.1 show that while both methods appear to produce good yields, the method using Resin A (solid supported cyanoborohydride) produced very little of the product, and was mostly starting material as determined by ^{1}H NMR and particularly electrospray mass spectrometry. However, the result using resin B (solid supported borohydride) seemed to be more suitable, giving a yield of 83 % and no remaining starting material was detected by ^{1}H NMR or mass spectrometry. The original scale for these reactions was based on using 200 mg of 2,5-anhydro-D-mannose **22**. In order to test this method further, the reaction was tested on a larger scale in the synthesis of both **37** and **70** (based on 600 mg of 2,5-anhydro-D-mannose **22** starting material). Furthermore, the reactions were also tested on a small scale (50 mg with respect to aldehyde **22**) in order to investigate whether this reaction would also be suitable small-scale parallel synthesis. Figure 4.7 shows the scheme and conditions for these reactions and Table 4.2 shows the results obtained.

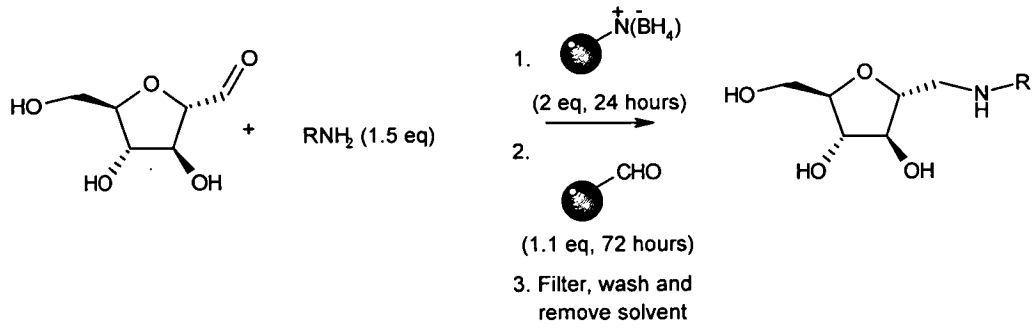

Figure 4.7 New synthetic scheme for *N*-substituted-1-amino-2,5-anhydro-1-deoxy-D-mannitol derivative synthesis.

Compound	Yield (%)
37*	84
70*	94
57	78
59	95
60	33†
76	99
77	87
78	96
87	80

Table 4.2 Results of synthesis using procedure shown in Figure 4.7. *Large scale, based on 600 mg of aldehyde **22**; 50 mg scale otherwise. †Low yield caused by leakage from the reaction cartridge.

It can be seen from Table 4.2 that the new reductive amination procedure is versatile enough to be used in both combinatorial scale and preparative scale syntheses, allowing for further inhibitor development. (Amine **87** is shown in Figure 4.8. This is a diastereo-mixture of **62** and **63**, synthesised from the racemic amine, as neither the *R* or *S* amine starting materials were commercially available).

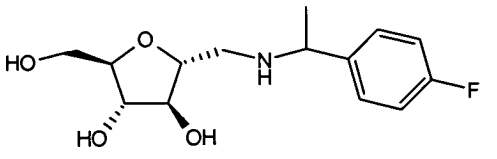

87

Figure 4.8 Amine **87**.

4.3.2 Methods towards the oxidation of *N*-substituted-1-amino-2,5-anhydro-1-deoxy-D-mannitol derivatives.

In choosing (and developing) a method for the oxidation of the 6-position hydroxyl, it was necessary to find procedures that were mild enough to not oxidise any other

functions within the molecule. Crucially, selectivity would be needed between the primary and secondary hydroxyl groups. Owing to the poor solubility of these compounds in organic solvents (other than methanol), any procedures would preferably use water as the solvent. Initially, oxidation was attempted on **15**, using ruthenium(III)trichloride monohydrate in the presence of sodium periodate to form ruthenium tetraoxide[94] and is shown in Figure 4.9.

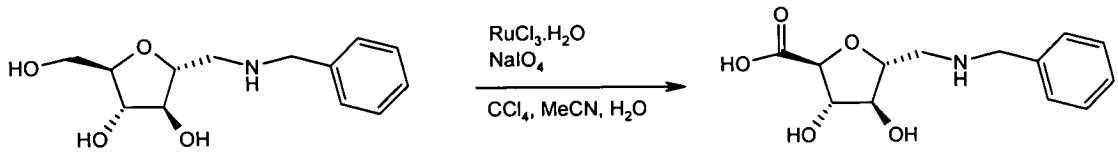

Figure 4.9 Attempted ruthenium tetraoxide catalysed oxidation.[94]

In this reaction, 2.2 molar % of ruthenium(III) trichloride and 3 equivalents of sodium periodate were used. The reaction was allowed to continue for a total of seven hours, as no product had been detected by electrospray mass spectrometry. However, after the reaction work up, not only was there no product, but there was also no recovered starting material. (The starting material could also not be detected in the crude reaction mixture by mass spectrometry). This led to the conclusion that the ruthenium tetraoxide catalysed oxidation was unsuitable and would therefore not be pursued any further.

Carrettin *et al* reported the selective oxidation of a primary hydroxyl group using a gold catalyst in the presence of aqueous sodium hydroxide, in the oxidation of glycerol to glyceric acid[95] (Figure 4.10). However, the use of elevated temperatures

and pressures deemed this approach unsuitable for development with *N*-substituted-1-amino-2,5-anhydro-1-deoxy-D-mannitol derivatives.

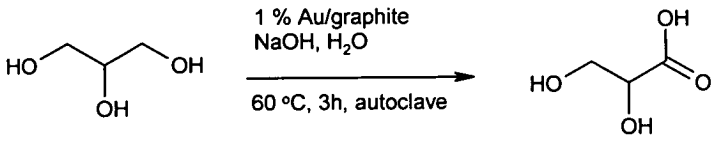

Figure 4.10 Gold catalysed oxidation of glycerol.[95]

However, the method that seemed the most promising was the use of TEMPO free radical mediated oxidation (in the presence of a bulk oxidant), owing to its mild conditions. Also, under basic conditions the rate of oxidation of primary alcohols is faster than that of secondary alcohols,[96,97] therefore, implying that there is selectivity for the oxidation of primary alcohols in the presence of secondary alcohols. Interestingly, when this method is performed on primary alcohols in organic solvents, the products obtained are the corresponding aldehydes.[97] When a biphasic solvent mixture was used (organic-aqueous), it was found that hydrophilic compounds were oxidised to the corresponding carboxylic acids.[98] When the reaction is performed in an aqueous solvent, only the carboxylic acid is obtained.[96] This method therefore seemed ideal for the oxidation of the 6-position hydroxyl group in *N*-substituted-1-amino-2,5-anhydro-1-deoxy-D-mannitol derivatives.

An initial attempt at this oxidation was carried out using a slightly modified method as described by de Nooy *et al*[99] which used a catalytic amount of TEMPO and sodium bromide. This is shown in Figure 4.11.

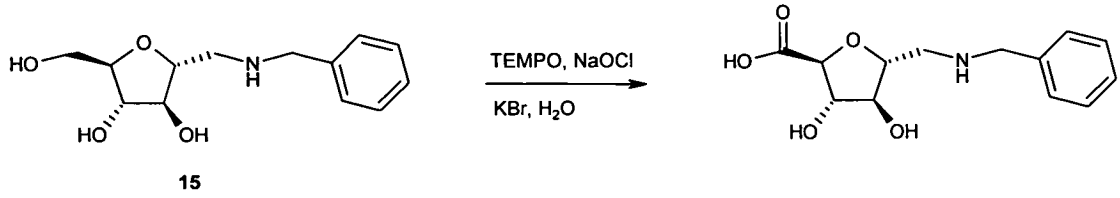

Figure 4.11 Attempted TEMPO-mediated oxidation.[99]

Although this reaction was allowed to continue for 72 hours, only starting material was detected in the reaction mixture (using the same methods as mentioned previously). Indeed, only the starting material, mixed with inorganic salts was, eventually, isolated. At this point a new problem was faced should oxidation be successful; the isolation of the oxidised product. Owing to the fact that the starting material and the product were highly water soluble, isolation and separation of these from the water soluble inorganic salts would be a problem. It was therefore decided that it would be necessary to BOC-protect the nitrogen of these compounds, which would aid solubility in organic solvents. This would then still be able to undergo a TEMPO-mediated oxidation by making use of the biphasic reaction and conditions.[96,98,100]

Although BOC-protection may seem to be a facile procedure for these compounds, this was not necessarily the case. Developing this reaction exclusively with **37**, the best conditions used di-*tert*-butyl dicarbonate (BOC-anhydride, administered in dioxane) in a 1:1, water : acetonitrile solution (used to solubilise the starting materials) with a final addition of 0.25 equivalents of 4-dimethylaminopyridine (DMAP, Figure 4.12). This gave yields within the range of 50 – 60 %, on which no improvement was made. However, when applying the same reaction conditions to

70, no product formation was observed, and only starting material was isolated; no BOC-anhydride was isolated either.

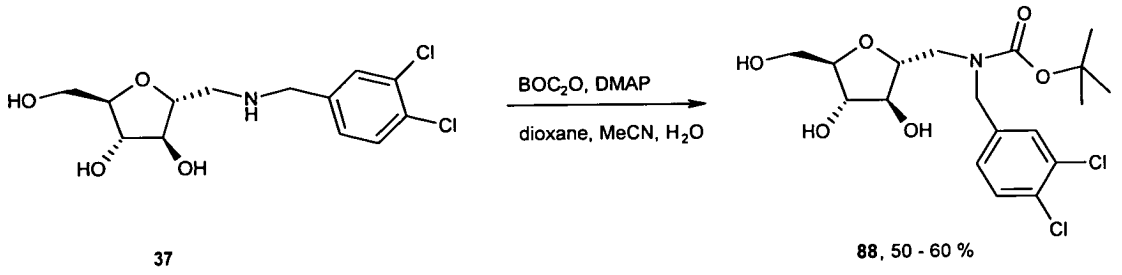

Figure 4.12 Initial BOC-protection of **37**.

DMAP acts by activating BOC-anhydride, so the activated species then acts as an electrophile towards amines. However, in the presence of a vast excess of water, it could be conceivable that water (or any hydroxide ions present) can also act as a nucleophile, resulting in hydrolysis of the activated species. This could also explain why the yield of the BOC protection of **37** was never greater than 60 %.

It was therefore decided to minimise the amount of water in the reaction mixture. This was achieved by suspending the *N*-substituted-1-amino-2,5-anhydro-1-deoxy-D-mannitol in acetonitrile and adding water dropwise until the compound was fully dissolved. The same procedure was then followed as previously. Figure 4.13 shows the procedure and the results.

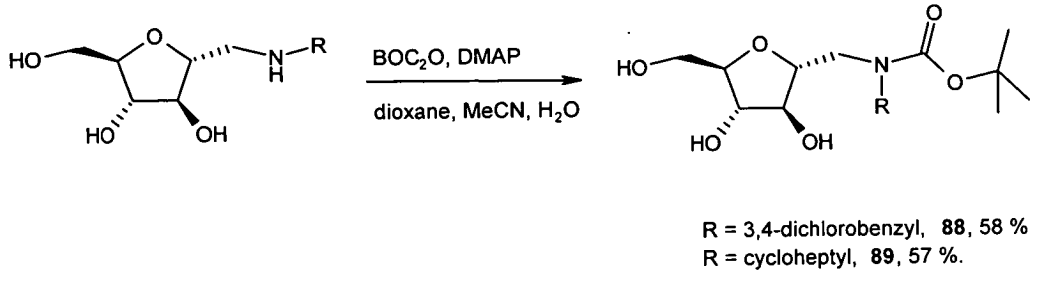

Figure 4.13 BOC protection of *N*-substituted-1-amino-2,5-anhydro-1-deoxy-D-mannitol derivatives.

The alteration to this method appeared to solve the problem as the synthesis of *N*-BOC-2,5-anhydro-1-deoxy-1-(cycloheptylamino)-D-mannitol **89**, occurred in a 57 % yield, and the yield for the synthesis of *N*-BOC-2,5-anhydro-1-deoxy-1-(3,4-dichlorobenzylamino)-D-mannitol **88** remained unaffected. Purification of **88** and **89** by flash column chromatography was attempted but drastically reduced the final yield. Consequently, the crude material was used for the next step. BOC protection was confirmed for both these amines by the presence of a signal in the ^{13}C NMR spectrum at δ = 156 – 157 ppm corresponding to the BOC carbonyl carbon atom. Further confirmation was gained by FTIR spectroscopy by the presence of a signal at 1672 cm^{-1}, a typical vibration for BOC carbonyl stretches.

Having achieved a successful BOC protection for both **37** and **70**, the next step was to reattempt the oxidation using a biphasic system. This was attempted using the method set out by Davis and Flitsch[100] and is shown in Figure 4.14.

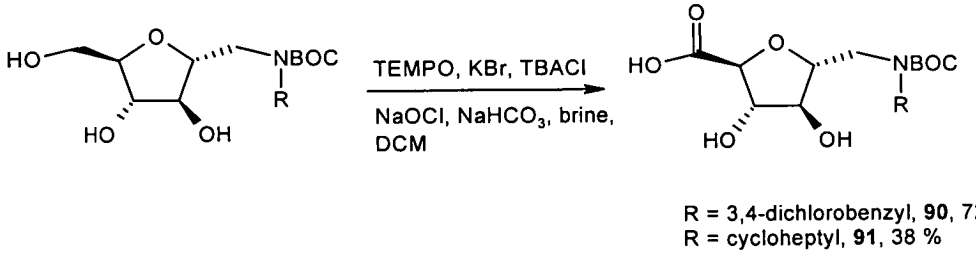

Figure 4.14 Biphasic oxidation method.[100]

To the biphasic mixture that contained the BOC-protected starting material and TEMPO in dichloromethane and a sodium bicarbonate solution of potassium bromide and tetrabutylammonium chloride, reagent grade sodium hypochlorite and brine in a sodium bicarbonate solution was added. Initial attempts at this reaction were unsuccessful, yielding only starting material. No oxidation products could be

detected either by NMR or by mass spectrometry. It was unclear, at first, why this reaction did not work, especially as other TEMPO-mediated oxidation procedures used very similar conditions to those above.[97] In fact, synthesis of some other sugar amino acids also used TEMPO-mediated oxidation.[84,101-103] It was decided that, because no oxidation product was being detected, an alternative bulk oxidant would be tested, based on an assumption that the reagent grade sodium hypochlorite may not be strong enough to re-oxidise the TEMPO oxidation mediator. Therefore, it was decided to replace sodium hypochlorite with oxone, as it is known that TEMPO/oxone catalyses the oxidation of alcohols to the aldehyde or ketone.[104] Adopting this strategy, the aldehyde could be isolated and another method could possibly be employed to oxidise the aldehyde to the acid. However, in keeping the same conditions as used in Figure 4.13, it was hoped that the acid would be synthesised in one pot, as oxone is also known to oxidise aldehydes to acids.[105] Unfortunately, this reaction also recovered starting material only, and no oxidation product was observed.

Returning to the idea that the reagent grade sodium hypochlorite was not strong enough, the concentration was checked by titrating against a standardised sodium thiosulfate solution (the method and calculations for this can be found in the appendix). The concentration of the reagent grade sodium hypochlorite was determined as 0.086 M. The concentration needed for the oxidation reaction is 1.3 M.[100] This is over fifteen times weaker than what is needed. Therefore, the concentration of industrial bleach was determined (1.69 M) and was diluted for use for the oxidation reaction. Unsurprisingly, the oxidation reaction was now successful, affording *N*-BOC-2,5-anhydro-1-deoxy-1-(3,4-dichlorobenzylamino)-D-mannonic

acid (compound **90**) in a 72 % yield and *N*-BOC-2,5-anhydro-1-deoxy-1-(cycloheptylamino)-D-mannonic acid (compound **91**) in a 38 % yield. The ^{13}C NMR spectrum gave confirmation of successful oxidation by a signal at δ = 174 ppm corresponding to the acid carbon atom, and disappearance of signal at δ = 62 ppm corresponding to the now oxidised methylene carbon atom. Again, attempts to purify these compounds by flash column chromatography proved unsuccessful as no product was returned. The crude material was therefore carried forward for use in the next step.

4.3.3 Amine coupling and deprotection of *N*-BOC protected mannonic acid derivatives.

Having successfully found a route to *N*-BOC protected mannonic acid derivatives, the objective now (as previously mentioned in section 4.1.2) was to perform amine coupling reactions. If successful, these reactions would be used to synthesis a small library which, after deprotection, could be tested against the target enzymes.

Coupling reactions to form amides are widely used and well documented (especially in the area of peptide synthesis).[13,83] There are many different reagents available depending on the conditions needed, but for this particular reaction it was decided to use standard BOC coupling conditions and aromatic amines. The reaction that was used as a test is shown in Figure 4.15.

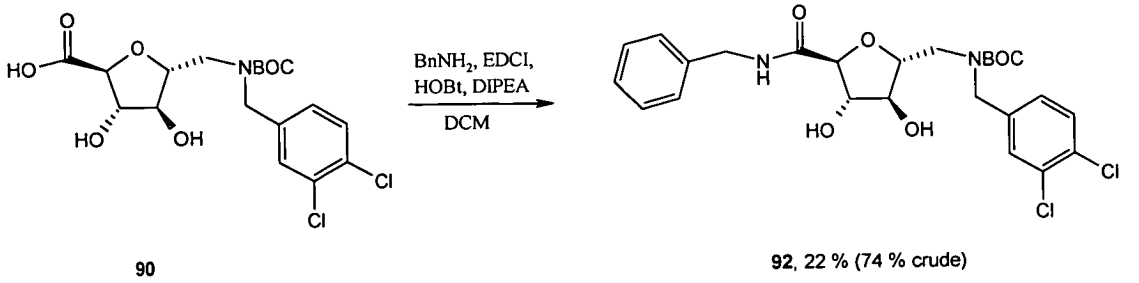

90 **92**, 22 % (74 % crude)

Figure 4.15 Amine coupling reaction in the synthesis of **92**.

The reaction shown in Figure 4.15 was successful, and after work up afforded **92** in a yield of 74 %. However, this was shown to contain some unreacted starting material so was purified using flash column chromatography. Although the overall yield of 22 % was disappointing, it still left sufficient material to undergo deprotection and purification. Coupling was confirmed by the psresence of 2 bands in the IR spectrum at 1666 and 1539 cm^{-1} corresponding to the secondary amide. Deprotection was carried out using a standard TFA/dichloromethane procedure (Figure 4.16) and afforded 2,5-anhydro-1-deoxy-1-(3,4-dichlorobenzylamino)-D-benzylmannonamide **93** in a yield of 71 % after purification by mass directed methods.

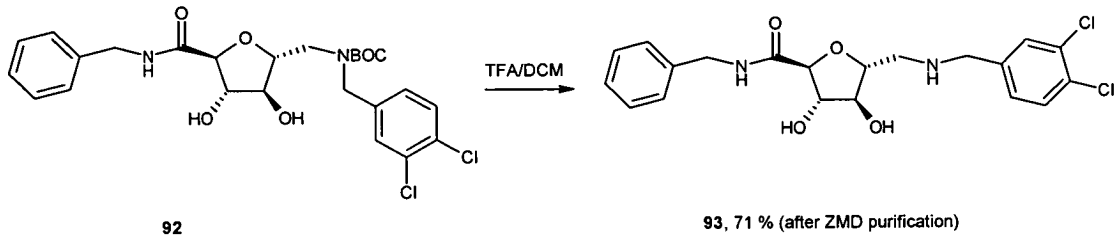

Figure 4.16 BOC-deprotection of **92**.

4.4 Library 3.

4.4.1 Library 3 synthesis.

Having successfully identified a synthetic route towards the synthesis of *N,N'*-substituted-1-amino-2,5-anhydro-1-deoxy-1-D-mannonamide derivatives, the next stage was to synthesise a small library of these compounds based on the structures of inhibitors **37** and **70** (Figure 4.17). All the reactions would be synthesised in parallel, and purification, after the amine coupling step, would be facilitated by parallel flash column chromatography system (Quad3) using pre-packed columns. Table 4.3 shows

the results of this synthesis, applying the schemes shown in Figures 4.15 and 4.16.

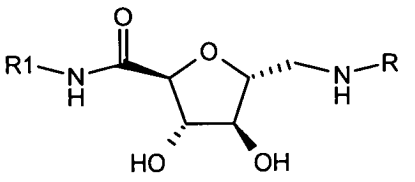

where R = 3,4-dichlorobenzyl or, cycloheptyl

Figure 4.17 General structure of library 3 compounds.

Library 3 was synthesised successfully, with yields for the amine coupling ranging between 15 – 39 %, and yields for the deprotection yielding between 20 – 99 % (both yields being after purification). Due to the low yields of the amine coupling reactions and the fact that the products of these reactions were only an intermediate in the overall library synthesis, some compounds were used directly in the deprotection reaction without any ^{1}H NMR or mass spectrometry characterisation (see Chapter 6). The structures of the final compounds were confirmed by ^{1}H NMR and, where possible, ^{13}C NMR. Full characterisation was achieved for amide **111** showing the characteristic signals in the IR spectrum at 1674 and 1541 cm^{-1} corresponding to the secondary amide. Other typical signals include the doublet of doublets corresponding to the diasteriotopic C1 methylene protons in the ^{1}H NMR spectrum at $\delta = 3.2 - 3.5$ ppm, and the carbonyl carbon signal at $\delta = 169.5$ in the ^{13}C NMR spectrum. As for libraries 1 and 2, the final compounds were established to have high purity by ^{13}C NMR with the baseline showing no impurities.

R groups / R1 groups	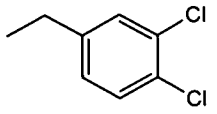	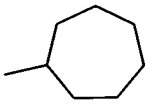
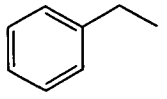	**92**, 22 % **93**, 71 %	**100**, 26 % **113**, 60 %
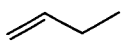	**94**, 29 % **107**, 82 %	**101**, 39 % **114**, 43 %
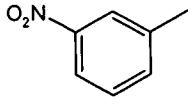	**95**, 30 % **108** 23 %	**102**, 33 % **115**, 36 %
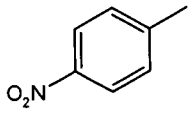	**96**, 25 % **109**, 20 %	**103**, 21 % **116**, 50 %
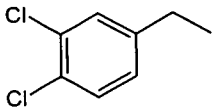	**97**, 25 % **110**, 58 %	**104**, 16 % **117**, 77 %
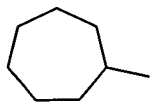	**98**, 24 % **111**, 48 %	**105**, 16 % **118**, 99 %
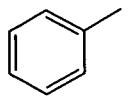	**99**, 25 % **112**, 50 %	**106**, 15 % **119**, 50 %

Table 4.3 Library 3 synthesis results. First entry; compound number and yield for coupling reaction. Second entry; compound number and yield for deprotection.

4.4.2 Library 3 screening results against *Tb* PFK.

Library 3 was designed so that inhibitors were synthesised to target not only *Tb* PFK, but *Lm* PyK as well; those compounds with a 3,4-dichlorobenzyl motif would be screened against *Tb* PFK, and those with a cycloheptyl motif would be screened against *Lm* PyK. Hence, it is clear from Table 4.3 that compounds **111** and **117** would be screened against both enzymes, as these compounds contain both motifs.

Due to the overall low yield of library 3, the inhibitor screen was carried out at a final concentration of 1 mM with respect to each inhibitor.

The results of the 1 mM screen of 8 compounds in library 3, against *Tb* PFK, are shown in Table 4.4 and in Figure 4.18.[106] The compounds are shown in Figure 4.19.

Compound	Percentage (%) remaining activity
93	4.0
107	2.0
108	1.7
109	0.8
110	0.9
111	4.7
112	5.5
117	0.4

Table 4.4 Results of the 1 mM library 3 screen against *Tb* PFK.[106]

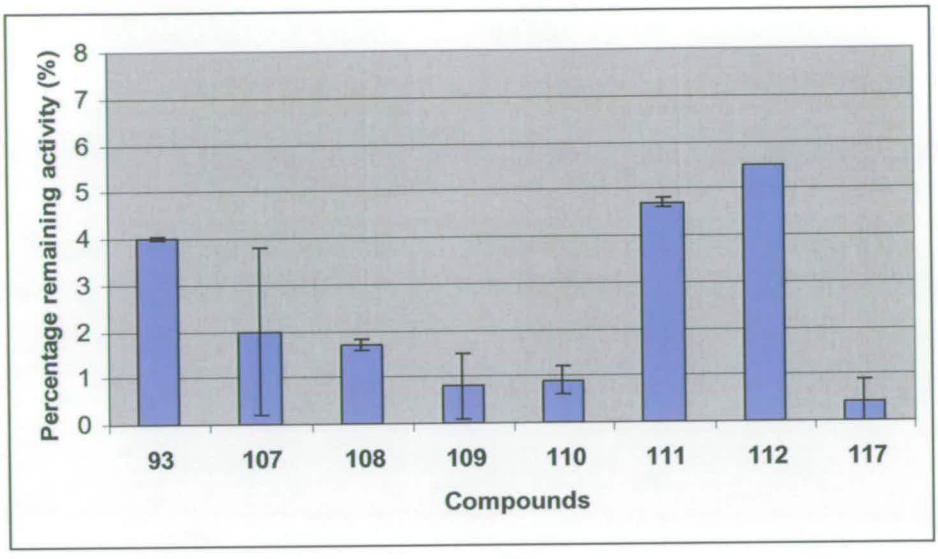

Figure 4.18 A graph showing the 1 mM screening results of a library 3 screen against *Tb* PFK.[106]

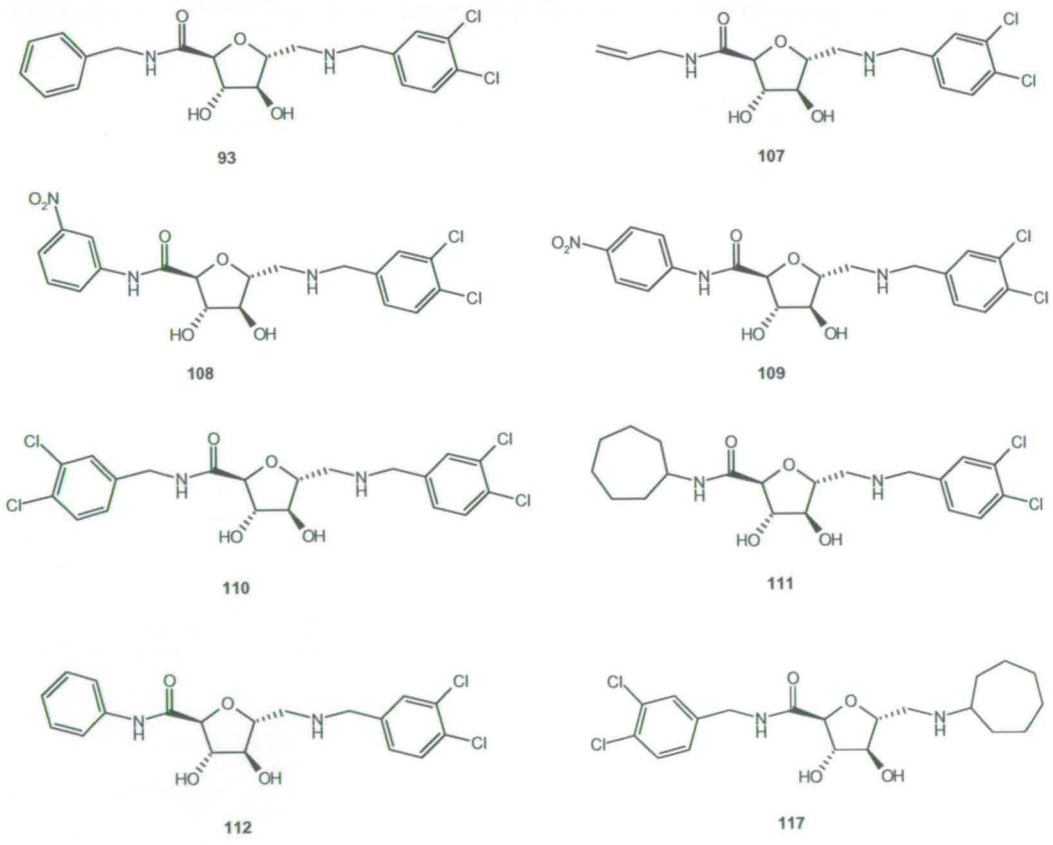

Figure 4.19 Compounds from library 3 screened against *Tb* PFK.

A comparison of the results shown in Table 4.4 and Figure 4.18 with the previous results shows a great improvement in inhibitory activity. Previously, the most potent inhibitor against *Tb* PFK was **37**, which inhibited the enzyme to 4.7 % of its original activity at a concentration of 5 mM. However, the screening results from library 3 show a comparable inhibitory effect, but at the lower concentration of 1 mM, suggesting that these inhibitors are more potent. Therefore, the IC_{50} values for four of the above inhibitors were determined; the choice of inhibitors was based on the amount of material available for testing. The results are shown in Table 4.5.[106]

Compound	IC_{50} (μM)
107	50
110	23
111	80
117	49

Table 4.5 IC_{50} values of four compounds from library 3. The dose-response curves can be found in the appendix.[106]

Table 4.5 shows that the inhibitors from library 3 have about a 10-fold increase in IC_{50} values compared with the previous lead compounds for *Tb* PFK (**21**, IC_{50} = 0.45 mM; **37**, IC_{50} = 0.41 mM), and that inhibitor **110** is a new lead compound with an IC_{50} value of 23 μM. Possible reasons for the inhibitory activity are discussed in section 4.4.3.

In order to ascertain whether the inhibitors bind to the F6P or ATP binding site, preliminary competition experiments were also carried out using inhibitor **110**.[106] These results showed that K_M value for ATP in the presence of the inhibitor remained constant whilst the V_{max} decreased, indicating that that the inhibitor is

unlikely to compete with ATP and therefore is also unlikely to exhibit its inhibitory effect by binding at the ATP binding site. However, for F6P the K_M value increased whilst a decrease is V_{max} was observed, indicating that the inhibitor may compete with F6P and, therefore, could inhibit *Tb* PFK by binding at the F6P binding site.

4.4.3 Molecular docking model.

In section 4.4.2 it was seen that inhibitors from library 3 gave IC_{50} values in the micromolar range against *Tb* PFK, which was a marked improvement on the existing lead compounds. It was also discovered that the inhibitors are likely to induce their effect by binding to the F6P binding site. Using this information, a model of inhibitor **110** in the F6P binding site of *Tb* PFK was produced, where the furanose scaffold of **110** is positioned in the same orientation as the F6P.[107] The models can be seen in Figures 4.20 and 4.21.

From the model shown in Figure 4.20, it is possible to identify potential reasons for why the sugar amino amide inhibitors, from library 3, show improved inhibitory activity on previous lead compounds. Firstly, the extension of the furanose scaffold at the 6-position allows the inhibitor to probe further into the binding pocket and, hence, gain favourable interactions. The figure also shows that the pocket is large and, therefore, there is scope further for inhibitor development. The use of larger groups at the 6-position would act as to probe this pocket more fully in the hope of attaining more binding interactions.

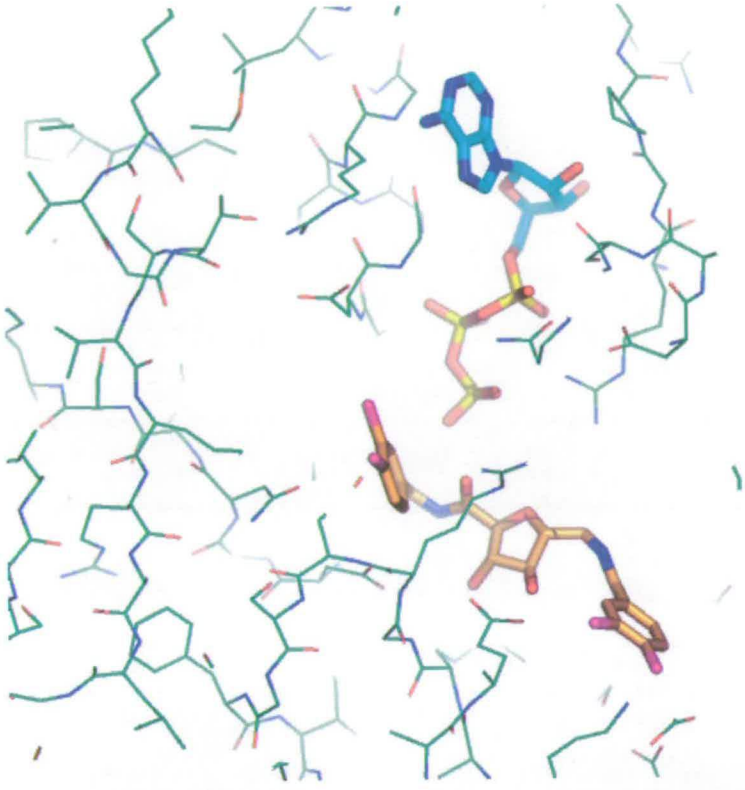

Figure 4.20 Model of inhibitor **110** in the F6P binding site of *Tb* PFK. ATP is also shown.[107]

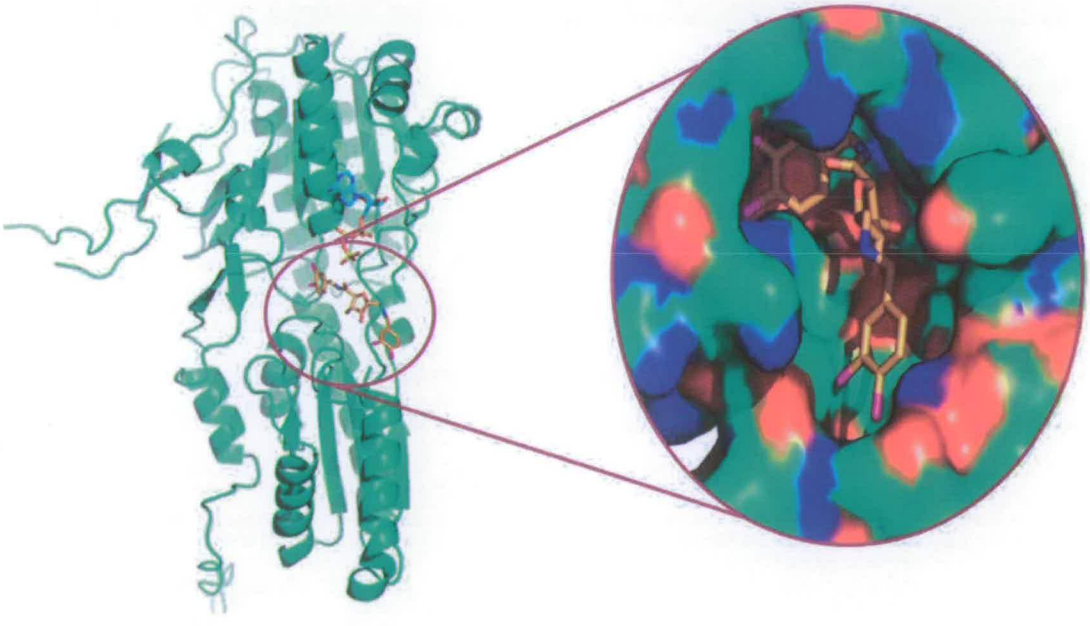

Figure 4.21 A ribbon representation of inhibitor **110** in the F6P binding site of *Tb* PFK (left), with a space filled close up of the binding site (right).[107]

Secondly, both Figures 4.20 and 4.21 how that there is a potential interaction between the carbonyl of amide functionality of the inhibitor and a close by arginine residue. This could provide a specific interaction and, as such, would mean that the sugar amino amides would bind more strongly to the protein. Previously, this position would have been occupied by a hydroxyl group and would, therefore, not be an as favourable interaction.

4.4.4 Library 3 screening results against *Lm* PyK.

As has been previously mentioned, library 3 was also designed to include inhibitors targeted against *Lm* PyK. Table 4.6 and Figure 4.21 show the results of a 5 mM screen of 7 compounds from library 3 screened against *Lm* PyK. (Unfortunately **117** could not be tested as it had already been consumed.) The compounds are shown in Figure 4.22.

Compound	Percentage (%) remaining activity
111	88.2
113	11.5
114	19.1
115	7.6
116	12.5
118	1.9
119	24.8

Table 4.6 Results of library 3 screen against *Lm* PyK.

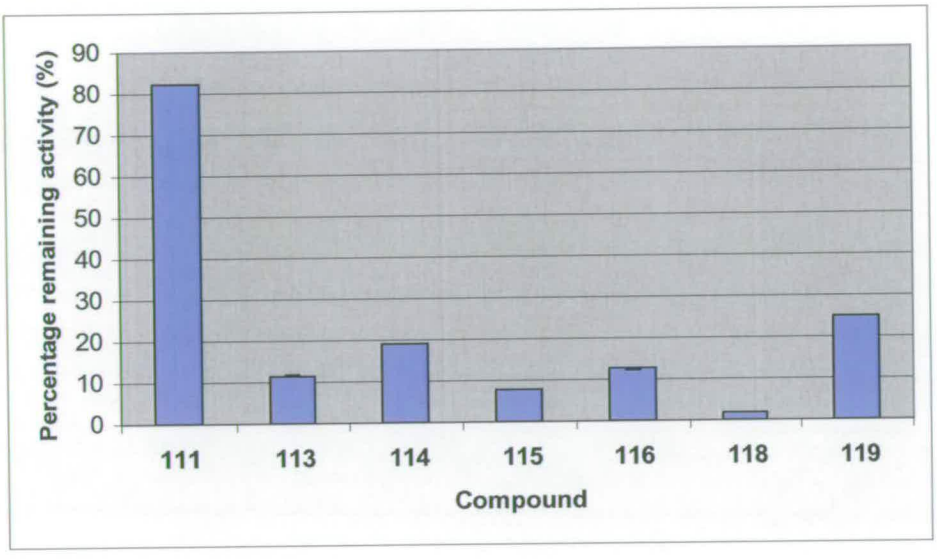

Figure 4.21 A graph showing the screening results of library 3 against *Lm* PyK.

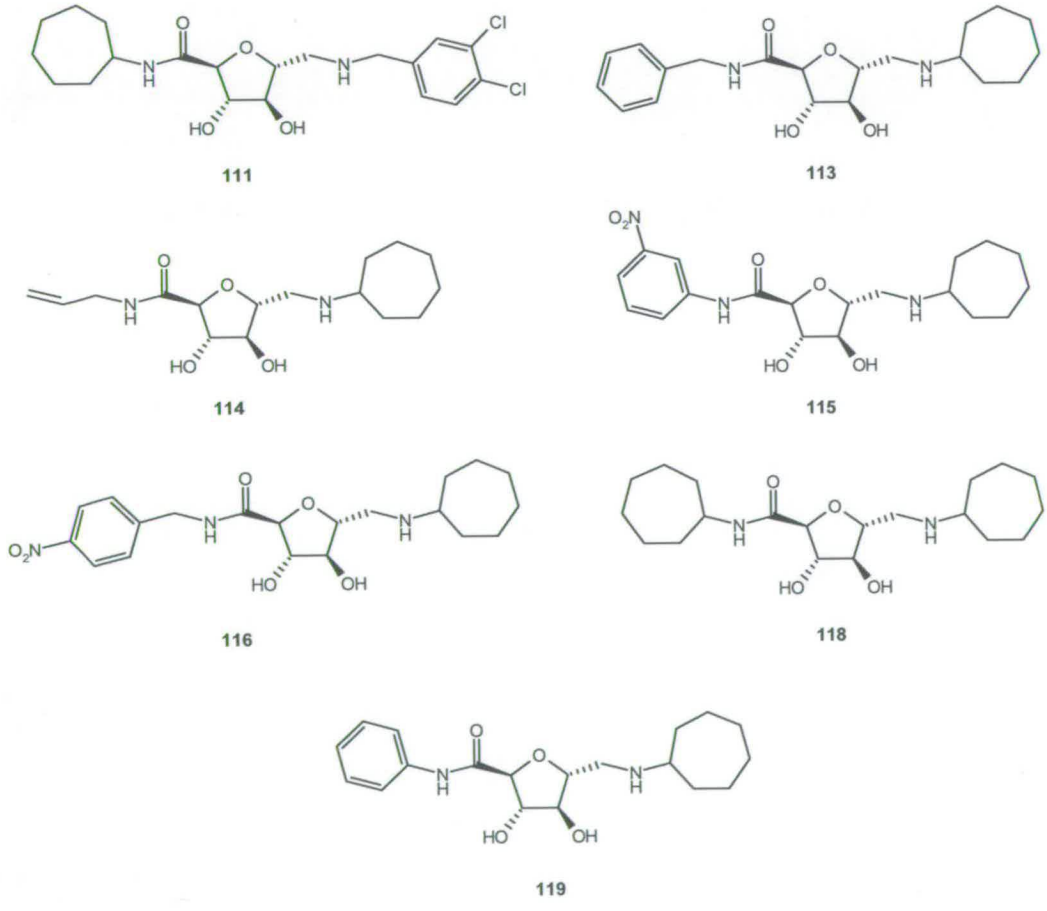

Table 4.6 Compounds from library 3 screened against *Lm* PyK.

The results shown in Table 4.6 and Figure 2.12 suggest that the compounds from library 3 show good inhibition against *Lm* PyK. When compared to the previous results from library 2, in particular inhibitor **70**, two compounds show similar or better inhibition (inhibitors **115** and **118**), while most of the other inhibitors tested still showed good inhibition. Interestingly, inhibitor **111** exhibited little inhibitory effect on *Lm* PyK, suggesting that the cyclohexyl motif can no longer bind effectively to the hydrophobic pocket in the effector site of *Lm* PyK, presumably due to a repulsive interaction caused by the amide functionality. Unfortunately, there was insufficient material available to these inhibitors further and obtain IC_{50} values.

4.5 Conclusion.

In order to develop further the inhibitors discovered in Chapters 2 and 3, an alterative method for reductive amination was identified. This made use of solid supported borohydride and the scavenger resin, 4-benzoxybenzaldehyde polystyrene. This also bypassed the need for any further purification and resulted in vastly improved yields, generally in the range of 78 – 99 %. In the interest of developing the inhibitors further, oxidation of the 6-position hydroxyl was investigated. At this point, improving the solubility of these compounds in organic solvent was needed, so a general method for the BOC-protection of the secondary amine was identified. Oxidation was attempted using a biphasic TEMPO mediated method and was initially unsuccessful. However, after discovering that the concentration of sodium hypochlorite used was too weak, the oxidation was re-attempted and was successful, giving the desired 6-position carboxylic acids in yields of 38 – 72 %. These acids were then used in a series of amine coupling reactions (using standard BOC reagents

and conditions) and deprotection reactions to give rise to library 3; a 14 member *N,N'*-substituted-1-amino-2,5-anhydro-1-deoxy-1-D-mannonamide library. Library 3 was then screened against both *Tb* PFK and *Lm* PyK. Against *Tb* PFK, all compounds exhibited a higher level of inhibition than shown by previous lead compounds. The inhibitors were found to have IC_{50} values in the micromolar range, the best of which was inhibitor **110** which gave an IC_{50} value of 23 μM. Modelling of this inhibitor in the F6P binding site suggests that the amide carbonyl may be making a binding interaction with the protein which could explain the higher degree of inhibition. Also, extension of the furanose scaffold at the 6-position allows the inhibitors to probe deeper into the F6P binding pocket, potentially gaining more binding interactions. There is the potential for further inhibitor development to probe this pocket even further. Against *Lm* PyK, several compounds showed similar inhibitory activity as the lead compound, inhibitor **70**. Inhibitor **118** appeared to inhibit the enzyme to a higher degree; this cannot be confirmed, however, as there was insufficient material available to obtain an IC_{50} value.

Chapter 5

Non-Library Inhibitor Development

5 Non-Library Inhibitor Development.

5.1 Overview.

In Chapter 4 it was discussed how the initial *N*-substituted-2,5-anhydro-1-deoxy-D-mannitol scaffold was developed in order to make sugar amino amide derivatives, which, when tested against *Tb* PFK, were shown to have inhibitory activity. The final results and discussion chapter continues on the theme of further inhibitor development, concentrating not only on further modifications to the 6-position hydroxyl group, but also introducing additional functionality as shown in Figure 5.1.

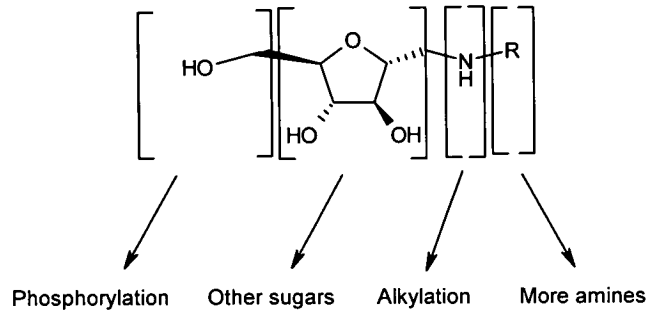

Figure 5.1 Potential modifications to general inhibitor structure.

Most of this development work was performed to try and gain an understanding of how changes affect inhibition of the respective enzyme targets, rather than with a view towards library synthesis (although, as will become evident, library synthesis is certainly feasible).

Finally, due to the fact that specificity between target and host enzymes is a very important aspect in drug design and drug discovery, the results of some specificity

experiments are reported.

5.2 Further inhibitor development.

5.2.1 Further modifications of the 6-position hydroxyl.

Work by Claustre *et al*[62] has suggested that the introduction of a electronegative group at the 6-position may improve inhibitor-protein binding (discussed in Chapter 2). Using chemistry already developed for the synthesis of *N*-BOC protected sugar amino amides (discussed in Chapter 4), the easiest method of introducing electronegativity at the 6-position would simply be to deprotect the *N*-BOC sugar amino acid derivatives, as shown in Figure 5.2. This was attempted by using standard BOC-deprotection conditions (TFA in dichloromethane), and the yields after mass directed purification are also shown in Figure 5.2. The sugar amino acids **120** and **121** still await testing against *Tb* PFK and *Lm* PyK.

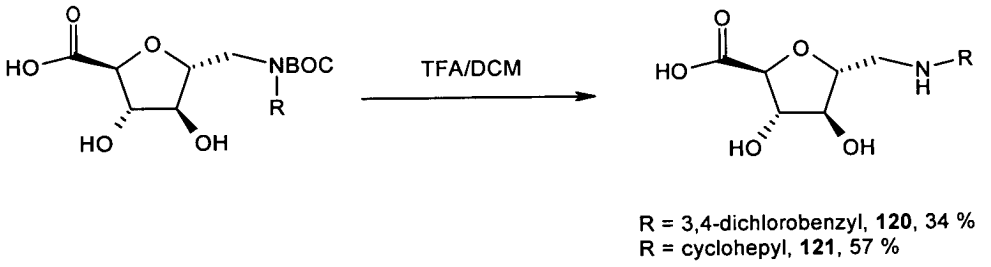

Figure 5.2 BOC-deprotection of sugar amino acids.

In Chapter 2, it was mentioned that phosphorylation at the 6-position hydroxyl could lead to more potent inhibitors, especially for *Tb* PFK.[62] Therefore attempts were made to synthesise phosphorylated derivatives in a manner that would be suitable for library synthesis. The main method used by Claustre *et al*[62] is shown in Figure 5.3

and employed chlorodiphenylphosphine as the phosphorylating agent. Subsequent deprotection of phosphate group was achieved by catalytic hydrogenation.

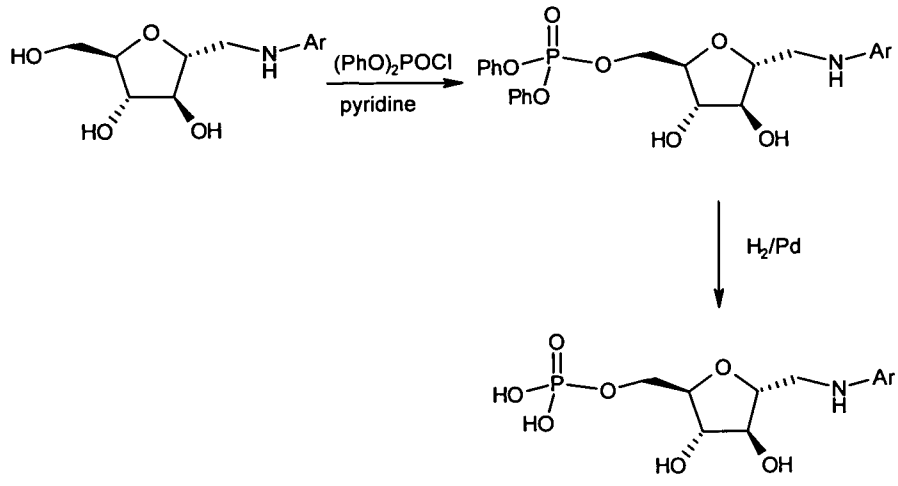

Figure 5.3 General phosphorylation procedure.[62]

However, the route shown in Figure 5.3 was deemed unsuitable for further development for library synthesis as the deprotection step would be difficult to perform in parallel on a multi-reaction basis. Furthermore, the yields of this route varied quite widely, depending on the initial substrate.[62,63] It was therefore necessary to try to find an alternative method that selectively phosphorylated primary hydroxyl groups in the presence of secondary hydroxyl groups. Commercially available phosphoramidite reagents seemed an ideal method for this synthesis. Perich and Johns[108] had shown that the di-*tert*-butyl *N,N*-diethylphosphoramidite could phosphitylate primary hydroxyl groups which could be subsequently converted to the phosphate by oxidation with *m*-CPBA to give the di-*tert*-butyl phosphate ester in high yields (93 - 98 %). It was hoped that this could also be achieved in a selective manner, thereby selectively phosphorylating *N*-sustituted-2,5-anydro-1-deoxy-D-

mannitol derivatives. The *tert*-butyl protecting groups could then be removed easily using mildly acidic conditions. This method is shown in Figure 5.4.

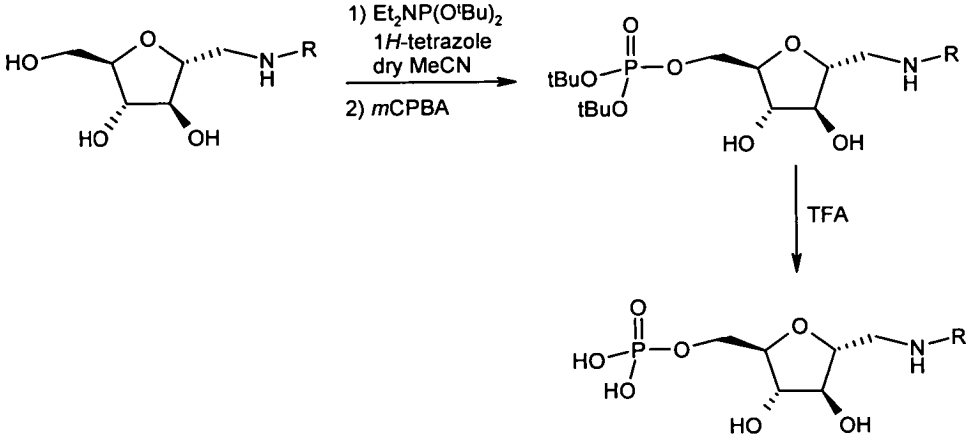

Figure 5.4 Proposed phosphorylation of *N*-substituted-2,5-anhydro-1-deoxy-D-mannitol derivatives.

The reaction was attempted with both **15** (benzyl derivative) and **37**, but no desired products were isolated, possibly attributed to the poor solubiltity of the *N*-sustituted-2,5-anydro-1-deoxy-D-mannitol derivatives in organic solvents. Therefore, it was decided to try the same reaction on the *N*-BOC protected substrates, thereby increasing the solubility of the compounds in organic solvent, and removing the potential for the nitrogen to act as a nucleophile towards the phosphitylating agent, and in doing so, hindering the reaction progression. The reaction was attempted using the *N*-BOC protected amine **88**; however, no product was yielded and only starting material was recovered. The method was therefore deemed suitable for further investigation.

Research by Sowa and Oucho[109] showed that selective phosphorylation of 5'-nucleotides was possible by using phosphorus oxychloride in the presence of water

and pyridine in acetonitrile. It was discovered that by using a ratio of 2 : 1 : 2 of phosphorus oxychloride, water and pyridine, tetrachloropyrophosphate would be formed *in situ* which would act as the phosphorylating agent (Figure 5.5).

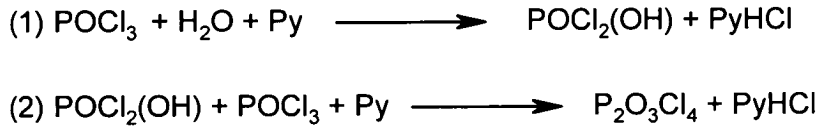

Figure 5.5 *In situ* generation of tetrachloropyrophosphate.[109]

Dichlorophosphoric acid is formed by the reaction of water with phosphorus oxychloride (reaction (1) in Figure 5.5) which then reacts with a further equivalent of phosphorus oxychloride to form tetrachloropyrophosphate (reaction (2) in Figure 5.5). It is this species that dichlorophosphorylates primary alcohols, which are subsequently hydrolysed to the phosphate in the presence of further equivalents of water. The substrates for the reaction were limited to the *N*-BOC protected derivatives, as acetonitrile was the required solvent; hence the reaction was performed using **88**. Monitoring the reaction by TLC and electrospray mass spectrometry, it was initially thought that the reaction had not worked; the TLC only showed base-line spots, and there were no peaks in the mass spectrometry spectrum at 500 and 502 (negative mode) which would have been expected for the BOC-protected phosphorylated product. However, after further inspection of the mass spectrum, peaks at 400 and 402 were found. It was thought that because hydrolysis of the dichlorophosphate would lead to the production of two moles of hydrochloric acid as a side product (as well as the formation of phosphoric acid caused by

hydrolysis of other side products), these highly acidic conditions would facilitate the removal of the BOC group. Therefore, the overall product of this reaction would in fact be 2,5-anhydro-1-deoxy-1-(3,4-dichlorobenzylamino)-D-mannitol-6-phosphate **122** (as shown in Figure 5.6), which corresponds to the peaks identified in the mass spectrum. The reaction was therefore worked up in a manner that would allow for isolation of the aqueous layer. After lyophilisation, the crude product was obtained in a yield of 95 %. However, because this was likely to include the product in a mixture with inorganic salts, it was purified using mass directed methods but led to an overall yield of 5 %.

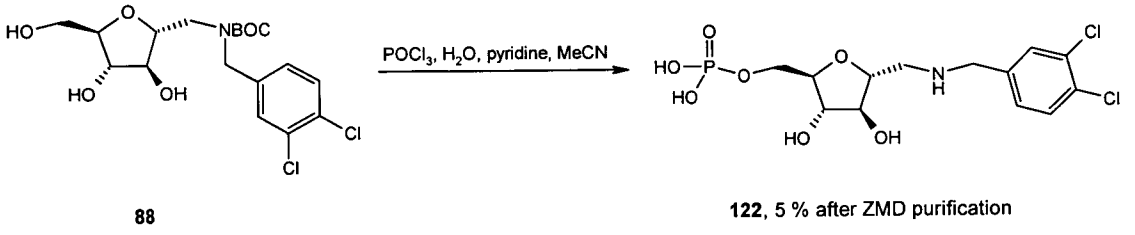

88 **122**, 5 % after ZMD purification

Figure 5.6 Synthesis of 2,5-anhydro-1-deoxy-1-(3,4-dichlorobenzylamino)-D-mannitol-6-phosphate **122**.

The reason for the low yield may not be solely due to loss of material by the purification method (as discussed in Chapter 4), but could also be due to high reactivity of phosphorus oxychloride and all other phosphorus intermediates. Indeed, when this reaction was attempted on a small scale, no product was obtained either for the reaction with **88**, or with **89** (cycloheptyl derivative). This was thought to be due to the fact that the amount of water needed for the formation of the tetrachloropyrophosphate intermediate is so small that it is very difficult to control. Furthermore, all equipment would need to be rigorously dried, which is a practice

that was hoped could be avoided. Due to this reason, and also because phosphorylation of these types of compounds do not necessarily lend themselves towards further development with regards to making drug-like compounds (based on the Lipinski rule of 5[19]), further attempts at phosphorylation were disregarded. Phosphate **122** was tested against *Tb* PFK and the results are shown in section 5.3.

5.2.2 Furanose scaffold modifications.

The furanose scaffold structure for all the inhibitors discussed so far is derived from 2,5-anhydro-D-mannitol and, as has already been shown in Chapter 2, is formed by the synthesis of 2,5-anhydro-D-mannose **22** from the nitrous deamination of D-glucosamine hydrochloride.[61] Aldehyde **22** subsequently undergoes a reductive amination reaction to synthesise the target compound. Therefore, the easiest method by which to obtain inhibitors with a different furanose scaffold would be to repeat the nitrous deamination reaction, but using alternative amino-sugars. This, in itself, is slightly restrictive as the only other commercially available amino-sugars are D-galactosamine hydrochloride and D-mannosamine hydrochloride (Figure 5.7).

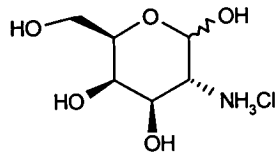

D-Galactosamine hydrochloride

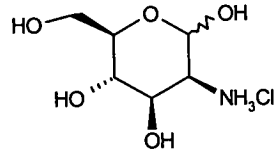

D-Mannosamine hydrochloride

Figure 5.7 Structures of D-galactosamine hydrochloride and D-mannosamine hydrochloride.

The nitrous deamination reaction was attempted with both substrates to synthesise 2,5-anhydro-D-talose **123** and 2,5-anhydro-D-glucose (Figure 5.8). The talose derivative, **123**, was successfully synthesised in a yield of 87 %, and its structure confirmed by comparison of ^{1}H and ^{13}C NMR spectra with previously published spectra.[110] However, the glucose derivative was not formed as analysed by ^{1}H and ^{13}C NMR.

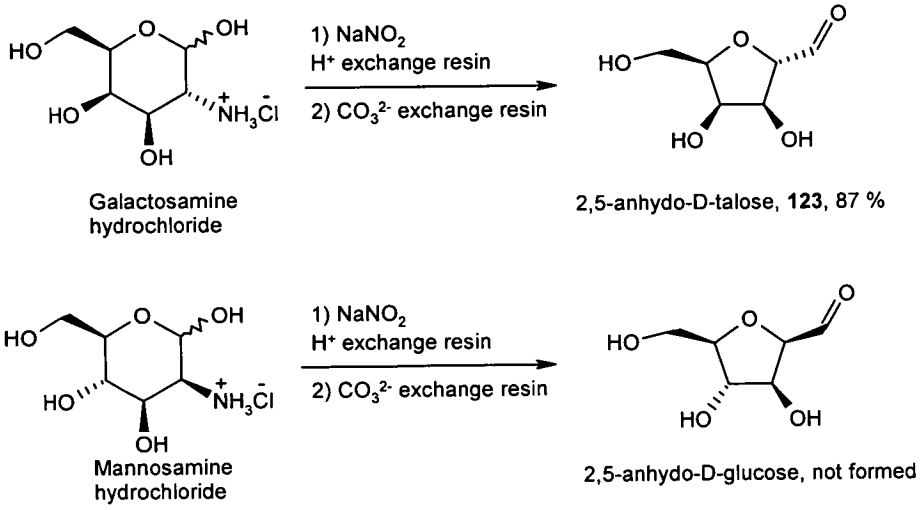

Figure 5.8 Nitrous deamination of amino-sugar substrates.

The reason for this outcome can be potentially explained by revisiting the mechanism for the synthesis of the furanose scaffold. After formation of the diazonium ion, the pyranose oxygen facilitates an intramolecular substitution reaction by rearside attack of the diazonium carbon. In the case where D-glucosamine hydrochloride (Figure 2.4, Chapter 2) and D-galactosamine hydrochloride (Figure 5.9) are the starting materials, this reaction is possible as, in the thermodynamically most stable conformation, the pyranose oxygen is aligned correctly for rearside attack in an S_N2 type manner (Figure 5.9). However, this is not

the case for D-mannosamine hydrochloride; when it has adopted its thermodynamically most stable conformation, rearside attack of the pyranose oxygen is not favoured, as the leaving group (the diazonium ion) is perpendicular to this attack. Therefore, in order for 2,5-anhydro-D-glucose to form, the reaction must proceed via the thermodynamically unstable conformation, caused by a ring flip (Figure 5.9). As the reactions are carried out at temperatures between 0 and 5 °C, it is postulated that 2,5-anhydro-D-glucose would not be formed. Due to this and the expense of the starting material D-mannosamine hydrochloride, this reaction was not pursued any further.

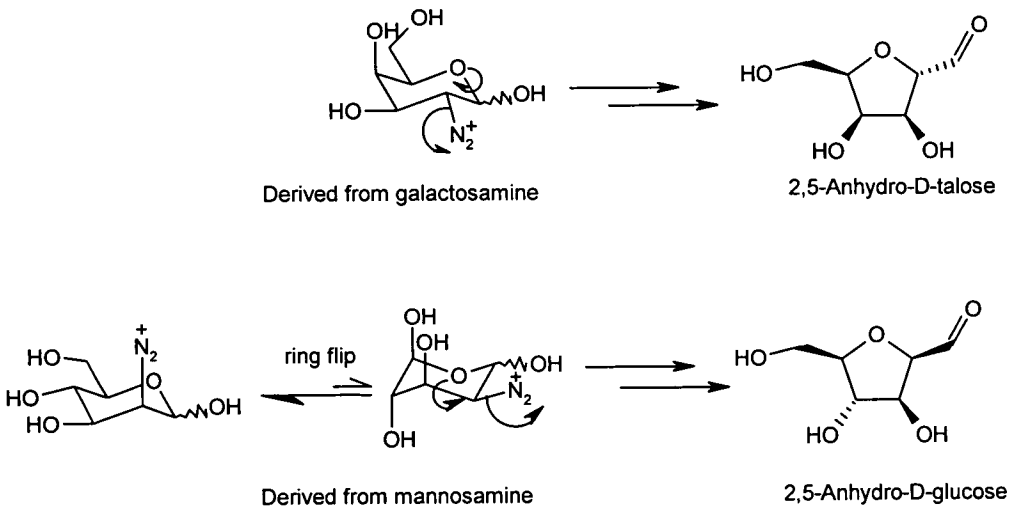

Figure 5.9 Mechanisms of formation of 2,5-anhydro-D-talose and 2,5-anhydro-D-glucose. (See Figure 2.4, Chapter 2, for full mechanism).

Having successfully achieved the synthesis for a different furanose scaffold (in a good yield), this meant that a route to a new family of compounds was available, and a new library could potentially be synthesised. However, partly due to cost and partly due to the fact that the talose structure only differs from the mannose structure by the

opposite stereochemistry of one hydroxyl group at the C3 position, it was decided only to synthesise two compounds. These are shown in Figure 5.10, and correspond to the best inhibitors from the library 1 5 mM screen against *Tb* PFK. It was hoped that this subtle change in stereochemistry would cause either reduced or enhanced activity of the inhibitor.

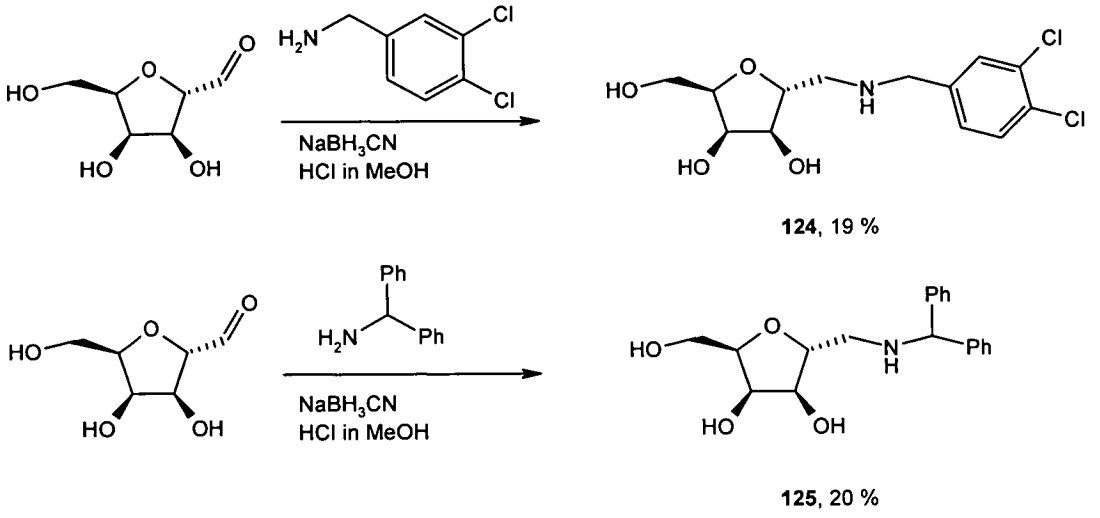

Figure 5.10 Synthesis of 2,5-anhydro-1-deoxy-1-(3,4-dichlorobenzylamino)-D-talitol **124**, and 2,5-anhydro-1-deoxy-1-(benzhydrylamino)-D-talitol **125**.

Both compounds were synthesised successfully using the original reductive amination procedure as described in section 2.2.1, and were purified using mass directed methods. However, both compounds await testing against *Tb* PFK.

5.2.3 Tertiary amine formation.

Until now, all inhibitors that have been synthesised have been secondary amines. In the absence of a crystal structure, and in the interest of determining whether the secondary amine is essential for inhibitor activity against both *Tb* PFK and *Lm* PyK,

it was decided that some tertiary amines should be synthesised, based on existing inhibitor structures. For these reasons, *N*-methylation was chosen as a starting point and any further attempts at *N*-alkylation (or indeed library synthesis) would follow biological evaluation, if needed.

Having had great success using solid supported reagents and scavenging reagents for the reductive amination reaction described in section 4.3.1, it was decided to utilise them again in the synthesis of tertiary amines. In the previous reductive amination reactions, the aldehyde was the limiting reagent and the primary amine was in excess Therefore 4-benzoxybenzaldehyde polystyrene was used to scavenge the excess amine. However, this time a new scavenger amine was needed as the secondary amine would be the limiting reagent and the aldehyde would be in excess. Solid supported tris(2-aminoethyl)amine (Figure 5.11) is known to scavenge carbonyl compounds from solution[93] and hopefully could be employed to scavenge aldehydes, in particular formaldehyde, which would be used for *N*-methylation.

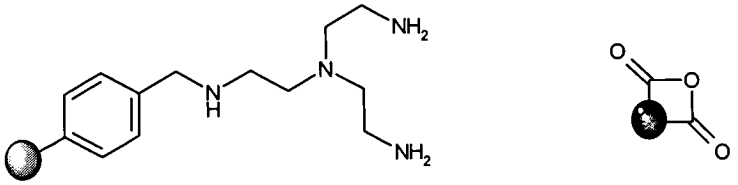

Figure 5.11 Solid supported tris(2-aminoethyl)amine and MP-anhydride resin.

The reaction was carried out using similar conditions to those used previously, although the reaction with solid supported borohydride was allowed to continue for 48 hours as opposed to 24 hours (Figure 5.12). However, monitoring the reaction by

electrospray mass spectrometry showed that not all of the starting material had reacted. Although by using this method of reaction monitoring the amount of starting material cannot be quantified, its presence in the mass spectrum does confirm its presence in the reaction mixture.

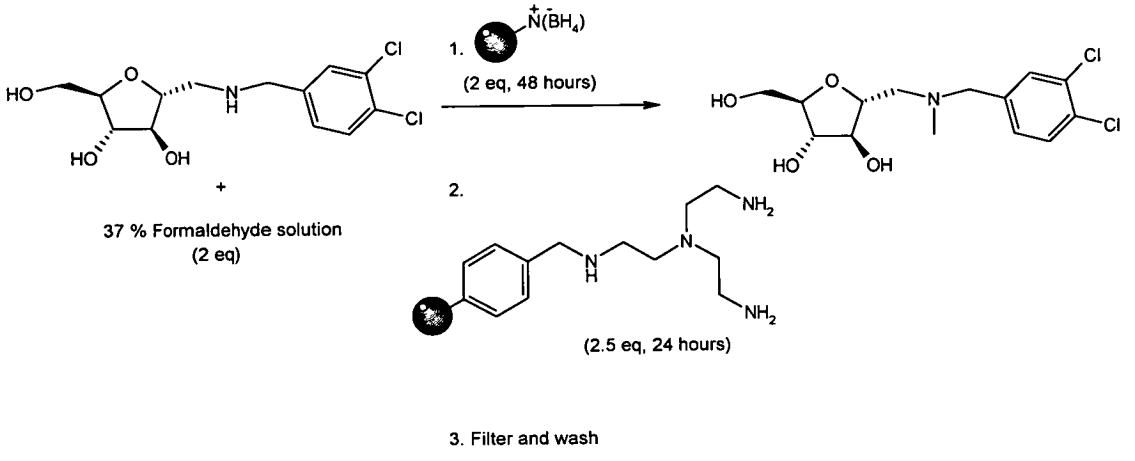

Figure 5.12 Attempted synthesis of *N*-methyl-2,5-anhydro-1-deoxy-(3,4-dichlorobenzylamino)-D-mannitol.

Therefore, an attempt was made to try to remove the starting material using yet another scavenging resin. Previously it was discussed that solid supported 4-benzoxybenzaldehyde resin scavenged for primary amines selectively (Chapter 4). However, in this instance, the starting material is a secondary amine, so the choice in scavenger resin needed to reflect this. MP-Anhydride resin (Figure 5.11) is known to scavenge secondary amines,[90] therefore two equivalents were added to the reaction. However, after a further 120 hours, the mass spectrum still showed a significant peak corresponding to the starting material. After work up (which simply involved filtering, washing and solvent removal), the proton NMR spectrum showed not only a complex pattern (confirming presence of both product and starting material) but

also showed the presence of formaldehyde (δ = 9.6 ppm), indicating that it also had not been scavenged successfully. Therefore, due to this, the high costs of the various resins and the long reaction times, a different approach was investigated.

An alternative method for the methylation of amines is by use of the Eschweiler-Clarke reaction.[111,112] This involves the use of formaldehyde in the presence of formic acid under reflux conditions and has been used successfully in organic synthesis.[113,114] However, recent advances have led to a modification of this procedure whereby the reactions can now be carried out quickly and efficiently using microwave conditions.[115,116] It was therefore decided to attempt *N*-methylation using the modified Eschweiler-Clarke conditions (Figure 5.13).

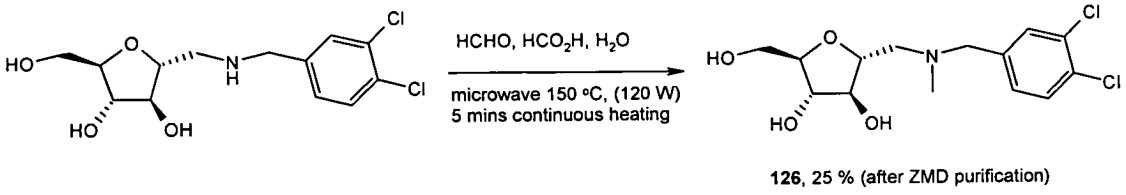

Figure 5.13 Microwave assisted Eschweiler-Clarke synthesis of *N*-methyl-2,5-anhydro-1-deoxy-(3,4-dichlorobenzylamino)-D-mannitol **126**.

After mass directed purification, tertiary amine **126** was isolated with a yield of 25 %. To test this reaction further, *N*-methylation of **70** (cycloheptyl derivative) was attempted, along with the *N*-ethylation of **37** (using acetaldehyde instead of formaldehyde). The results of these reactions are shown in Figure 5.14.

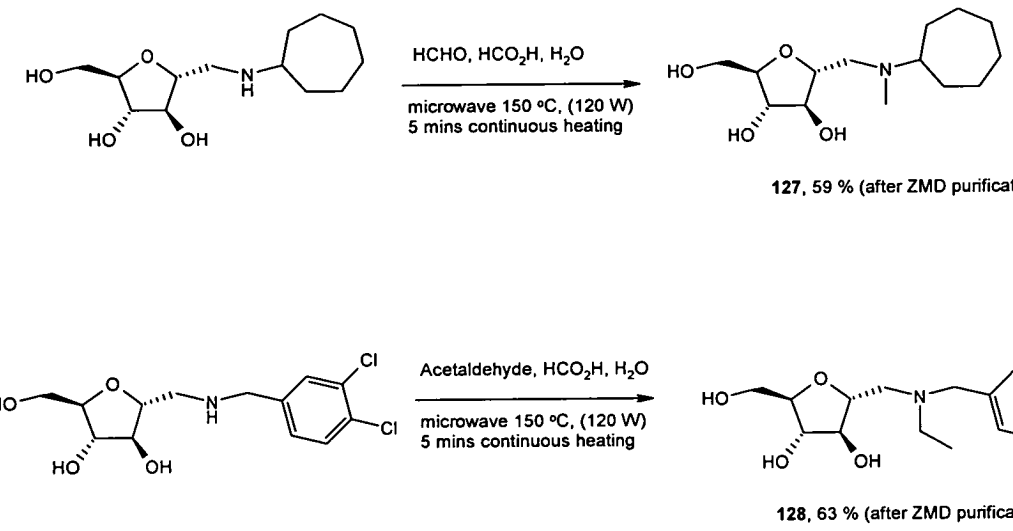

Figure 5.14 Synthesis of *N*-methyl-2,5-anhydro-1-deoxy-1-(cycloheptylamino)-D-mannitol **127** and *N*-ethyl-2,5-anhydro-1-deoxy-1-(3,4-dichlorobenzylamino)-D-mannitol **128**.

Having successfully performed *N*-methylation on both **37** and **70**, and also performed *N*-ethylation on **37**, these results indicate that the microwave assisted Eschweiler-Clarke reaction is an ideal method for the formation of tertiary amines. This process becomes even more attractive when taking in to account the short reaction times, making this method ideal for library synthesis, should the need arise.

Amines **126** and **128** were screened for inhibitory activity against *Tb* PFK and the results are discussed in section 5.3; **127** still awaits testing against *Lm* PyK.

5.3 Biological results for non-library synthesised compounds.

5.3.1 Overview.

Some of the compounds that were synthesised from Chapter 5, along with one other, **42**, that was synthesised as a consequence of the library 1 screening results, were screened (using the 5 mM inhibition screen or obtaining a K_d value) against either *Tb*

PFK or *Lm* PyK. This section reports and comments on these final results, and any other results, that were obtained.

5.3.2 Biological results.

As described in Chapter 2, 2,5-anhydro-1-deoxy-1-(3,4-difluorobenzylamino)-D-mannitol **42**, (Figure 5.15) was synthesised because the library 1 screening results seemed to suggest that this may be a more potent inhibitor of *Tb* PFK than the lead compound, 2,5-anhydro-1-deoxy-1-(3,4-dichlorobenzylamino)-D-mannitol **37**.

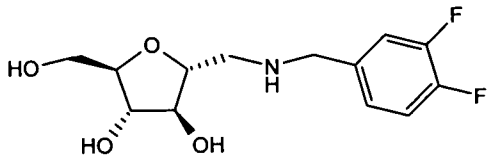

Figure 5.15 2,5-Anhydro-1-deoxy-1-(3,4-difluorobenzylamino)-D-mannitol **42**.

The K_d of **42** was determined for *Tb* PFK[74] and found to be 85 μM. This is a higher value when compared with that of **37** (K_d = 61 μM) and indeed when compared to **32** (K_d = 58 μM). This shows that **42** does not bind as strongly to *Tb* PFK as either **37** or **32**, and therefore is likely to be a poorer inhibitor. Although results from the library 1 screen may have suggested that **42** should be a more potent inhibitor, it still shows that it does indeed bind strongly to the target enzyme. As was mentioned in Chapter 2, trends between the fluoro, methyl and chloro substituted compounds did showed similar activities, whilst no di-substituted fluoro compounds had been tested. This could also account for the reason why **42** is less potent than **37**.

Continuing with K_d values, the value for 2,5-anhydro-1-deoxy-1-(3,4-dichlorobenzylamino)-D-mannitol-6-phosphate **122** against *Tb* PFK was also determined and found to be 110 μM.[74] Again, this is higher than the value for **37**, and indeed for other phosphorylated compounds as investigated by Claustre *et al.*[62] It shows that phosphate **122** is less potent than the **37**, and it is also likely to be less potent than other phosphorylated derivatives as previously discussed (Chapter 2). It also confirms that phosphorylation at the 6-position does not necessarily lead to improvement in inhibition, as alluded to in Chapter 2.

The final biological results are concerned with tertiary amines **126** and **128** (from section 5.2.3). These were screened against *Tb* PFK using the 5 mM screen protocol[82] and are shown in Table 5.1 and Figure 5.16, alongside the results for **37**.

Compound	Percentage (%) remaining activity
37	4.7
126	2.4
128	3.7

Table 5.1 Results of inhibitor screening of amines **126** and **128** against *Tb* PFK compared with compound **37**.[82]

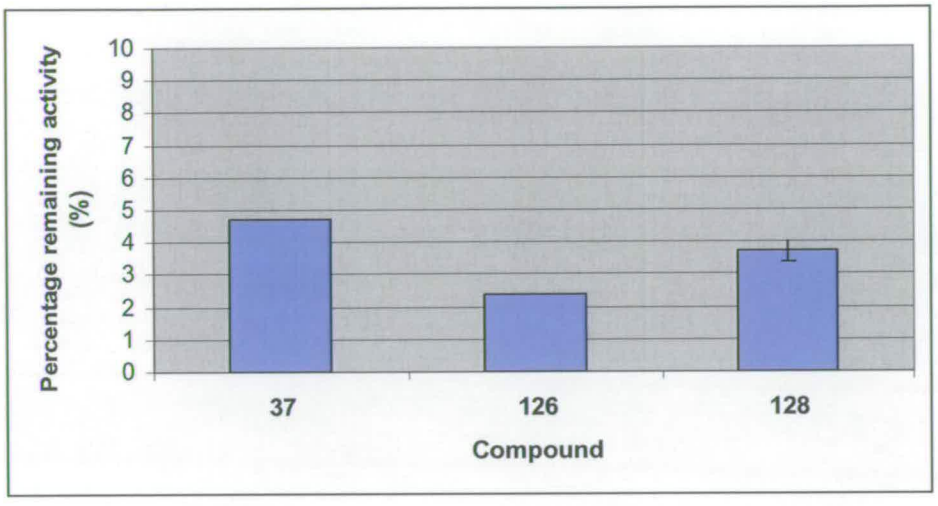

Figure 5.16 A Graph showing the inhibitor screening results for amines **126** and **128** against *Tb* PFK compared with **37**.[82]

The results shown in Table 5.1 and Figure 5.16 shows that inhibition of *Tb* PFK caused by **126** and **128** is similar to that caused by **37**. As the results are low and similar in value, it is difficult to comment further. An IC_{50} value was determined for **126** and was found to be 0.33 mM, an improvement on the IC_{50} value for inhibitor **37** (0.41 mM). This clearly shows that the secondary amine is not essential for inhibitory activity, and the *–NH* appears not to make any hydrogen bonding interactions with the enzyme. Therefore, further synthesis of tertiary amines would be necessary to optimise inhibition, especially using the sugar amino amide inhibitors from library 3.

In the absence of a crystal structure of *Tb* PFK with inhibitors bound, competition experiments were also carried out with **126**[82] to help ascertain whether these compounds compete with F6P or ADP, and therefore indicate the mode of binding. These results[82] are shown in Table 5.2.

Inhibitor	K_M ATP (mM)	K_M F6P (mM)	V_{max} ATP	V_{max} F6P
No inhibitor	0.053	0.29	100	100
126	0.052	1.65	56.9	65.5

Table 5.2 Results of competition experiments of inhibitor **126** against *Tb* PFK. [82]

The competition experiment results show that there is a change in both the K_M and V_{max} values for F6P when incubated with inhibitor **126** (K_M shows a 6-fold increase), whereas for ATP, there is no change in K_M value. This indicates that **126** competes with F6P and is therefore highly likely to bind to the F6P binding site,[82] as was also shown with inhibitor **110** from library 3.

5.3.3 *In vivo* screening results.

In inhibitor design and development, it is important (as has been mentioned earlier) to take in to account factors that may affect bioavailability (such as the Lipinski Rule of 5[19]). However, these are only guidelines and do not guarantee inhibitors or potential drugs to have *in vivo* activity. Therefore, ED_{50} values were determined for four compounds; **37**, the lead against *Tb* PFK from library 1; **70**, the lead against *Lm* PyK from library 2, and two other inhibitors from library 2, **57** and **59**. These results are shown in Table 5.3.[117]

Inhibitor	ED_{50} (mM)
37	0.15
57	0.88
59	0.41
70	1.88

Table 5.3 Results of *in vivo* screening of a selection of inhibitors on trypanosomatid cells.[117]

The results shown in Table 5.3 show that the inhibitors developed do indeed inhibit trypanosomatid cell growth in the *in vivo* assay. It is interesting to note that the best of these inhibitors is **37** with an ED_{50} of 0.15 mM. The results are encouraging as they show that the inhibitors are not only active against their target enzymes, but also show *in vivo* activity which is crucial if further lead and drug development is to be successful.

5.4 Inhibitor specificity.

It is important in the context of drug discovery, design and development that specificity between target and non-target proteins is achieved. Particularly important in the area of infectious disease is the specificity needed between the host and target (in this case parasite) proteins. As was reported in Chapter 1, trypanosomatid glycolytic enzymes are considered ideal targets due to the low similarity with their mammalian counterparts. For obvious reasons, it is undesirable to have a drug that affects the patient as well as the disease, although this has not always been possible for the treatment of trypanosomal diseases.[34,36] In performing the inhibition assays, it is also important that enzymes in the assay couple are not being inhibited by the compounds being tested. This ensures that the results obtained are due to inhibition

of the target enzyme, and not to a side inhibition of enzymes present in the coupled assay.

Therefore, inhibitor **126** was screened against mammalian (rabbit muscle) PFK to ascertain whether it was specific for the trypanosomatid enzyme (see Figure 5.17) and was also tested against the auxiliary enzymes involved in the enzyme couple: these results are also shown in Figure 5.17.

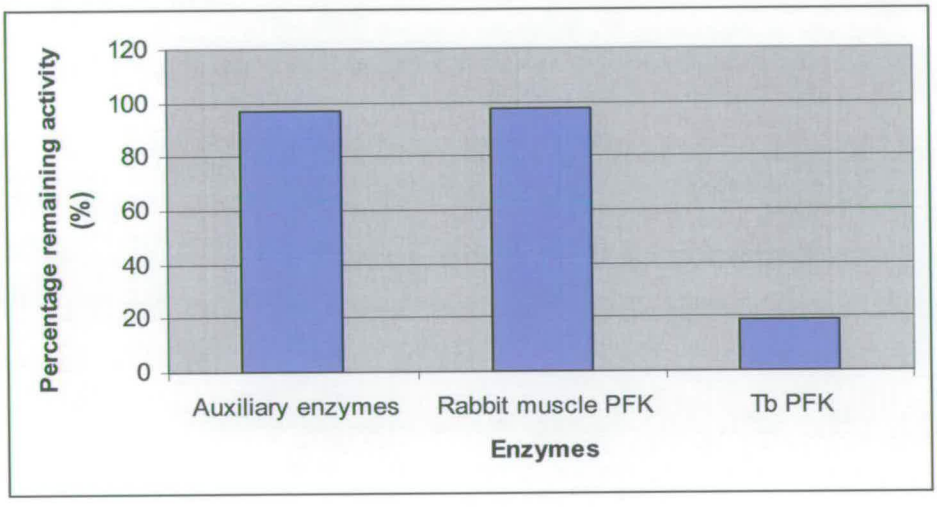

Figure 5.17 Screening results of inhibitor **126** against auxiliary assay and mammalian enzymes (inhibitor concentration = 1 mM, average of 2 results).[75]

It is clear from these results that inhibitor **126** is completely selective for the *Tb* PFK and does not inhibit the mammalian enzyme. Confidence is also gained by the fact that the screening results are solely due to inhibition of *Tb* PFK and cannot be attributed to inhibition of any other enzymes in the assay.

5.5 Overall summary and conclusion.

The primary aim of this research was to improve on already existing inhibitors for *Tb* PFK as well as identifying new inhibitors of *Lm* PyK. Methods to try to achieve this include library synthesis and screening (based on already known inhibitors) and rational inhibitor development.

By means of library design and synthesis, a new lead compound for *Tb* PFK was identified; 2,5-anhydro-1-deoxy-1-(3,4-dichlorobenzylamino)-D-mannitol **37** which has an IC_{50} value of 0.41 mM. Further to this, 2,5-anhydro-1-deoxy-1-(cycloheptylamino)-D-mannitol **70** was identified as a lead compound for the inhibition of *Lm* PyK, with an IC_{50} of 58 μM. A comparison of all the results from the biological screens of the libraries synthesised, allowed for the compilation of structure activity relationships. Competition and *in silico* docking experiments[80] for *Lm* PyK inhibitors suggested that **70** competes with F2,6BP and, therefore, binds to the effector site: potential protein-ligand interactions were also identified.

Further inhibitor development identified four main areas where modification can be achieved. Notably, this lead to the development of a third library, the δ-furanoid sugar amino amides. Biological testing of these compounds against *Tb* PFK showed much improved inhibition and identified a new lead compound, 2,5-anhydro-1-deoxy-1(3,4-dichlorobenzylamino)-D-3,4-dichlorobenzylmannonamide **110**, with an IC_{50} value of 23 μM. Testing of these compounds against *Lm* PyK again showed that the sugar amino amides have at least comparable inhibitory activity compared with **70**, although IC_{50} values have not been determined.

Other areas of inhibitor development identified routes to inhibitors with an alternative sugar scaffold, and with a tertiary amine function (as opposed to a

secondary amine in the case of all the other inhibitors), both of which can be easily adapted for further library synthesis. This led to the identification of the tertiary amine *N*-methyl-2,5-anhydro-1-deoxy-(3,4-dichlorobenzylamino)-D-mannitol **126** as an improved inhibitor of *Tb* PFK, compared with the initial lead compounds **21** and **37**, with an IC_{50} of 0.33 mM. Figure 5.18 shows the progress of lead development, and the structures and results of the main inhibitors.

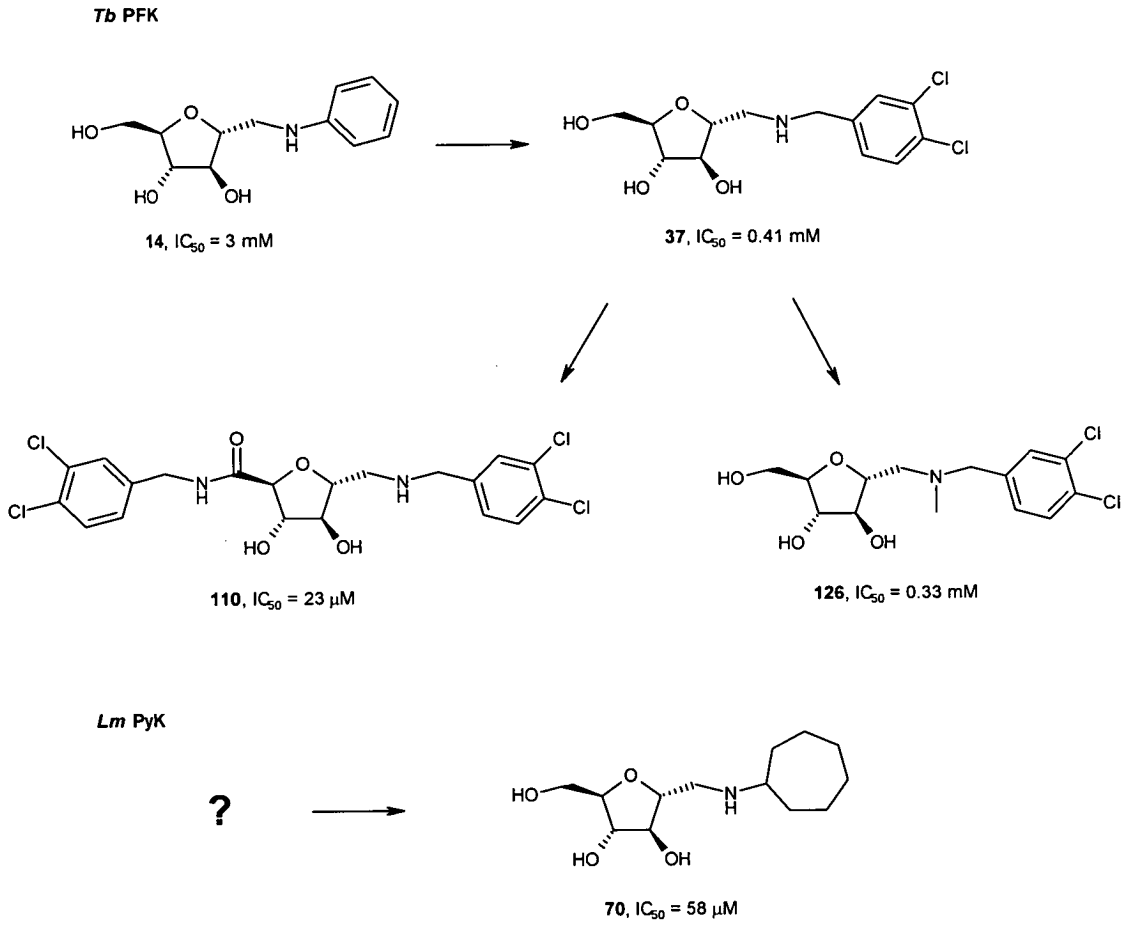

Figure 5.18 A scheme showing the main areas of inhibitor development for both *Tb* PFK and *Lm* PyK.

Finally, specificity experiments had also shown that **126** is specific for the trypanosmatid enzyme, and does not affect the mammalian enzyme.

Overall, not only has the primary objective been achieved, but the way has been paved for further inhibitor design and synthesis, due to the routes developed. All inhibitors fall within the Lipinski rule of 5 boundaries (see appendix), and coupled with the specificity data, make all the inhibitors mentioned, suitable lead compounds for further development.

Chapter 6

Experimental

6 Experimental.

6.1 General techniques.

6.1.1 Instrumentation.

^{1}H and ^{13}C NMR were recorded on Bruker AC 250 or AC 360 instruments. Chemical shifts (δ) are recorded in parts per million (ppm) downfield of tetramethylsilane and were referred to residual undeuterated solvent present in the deuterated solvent of the sample (e.g. CH_3OH in CD_3OD).

Electrospray ionisation mass spectroscopy (ESI) was carried out on a Micromass VG Platform II instrument. Solvents used were either water or acetonitrile : water (1 : 1, 0.1 % acetic acid) in either positive or negative scan modes. Fast Atom Bombardment (FAB) high resolution mass spectra were recorded on a Kratos MS50TC instrument.

Infra-red absorption spectroscopy was performed on a Perkin-Elmer FT-IR Paragon 1000 spectrometer, and ν_{max} values are quoted in cm^{-1}.

Optical rotations were performed at room temperature on an AA1000 polarimeter from Optical Activity Ltd (measurements made at the sodium D-line). Concentrations are given in g/100ml.

Thin layer chromatography was performed on Merck DC-Alufolien Kieselgel $60F_{245}$ 0.2 mm pre-coated plates. Components were visualised by u.v. fluorescence or by potassium permanganate or ninhydrin stains.

Melting points were obtained on Gallenkamp melting point apparatus.

Parallel synthesis was peformed using the following instruments: Bohdan Neptune reagent dispenser, Bohdan MiniBlock Synthesiser and shaker, and Christ β-RVC

solvent evaporator.

Microwave synthesis was performed using the CEM Discover microwave and Explorer autosampler.

Mass directed purification was carried out on a Waters ZMD mass spectrometer with Waters 600 HPLC using MassLynx version 3.5 and FractionLynx software. The HPLC column used was a Waters Xterra, C18, 60 x 21.20 mm, 5 u microns.

Parallel flash column chromatography was carried out using Quad3 parallel purification system using pre-packed columns.

6.1.2 Mass directed purification methods.

All samples for purification were made to ca 50 mg/ml in acetonitrile : water (1 : 1, 0.1 % acetic acid). A flow rate of 20 ml/min was used, and the sample injection volume was 500 µl. The following methods were used sample elution:

ZMD Method 1.

Positive ion mode, CV = 25

Run time = 12 minutes.

Time (minutes)	Water, (0.1 % TFA) %	MeCN (%)
0	98	2
1	98	2
9	70	30
10	98	2
12	98	2

ZMD Method 1a.

Negative ion mode, CV = 25

Run time = 12 minutes.

Time (minutes)	Water, (0.1 % TFA) %	MeCN (%)
0	98	2
1	98	2
9	70	30
10	98	2
12	98	2

ZMD Method 2.

Run time = 12 minutes

Time (minutes)	10 mM $NH_4(HCO_3)$, %	MeCN (%)
0	98	2
1	98	2
9	70	30
10	98	2
12	98	2

ZMD Method 2a.

Run time = 16 minutes

Time (minutes)	10 mM $NH_4(HCO_3)$, %	MeCN (%)
0	98	2
1	98	2
14	70	30
16	98	2

ZMD Method 2b.

Run time = 20 minutes

Time (minutes)	10 mM $NH_4(HCO_3)$, %	MeCN (%)
0	98	2
1	98	2
17	70	30
18	98	2
20	98	2

ZMD Method 2c.

Run time = 26 minutes

Time (minutes)	10 mM $NH_4(HCO_3)$, %	MeCN (%)
0	98	2
1	98	2
24	70	30
26	98	2

6.2 Library 1: Design, Synthesis and Evaluation.

6.2.1 Synthesis of 2,5-anhydro-D-mannose, 22.[61]

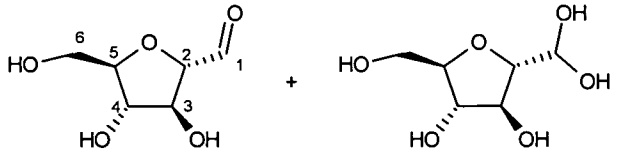

D-Glucosamine hydrochloride (2.0 g) was dissolved in water (50 ml) and stirred at 0 °C for approximately 5 hours. Sodium nitrite (1.6 g, 2.5 eq.) was then added, followed by cautious addition of Amberlite 120 H^+ resin (47 ml), maintaining the temperature between 0 – 5 °C. The reaction was then left to stir at 0 °C for 18 hours before the resin was removed by filtration. The solution was then neutralised by portion-by-portion addition of Dowex CO_3^{2-} resin. The resin was removed by

filtration and the remaining solution was lyophilised to yield the title compound as a pale yellow hygroscopic solid (1.33 g, 88%).

$R_f = 0.42$,[63] CH_2Cl_2 : MeOH (8 : 2)

^{1}H NMR (250 MHz, D_2O), δ (ppm): 3.50 – 3.75 (3H, m, H-2, 2 x H-6), 3.78 – 3.86 (1H, m, H-5), 3.95 (1H, t, $J_{4,3}$ = $J_{4,5}$ = 5.5 Hz, H-4), 4.10 (1H, t, $J_{3,4}$ = $J_{3,2}$ = 5.5 Hz, H-3), 5.00 (1H, d, $J_{1,2}$ = 5.5 Hz, H-1 gem-diol), 8.35 (s, H-1 aldehyde).

^{13}C NMR (63 MHz, D_2O), δ (ppm): 61.2 (C6), 76.8 (C4), 77.8 (C3), 83.2 (C5), 84.6 (C2), 90.0 (C-1 gem-diol).

6.2.2 Synthesis of 2,5-anhydro-1-deoxy-1-phenylamino-D-mannitol, 14.[61]

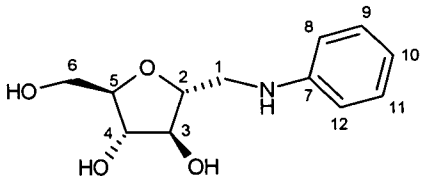

Sodium cyanoborohydride (0.15 g, 0.7 eq.) was added to a solution of **22** (0.55 g, 1 eq.) and aniline (0.29 ml, 1 eq.) in methanol (10 ml). The solution was stirred for 2 hours maintained at pH 6, by dropwise addition of HCl (0.5 M) in methanol. The solvent was then removed under reduced pressure, and the resulting residue was dissolved in acetonitrile : water (1 : 1, 0.1 % acetic acid) and purified using mass directed purification (ZMD Method 1). Removal of the solvent by lyophilisation afforded the title compound as an off-white solid (0.41 g, 50 %).

^{1}H NMR (250 MHz, CD_3OD), δ (ppm): 3.23 (1H, dd, J_{gem} = 13.0 Hz, $J_{1a,2}$ = 7.0 Hz, 1 x H-1), 3.36 (1H, dd, J_{gem} = 13.0 Hz, $J_{1b,2}$ = 3.5 Hz, 1 x H-1), 3.65 (1H, dd, J_{gem} =

12.0 Hz, $J_{5,6a}$ = 5.61, 1 x H-6), 3.70 (1H, dd, J_{gem} = 12.0 Hz, $J_{5,6b}$ = 3.5 Hz, 1 x H-6), 3.93 – 3.98 (1H, m, H-5), 4.01 - 10 (3H, m, H-2, H-3, H-4), 6.65 – 6.85 (3H, m, H-9, H-10, H-11), 7.15 – 7.25 (2H, m, H-8, H-12).

^{13}C NMR (63 MHz, CD_3OD), δ (ppm): 46.2 (C1), 62.2 (C6), 77.9 (C4), 79.5 (C3), 82.1 (C2), 84.1 (C5), 113.1 (C9, C11), 117.2 (C10), 128.9 (C8, C12), 149.0 (C7).

ESI$^+$: $[M + H]^+$ = 240.2

6.2.3 Synthesis of 2,5-anhydro-1-deoxy-1-benzylamino-D-mannitol, 15.[61]

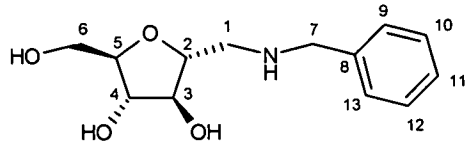

Sodium cyanoborohydride (0.23 g, 0.7 eq.) was added to a solution of **22** (0.87 g, 1 eq.) and benzylamine (0.59 ml, 1 eq.) in methanol (15 ml). The solution was stirred 2 hours at pH 6, maintained by dropwise addition of HCl (0.5 M) in methanol. The solvent was then removed under reduced pressure and the resulting residue was dissolved in acetonitrile:water (1:1, 0.1 % acetic acid) and purified using mass directed purification (ZMD Method 1). Removal of the solvent by lyophilisation afforded the title compound as a white solid (1.30 g, 96 %).

^{1}H NMR (250 MHz, CD_3OD), δ (ppm): 2.73 (1H, dd, J_{gem} = 12.5 Hz, $J_{1a,2}$ = 7.5 Hz, 1 x H-1), 2.82 (1H, dd, J_{gem} = 12.5 Hz, $J_{1b,2}$ = 3.59 Hz, 1 x H-1), 3.58 – 3.75 (3H, m, H-2, 2 x H-6), 3.77 – 3.83 (3H, m, H-5, 2 x H-7), 3.89 – 3.97 (2H, m, H-3, H-4), 7.10 – 7.30 (5H, m, H-9 to H-13).

^{13}C NMR (63 MHz, CD_3OD), δ (ppm): 43.1 (C1), 51.2 (C7), 61.9 (C6), 77.4 (C4),

79.5 (2C, C2, C3), 85.2 (C5), 128.8 – 129.9 (5C, C9 to C13), 131.3 (C8).

ESI^+: $[M + Na]^+ = 276.1$

6.2.4 Procedure for the synthesis of *N*-aryl-1-amino-2,5-anhydro-1-deoxy-1-D-mannitols using parallel synthetic method: A 4-membered test library.

Using the Bohdan Neptune reagent manager, a methanolic solution of **22** (0.35 M, 1 eq.) was added to four, 2 ml reactors, contained within the Bohdan MiniBlock synthesiser. An arylamine (1 eq.) was then added to each reactor. The MiniBlock synthesiser was then shaken for 20 minutes before addition of a methanolic solution of sodium borohydride (2.4 M, 0.7 eq.). HCl in methanol (0.5 M) was added dropwise to each reactor so that each solution was maintained at pH 6. The Mini-Block was shaken for a further 30 minutes. The pH was again adjusted (if necessary) by dropwise addition of HCl in methanol (0.5 M). The MiniBlock was then shaken for a further 90 minutes, checking the pH of the reactors every 30 minutes. The reaction mixtures where then transferred to a microtitre plate and the solvent removed under vacuum. The residues were then dissolved in acetonitrile : water (1 : 1, 0.1 % acetic acid) and purified using mass directed purification.

6.2.4.1 2,5-Anhydro-1-deoxy-1-phenylamino-D-mannitol, 14.[61]

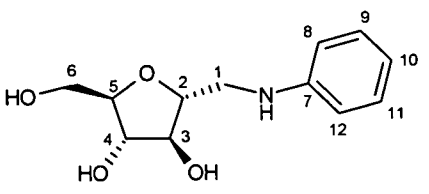

From aniline, using ZMD Method 1, gave **14** as a brown solid (20 %).

6.2.4.2 2,5-Anhydro-1-deoxy-1-benzylamino-D-mannitol, 15.[61]

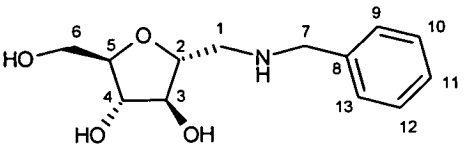

From benzylamine, using ZMD Method 1, gave **15** as a yellow oil (30 %).

6.2.4.3 2,5-Anhydro-1-deoxy-1-(m-carboxyl-phenylamino)-D-mannitol, 16.[61]

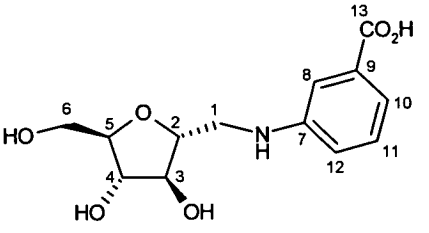

From *m*-aminobenzoic acid, using ZMD method 1a, gave **16** as a yellow oil (20 %).

^{1}H NMR (250 MHz, CD_3OD), δ (ppm): 3.38 – 3.42 (2H, m, 2 x H-1), 3.60 – 3.90 (3H, m, H-2, 2 x H-6), 4.00 – 4.10 (1H, m, H-5), 4.10 – 4.25 (2H, m, H-3, H-4), 7.45 – 7.60 (1H, m, H-12), 7.70 – 7.90 (1H, m, H-11), 8.15 – 8.3 (2H, m, H-8, H-10).

^{13}C NMR (63 MHz, CD_3OD), δ (ppm): 45.9 (C1), 62.2 (C6), 77.9 (C4), 79.4 (C3), 82.0 (C2), 84.1 (C5), 113.5 (C8), 117.0 (C10), 118.2 (C12), 128.8 (C11), 133.0 (C9), 151.1 (C7), 169.0 (C13).

ESI$^-$: $[M - H]^-$ = 282.0 (exp. 282.3).

6.2.4.4 2,5-Anhydro-1-deoxy-1-(m-nitrophenylamino)-D-mannitol, 17.[61]

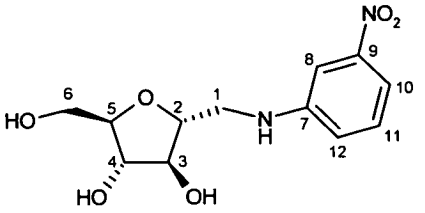

From 3-nitroaniline, using ZMD Method 1a, gave **17** as yellow solid (50%).

^{1}H NMR (250 MHz, CD_3OD), δ (ppm): 3.38 (2H, 2dd, J_{gem} = 14.5 Hz, $J_{1a,2}$ = 6.0 Hz, $J_{1b,2}$ = 3.5 Hz, 2 x H-1), 3.68 (2H, 2dd, J_{gem} = 12.0 Hz, $J_{5,6a}$ = 5.5 Hz, $J_{5,6b}$ = 3.5 Hz, 2 x H-6), 3.83 – 3.90 (1H, m, H-2), 3.93 – 4.03 (3H, m, H-3, H-4, H-5), 6.95 – 7.05 (1H, m, H-10), 7.20 – 7.32 (1H, m, H-11), 7.38 – 7.48 (2H, m, H-8, H-12).

^{13}C NMR (63 MHz, CD_3OD), δ (ppm): 44.6 (C1), 61.3 (C6), 76.9 (C4), 78.4 (C3), 81.2 (C2), 83.3 (C5), 107.4 (C8), 110.4 (C10), 119.5 (C12), 120.9 (C11), 149.0 – 149.5 (2C, C7, C9).

ESI$^-$: $[M - H]^-$ = 283.1 (exp. 283.2).

6.2.5 Synthesis of library 1: *N*-benzyl-1-amino-2,5-anhydro-1-deoxy-D-mannitol derivatives.

Using the Bohdan Neptune reagent manager, a methanolic solution of **22** (0.7 M) was added to 17 x 2 ml reactors each containing a benzylamine derivative (100 mg, pre-weighed by Sigma-Aldrich Filling Station) in equimolar quantities. The Bohdan MiniBlock synthesiser that contained the reactors was then shaken for 15 minutes. Sodium cyanoborohydride in methanol (2.4 M, 0.7 eq.) was added to each reactor, before adjusting the pH to 6 by dropwise addition of HCl in methanol (0.5 M). The

MiniBlock was then shaken for a further 2 hours, monitoring the pH of each reactor, and adjusting the pH if necessary. The reaction mixtures were then transferred to a microtitre plate and the solvent removed under reduced pressure. The residues were dissolved in acetonitrile : water (1:1, 0.1 % acetic acid) and purified using mass directed purification (ZMD Method 1).

6.2.5.1 2,5-Anhydro-1-deoxy-1-(2,4-dichlorobenzylamino)-D-mannitol, 25.

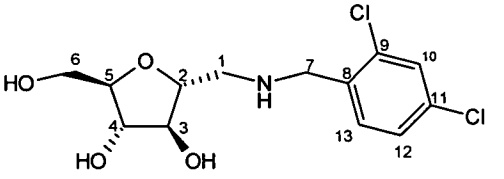

From 2,4-dichlorobenzylamine, yield = 28 mg, 15 %.

^{1}H NMR (250 MHz, CD_3OD), δ (ppm): 3.30 – 3.37 (2H, m, 2 x H-1), 3.70 (2H, 2dd, J_{gem} = 11.5 Hz, $J_{5,6a}$ = 5.5 Hz, $J_{5,6b}$ = 3.5 Hz, 2 x H-6), 3.89 – 34.02 (3H, m, H-2, H-3, H-5), 4.17 – 4.27 (3H, m, H-4, 2 x H-7), 7.28 – 7.57 (3H, m, Ar-H).

^{13}C NMR (63 MHz, CD_3OD), δ (ppm): 39.2 (C1), 48.1 (C7), 61.2 (C6), 76.7 (C4), 78.9 (C3, C2), 84.9 (C5), 127 – 131 (3C, C10, C12, C13), 132 – 135 (2C, C9, C11).

ESI$^+$: $[M + H]^+$ = 322.0 [^{35}Cl – ^{35}Cl].

6.2.5.2 2,5-Anhydro-1-deoxy-1-(3-chlorobenzylamino)-D-mannitol, 26.

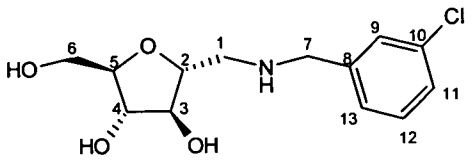

From 3-chlorobenzylamine, yield = 14 mg, 7 %.

^{1}H NMR (250 MHz, CD_3OD), δ (ppm): 3.01 – 3.15 (2H, m, 2 x H-1), 3.47 – 4.11 (8H, m, H-2, H-3, H-4, H-5, 2 x H-6, 2 x H-7), 7.01 – 7.47 (4H, m, 4 x Ar-H).

ESI$^+$: $[M + H]^+$ = 288.0 [^{35}Cl], 289.9 [^{37}Cl].

6.2.5.3 2,5-Anhydro-1-deoxy-1-(4-chlorobenzylamino)-D-mannitol, 27.

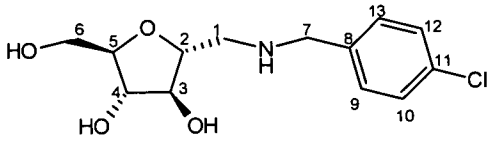

From 4-chlorobenzylamine, yield = 15 mg, 7 %.

^{1}H NMR (250 MHz, CD_3OD), δ (ppm): 3.30 – 3.35 (2H, m, 2 x H-1), 3.73 (2H, 2dd, J_{gem} = 12.0 Hz, $J_{5,6a}$ = 6.0 Hz, $J_{5,6b}$ = 3.0 Hz, 2 x H-6), 3.95 – 4.07 (3H, m, H-2, H-3, H-5), 4.16 – 4.79 (3H, m, H-4, 2 x H – 7), 7.49 – 7.68 (4H, m, 4 x Ar-H).

ESI$^+$: $[M + H]^+$ = 288.0 [^{35}Cl], 290.1 [^{37}Cl].

6.2.5.4 2,5-Anhydro-1-deoxy-1-(2-chlorobenzylamino)-D-mannitol, 28.

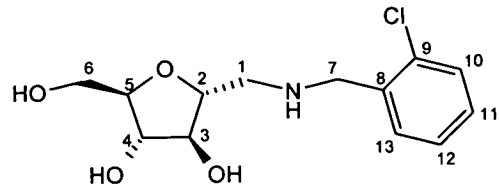

From 2-chlorobenzylamine, yield = 12 mg, 6 %.

^{1}H NMR (250 MHz, CD_3OD), δ (ppm): 3.37 – 3.40 (2H, m, 2 x H-1), 3.62 – 3.80 (3H, m , H-3, 2 x H-6), 3.97 – 4.09 (2H, m, H-2, H-5), 4.32 – 4.49 (3H, m, H-4, 2 x H-7), 7.44 – 7.57 (4H, m, 4 x Ar-H).

ESI$^+$: $[M + H]^+$ = 288.1 [^{35}Cl], 290.1 [^{37}Cl].

6.2.5.5 2,5-Anhydro-1-deoxy-1-(4-methylbenzylamino)-D-mannitol, 29.

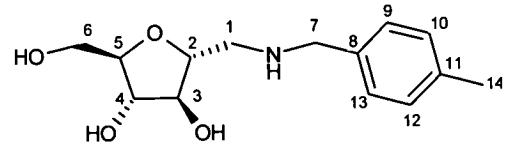

From 4-methylbenzylamine, yield = 82 mg, 37 %.

^{1}H NMR (250 MHz, CD_3OD), δ (ppm): 2.33 (3H, s, 3 x H-14), 3.26 – 3.29 (2H, m, 2 x H-1), 3.76 – 3.80 (3H, m, H-3, 2 x H-6), 3.95 – 4.26 (5H, m, H-2, H-4, H-5, 2 x H-7), 7.22 – 7.51 (4H, m, Ar-H).

ESI$^+$: $[M + H]^+$ = 268.0.

6.2.5.6 2,5-Anhydro-1-deoxy-1-(3-methylbenzylamino)-D-mannitol, 30.

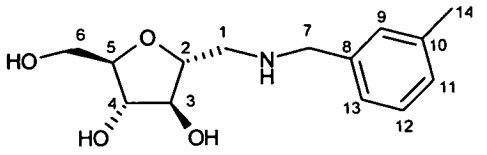

From 3-methylbenzylamine, yield = 80 mg, 36 %.

^{1}H NMR (250 MHz, CD_3OD), δ (ppm): 2.33 (3H, s, 3 x H-14), 3.27 – 3.28 (2H, m, 2 x H-1), 3.61 – 3.72 (3H, m, H-3, 2 x H-6), 3.91 – 4.23 (5H, m, H-2, H-4, H-5, 2 x H-7), 7.17 – 7.38 (4H, m, Ar-H).

ESI^+: $[M + H]^+ = 268.0$.

6.2.5.7 2,5-Anhydro-1-deoxy-1-(2-methylbenzylamino)-D-mannitol, 31.

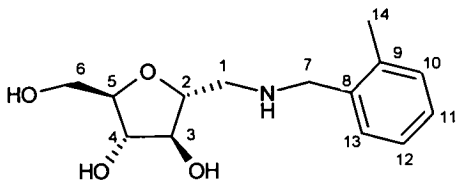

From 2-methylbenzylamine, yield = 179 mg, 81 %.

^{1}H NMR (250 MHz, CD_3OD), δ (ppm): 2.45 (3H, s, H-14), 3.32 – 3.37 (2H, m, 2 x H-1), 3.67 – 3.75 (3H, m, H-3, 2 x H-6), 3.95 – 4.05 (2H, m, H-2, H-5), 4.18 – 4.42 (3H, m, H-4, 2 x H-7), 7.26 – 7.49 (4H, m, Ar-H).

^{13}C NMR (63 MHz, CD_3OD), δ (ppm): 17.5 (Me), 39.6 (C1), 47.6 (C7), 61.0 (C6), 76.5 (C4), 78.4 (C3), 78.7 (C2), 84.1 (C5), 128.3 – 130.2 (4C, C10 – C13), 136.2 – 137.0 (2C, C8, C9).

ESI$^+$: $[M + H]^+$ = 268.0 (exp. 268.3).

6.2.5.8 2,5-Anhydro-1-deoxy-1-(benzhydrylamino)-D-mannitol, 32.

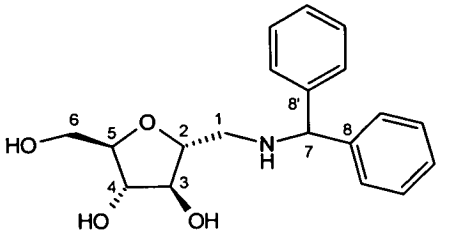

From benzhydrylamine, yield = 32 mg, 18 %.

^{1}H NMR (250 MHz, CD_3OD), δ (ppm): 3.20 – 3.23 (2H, m, 2 x H-1), 3.67 – 3.80 (3H, m, H-3, 2 x H-6), 3.92 – 3.97 (2H, m, H-2, H-4), 4.14 – 4.17 (1H, m, H-5), 5.64 (1H, s, H-7), 7.41 – 7.53 (10H, m, Ar-H).

^{13}C NMR (63 MHz, CD_3OD), δ (ppm): 48.0 (C1), 61.2 (C6), 65.2 (C7), 76.7 (C4), 78.9 (C2 and C3), 84.6 (C5), 126.4 – 128.6 (10C, 10 x ArC-H), 135.0 – 136.7 (2C, C8, C8′).

ESI$^+$: $[M + H]^+$ = 330.2.

6.2.5.9 2,5-Anhydro-1-deoxy-1-(trifluoromethylbenzylamino)-D-mannitol, 33.

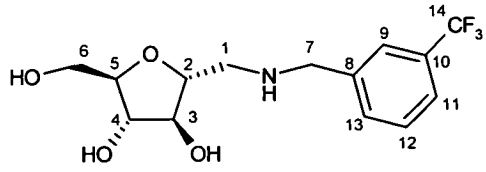

From trifluoromethyl benzylamine, yield = 80 mg, 36 %.

^{1}H NMR (250 MHz, CD_3OD), δ (ppm): 3.31 – 3.36 (2H, m, 2 x H-1), 3.67 – 4.05 (5H, m, H-2, H-3, H-4, 2 x H-6), 4.19 – 4.41 (3H, m, H-5, 2 x H-7), 7.42 – 7.98 (4H, m, Ar-H).

6.2.5.10 2,5-Anhydro-1-deoxy-1-(2-fluorobenzylamino)-D-mannitol, 34.

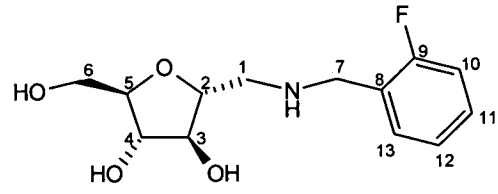

From 2-fluorobenzylamine, yield = 184 mg, 85 %.

^{1}H NMR (250 MHz, CD_3OD), δ (ppm): 3.38 – 3.41 (2H, m, 2 x H-1), 3.72 – 3.87 (3H, m, H-3, 2 x H-6), 4.02 – 4.02 (2H, m, H-2, H-4), 4.41 – 4.56 (3H, m, H-5, 2 x H-7), 7.39 – 7.77 (4H, m, Ar-H).

^{13}C NMR (63 MHz, CD_3OD), δ (ppm): 43.7 (C1), 48.1 (C7), 60.7 (C6), 76.1 (C4), 78.0 (C3), 78.3 (C2), 83.5 (C5), 115.1 – 131.5 (5C, ArC), 158.6 (ArC-F).

^{19}F NMR (235 MHz, CD_3OD), δ (ppm): -78.3.

ESI^+: $[M + H]^+ = 272.1$.

6.2.5.11 2,5-Anhydro-1-deoxy-1-(4-fluorobenzylamino)-D-mannitol, 35.

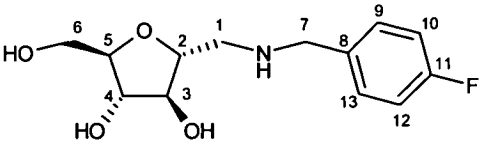

From 4-fluorobenzylamine, yield = 139 mg, 64 %.

^1H NMR (250 MHz, CD_3OD), δ (ppm): 3.12 - 3.27 (2H, m, 2 x H-1), 3.63 – 3.72 (3H, m, H-3, 2 x H-6), 3.89 – 3.98 (2H, m, H-2, H-4), 4.10 – 4.25 (3H, m, H-5, 2 x H-7), 7.08 – 7.18 (2H, m, H-10, H-12), 7.44 – 7.57 (2H, m, H-9, H-13).

^{13}C NMR (63 MHz, CD_3OD), δ (ppm): 41.9 (C1), 49.9 (C7), 61.0 (C6), 76.4 (C4), 78.1 (C3), 78.5 (C2), 83.6 (C5), 115.5 (2C, C10, C12), 128.4 (C8), 130.7 – 131.9 (2C, C9, C13), 164.6 (C11).

^{19}F NMR (235 MHz, CD_3OD), δ (ppm): -76.6.

ESI^+: $[M + H]^+ = 271.9$.

6.2.5.12 2,5-Anhydro-1-deoxy-1-(3-fluorobenzylamino)-D-mannitol, 36.

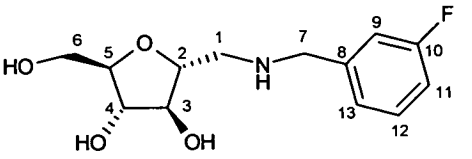

From 3-fluorobenzylamine, yield = 44 mg, 20 %.

^{1}H NMR (250 MHz, CD_3OD), δ (ppm): 3.17 – 3.47 (2H, m, 2 x H-1), 3.63 – 4.03 (5H, m, H-2, H-3, H-4, 2 x H-6), 4.17 – 4.32 (3H, m, H-5, 2 x H-7), 7.17 – 7.36 (3H, m, H-9, H-11, H-13), 7.44 – 7.50 (1H, m, H-12).

ESI^+: $[M + H]^+ = 272.1$.

6.2.5.13 2,5-Anhydro-1-deoxy-1-(3,4-dichlorobenzylamino)-D-mannitol, 37.

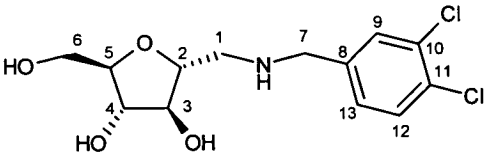

From 3,4-dichlorobenzylamine, yield = 12 mg, 7 %.

$[\alpha]_D$ = + 5.7 ° (*c* 0.7, MeOH).

^{1}H NMR (250 MHz, CD_3OD), δ (ppm): 2.72 (1H, dd, J_{gem} = 12.5 Hz, $J_{1a,2}$ = 7.5 Hz, H-1a), 2.79 (1H, dd, J_{gem} = 12.5 Hz, $J_{1b,2}$ = 3.5 Hz, H-1b), 3.61 – 4.03 (8H, m, H-2, H-3, H-4, H-5, 2 x H-6, 2 x H-7), 7.24 (1H, dd, $J_{12,13}$ = 8.0 Hz, $J_{9,13}$ = 2.0 Hz, H-13), 7.40 (1H, d, $J_{12,13}$ = 8.0 Hz, H-12), 7.58 (1H, d, $J_{9,13}$ = 2.0 Hz, H-9).

^{13}C NMR (63 MHz, CD_3OD), δ (ppm): 50.1 (C1), 51.3 (C7), 61.5 (C6), 76.9 (C2), 79.2 (C5), 81.7 (C4), 83.5 (C3), 127.4 – 129.6 (3C, C9, C12, C13), 129.9 – 131.3 (2C, C10, C11), 139.9 (C8).

ESI$^+$: $[M + H]^+ = 322.1$ [$^{35}Cl - ^{35}Cl$].

HRMS FAB (+ve) found m/z = 322.06074 and 324.05862 $[M + H]^+$, $C_{13}H_{18}NO_4Cl_2$ requires 322.06129 (2 x ^{35}Cl) and 324.05834 ($^{35}Cl + ^{37}Cl$).

Decomposes > 190 °C.

6.2.5.14 2,5-Anhydro-1-deoxy-1-(2,5-dimethylbenzylamino)-D-mannitol, 38.

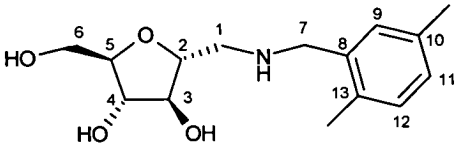

From 2,5-dimethylbenzylamine, yield = 42 mg, 20 %.

^1H NMR (250 MHz, CD_3OD), δ (ppm): 2.24 (3H, s, ArC**H**$_3$), 2.29 (3H, s, ArC**H**$_3$), 3.19 – 3.30 (2H, m, 2 x H-1), 3.56 (1H, dd, J_{gem} = 11.5 Hz, $J_{5,6a}$ = 5.5 Hz, H-6a), 3.64 (1H, dd, J_{gem} = 11.5 Hz, $J_{5,6b}$ = 3.5 Hz, H-6b), 3.80 (1H, t, $J_{2,3} = J_{3,4}$ = 4.5 Hz, H-3), 3.83 – 3.97 (2H, m, H-2, H-4), 3.98 – 4.19 (3H, m, H-5, 2 x H-7), 7.00 – 7.24 (3H, m, Ar-H).

ESI$^+$: $[M + H]^+ = 282.1$.

6.2.5.15 2,5-Anhydro-1-deoxy-1-(2,4-dimethylbenzylamino)-D-mannitol, 39.

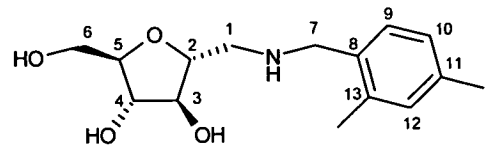

From 2,4-dimethylbenzylamine, yield = 81 mg, 39%.

^{1}H NMR (250 MHz, CD_3OD), δ (ppm): 2.32 (3H, s, ArC**H**$_3$), 2.39 (3H, s, ArC**H**$_3$), 3.31 – 3.35 (2H, m, 2 x H-1), 3.68 (1H, dd, J_{gem} = 11.5 Hz, $J_{5,6a}$ = 5.5 Hz, H-6a), 3.76 (1H, dd, J_{gem} = 11.5 Hz, $J_{5,6b}$ = 3.5 Hz, H-6b), 3.93 – 4.06 (3H, m, H-2, H-3, H-4), 4.12 – 4.30 (3H, m, H-5, 2 x H-7), 7.07 - 7.51 (3H, m, Ar-H).

^{13}C NMR (63 MHz, CD_3OD), δ (ppm): 17.3 (Me-C), 19.2 (Me-C) 39.4 (C1), 48.5 (C7), 61.2 (C6), 76.7 (C4), 78.7 (C3), 78.9 (C2), 84.5 (C5), 126.4 – 129.6 (3C, C10, C12, C13), 136.8 - 139.0 (3C, C8, C9, C11).

ESI$^+$: $[M + H]^+$ = 282.1.

6.2.5.16 2,5-Anhydro-1-deoxy-1-(3,4-dimethylbenzylamino)-D-mannitol, 40.

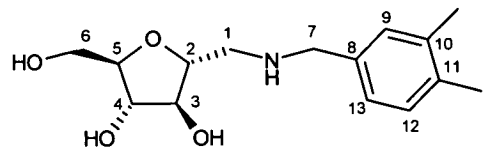

From 3,4-dimethylbenzylamine, yield = 44 mg, 21 %

^{1}H NMR (250 MHz, CD_3OD), δ (ppm): 2.29 (6H, s, 2 x ArC**H**$_3$), 3.22 – 3.43 (2H, m, 2 x H-1), 3.65 (1H, dd, J_{gem} = 11.5 Hz, $H_{5,6a}$ = 5.5 Hz, H-6a), 3.74 (1H, dd, J_{gem} =

11.5 Hz, $J_{5,6b}$ = 3.5 Hz, H-6b), 3.67 – 4.20 (6H, m, H-2, H-3, H-4, H-5, 2 x H-7), 7.14 – 7.34 (3H, m, Ar-H).

^{13}C NMR (63 MHz, CD_3OD), δ (ppm): 17.8 (2 x Me-C), 42.2 (C1), 50.2 (C7), 61.2 (C6), 76.7 (C4), 78.7 (2C, C2, C3), 84.3 (C5), 125.5 – 130.2 (3C, C9, C12, C13), 136.8 – 137.5 (3C, C8, C10, C11).

ESI$^+$: $[M + H]^+$ = 282.1 (exp. 282.2).

6.2.5.17 2,5-Anhydro-1-deoxy-1-(4-phenylbenzylamino)-D-mannitol, 41.

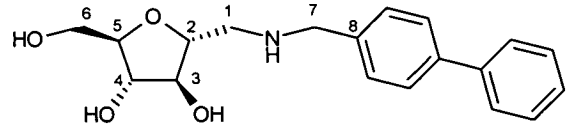

From 4-phenylbenzylamine, yield = 42 mg, 23 %.

^{1}H NMR (250 MHz, CD_3OD), δ (ppm): 2.12 – 2.29 (2H, m, 2 x H-1), 3.47 – 4.24 (8H, m, H-2, H-3, H-4, H-5, 2 x H-6, 2 x H-7), 7.43 – 7.81 (9H, m, Ar-H).

ESI$^+$: $[M + H]^+$ = 330.1 (exp. 330.2).

6.2.6 Biological screens.

6.2.6.1 5 mM Inhibitor screen vs Tb PFK.

In a 1 ml cuvette was placed 100 mM inhibitor solution (40 µl, made up with 0.1 M triethanolamine, pH 8.0), 12.5 µg/ml PFK (16 µl), made up to 760 µl with 0.1 M triethanolamine, pH 8.0 and was incubated for 2 minutes. The reaction was started by

addition of the substrate mix (40 µl, 40 mM $MgCl_2$, 40 mM F6P, 20 mM ATP, 6 mM NADH, 34 units/ml G3PDH, 18 units/ml aldolase, 20 units/ml TIM), gently agitated and the decrease in absorbance at 340 nm measured for 2 minutes (using Lambda Bio). The initial rate was then calculated using UV kinlab. A control rate with no inhibitor present was also determined. The rate for each inhibitor assay was expressed as a percentage of the control assay.

6.2.6.2 5 mM Inhibitor screen vs Lm PyK.

To a 1 ml cuvette was added the substrate mix (500 µl, 50 mM triethanolamine, pH 7.2, 50 mM KCl, 6 mM $MgSO_4$, 0.6 mM ADP, 0.84 mM NADH, 27.6 units/ml LDH), 0.04 mg/ml PyK (10 µl), 100 mM inhibitor solution (50 µl, made up with 0.1 M triethanolamine, pH 7.5) and made to 992 µl by addition of water. The mixture was incubated for 2 minutes before the reaction was started by addition of 50 µM PEP (50 µl). The mixture was gently agitated and the decrease in absorbance at 340 nm was measured for 2 minutes (using Lambda Bio). The initial rate was then calculated using UV kinlab. A control rate with no inhibitor present was also determined. The rate for each inhibitor assay was expressed as a percentage of the control assay.

6.2.7 Synthesis of 2,5-anhydro-1-deoxy-1-(3,4-difluorobenzylamino)-D-mannitol, 42.

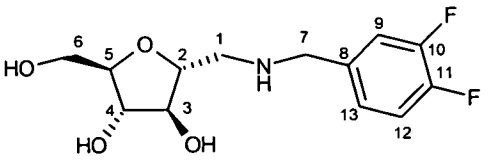

Aldehyde **22** (0.5 g, 1 eq.) and 3,4-difluorobenzylamine (0.36 ml, 1 eq.) were dissolved in methanol (10 ml) and stirred for 20 minutes. Sodium cyanoborohydride (0.13 g, 0.7 eq.) was added and the reaction was stirred for 3 hours, maintaining the pH at 6 by dropwise addition of HCl in methanol (0.5 M). The solvent was then removed under reduced pressure and the resulting residue was dissolved in acetonitrile:water (1:1, 0.1 % acetic acid) and purified using mass directed purification (ZMD Method 2). The resulting solution was lyophilised and the title compound was afforded as a white solid (74 mg, 8 %).

^{1}H NMR (250 MHz, CD_3OD), δ (ppm): 2.74 (1H, dd, J_{gem} = 12.5 Hz, $J_{1a,2}$ = 7.5 Hz, H-1a), 2.82 (1H, dd, J_{gem} = 12.5 Hz, $J_{1b,2}$ = 4.0 Hz, H-1b), 3.63 (1H, dd, J_{gem} = 11.5 Hz, $J_{5,6a}$ = 6.0 Hz, H-6a), 3.74 (1H, d, J_{gem} = 11.5 Hz, $J_{5,6b}$ = 3.5 Hz, H-6b), 3.79 (2H, s, 2 x H-7), 3.81 – 3.97 (4H, m, H-2, H-3, H-4, H-5), 7.15 – 7.33 (5H, m, 5 x Ar-H).

^{13}C NMR (63 MHz, CD_3OD), δ (ppm): 50.0 (C1), 51.4 (C7), 61.5 (C6), 76.9 (C4), 79.2 (C3), 81.7 (C5), 83.6 (C2), 116.1 – 124.1 (3C, C9, C12, C13), 136.3 (C8), 147.5 – 152.5 (2C, C10, C11).

ESI$^+$: $[M + H]^+$ = 290.0.

6.3 Library 2: Design, Synthesis and Evaluation.

6.3.1 Synthesis of library 2: *N*-substituted-1-amino-2,5-anhydro-1-deoxy-D-mannitol derivatives.

Using the Bohdan Neptune reagent manager, a methanolic solution of **22** (0.5 M) was dispensed in to 39 x 5 ml reactors, each containing an amine in equimolar quantities. The Bohdan MiniBlock synthesiser that contained the reactors was shaken for 15 minutes. Sodium cyanoborohydride in methanol (2.4 M, 0.7 eq.) was added to each reactor before adjusting the pH to 6 by dropwise addition of HCl in methanol (0.5 M). The MiniBlock was then shaken for a further 2 hours, monitoring the pH of each reactor, and adjusting the pH if necessary. The reaction mixtures were then transferred to a microtitre plate and the solvent removed under pressure. The residues were dissolved in water : acetonitrile (1:1, 0.1 % acetic acid) and purified using the mass directed purification.

6.3.1.1 2,5-Anhydro-1-deoxy-1-(cyclopentylamino)-D-mannitol, 48.

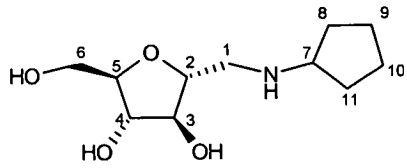

From cyclopentylamine, using ZMD Method 2, yield = 179 mg, 90 %.

^{1}H NMR (250 MHz, CD_3OD), δ (ppm): 1.62 – 2.08 (8H, m, H-8 – H-11), 3.15 – 3.30 (3H, m, 2 x H-1, H-7), 3.59 – 4.15 (6H, m, H-2, H-3, H-4, H-5, 2 x H-6).

^{13}C NMR (63 MHz, CD_3OD), δ (ppm): 22.9 (2C, C9, C10), 30.0 (2C, C8, C11), 48.0

(C1), 58.8 (C7), 61.1 (C6), 76.6 (C4), 78.6 – 78.8 (2C, C2, C3), 83.8 (C5).

ESI^+: $[M + H]^+ = 232.1$.

6.3.1.2 2,5-Anhydro-1-deoxy-1-N-(2S-2-amino-3-phenyl-1-hydroxypropyl)-D-mannitol, 49.

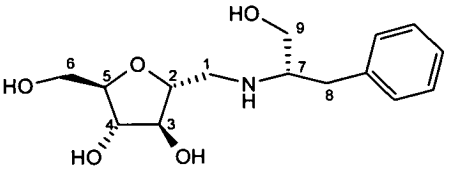

From L-(-)-2-amino-3-phenyl-1-propanol using, ZMD Method 2, yield = 74 mg, 37 %.

^1H NMR (250 MHz, CD_3OD), δ (ppm): 2.82 – 3.33 (5H, m, 2 x H-1, H-7, 2 x H-8), 3.47 – 3.77 (5H, m, H-2, 2 x H-6, 2 x H-9), 3.92 – 4.17 (3H, H-3, H-4, H-5), 7.24 – 7.36 (5H, m, Ar-H).

^{13}C NMR (63 MHz, CD_3OD), δ (ppm): 34.0 (C8), 46.9 (C1), 58.2 (C9), 60.2 (C7), 61.2 (C6), 76.8 (C4), 78.9 (C3), 79.9 (C2), 84.2 (C5), 126.0 – 128.5 (5C, Ar-CH), 136.2 (ArC-R).

ESI^+: $[M + H]^+ = 298.2$.

6.3.1.3 2,5-Anhydro-1-deoxy-1-(2-pentylamino)-D-mannitol, 50.

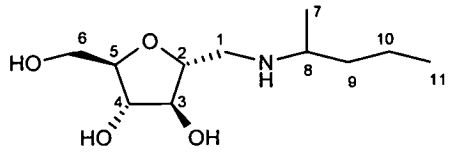

From 2-pentylamine using, ZMD Method 2, yield = 64 mg, 32 %.

^{1}H NMR (250 MHz, CD_3OD), δ (ppm): 0.97 (3H, t, $J_{10,11}$ = 7.0 Hz, 3 x H-11), 1.29 (3H, d, $J_{7,8}$ = 6.5, 3 x H-7), 1.64 – 2.12 (4H, m, 2 x H-9, 2 x H-10), 3.07 – 3.32 (3H, m, 2 x H-1, H-8), 3.52 – 3.92 (6H, m, H-2, H-3, H-4, H-5, 2 x H-6).

ESI^+: $[M + H]^+$ = 234.1.

6.3.1.4 2,5-Anhydro-1-deoxy-1-(1-hydroxy-1-phenylprop-2-ylamino)-D-mannitol, 52.

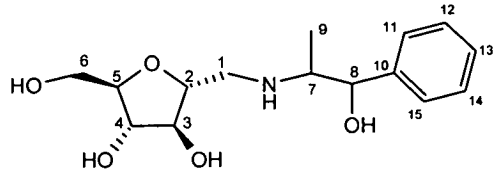

From (±)-phenylpropanolamine hydrochloride, using ZMD Method 2, yield = 23 mg, 11 %.

^{1}H NMR (250 MHz, CD_3OD), δ (ppm): 1.01 (3H, dd, J = 2.5 Hz, J = 6.5 Hz, 3 x H-9), 2.76 – 3.11 (3H, m, 2 x H-1, H-7), 3.56 – 3.73 (2H, m, 2 x H-6), 3.78 – 3.85 (2H,

m, H-2, H-3), 3.91 – 4.01 (2H, m, H-4, H-5), 4.79 (1H, t, $J_{7,8}$ = 4.5 Hz, H-8), 7.23 – 7.44 (5H, m, Ar-H).

^{13}C NMR (63 MHz, CD_3OD), δ (ppm): 12.0 and 12.4 (C9), 48.1 (C1), 57.9 and 58.4 (C7), 61.3 (C6), 73.5 (C4), 76.9 (C3), 79.4 (C2), 81.9 (C5), 83.8 and 84.2 (C8), 125.5 (2C, C11, C15), 126.5 (C13), 127.4 (2C, C12, C14), 141.7 (C10).

ESI$^+$: $[M + H]^+$ = 298.2.

6.3.1.5 2,5-Anhydro-1-deoxy-1-(2R-1-hydroxy-3-phenylprop-2-ylamino)-D-mannitol, 53.

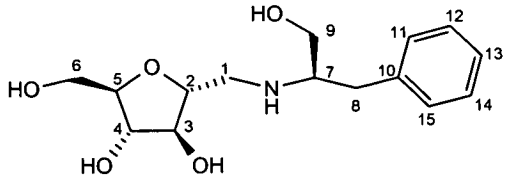

From D-(+)-2-amino-3-phenyl-1-propanol, using ZMD Method 2, yield = 26 mg, 13 %.

^{1}H NMR (250 MHz, CD_3OD), δ (ppm): 2.65 – 3.00 (5H, m, 2 x H-1, H-7, 2 x H-8), 3.35 – 3.78 (5H, H-2, 2 x H-6, 2 x H-9), 3.80 – 4.05 (3H, m, H-3, H-4, H-5), 7.23 – 7.36 (5H, m, Ar-H).

^{13}C NMR (63 MHz, CD_3OD), δ (ppm): 36.3 (C8), 48.7 (C1), 60.6 (C7), 61.4 (C9), 61.7 (C6), 76.9 (C4), 79.2 (C3), 82.1 (C2), 83.7 (C5), 125.5 (C13), 127.7 (2C, C11, C15), 128.4 (2C, C12, C14), 138.2 (C10).

ESI$^+$: $[M + H]^+$ = 298.2.

6.3.1.6 2,5-Anhydro-1-deoxy-1-(2-indanamino)-D-mannitol, 54.

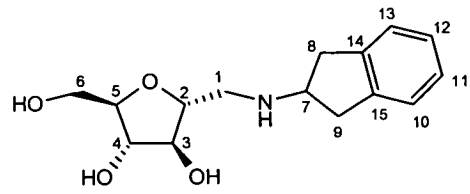

From 2-aminoindan hydrochloride, using ZMD Method 2, yield = 30 mg, 15 %.

^{1}H NMR (250 MHz, CD_3OD), δ (ppm): 2.60 – 2.82 (4H, m, 2 x H-1, 1 x H-8, 1 x H-9), 3.07 (2H, ddd, H_{gem} = 15.5 Hz, $J_{7,8\ anti} = J_{7,9\ anti}$ = 7.0 Hz, $J_{7,8\ syn} = J_{7,9\ syn}$ = 3.5 Hz, 1 x H-8, 1 x H-9), 3.45 – 3.63 (3H, m, 2 x H-6, H-7), 3.68 – 3.87 (4H, m, H-2 – H-5), 6.97 – 7.08 (4H, m, H-10 – H-13).

^{13}C NMR (63 MHz, CD_3OD), δ (ppm): 38.3 (2C, C8, C9), 49.4 (C1), 58.7 (C7), 61.5 (C6), 77.0 (C4), 79.4 (C3), 81.8 (C5), 83.7 (C2), 123.6 (2C, C11, C12), 125.7 (2C, C10, C13), 140.6 (C14, C15).

ESI$^+$: $[M + H]^+$ = 280.2 (exp. 280.2).

6.3.1.7 2,5-Anhydro-1-deoxy-1-(1R,2S-2-hydroxy-1-indanamino)-D-mannitol, 55.

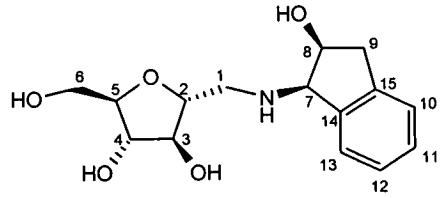

From (1*R*, 2*S*)-1-amino-2-indanol, using ZMD Method 2, yield = 26 mg, 13 %.

^{1}H NMR (250 MHz, CD_3OD), δ (ppm): 2.87 – 3.15 (4H, m, 2 x H-1, 2 x H-9), 3.64 (1H, dd, J_{gem} = 12.0 Hz, $J_{5,6a}$ = 5.5 Hz, H-6a), 3.73 (1H, dd, J_{gem} = 12.0 Hz, $J_{5,6b}$ = 3.5 Hz, H-6b), 3.82 – 4.04 (4H, m, H-2 – H-5), 4.08 (1H, d, $J_{7,8}$ = 5.0 Hz, H-7), 4.58 (1H, dt, $J_{7,8} = J_{8,9\ syn}$ = 5.0 Hz, $J_{8,9\ anti}$ = 4.0 Hz, H-8), 7.17 – 7.44 (4H, m, H-10 – H-13).

^{13}C NMR (63 MHz, CD_3OD), δ (ppm): 38.3 (C9), 49.2 (C1), 61.4 (C6), 65.3 (C7), 71.2 (C8), 77.0 (C4), 79.3 (C3), 82.1 (C5), 83.5 (C2), 123.8 – 127.0 (4C, C10 – C13), 140.2 – 141.7 (2C, C14, C15).

ESI$^+$: $[M + H]^+$ = 296.1.

6.3.1.8 2,5-Anhydro-1-deoxy-1-(1S,2R-2-hydroxy-1-indanamino)-D-mannitol, 56.

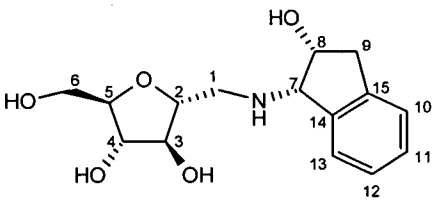

From (1*S*,2*R*)-1-amino-2-indanol, using ZMD Method 2, yield = 12 mg, 6 %.

^{1}H NMR (250 MHz, CD_3OD), δ (ppm): 2.90 – 3.17 (4H, m, 2 x H-1, 2 x H-9), 3.61 – 3.74 (2H, m, 2 x H-6), 3.88 – 4.06 (4H, m, H-2 – H-5), 4.10 (1H, d, $J_{7,8}$ = 5.0 Hz, H-7), 4.56 (1H, dt, $J_{7,8} = J_{8,9\ syn}$ = 5.0 Hz, $J_{8,9\ anti}$ = 3.5 Hz, H-8), 7.15 – 7.40 (H, m, H-10 – H-13).

ESI$^+$: $[M + H]^+$ = 296.2.

6.3.1.9 2,5-Anhydro-1-deoxy-1-(1,2,3,4-tetrahydro-1-naphthylamino)-D-mannitol, 57.

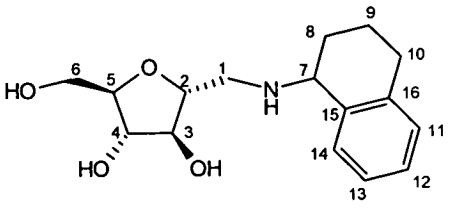

From 1,2,3,4-tetrahydro-1-naphthylamine hydrochloride, using ZMD Method 2a, yield = 24 mg, 12 %.

^{1}H NMR (250 MHz, CD_3OD), δ (ppm): 1.68 – 1.94 (4H, m, 2 x H-8, 2 x H-9), 2.67 – 3.03 (4H, m, 2 x H-1, 2 x H-10), 3.55 – 3.75 (2H, m, 2 x H-6), 3.79 – 4.05 (5H, m, H-2, H-3, H-4, H-5, H-7), 7.08 – 7.36 (4H, m, H-11 – H-14).

^{13}C NMR (63 MHz, CD_3OD), δ (ppm): 18.5 (C9), 27.0 (C8), 28.4 (C10), 48.5 (C1), 55.0 (C7), 61.5 (C6), 77.0 (C4), 79.5 (C3), 82.5 (C5), 84.0 (C2), 125.0 – 128.3 (4C, C11 – C14), 136.0 – 137.5 (2C, C15, C16).

ESI$^+$: $[M + H]^+$ = 294.3.

6.3.1.10 2,5-Anhydro-1-deoxy-1-(cyclobutylamino)-D-mannitol, 58.

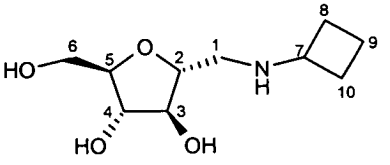

From cyclobutylamine hydrochloride, using ZMD Method 2a, yield = 31 mg, 16 %.

^{1}H NMR (250 MHz, CD_3OD), δ (ppm): 1.82 – 2.32 (6H, m, 2 x H-8, 2 x H-9, 2 x H-10), 3.07 – 3.10 (2H, m, 2 x H-1), 3.66 – 4.03 (7H, m, H-2, H-3, H-4, H-5, 2 x H-6, H-7).

^{13}C NMR (63 MHz, CD_3OD), δ (ppm): 13.6 (C9), 25.8 – 26.3 (2C, C8, C10), 46.5 (C1), 51.4 (C7), 61.2 (C6), 76.9 (C4), 78.7 (C3), 79.1 (C5), 84.4 (C2).

ESI$^+$: $[M + H]^+ = 218.1$.

6.3.1.11 2,5-Anhydro-1-deoxy-1-(hexylamino)-D-mannitol, 59.

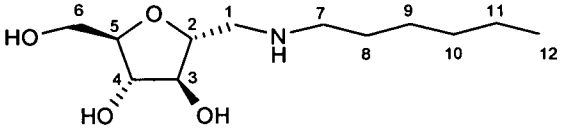

From hexylamine, using ZMD Method 2, yield = 12 mg, 6 %.

^{1}H NMR (250 MHz, CD_3OD), δ (ppm): 0.87 (3H, t, $J_{11,12}$ = 6.5 Hz, 3 x H-12), 1.24 – 1.64 (8H, m, H-8 – H-11), 2.60 – 2.89 (4H, m, 2 x H-1, 2 x H-7), 3.60 (1H, dd, J_{gem} = 11.5 Hz, $J_{5,6a}$ = 5.5 Hz, H-6a), 3.69 (1H, dd, J_{gem} = 11.5 Hz, $J_{5,6b}$ = 3.5 Hz, H-6b), 3.78 – 3.96 (4H, m, H-2, H-3, H-4, H-5).

ESI$^+$: $[M + H]^+ = 248.3$.

6.3.1.12 2,5-Anhydro-1-deoxy-1-(S-1-(4-methoxyphenyl)ethylamino)-D-mannitol, 60.

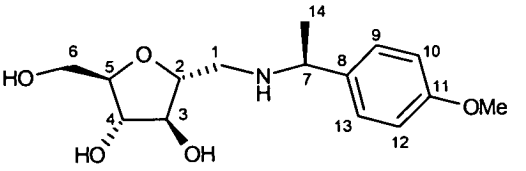

From (*S*)-(−)-1-(4-methoxyphenyl)-ethylamine, using ZMD Method 2, yield = 8 mg, 4 %.

^{1}H NMR (250 MHz, CD_3OD), δ (ppm): 1.36 (3H, d, $J_{7,14}$ = 6.5 Hz, 3 x H-14), 2.59 – 2.63 (2H, m, 2 x H-1), 3.57 – 3.93 (9H, m, H-2, H-3, H-4, H-5, 2 x H-6, -OC**H**$_3$), 4.06 (1H, q, $J_{7,14}$ = 6.5 Hz, H-7), 6.84 – 6.92 (2H, m, H-10, H-12), 7.24 – 7.32 (2H, m, H-9, H-13).

^{13}C NMR (63 MHz, CD_3OD), δ (ppm): 21.3 (C14), 48.7 (C1), 54.0 (-O**C**H$_3$), 57.1 (C7), 61.2 (C6), 76.7 (C4), 79.2 (C3), 81.3 (C5), 83.3 (C2), 113.1 (2C, C10, C12), 127.2 (2C, C9, C13), 134.8 (C8), 158.3 (C11).

ESI$^+$: $[M + H]^+$ = 298.1 (exp. 298.2).

6.3.1.13 2,5-Anhydro-1-deoxy-1-(R-1-(4-methoxyphenyl)ethylamino)-D-mannitol, 61.

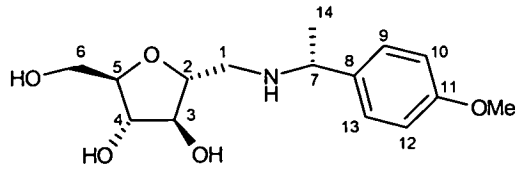

From (*R*)-(+)-1-(4-methoxyphenyl)-ethylamine using ZMD method 2, yield = 35 mg, 18 %.

^{1}H NMR (250 MHz, CD_3OD), δ (ppm): 1.41 (3H, d, $J_{7,14}$ = 6.5 Hz, 3 x H-14), 2.56 (1H, dd, J_{gem} = 12.5 Hz, $J_{1a,2}$ = 8.0 Hz, H-1a), 2.73 (1H, dd, J_{gem} = 12.5 Hz, $J_{1b,2}$ = 3.0 Hz, H-1b), 3.65 – 4.05 (10H, m, H-2, H-3, H-4, H-5, 2 x -6, H-7, -OC**H$_3$**), 6.98 (2H, d, $J_{9,10} = J_{12,13}$ = 9.0 Hz, H-10, H-12), 7.32 (2H, d, $J_{9,10} = J_{12,13}$ = 9.0 Hz, H-9, H-13).

^{13}C NMR (63 MHz, CD_3OD), δ (ppm): 22.0 (C14), 49.5 (C1), 54.5 (-O**C**H$_3$), 56.7 (C7), 61.3 (C6), 76.8 (C4), 79.3 (C3), 81.5 (C5), 83.4 (C2), 113.4 (2C, C10, C12), 127.4 (C9, C13), 135.9 (C8), 158.0 (C11).

ESI$^+$: $[M + H]^+$ = 298.1.

HRMS FAB (+ve) found m/z = 298.16550 $[M + H]^+$, $C_{15}H_{24}NO_5$ requires 298.16545.

Decomposes > 150 °C.

6.3.1.14 2,5-Anhydro-1-deoxy-1-(S-(4-fluorophenyl)ethylamino)-D-mannitol, 62.

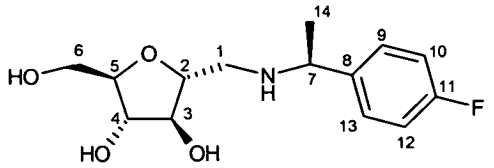

From (*S*)-(4-fluorophenyl)-ethylamine, using ZMD Method 2, yield = 23 mg, 13 %.

^{1}H NMR (250 MHz, CD_3OD), δ (ppm): 1.36 (3H, d, $J_{7,14}$ = 6.5 Hz, 3 x H-14), 2.61 (2H, d, $J_{1a,2} = J_{1b,2}$ = 5.5 Hz, 2 x H-1), 3.56 – 3.93 (7H, m, H-2, H-3, H-4, H-5, 2 x H-6, H-7), 7.01 – 7.10 (2H, m, H-10, H-12), 7.34 – 7.42 (2H, m, H-9, H-13).

^{13}C NMR (63 MHz, CD_3OD), δ (ppm): 21.9 (C14), 49.1 (C1), 57.1 (C7), 61.5 (C6), 77.0 (C4), 79.5 (C3), 81.9 (C5), 83.6 (C2), 114.4 (2C, C10, C12), 127.7 (2C, C9, C13), 139.5 (C8), 159.5 (C11).

ESI$^+$: $[M + H]^+$ = 286.1.

6.3.1.15 2,5-Anhydro-1-deoxy-1-(R-(4-fluorophenyl)ethylamino)-D-mannitol, 63.

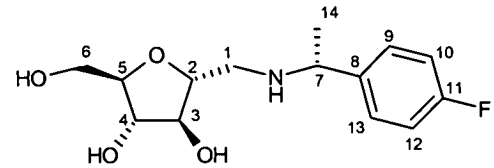

From (*R*)-(4-fluorophoenyl)-ethylamine, using ZMD Method 2a, yield = 20 mg, 10 %.

^{1}H NMR (250 MHz, CD_3OD), δ (ppm): 1.38 (3H, d, $J_{7,14}$ 6.5 Hz, 3 x H-14), 2.53 (1H, dd, J_{gem} = 12.5 Hz, $J_{1a,2}$ = 7.5 Hz, H-1a), 2.71 (1H, dd, J_{gem} = 12.5 Hz, $J_{1b,2}$ = 3.5 Hz, H-1,), 3.63 – 3.96 (7H, m, H-2, H-3, H-4, H-5, 2 x H-6, H-7), 7.03 – 7.12 (2H, m, H-10, H-12), 7.34 – 7.44 (2H, m, H-9, H-13).

^{13}C NMR (63 MHz, CD_3OD), δ (ppm): 22.0 (C14), 48.6 (C1), 56.7 (C7), 61.6 (C6), 77.1 (C4), 79.4 (C3), 81.9 (5), 84.0 (C2), 114.5 (2C, C10, C12), 127.8 (2C, C9, C13), 139.9 (C11), 159.9 (C11).

ESI$^+$: $[M + H]^+$ = 286.2.

6.3.1.16 2,5-Anhydro-1-deoxy-1-(S-(4-chlorophenyl)ethylamino)-D-mannitol, 64.

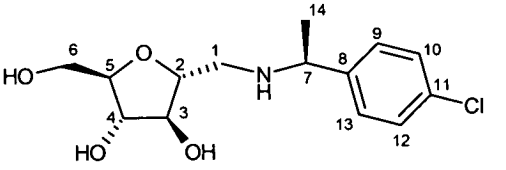

From (*S*)-(4-chlorophoenyl)-ethylamine, using ZMD Method 2a, yield = 18 mg, 9 %.

^{1}H NMR (250 MHz, CD_3OD), δ (ppm): 1.37 (3H, d, $J_{7,14}$ = 6.5 Hz, 3 x H-14), 2.61 (2H, d, $J_{1a,2}$ = $J_{1b,2}$ = 5.5 Hz, 2 x H-1), 3.57 – 3.94 (7H, m, H-2, H-3, H-4, H-5, 2 x H-6, H-7), 7.36 (4H, s, H-9, H-10, H-12, H-13).

ESI$^+$: $[M + H]^+$ = 302.0 [^{35}Cl], 304.0 [^{37}Cl].

6.3.1.17 2,5-Anhydro-1-deoxy-1-(R-(4-chlorophenyl)ethylamino)-D-mannitol, 65.

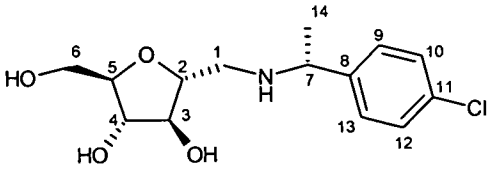

From (*R*)-(4-chlorophoenyl)-ethylamine, using ZMD Method 2a, yield = 15 mg, 8 %.

^{1}H NMR (250 MHz, CD_3OD), δ (ppm): 1.37 (3H, d, $J_{7,14}$ = 6.5 Hz, 3 x H-14), 2.51 (1H, dd, J_{gem} = 12.5 Hz, $J_{1a,2}$ = 8.0 Hz, H-1a), 2.70 (1H, dd, J_{gem} = 12.5 Hz, $J_{1b,2}$ = 3.0 Hz, H-1b), 3.59 – 3.97 (7H, m, H-2, H-3, H-4, H-5, 2 x H-6, H-7), 7.36 (4H, s, H-9, H-10, H-12, H-13).

ESI$^+$: $[M + H]^+$ = 302.2 [^{35}Cl], 304.2 [^{37}Cl].

6.3.1.18 2,5-Anhydro-1-deoxy-1-(cyclohexylamino)-D-mannitol, 66.

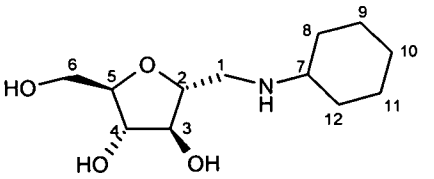

From cyclohexylamine, using ZMD Method 2, yield = 23 mg, 12 %.

^{1}H NMR (250 MHz, CD_3OD), δ (ppm): 1.11 – 1.43 (10H, m, 5 x -CH_2- cyclohexane), 2.61 – 2.72 (1H, m, H-7), 2.88 (1H, dd, J_{gem} = 12.5 Hz, $J_{1a,2}$ = 8.0 Hz, H-1a), 2.99 (1H, dd, J_{gem} = 12.5 Hz, $J_{1b,2}$ = 3.5 Hz, H-1b), 3.62 (1H, dd, J_{gem} = 12.0

Hz, $J_{5,6a}$ = 5.5 Hz, H-6a), 3.72 (1H, J_{gem} = 12.0 Hz, $J_{5,6b}$ = 3.5 Hz, H-6b), 3.82 – 4.00 (4H, m, H-2, H-3, H-4, H-5).

^{13}C NMR (63 MHz, CD_3OD), δ (ppm): 24.0 (2C, C9, C11), 25.0 (C10), 30.9 (2C, C8, C12), 47.4 (C1), 56.3 (C7), 61.5 (C6), 77.0 (C4), 79.4 (C3), 81.2 (C5), 84.1 (C2).

ESI$^+$: $[M + H]^+$ = 246.3.

6.3.1.19 2,5-Anhydro-1-deoxy-1-(S-1-(1-naphthyl)ethylamino)-D-mannitol, 67.

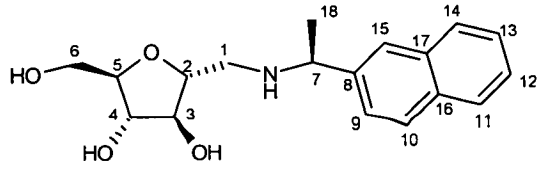

From (*S*)-(−)-1-(1-naphthyl)-ethylamine, using ZMD Method 2b, yield = 35 mg, 18 %.

^{1}H NMR (250 MHz, CD_3OD), δ (ppm): 1.52 (3H,d, $J_{7,18}$ = 6.5 Hz, 3 x H-18), 2.71 (1H, dd, J_{gem} = 12.5 Hz, $J_{1a,2}$ = 7.0 Hz, H-1a), 2.81 (1H, dd, J_{gem} = 12.5 Hz, $J_{1b,2}$ = 4.0 Hz, H-1b), 3.61 (1H, d, J_{gem} = 11.5 Hz, $J_{5,6a}$ = 5.5 Hz, H-6a), 3.72 (1H, dd, J_{gem} = 11.5 Hz, $J_{5,6b}$ = 3.5 Hz, H-6b), 3.76 – 3.99 (4H, m, H-2, H-3, H-4, H-5), 4.79 (1H, q, $J_{7,18}$ = 6.67 Hz, H-7), 7.46 – 8.22 (7H, m, Ar-H).

^{13}C NMR (63 MHz, CD_3OD), δ (ppm): 21.4 (C18), 49.1 (C1), 52.4 (C7), 61.5 (C6), 77.0 (C4), 79.4 (C3), 82.0 (C5), 83.7 (C2), 121.9 – 128.1 (7C, Ar-CH), 129.0 – 131.5 (2C, C16, C17), 134.0 (C8).

ESI$^+$: $[M + H]^+$ = 318.2.

6.3.1.20 2,5-Anhydro-1-deoxy-1-(R-1-(1-naphthyl)ethylamino)-D-mannitol, 68.

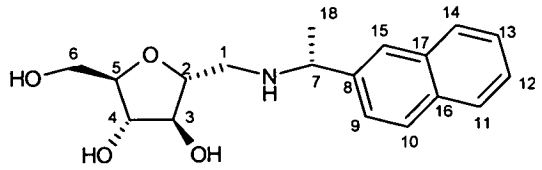

From (*R*)-(+)-1-(1-naphthyl)-ethylamine, using ZMD Method 2c, yield = 26 mg, 13 %.

^{1}H NMR (250 MHz, CD_3OD), δ (ppm): 1.53 (3H, d, $J_{7,18}$ = 6.5 Hz, 3 x H-18), 2.71 (1H, dd, J_{gem} = 12.5 Hz, $J_{1a,2}$ = 7.5 Hz, H-1a), 2.84 (1H, dd, J_{gem} = 12.5 Hz, $J_{1b,2}$ = 3.5 Hz, H-1b), 3.63 (1H, dd, J_{gem} = 12.0 Hz, $J_{5,6a}$ = 5.5 Hz, H-6a), 3.71 (1H, dd, J_{gem} = 12.0 Hz, $J_{5,6b}$ = 3.5 Hz, H-6b), 3.77 – 3.99 (4H, m, H-2, H-3, H-4, H-5), 4.79 (1H, q, $J_{7,18}$ = 6.70 Hz, H-7), 7.48 – 8.19 (7H, m, Ar-H).

ESI$^+$: $[M + H]^+$ = 318.1.

6.3.1.21 2,5-Anhydro-1-deoxy-1-N-(6-amino-2-methyl-2-hydroxyheptyl)-D-mannitol, 69.

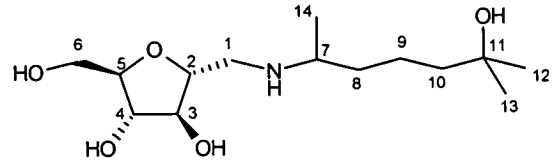

From 6-amino-2-methylheptanol, using ZMD Method 2b, yield = 23 mg, 7 %.

^{1}H NMR (250 MHz, CD_3OD), δ (ppm): 1.13 (3H, d, $J_{7,14}$ = 6.5 Hz, 3 x H-14), 1.18 (6H, s, 3 x H-12, 3 x H-13), 1.23 – 1.50 (6H, m, 2 x H-8, 2 x H-9, 2 x H-10), 2.73 – 2.98 (3H, m, 2 x H-1, H-7), 3.63 (1H, dd, J_{gem} = 11.5 Hz, $J_{5,6a}$ = 5.5 Hz, H-6a), 3.70 (1H, dd, J_{gem} = 11.5 Hz, $J_{5,6b}$ = 3.5 Hz, H-6b), 3.80 – 3.96 (4H, m, H-2, H-3, H-4, H-5).

ESI$^+$: $[M + H]^+$ = 292.3.

6.3.1.22 2,5-Anhydro-1-deoxy-1-(cycloheptylamino)-D-mannitol, 70.

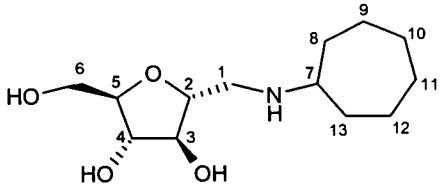

From cycloheptylamine, using ZMD Method 2, yield = 66 mg, 33 %.

$[\alpha]_D$ = 6.7 ° (*c* 1.7, MeOH).

^{1}H NMR (250 MHz, CD_3OD), δ (ppm): 1.27 – 1.91 (12H, m, 6 x –$\mathbf{CH_2}$-cycloheptane), 2.65 – 2.84 (3H, m, 2 x H-1, H-7), 3.60 (1H, dd, J_{gem} = 12.0 Hz, $J_{5,6a}$ = 5.5 Hz, H-6a), 3.68 (1H, dd, J_{gem} = 12.0 Hz, $J_{5,6b}$ = 3.5 Hz, H-6b), 3.78 – 3.93 (4H, m, H-2, H-3, H-4, H-5).

^{13}C NMR (63 MHz, CD_3OD), δ (ppm): 23.6 (2C, C9, C12), 27.3 (2C, C10, C11), 33.0 (2C, C8, C13), 48.4 (C1), 58.6 (C7), 61.5 (C6), 77.0 (C4), 79.5 (C3), 81.6 (C2), 84.1 (C5).

ESI$^+$: $[M + H]^+$ = 260.2.

HRMS FAB (+ve) found m/z = 260.18594 $[M + H]^+$, $C_{13}H_{26}NO_4$ requires 260.18618.

Decomposes > 225 °C.

6.3.1.23 2,5-Anhydro-1-deoxy-1-(cyclooctylamino)-D-mannitol, 71.

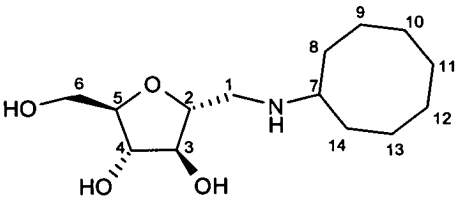

From cyclooctylamine, using ZMD Method 2a, yield = 54 mg, 27 %.

^{1}H NMR (250 MHz, CD_3OD), δ (ppm): 1.51 – 1.82 (14H, m, 7 x –C**H**$_2$- cylooctane), 2.73 – 2.85 (2H, m, 1 x H-1, H-7), 2.91 (1H, dd, J_{gem} = 12.5 Hz, $J_{1b,2}$ = 3.5 Hz, H-1a), 3.64 (1H, dd, J_{gem} = 11.5 Hz, $J_{5,6a}$ = 5.5 Hz, H-6a), 3.72 (1H, dd, J_{gem} = 11.5 Hz, $J_{5,6b}$ = 3.5 Hz, H-6b), 3.82 – 3.98 (4H, m, H-2, H-3, H-4, H-5).

^{13}C NMR (63 MHz, CD_3OD), δ (ppm): 23.4 (2C, C9, C13), 25.0 (C11), 26.1 (2C, C10, C12), 31.0 (2C, C8, C14), 48.4 (C1), 57.4 (C7), 61.5 (C6), 77.0 (C4), 79.5 (C3), 81.7 (C5), 84.1 (C2).

ESI$^+$: $[M + H]^+$ = 274.3.

6.3.1.24 2,5-Anhydro-1-deoxy-1-(S-3-methyl-2-butylamino)-D-mannitol, 72.

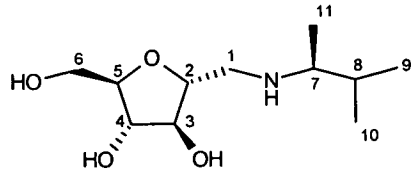

From (*S*)-3-methyl-2-butylamine, using ZMD Method 2, yield = 31 mg, 16 %.

^{1}H NMR (250 MHz, CD_3OD), δ (ppm): 0.89 (3H, d, $J_{8,9}$ = 7.0 Hz, 3 x H-9), 0.94 (3H, d, $J_{8,10}$ = 7.0 Hz, 3 x H-10), 1.74 – 1.90 (1H, m, H-8), 2.52 – 2.63 (1H, m, H-7), 2.75 – 2.88 (2H, m, 2 x H-1), 3.63 (1H, dd, J_{gem} = 11.5 Hz, $J_{5,6a}$ = 5.5 Hz, H-6a), 3.70 (1H, dd, J_{gem} = 11.5 Hz, $J_{5,6b}$ = 4.0 Hz, H-6a), 3.82 – 3.99 (4H, m, H-2, H-3, H-4, H-5).

^{13}C NMR (63 MHz, CD_3OD), δ (ppm): 13.1 (C9), 15.3 (C10), 18.0 (C11), 31.0 (C8), 48.2 (C1), 57.6 (C7), 61.5 (C6), 77.1 (C4), 79.6 (C3), 81.8 (C5), 84.4 (C2).

ESI$^+$: $[M + H]^+$ = 233.9.

6.3.1.25 2,5-Anhydro-1-deoxy-1-(R-3-methyl-2-butylamino)-D-mannitol, 73.

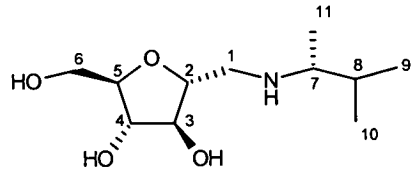

From (*R*)-3-methyl-2-butylamine, using ZMD Method 2a, yield = 37 mg, 19 %.

^{1}H NMR (250 MHz, CD_3OD), δ (ppm): 0.87 (3H, d, $J_{8,9}$ = 7.0 Hz, 3 x H-9), 0.92 (3H, d, $J_{8,10}$ = 7.0 Hz, 3 x H-10), 1.71 (1H, m, H-8), 2.50 – 2.60 (1H, m, H-7), 2.70 (1H, dd, J_{gem} = 12.5 Hz, $J_{1a,2}$ = 8.5 Hz, 1 x H-1), 2.91 (1H, dd, J_{gem} = 12.5 Hz, $J_{1b,2}$ = 3.0 Hz, 1x H-1), 3.64 (1H, dd, J_{gem} = 12.0 Hz, $J_{5,6a}$ = 5.5 Hz, 1 x H-6), 3.71 (1H, dd, J_{gem} = 12.0 Hz, $J_{5,6b}$ = 3.5 Hz, 1 x H-6), 3.82 – 3.98 (4H, m, H-2, H-3, H-4, H-5).

^{13}C NMR (63 MHz, CD_3OD), δ (ppm): 13.2 (C9), 15.4 (C10), 17.9 (C11), 30.8 (C8), 48.7 (C1), 58.2 (C7), 61.2 (C6), 76.7 (C4), 79.3 (C3), 81.6 (C5), 83.6 (C2).

ESI$^+$: $[M + H]^+$ = 234.2.

6.3.1.26 2,5-Anhydro-1-deoxy-1-N-(2-amino-5-methylhexyl)-D-mannitol, 74.

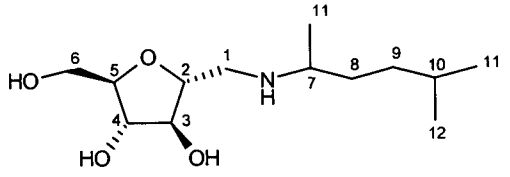

From 2-amino-5-methylhexane, using ZMD Method 2a, yield = 49 mg, 25 %.

^{1}H NMR (250 MHz, CD_3OD), δ (ppm): 0.93 (6H, d, $J_{10,11}$ = $J_{10,12}$ = 6.5 Hz, 3 x H-11, 3 x H-12), 1.09 (3H, d, $J_{7,13}$ = 6.5 Hz, 3 x H-13), 1.19 – 1.64 (5H, m, 2 x H-8, 2 x H-9, H-10), 2.59 – 2.94 (3H, m, 2 x H-1, H-7), 3.63 (1H, dd, J_{gem} = 11.5 Hz, $J_{5,6a}$ = 5.5 Hz, H-6a), 3.71 (1H, dd, J_{gem} = 11.5 Hz, $J_{5,6b}$ = 3.5 Hz, H-6b), 3.81 – 3.96 (4H, m, H-2, H-3, H-4, H-5).

^{13}C NMR (63 MHz, CD_3OD), δ (ppm): 17.8 (C13), 21.0 (C11), 21.2 (C12), 27.5 (C10), 33.4 (C9), 34.4 (C8), 48.6 (C1), 52.7 (C7), 61.5 (C6), 77.0 (C4), 79.5 (C3),

82.0 (C5), 84.0 (C2).

ESI$^+$: $[M + H]^+ = 262.3$.

6.3.1.27 2,5-Anhydro-1-deoxy-1-N-(2-amino-6-methylheptyl)-D-mannitol, 75.

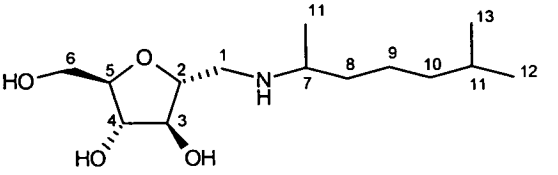

From (±)-L-amino-6-methylheptane, using ZMD Method 2b, yield = 41 mg, 21 %.

^{1}H NMR (250 MHz, CD_3OD), δ (ppm): 0.90 (6H, d, $J_{11,12} = J_{11,13} = 6.5$ Hz, 3 x H-12, 3 x H-13), 1.10 (3H, d, $J_{7,14} = 6.5$ Hz, 3 x H-14), 1.16 – 1.64 (7H, m, 2 x H-8, 2 x H-9, 2 x H-10, H-11), 2.68 – 2.95 (3H, m, 2 x H-1, H-7), 3.62 (1H, dd, $J_{gem} = 11.5$ Hz, $J_{5,6a} = 5.5$ Hz, H-6a), 3.71 (1H, d, $J_{gem} = 11.5$ Hz, $J_{5,6b} = 3.5$ Hz, H-6b), 3.80 – 3.96 (4H, m, H-2, H-3, H-4, H-5).

^{13}C NMR (63 MHz, CD_3OD), δ (ppm): 17.4 (C9), 21.0 – 22.9 (3C, C12, C13, C14), 27.2 (C11), 35.6 (C10), 38.4 (C8), 48.6 (C1), 52.9 (C7), 61.5 (C6), 77.0 (C4), 79.5 (C3), 81.8 (C5), 84.0 (C2).

ESI$^+$: $[M + H]^+ = 276.3$.

6.3.1.28 2,5-Anhydro-1-deoxy-1-(R-sec-butylamino)-D-mannitol, 76.

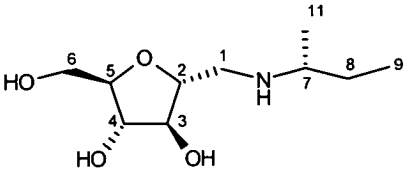

From (*R*)-sec-butylamine, using ZMD Method 2a, yield = 32 mg, 16 %.

^{1}H NMR (250 MHz, CD_3OD), δ (ppm): 1.00 (3H, t, $J_{8,9}$ = 7.5 Hz, 3 x H-9), 1.26 (3H, d, $J_{7,10}$ = 6.5 Hz, 3 x H-10), 1.41 – 1.85 (2H, m, 2 x H-8), 2.97 – 3.25 (3H, m, 2 x H-1, H-7), 3.66 (1H, dd, J_{gem} = 12.0 Hz, $J_{5,6a}$ = 5.5 Hz, H-6a), 3.74 (1H, dd, J_{gem} = 12.0 Hz, $J_{5,6b}$ = 3.5 Hz, H-6b), 3.91 – 4.16 (4H, m, H-2, H-3, H-4, H-5).

^{13}C NMR (63 MHz, CD_3OD), δ (ppm): 8.1 (C9), 14.7 (C10), 25.2 (C8), 46.0 (C1), 54.9 (C7), 60.7 (C6), 76.1 (C4), 78.3 (C3), 78.8 (C5), 83.0 (C2).

ESI$^+$: $[M + H]^+$ = 220.2.

6.3.1.29 2,5-Anhydro-1-deoxy-1-N-(endo-2-aminonorbornyl)-D-mannitol, 77.

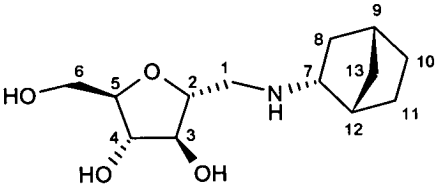

From *endo*-2-aminonorbornane hydrochloride, using ZMD Method 2a, yield = 23 mg, 12 %.

^{1}H NMR (250 MHz, CD_3OD), δ (ppm): 1.32 – 2.48 (8H, m, 4 x –C**H**$_2$- norbornane), 2.71 – 2.92 (2H, m, 2 x H-1), 3.10 – 3.16 (1H, m, H-7), 3.67 – 3.72 (2H, m, 2 x H-6), 3.85 – 3.99 (4H, m, H-2, H-3, H-4, H-5).

ESI$^+$: $[M + H]^+ = 258.2$.

6.3.1.30 2,5-Anhydro-1-deoxy-1-N-(exo-2-aminonorbornyl)-D-mannitol, 78.

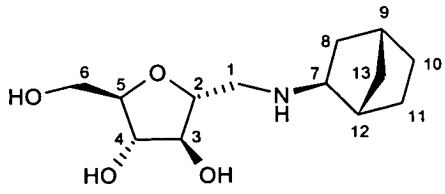

From *exo*-2-aminonorbornane, using ZMD Method 2a, yield = 30 mg, 15 %.

^{1}H NMR (250 MHz, CD_3OD), δ (ppm): 1.15 – 1.75 (8H, m, 4 x –C**H**$_2$- norbornane), 2.68 – 2.95 (3H, m, 2 x H-1, H-7), 3.62 (1H, dd, J_{gem} = 11.5 Hz, $J_{5,6a}$ = 5.5, H-6a), 3.68 (1H, dd, J_{gem} = 11.5 Hz, $J_{5,6b}$ = 3.5 Hz, H-6b), 3.76 – 3.97 (4H, m, H-2, H-3, H-4, H-5).

^{13}C NMR (63 MHz, CD_3OD), δ (ppm): 26.1 (C11), 27.3 (C10), 33.7 (C9), 35.1 (C13), 38.1 (C8), 39.4 (C12), 48.7 (C1), 61.2 (C7), 61.5 (C6), 77.0 (C4), 79.6 (C3), 81.6 (C5), 84.4 (C2).

ESI$^+$: $[M + H]^+ = 258.3$.

6.3.1.31 2,5-Anhydro-1-deoxy-1-(1-methyl-3-phenylpropylamino)-D-mannitol, 79.

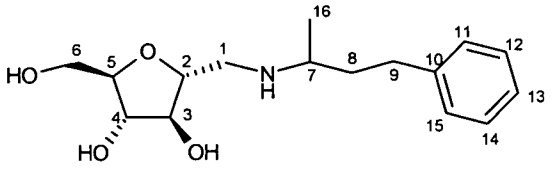

From 1-methyl-3-phenylpropylamine, using ZMD Method 2a, yield = 31 mg, 16 %.

^{1}H NMR (250 MHz, CD_3OD), δ (ppm): 1.12 (3H, dd, $J_{7R,14}$ = 6.0 Hz, $J_{7S,14}$ = 2.5 Hz, 3 x H-14), 1.51 – 1.92 (2H, m, 2 x H-8), 2.53 – 2.90 (5H, m, 2 x H-1, H-7, 2 x H-9), 3.57 – 3.94 (6H, m, H-2, H-3, H-4, H-5, 2 x H-6), 7.09 – 7.27 (5H, m, Ar-H).

^{13}C NMR (63 MHz, CD_3OD), δ (ppm): 17.7 (C16), 31.4 (C8), 37.6 (C9), 48.5 (C1), 52.2 (C7), 61.5 (C6), 77.0 (C4), 79.5 (C3), 82.0 (C5), 83.9 (C2), 125.0 (C13), 127.5 (4C, C11, C12, C14, C15), 141.4 (C10).

ESI$^+$: $[M + H]^+$ = 296.4.

6.3.1.32 2,5-Anhydro-1-deoxy-1-N-(R-2-amino-4-methyl-1-hydroxybutyl)-D-mannitol, 80.

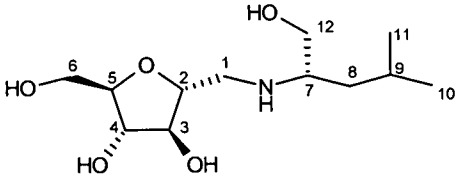

From (*R*)-leucinol, using ZMD Method 2a, yield = 28 mg, 14 %.

^{1}H NMR (250 MHz, CD_3OD), δ (ppm): 0.95 (6H, d, $J_{9,10} = J_{9,11}$ = 6.5 Hz, 3 x H-10, 3 x H-11), 1.23 – 1.42 (2H, m, 2 x H-8), 1.61 – 1.77 (1H, m, H-9), 2.70 – 2.82 (2H, m, 1 x H-1, H-7), 2.94 (1H, dd, J_{gem} = 12.0 Hz, $J_{1b,2}$ = 3.5 Hz, H-1b), 3.33 – 3.74 (4H, m, 2 x H-6, 2 x H-12), 3.81 – 3.99 (4H, m, H-2, H-3, H-4, H-5).

ESI$^+$: $[M + H]^+$ = 264.1.

6.3.1.33 2,5-Anhydro-1-deoxy-1-N-(S-2-amino-4-methyl-1-hydroxybutyl)-D-mannitol, 81.

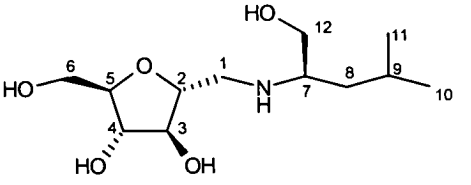

From (*S*)-leucinol, using ZMD Method 2a, yield = 29 mg, 15 %.

^{1}H NMR (250 MHz, CD_3OD), δ (ppm): 0.95 (6H, d, $J_{9,10} = J_{9,11}$ = 6.5 Hz, 3 x H-10, 3 x H-11), 1.30 (2H, t, $J_{7,8} = J_{8,9}$ = 7.0 Hz, 2 x H-8), 1.60 – 1.77 (1H, m, H-9), 2.68 – 2.83 (2H, m, 1 x H-1, H-7), 2.92 (1H, dd, J_{gem} = 12.5 Hz, $J_{1b,2}$ = 3.5 Hz, H-1b), 3.38 – 3.72 (4H, m, 2 x H-6, 2 x H-12), 3.81 – 3.96 (4H, m, H-2, H-3, H-4, H-5).

ESI$^+$: $[M + H]^+$ = 264.2.

6.3.1.34 2,5-Anhydro-1-deoxy-1-(S-2-1-methoxy-2-propylamino)-D-mannitol, 82.

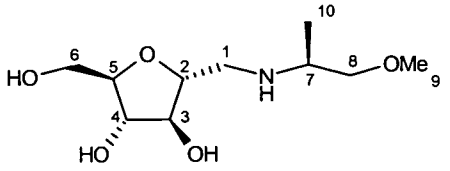

From (*S*)-methoxy-2-propylamine, using ZMD Method 2a, yield = 39 mg, 20 %.

^{1}H NMR (250 MHz, CD_3OD), δ (ppm): 1.03 (3H, d, $J_{7,10}$ = 6.55 Hz, 3 x H-10), 2.82 – 3.00 (3H, m, 2 x H-1, H-7), 3.21 – 3.27 (5H, m, 2 x H-8, 3 x H-9), 3.56 (1H, dd, J_{gem} = 11.5 Hz, $J_{5,6a}$ = 5.5 Hz, H-6a), 3.64 (1H, dd, J_{gem} = 11.5 Hz, $J_{5,6b}$ = 3.65 Hz, H-6b), 3.76 – 3.92 (4H, m, H-2, H-3, H-4, H-5).

ESI$^+$: $[M + H]^+$ = 236.2.

6.3.1.35 2,5-Anhydro-1-deoxy-1-N-(2-amino-1-hydroxybutyl)-D-mannitol, 83.

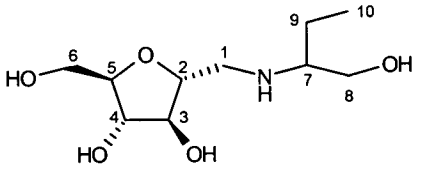

From (±)-2-amino-1-butanol, using ZMD Method 2a, yield = 26 mg, 13 %.

^{1}H NMR (250 MHz, CD_3OD), δ (ppm): 0.92 (3H, t, $J_{9,10}$ = 7.5 Hz, 3 x H-10), 1.35 – 1.64 (2H, m, 2 x H-9), 2.55 – 2.05 (3H, m, 2 x H-1, H-7), 3.38 – 3.98 (8H, m, H-2, H-3, H-4, H-5, 2 x H-6, 2 x H-8).

ESI$^+$: $[M + H]^+ = 236.2$.

6.3.1.36 2,5-Anhydro-1-deoxy-1-(1-indanamino)-D-mannitol, 84.

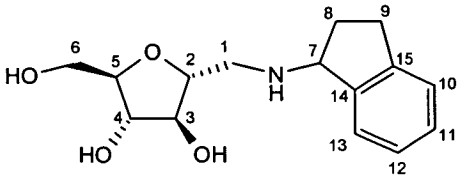

From 1-aminoindan, using ZMD Method 2a, yield = 19 mg, 10 %.

^{1}H NMR (250 MHz, CD_3OD), δ (ppm): 1.85 – 1.99 (1H, m, 1 x H-8), 2.32 – 2.46 (1H, m, 1 x H-8), 2.77 – 3.10 (4H, m, 2 x H-1, 2 x H-9), 3.62 (1H, dd, J_{gem} = 11.5 Hz, $J_{5,6a}$ = 6.0 Hz, H-6a), 3.70 (1H, dd, J_{gem} = 11.5 Hz, $J_{5,6b}$ = 3.5 Hz, H-6b), 3.81 – 4.00 (4H, m, H-2, H-3, H-4, H-5), 4.33 (1H, m, H-7), 7.15 – 7.42 (4H, m, 4 x Ar-H).

ESI$^+$: $[M + H]^+ = 280.1$.

6.3.1.37 2,5-Anhydro-1-deoxy-1-N-(3-amino-3-phenyl-1-hydroxypropyl)-D-mannitol, 85.

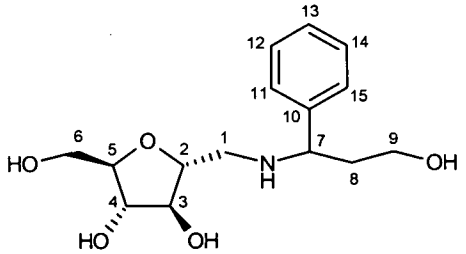

From 3-amino-3-phenyl-1-propanol, using ZMD Method 2a, yield = 35 mg, 18 %.

^{1}H NMR (250 MHz, CD_3OD), δ (ppm): 1.73 – 2.10 (2H, m ,2 x H-8), 2.45 – 2.69

(2H, m, 2 x H-1), 3.38 – 3.93 (9H, m, H-2, H-3, H-4, H-5, 2 x H-6, H-7, 2 x H-9), 7.21 – 7.33 (5H, m, 5 x Ar-H).

^{13}C NMR (63 MHz, CD_3OD), δ (ppm): 39.1 (C8), 48.5 (C1), 58.7 (C9), 60.0 (C7), 61.6 (C6), 77.1 (C4), 58.7 (C3), 82.0 (C5), 83.5 (C2), 125.7 (C13), 126.6 – 127.7 (4C, C11, C12, C14, C15), 142.2 (C10).

ESI$^+$: $[M + H]^+ = 298.1$.

6.3.1.38 2,5-Anhydro-1-deoxy-1-N-(2S-2-amino-3-phenyl-1-hydroxypropyl)-D-mannitol, 86.

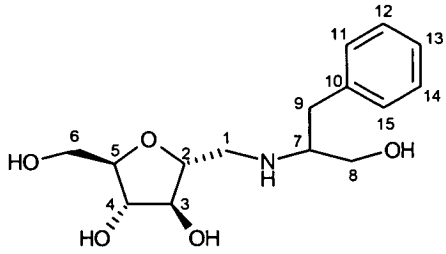

From L-(−)-2-amino-3-phenyl-1-propanol, using ZMD Method 2a, yield = 17 mg, 9 %.

^{1}H NMR (250 MHz, CD_3OD), δ (ppm): 2.65 – 2.94 (5H, m, 2 x H-1, H-7, 2 x H-9), 3.37 – 3.96 (8H, m, H-2, H-3, H-4, H-5, 2 x H-6, 2 x H-8), 7.15 – 7.32 (5H, m, 5 x Ar-H).

ESI$^+$: $[M + H]^+ = 298.3$.

6.4 Library 3: Design, Synthesis and Evaluation.

6.4.1 Synthesis of 2,5-anhydro-1-deoxy-1-(3,4-dichlorobenzylamino)-D-mannitol 37 using solid phase reagents and scavenger resins.

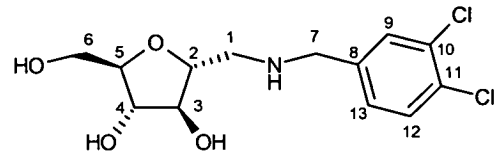

3,4-Dichlorobenzylamine (0.44 ml, 1.5 eq.), was added to a solution of aldehyde **22** (0.36 g, 1 eq.) in methanol (10 ml) in a solid phase reaction cartridge. The cartridge was sealed and placed on a shaker for 2 hours. Borohydride resin (1.17 g, 2 eq., 3.8 mmol/g) was added and the cartridge was shaken for a further 24 hours. 4-Benzoxybenzaldehyde polystyrene (0.76 g, 1.1 eq., 3.2 mmol/g) in dichloromethane (4 ml) was added before leaving the reaction to shake for a further 72 hours. After ESMS mass spectroscopy (positive) confirmed no more 3,4-dichlorobenzylamine to be present in solution, the resin was removed by filtration and was washed with methanol (3 x 5 ml) and dichloromethane (5 ml). All filtrates were combined and the solvent removed under reduced pressure to yield the title compound as a white solid (0.60 g, 84 %).

6.4.2 Synthesis of 2,5-anhydro-1-deoxy-1-(cycloheptylamino)-D-mannitol 70, using solid phase reagents and scavenger resins.

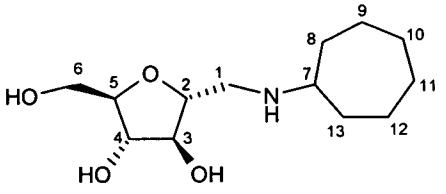

Cycloheptylamine (0.47 ml, 1.5 eq.), was added to a solution of aldehyde **22** (0.40 g, 1 eq.) in methanol (16 ml) in a solid phase reaction cartridge. The cartridge was sealed and placed on a shaker for 2 hours. Borohydride resin (1.30 g, 2 eq., 3.8 mmol/g) was added and the cartridge was shaken for a further 24 hours. 4-Benzoxybenzaldehyde polystyrene (0.78 g, 1.1 eq., 3.2 mmol/g) in dichloromethane (4 ml) was added before leaving the reaction to shake for a further 72 hours. After ESMS (positive) confirmed no more 3,4-dichlorobenzylamine to be present in solution, the resin was removed by filtration and was washed with methanol (3 x 5 ml) and dichloromethane (5 ml). All filtrates were combined and the solvent removed under reduced pressure to yield the title compound as a white solid (0.61 g, 94 %).

6.4.3 Parallel synthesis of amines 57, 59, 60, 76, 77, 78 and 87 using solid phase reagents and scavenger resins.

To separate solutions of aldehyde **22** (50 mg, 1 eq.) in methanol (2 ml) contained in solid phase reaction cartridges, were added different amines (1.5 eq.). The cartridges were shaken for 2 hours whereupon borohydride resin (0.16 g, 2 eq., 3.8 mmol/g) was added. The reactions were shaken for a further 24 hours before addition of 4-benzoxybenzaldehyde polystyrene (0.11 g, 1.1 eq., 3.2 mmol/g) in dichloromethane (1.5 ml). The reactions were again shaken for 72 hours before removal of the resin by filtration. The resins were washed with methanol (3 x 2 ml) and dichloromethane (2 ml) and the filtrates for each reaction were combined. The solvent was removed under reduced pressure to yield the desired compounds as white solids.

6.4.3.1 2,5-Anhydro-1-deoxy-1-(1,2,3,4-tetrahydro-1-naphthylamino)-D-mannitol, 57.

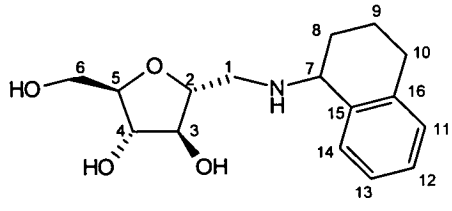

From 1,2,3,4-tetrahydro-1-naphthylamine hydrochloride, yield = 71 mg, 78 %.

6.4.3.2 2,5-Anhydro-1-deoxy-1-(hexylamino)-D-mannitol, 59.

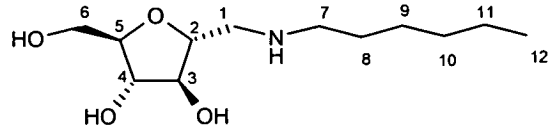

From hexylamine, yield = 73 mg, 95 %.

6.4.3.3 2,5-Anhydro-1-deoxy-1-(S-1-(4-methoxyphenyl)ethylamino)-D-mannitol, 60.

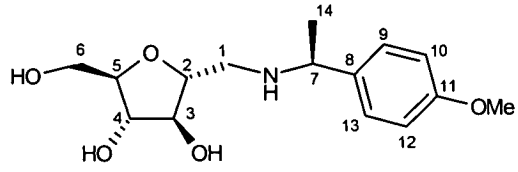

From (*S*)-(−)-1-(4-methoxyphenyl)-ethylamine, yield = 30 mg, 33 %.

6.4.3.4 2,5-Anhydro-1-deoxy-1-(R-sec-butylamino)-D-mannitol, 76.

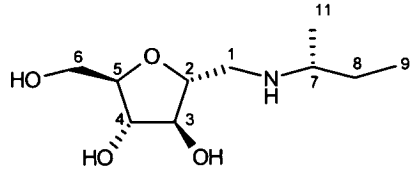

From (*R*)-*sec*-butylamine, yield = 67 mg, 99 %.

6.4.3.5 2,5-Anhydro-1-deoxy-1-N-(endo-2-aminonorbornyl)-D-mannitol, 77.

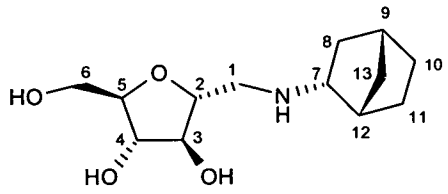

From *endo*-2-aminonorbornane hydrochloride, yield = 70 mg, 87 %.

6.4.3.6 2,5-Anhydro-1-deoxy-1-N-(exo-2-aminonorbornyl)-D-mannitol, 78.

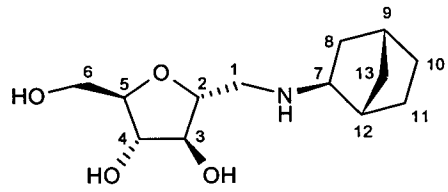

From *exo*-2-aminonorbornane, yield = 77 mg, 96 %.

6.4.3.7 2,5-Anhydro-1-deoxy-1-(4-fluorophenyl)ethylamino)-D-mannitol, 87.

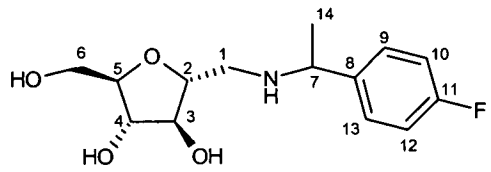

From (±)-(4fluorophenyl)-ethylamine, yield = 71 mg, 80 %.

^{1}H NMR (250 MHz, CD_3OD), δ (ppm): 1.42 (3H, dd, $J_{7R,14}$ = 6.5 Hz, $J_{7S,14}$ = 1.5 Hz, 3 x H-14), 2.54 – 2.79 (3H, m, 2 x H-1, H-7), 3.61 – 3.99 (6H, m, H-2, H-3, H-4, H-5, 2 x H-6), 7.08 (2H, m, H-10, H-12), 7.36 – 7.43 (2H, m, H-9, H-13).

^{13}C NMR (63 MHz, CD_3OD), δ (ppm): 21.5 (C14), 48.5 (C1), 54.9 (-OCH_3), 57.1 (C7), 62.2 (C6), 76.6 (C4), 79.1 (C3), 80.9 (C5), 83.0 (C2), 114.6 (2C, C10, C12), 128.3 (2C, C9, C13), 138.0 (C8), 157.5 (C11).

ESI$^+$: $[M + H]^+$ = 286.0.

6.4.4 Synthesis of *N*-BOC-2,5-anhydro-1-deoxy-1-(3,4-dichlorobenzylamino)-D-mannitol (BOC protection of amine 37), 88.

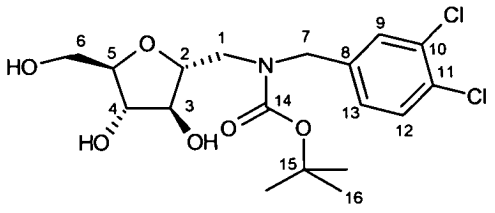

To a stirring mixture of amine **37** (0.96 g, 1 eq.) in acetonitrile (10 ml), water was added dropwise until **37** had dissolved. Di-*tert*-butyl dicarbonate (0.64 g, 1 eq.) in dioxane (2 ml) was added and the reaction was cooled to 0 °C. 4-Dimethylaminopyridine (0.091 g, 0.25 eq.) was added then and the reaction was stirred for 2 hours. After addition of water (10 ml), the reaction was extracted in to ethyl acetate (3 x 10 ml). The organic layer was washed with sat. $NaHCO_3$ (2 x 10 ml) and the combined aqueous layers were neutralised with 2M HCl before being re-extracted with ethyl acetate (2 x 10 ml). The combined aqueous layers were then

acidified to pH 1 before another re-extraction with ethyl acetate (3 x 10 ml). All organic layers were combined and washed with 5 % $NaHSO_4$ (2 x 5 ml), dried over Na_2SO_4, filtered and the solvent removed under reduced pressure to yield the title compound as a pale yellow oil (0.73 g, 58 %).

R_f = 0.27 CH_2Cl_2 : MeOH (9.5 : 0.5)

FTIR thin film (cm^{-1}): 3398 br (OH), 2978 and 2932 (CH), 1672 (C=O).

^1H NMR (250 MHz, $CDCl_3$), δ (ppm): 1.34 (9H, s, 9 x H-16), 3.24 – 3.46 (2H, m, 2 x H-1), 3.59 – 3.73 (2H, m, 2 x H-6), 3.75 – 4.14 (4H, m, H-2, H-3, H-4, H-5), 4.37 (2H, s, 2 x H-7), 6.98 (1H, dd, $J_{12,13}$ = 8.0 Hz, $J_{9,13}$ = 2.0 Hz, H-13), 7.24 (1H, d, $J_{9,13}$ = 2.0 Hz, H-9), 7.32 (1H, d, $J_{12,13}$ = 8.0 Hz, H-12).

^{13}C NMR (63 MHz, $CDCl_3$), δ (ppm): 28.2 (3C, 3 x C16), 48.2 (C2), 51.0 (C7), 62.1 (C6), 76.6 (C4), 78.5 (C3), 81.2 (C15), 82.3 (C5), 82.9 (C2), 126.4 – 130.3 (3C, C9, C12, C13), 131.0 – 132.3 (2C, C10, C11), 132.3 (C8), 156.6 (C14).

ESI$^+$: $[M + Na]^+$ = 444.2 [^{35}Cl – ^{35}Cl].

6.4.5 Synthesis of *N*-BOC-2,5-anhydro-1-deoxy-1-(cycloheptylamino)-D-mannitol (BOC protection of amine 70), 89.

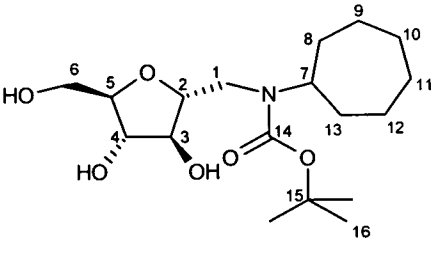

To a stirring mixture of amine **70** (1.10 g, 1 eq.) in acetonitrile (15 ml), water was

added dropwise until **70** had dissolved. Di-*tert*-butyl dicarbonate (0.93 g, 1 eq.) in dioxane (3 ml) was added and the reaction was cooled to 0 °C. 4-Dimethylaminopyridine (0.13 g, 0.25 eq.) was then added and the reaction was stirred for 2 hours. After addition of water (10 ml), the reaction was extracted in to ethyl acetate (3 x 10 ml). The organic layer was washed with sat. $NaHCO_3$ (2 x 10 ml) and the combined aqueous layers were neutralised with 2M HCl before being re-extracted with ethyl acetate (2 x 10 ml). The combined aqueous layers were then acidified to pH 1 before another re-extraction with ethyl acetate (3 x 10 ml). All organic layers were combined and washed with 5 % $NaHSO_4$ (2 x 5 ml), dried over Na_2SO_4, filtered and the solvent removed under reduced pressure to yield the title compound as a pale yellow oil (0.88 g, 57 %).

^{1}H NMR (250 MHz, $CDCl_3$), δ (ppm): 1.37 – 1.78 (21H, m, 6 x –C**H$_2$**- cycloheptane, 9 x H-16), 3.05 – 3.39 (2H, m, 2 x H-1), 3.64 – 4.32 (7H, m, H-2, H-3, H-4, H-5, 2 x H-6, H-7).

^{13}C NMR (63 MHz, $CDCl_3$), δ (ppm): 23.5 – 27.8 (4C, C9 – C12), 28.3 (3C, 3 x C16), 33.2 – 35.3 (2C, C8, C13), 47.2 (C1), 60.9 (C7), 62.6 (C6), 77.0 (C4), 78.4 (C3), 80.4 (C15), 83.4 (C5), 83.6 (C2), 156.9 (C14).

ESI$^+$: $[M + Na]^+ = 382.1$.

6.4.6 Synthesis of *N*-BOC-2,5-anhydro-1-deoxy-1-(3,4-dichlorobenzylamino)-D-mannonic acid (oxidation of 88), 90.

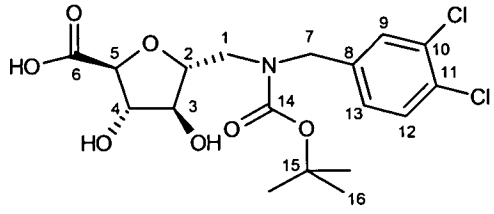

N-BOC protected amine **88** (0.13 g, 1 eq.) and TEMPO (3 mg, 6 mol %) were dissolved in CH_2Cl_2 (1 ml). A solution of KBr (0.4 M), tetrabutylammonium chloride (0.3 M) in sat. $NaHCO_3$ (1 ml) was added and the solution was cooled to 0 °C and stirred vigorously. A solution of sodium hypochlorite (1.3 M, 0.75 ml), sat. $NaHCO_3$ (0.33 ml) and brine (0.66 ml) were added dropwise over a period of 30 minutes. The reaction was then allowed to stir for a further 2 hours. The two layers were then separated and the organic phase was washed with water (3 x 10 ml). The aqueous layers were combined and acidified to pH 1 with HCl (2 M) before extracting with ethyl acetate (3 x 10 ml). The organic layer was then dried over Na_2SO_4, filtered and the solvent removed under reduced pressure to yield the title compound as an off white solid (97 mg, 72 %).

Decomposes > 150 °C

FTIR thin film (cm^{-1}): 3417 br (OH), 2978 and 2932 (CH), 1667 (2 x C=O).

^1H NMR (250 MHz, $CDCl_3$), δ (ppm): 1.47 (9H, s, 9 x H-16), 3.24 – 3.47 (2H, m, 2 x H-1), 3.84 – 4.40 (6H, m, H-2, H-3, H-4, H-5, 2 x H-7), 5.93 (1H, s broad, acid OH), 6.98 (1H, d, $J_{12,13}$ = 7.5 Hz, H-13), 7.24 (1H, s, H-9), 7.31 (1H, d, $J_{12,13}$ = 7.5 Hz, H-12).

^{13}C NMR (63 MHz, $CDCl_3$), δ (ppm): 28.2 (3 x C16), 48.0 (C1), 51.0 (C7), 78.0 (C4), 79.7 (C3), 81.5 (C15), 81.8 (C5), 83.9 (C2), 126.5 – 130.3 (3C, C9, C12, C13), 131.0 – 132.3 (2C, C10, C12), 138.3 (C8), 156.4 (C14), 174.1 (C6).

ESI⁻: $[M - H]^- = 434.1$ [$^{35}Cl - ^{35}Cl$].

6.4.7 Synthesis of *N*-BOC-2,5-anhydro-1-deoxy-1-(cycloheptylamino)-D-mannonic acid (oxidation of 89), 91.

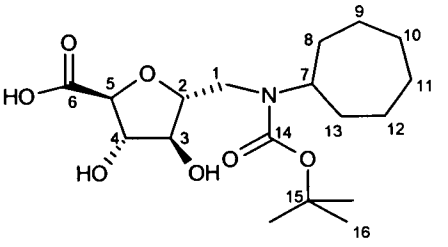

N-BOC protected **89** (0.49 g, 1 eq.) and TEMPO (3 mg, 2 mol %) were dissolved in CH_2Cl_2 (5 ml). A solution of KBr (0.4 M), tetrabutylammonium chloride (0.3 M) in sat. $NaHCO_3$ (5 ml) was added and the solution was cooled to 0 °C and stirred vigorously. A solution of sodium hypochlorite (1.3 M, 3.5 ml), sat. $NaHCO_3$ (1.6 ml) and brine (3.3 ml) were added dropwise over a period of 45 minutes. The reaction was then allowed to warm up to room temperature and stir for 24 hours. The two layers were then separated and the organic phase was washed with water (8 x 10 ml). The aqueous layers were combined and acidified to pH 1 with HCl (2 M) before extracting with ethyl acetate (8 x 10 ml). The organic layer was then dried over Na_2SO_4, filtered and the solvent removed under reduced pressure to yield the title compound as a viscous yellow oil (0.19 g, 38 %).

^1H NMR (250 MHz, $CDCl_3$), δ (ppm): 1.38 – 1.74 (21H, m, 6 x –CH_2- cycloheptane,

9 x H-16), 3.18 – 3.41 (2H, m, 2 x H-1), 3.42 – 5.06 (5H, m, H-2, H-3, H-4, H-5, H-7).

ESI⁻: $[M - H]^-$ = 372.1.

6.4.8 Synthesis of *N*-BOC-2,5-anhydro-1-deoxy-1-(3,4-dichlorobenzylamino)-D-benzylmannonamide, 92.

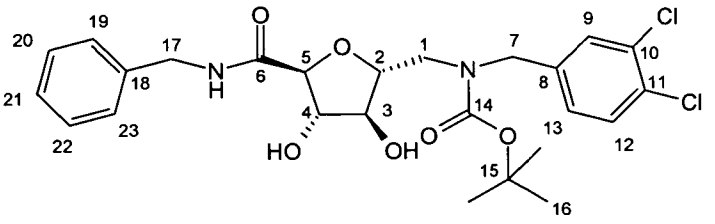

To a solution of **90** (0.1 g, 1 eq.) and benzylamine (25 µl, 1 eq.) in CH_2Cl_2 (1 ml), was added EDCI (0.11 g, 1.3 eq.), HOBt (0.09 g, 1.5 eq.) and DIPEA (0.18 ml, 2.2 eq.). The reaction was allowed to stir at room temperature for 20 hours before quenching with NaCl (2 M, 2 ml). The two layers were separated and the aqueous phase was extracted with CH_2Cl_2 (2 x 3 ml). All organic phases were combined and washed with water (2 x 3 ml) and HCl (0.5 M, 2 x 3 ml) before being dried over Na_2SO_4. The mixture was then filtered and the solvent removed under reduced pressure to yield an orange glassy solid (90 mg, 74 %). This was purified by flash column chromatography on silica gel eluting with CH_2Cl_2 : MeOH (9.5 : 0.5). The solvent was removed to yield the title compound as a glassy yellow solid (26 mg, 22 %).

R_f = 0.26 CH_2Cl_2 : MeOH (9.5 : 0.5)

FTIR thin film (cm^{-1}): 3398 br (OH), 2926 (CH), 1666 (C=O BOC, amide I), 1539 (C=O amide II).

^1H NMR (250 MHz, $CDCl_3$), δ (ppm): 1.34 (9H, s, 9 x H-16), 3.31 – 3.45 (2H, m, 2 x H-1), 3.91 – 4.09 (3H, m, H-2, H-3, H-4), 4.27 (1H, d, $J_{4,5}$ = 4.0 Hz, H-5), 4.37 – 4.53 (4H, m, 2 x H-7, 2 x H-17), 6.93 – 6.98 (2H, m, H-9, H-13), 7.15 – 7.31 (6H, H-13, H-19 – H-23).

^{13}C NMR (63 MHz, $CDCl_3$), δ (ppm): 28.2 (3C, 3 x C16), 42.8 (C17), 77.5 (C4), 79.7 (C3), 81.1 (C15), 83.2 (C2), 83.8 (C5), 126.3 -132.4 (10C, C9 – C13 and C19 – C23), 137.3 – 138.5 (2C, C8, C18), 156.1 (C14), 171.7 (C6).

ESI^+: $[M + H]^+ = 525.1$ [$^{35}Cl - ^{35}Cl$].

6.4.9 Synthesis of 2,5-anhydro-1-deoxy-1-(3,4-dichlorobenzylamino)-D-benzylmannonamide, 93.

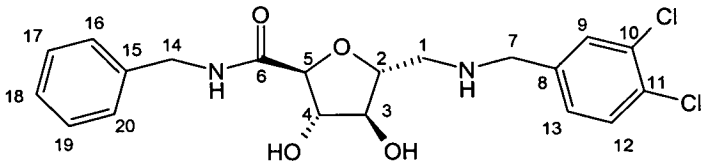

The *N*-BOC protected sugar amino amide **92** (22 mg) was dissolved in CH_2Cl_2 (2 ml) and trifluoroacetic acid (1 ml) was added. The reaction was stirred for 2 hours before quenching with water (1 ml). The two phases were separated and the aqueous phase was extracted with ethyl acetate (2 x 2 ml). The organic phases were combined, dried over Na_2SO_4, filtered and the solvent removed to yield a yellow oil. This was dissolved in acetonitrile : water (1:1, 0.1 % acetic acid) and purified using the mass

directed purification (ZMD Method 1). Removal of the solvent by lyophilisation afforded the title compound as a yellow solid (12 mg, 71 %).

FTIR thin film (cm^{-1}): 3330 br (OH), 3066 (amide NH), 2964 and 2845 (CH), 1671 (amide I), 1543 (amide II).

^1H NMR (250 MHz, CD_3OD), δ (ppm): 3.22 – 3.43 (2H, m, 2 x H-1), 3.99 (1H, t, $J_{2,3} = J_{3,4} = 2.0$ Hz, H-3), 4.24 (2H, s, 2 x H-7), 4.34 – 4.53 (5H, m, H-2, H-4, H-5, 2 x H-14), 7.22 – 7.31 (5H, m, H-16 – H-20), 7.33 (1H, dd, $J_{12,13} = 8.5$ Hz, $J_{9,13} = 2.0$ Hz, H-13), 7.62 (1H, d, $J_{12,13} = 8.5$ Hz, H-12), 7.72 (1H, d, $J_{9,13} = 2.0$ Hz, H-9).

^{13}C NMR (63 MHz, CD_3OD), δ (ppm): 41.7 (C14), 48.1 (C1), 49.2 (C7), 77.9 (C4), 79.5 (C3), 81.9 (C2), 85.2 (C5), 126.5 – 128.9 (3C, C9, C12, C13), 130.4 – 131.2 (2C, C10, C11), 137.7 (C8), 172.0 (C6).

ESI$^+$: $[M + H]^+ = 425.1$ [$^{35}Cl - ^{35}Cl$].

6.4.10 Synthesis of library 3: Synthesis of *N,N'*-substituted-1-amino-2,5-anhydro-1-deoxy-1-D-mannonamide derivatives. Part 1: Amine coupling.

The *N*-BOC protected sugar amino acids **90** and **91** (1 eq.) were dissolved in CH_2Cl_2 (1 ml) and placed in to 10 ml reaction tubes (6 x **90**, 7 x **91**). To each tube a different amine was added (1 eq., 7 amines used in total) along with EDCI (1.3 eq.), HOBt (1.5 eq.) and DIPEA (2.2 eq.). The reactions were allowed to stir for 20 hours before quenching with NaCl (2 M, 1 ml). For each reaction, the two phases were separated and the aqueous phase extracted with CH_2CH_2 (2 x 2 ml). The organic phases were combined and washed with water (2 x 2 ml) and HCl (0.5 M, 2 x 2 ml). The solutions were then dried over Na_2SO_4, filtered and the solvent removed under reduced

pressure to yield the crude products. The compounds were purified using the Quad3 parallel purification system, using pre-packed columns, eluting with CH_2Cl_2 : MeOH (9.5 : 0.5). Solvent removal yielded the desired compounds.

6.4.10.1 N-BOC-2,5-Anhydro-1-deoxy-1-(3,4-dichlorobenzylamino)-D-allylmannonamide, 94.

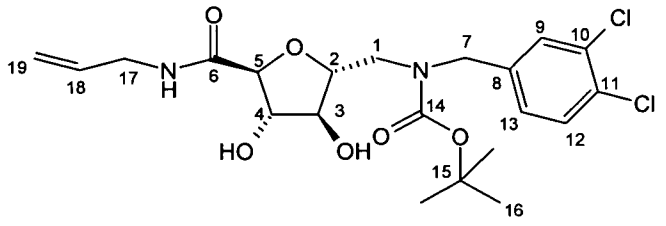

From allylamine and **90**, yield = 63 mg, 29 %.

FTIR thin film (cm^{-1}): 3399 br (OH), 2977 and 2927 (CH), 1665 (C=O BOC, amide I), 1536 (C=O amide II).

^1H NMR (250 MHz, $CDCl_3$), δ (ppm): 1.32 (9H, s, 9 x H-16), 3.35 – 3.46 (2H, m, 2 x H-1), 3.76 (1H, t, $J_{2,3} = J_{3,4} = 5.5$ Hz, H-3), 3.91 – 4.38 (7H, m, H-2, H-4, H-5, 2 x H-7, 2 x H-17), 5.02 – 5.14 (2H, m, 2 x H-19), 5.63 – 5.79 (1H, m, H-18), 6.77 (1H, s, NH amide), 6.99 (1H, d, $J_{12,13} = 7.5$, H-13), 7.24 – 7.58 (2H, m, H-9, H-12).

^{13}C NMR (63 MHz, $CDCl_3$), δ (ppm): 28.2 (3C, 3 x C16), 41.2 (C17), 48.5 (C1), 51.2 (C7), 77.7 (C4), 79.8 (C3), 81.0 (C15), 83.3 (C2), 84.0 (C5), 116.6 (C19), 126.2 – 130.3 (3C, C9, C12, C13), 131.0 – 132.4 (2C, C10, C11), 133.2 (C18), 138.6 (C8), 156.0 (C14), 171.7 (C6).

6.4.10.2 N-BOC-2,5-Anhydro-1-deoxy-1-(3,4-dichlorobenzylamino)-D-3-nitrophenylmannonamide, 95.

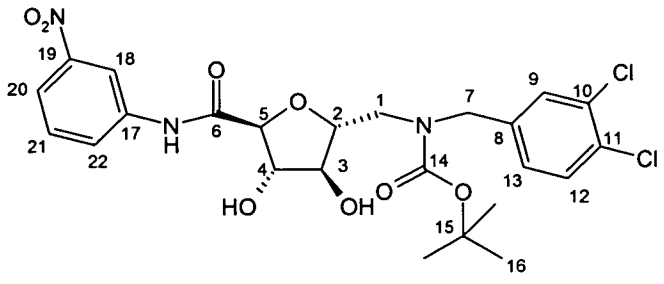

From 3-nitroaniline and **90**, yield = 76 mg, 30 %.

FTIR thin film (cm^{-1}): 3375 br (OH), 2926 (CH), 1671 (C=O BOC, amide I), 1532 (C=O amide II).

^1H NMR (250 MHz, $CDCl_3$), δ (ppm): 1.38 (9H, s, 9 x H-16), 3.31 – 3.55 (2H, m, 2 x H-1), 4.04 (1H, m, 1 x H-3), 4.16 – 4.78 (5H, m, H-2, H-4, H-5, 2 x H-7), 6.99 (1H, dd, $J_{12,13}$ = 8.0 Hz, $J_{9,13}$ = 1.5 Hz, H-13), 7.20 – 7.38 (3H, m, H-9, H-12, H-21), 7.72 – 7.84 (2H, m, H-20, H-22), 8.35 (1H, s, H-18), 8.67 (1H, s, **NH** amide).

^{13}C NMR (63 MHz, $CDCl_3$), δ (ppm): 28.2 (3C, 3 x C16), 48.3 (C1), 53.3 (C7), 77.6 (C4), 80.1 (C3), 81.3 (C15), 83.8 (C2), 84.5 (C5), 114.7 (C18), 119.2 (C20), 125.6 – 132.4 (7C, C9 – C13, C21, C22), 137.7 (C8), 138.4 (C17), 156.2 (C14), 170.3 (C6).

ESI$^-$: $[M - H]^-$ = 554.2 [$^{35}Cl - ^{35}Cl$].

6.4.10.3 N-BOC-2,5-Anhydro-1-deoxy-1-(3,4-dichlorobenzylamino)-D-4-nitrophenylmannonamide, 96.

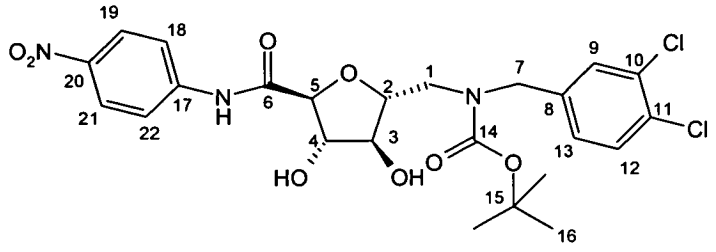

From 4-nitroaniline and **90**, yield = 30 mg, 25 %.

R_f = 0.20 CH_2Cl_2 : MeOH (9.5 : 0.5)

^{1}H NMR (250 MHz, $CDCl_3$), δ (ppm): 1.41 (9H, s, 9 x H-16), 3.32 – 4.47 (8H, m, 2 x H-1, H-2, H-3, H-4, H-5, 2 x H-7), 6.54 - 6.57 (1H, m, Ar-H), 6.98 – 7.36 (3H, m, H-9, H-12, H13), 7.63 – 7.66 (1H, m, Ar-H), 7.98 – 8.14 (2H, m, 2 x Ar-H).

6.4.10.4 N-BOC-2,5-Anhydro-1-deoxy-1-(3,4-dichlorobenzylamino)-D-3,4-dichlorobenzylmannonamide, 97.

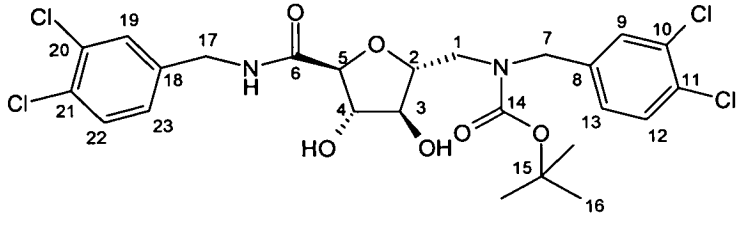

From 3,4-dichlorobenzylamine and **90**, yield = 33 mg, 25 %.

R_f = 0.14 CH_2Cl_2 : MeOH (9.5 : 0.5)

^{1}H NMR (250 MHz, $CDCl_3$), δ (ppm): 1.39 (9H, s, 9 x H-16), 3.28 – 3.48 (2H, m, 2

x H-1), 3.81 – 4.41 (8H, m, H-2, H-3, H-4, H-5, 2 x H-7, 2 x H-17), 6.99 (2H, H-13, H-23), 7.20 – 7.32 (4H, m, H-9, H-12, H-19, H-22).

6.4.10.5 N-BOC-2,5-Anhydro-1-deoxy-1-(3,4-dichlorobenzylamino)-D-cycloheptylmannonamide, 98.

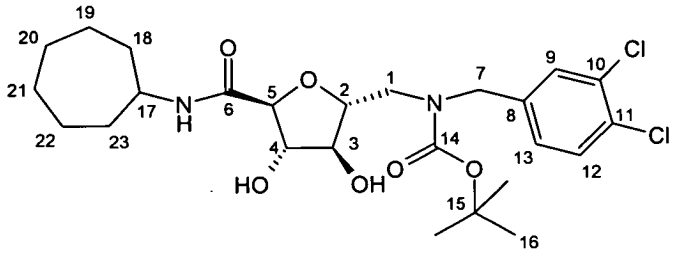

From cycloheptylamine and **90**, yield = 28 mg, 24 %.

R_f = 0.11 CH_2Cl_2 : MeOH (9.5 : 0.5)

^{1}H NMR (250 MHz, $CDCl_3$), δ (ppm): 1.31 – 1.55 (21H, m, 6 x –C**H$_2$**- cycloheptane, 9 x H-16), 3.31 – 3.51 (2H, m, 2 x H-1), 3.80 – 4.46 (7H, m, H-2, H-3, H-4, H-5, 2 x H-7, H-17), 6.99 (1H, d, $J_{12,13}$ = 8.0 Hz, H-13), 7.26 – 7.35 (2H, m, H-9, H-12).

6.4.10.6 N-BOC-2,5-Anhydro-1-deoxy-1-(3,4-dichlorobenzylamino)-D-phenylmannonamide, 99.

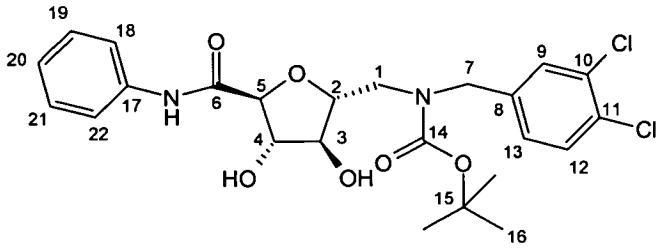

From aniline and **90**, yield = 28 mg, 25 %.

R_f = 0.11 CH_2Cl_2 : MeOH (9.5 : 0.5)

^{1}H NMR (250 MHz, $CDCl_3$), δ (ppm): 1.36 (9H, s, 9 x H-16), 3.28 – 3.50 (2H, m, 2 x H-1), 3.82 – 4.46 (6H, m, H-2, H-3, H-4, H-5, 2 x H-7), 6.94 – 7.31 (8H, m, H-9, H-12, H-13, H-18 – H-22).

6.4.10.7 N-BOC-2,5-Anhydro-1-deoxy-1-(cycloheptylamino)-D-benzylmannonamide, 100.

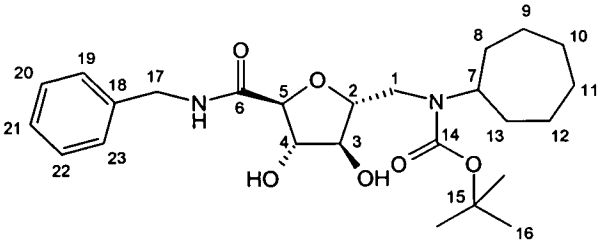

From benzylamine and **91**, yield = 36 mg, 26 %.

R_f = 0.13 CH_2Cl_2 : MeOH (9.5 : 0.5)

^{1}H NMR (360 MHz, $CDCl_3$), δ (ppm): 1.39 – 1.72 (21H, m, 6 x -C**H**$_2$- cycloheptane,

9 x H-16), 3.38 (2H, s, 2 x H-1), 3.45 – 3.54 (1H, m, H-7), 3.98 – 4.47 (6H, m, H-2, H-3, H-4, H-5, 2 x H-17), 7.07 (1H, s, NH amide), 7.21 – 7.32 (5H, m, 5 x Ar-H).

6.4.10.8 N-BOC-2,5-Anhydro-1-deoxy-1-(cycloheptylamino)-D-allylmannonamide, 101.

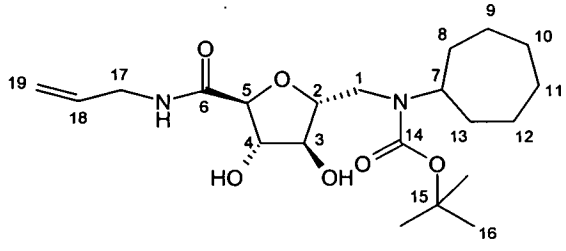

From allylamine and **91**, yield = 31 mg, 39 %.

^{1}H NMR (250 MHz, $CDCl_3$), δ (ppm): 1.27 – 1.67 (21H, m, 6 x -C**H**$_2$- cycloheptane, 9 x H-16), 3.30 – 4.45 (9H, m, 2 x H-1, H-2, H-3, H-4, H-5, H-7, 2 x H-17), 5.07 – 5.24 (2H, m, 2 x H-19), 5.68 – 5.85 (1H, m, H-18).

6.4.10.9 N-BOC-2,5-Anhydro-1-deoxy-1-(cycloheptylamino)-D-3-nitrophenylmannonamide, 102.

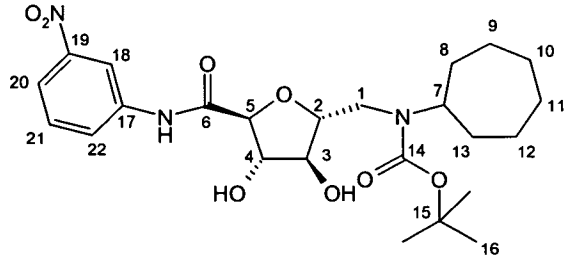

From 3-nitroaniline and **91**, yield = 31 mg, 33 %.

^{1}H NMR (250 MHz, $CDCl_3$), δ (ppm): 1.38 – 1.75 (21 H, m, 6 x -C**H**$_2$- cycloheptane,

9 x H-16), 3.31 – 4.56 (7H, m, 2 x H-1, H-2, H-3, H-4, H-5, H-7), 7.33 – 7.99 (4H, 4 x Ar-H).

6.4.10.10 N-BOC-2,5-Anhydro-1-deoxy-1-(cycloheptylamino)-D-4-nitrophenylmannonamide, 103.

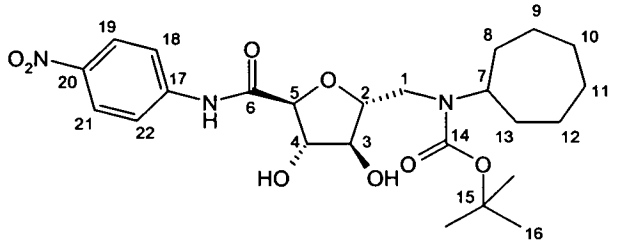

From 4-nitroaniline and **91**, yield = 30 mg, 21 %.

R_f = 0.09 CH_2Cl_2 : MeOH (9.5 : 0.5)

^{1}H NMR (360 MHz, $CDCl_3$), δ (ppm): 1.44 – 1.72 (21H, m, 6 x -C**H**$_2$- cycloheptane, 9 x H-16), 3.35 – 4.75 (7H, m, 2 x H-1, H-2, H3, H-4, H-5, H-7), 6.60 (2H, d, $J_{18,19}$ = $J_{21,22}$ = 9.0 Hz, H-18, H-22), 8.03 (2H, d, $J_{18,19}$ = $J_{21,22}$ = 9.0 Hz, H-19, H-21).

6.4.10.11 N-BOC-2,5-Anhydro-1-deoxy-1-(cycloheptylamino)-D-3,4-diclorobenzylmannonamide, 104.

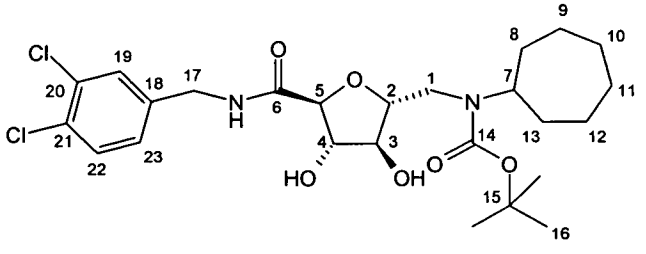

From 3,4-dichlorobenzylamine and **91**, yield = 16 mg, 16 %.

R_f = 0.14 CH_2Cl_2 : MeOH (9.5 : 0.5)

^{1}H NMR (250 MHz, $CDCl_3$), δ (ppm): 1.38 – 1.70 (21H, m, 6 x -C**H**$_2$- cycloheptane, 9 x H-16), 3.30 – 3.55 (3H, m, 2 x H-1, H-7), 3.94 – 4.42 (6H, m, H-2, H-3, H-4, H-5, 2 x H-17), 7.02 – 7.07 (1H, m, H-23), 7.27 – 7.34 (2H, m, H-19, H-22).

6.4.10.12 N-BOC-2,5-Anhydro-1-deoxy-1-(cycloheptylamino)-D-cycloheptylmannonamide, 105.

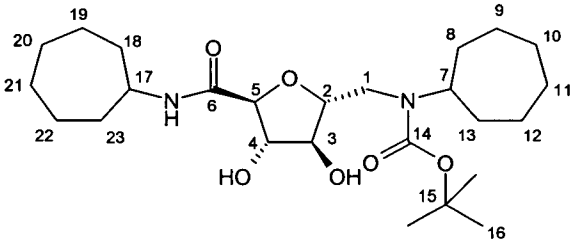

From cycloheptylamine and **91**, yield = 14 mg, 16 %.

R_f = 0.11 CH_2Cl_2 : MeOH (9.5 : 0.5).

6.4.10.13 N-BOC-2,5-Anhydro-1-deoxy-1-(cycloheptylamino)-D-phenylmannonamide, 106.

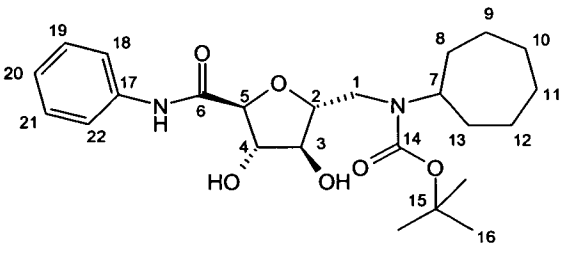

From aniline and **91**, yield = 13 mg, 15 %.

R_f = 0.13 CH_2Cl_2 : MeOH (9.5 : 0.5)

6.4.11 Synthesis of library 3: Synthesis of *N,N'*-substituted-1-amino-2,5-anhydro-1-deoxy-1-D-mannonamide derivatives. Part 2: BOC-deprotection.

BOC-protected amino mannonamides (from part 1) were dissolved in CH_2Cl_2 (1.5 ml). Trifluoroacetic acid (1 ml) was added and the reactions were stirred for 2 hours. The solvent was then removed under reduced pressure and the residue dissolved in acetonitrile : water (1 : 1, 0.1 % acetic acid) and purified using mass directed purification (ZMD Method 1). Removal of the solvent by lyophilisation afforded the desired compounds.

6.4.11.1 2,5-Anhydro-1-deoxy-1-(3,4-dichlorobenzylamino)-D-allylmannonamide, 107.

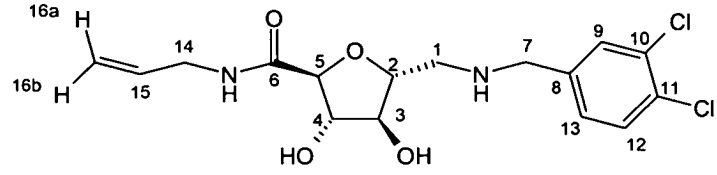

From **104**, yield = 41 mg, 82 %.

^{1}H NMR (250 MHz, CD_3OD), δ (ppm): 3.28 (1H, dd, J_{gem} = 13.0 Hz, $J_{1a,2}$ = 3.0 Hz, H-1a), 3.44 (1H, dd, J_{gem} = 13.0 Hz, $J_{1b,2}$ = 9.5 Hz, H-1b), 3.75 – 3.94 (2H, m, 2 x H-14), 3.97 (1H, t, $J_{2,3} = J_{3,4}$ = 2.0 Hz, H-3), 4.27 (1H, d, J_{gem} = 13.5 Hz, 1 x H-7), 4.33 (1H, d, J_{gem} = 13.5 Hz, 1 x H-7), 4.35 (1H, t, $J_{3,4} = J_{4,5}$ = 2.0 Hz, H-4), 4.38 – 4.41 (1H, m, H-2), 4.44 (1H, d, $J_{4,5}$ = 2.0 Hz, H-5), 5.08 (1H, dq, $J_{15,16b}$ = 10.5 Hz, $J_{14,16b} = J_{16a,16b}$ = 1.5 Hz, H-16b), 5.23 (1H, dq, $J_{15,16a}$ = 17.0 Hz, $J_{14,16a} = J_{16a,16b}$ = 1.5 Hz, H-16a), 5.75 – 5.90 (1H, m, H-15), 7.45 (1H, dd, $J_{12,13}$ = 8.5 Hz, $J_{9,13}$ = 2.0 Hz, H-13), 7.63 (1H, d, $J_{12,13}$ = 8.5 Hz, H-12), 7.73 (1H, d, $J_{9,13}$ = 2.0 Hz, H-9), 8.11 (1H, t, $J_{14,NH\text{-}amide}$ = 6.0 Hz, exchanges in D_2O, N**H**-amide).

^{13}C NMR (63 MHz, CD_3OD), δ (ppm): 40.4 (C14), 48.1 (C1), 49.0 (C7), 77.8 (C4), 79.6 (C3), 81.7 (C2), 85.4 (C5), 114.2 (C16), 129.0 – 131.3 (3C, C9, C12, C13), 132.2 – 132.9 (2C, C10, C11), 133.3 (2C, C8, C15), 170.9 (C6).

ESI$^+$: $[M + H]^+$ = 375.1 [^{35}Cl – ^{35}Cl].

6.4.11.2 2,5-Anhydro-1-deoxy-1-(3,4-dichlorobenzylamino)-D-3-nitrophenylmannonamide, 108.

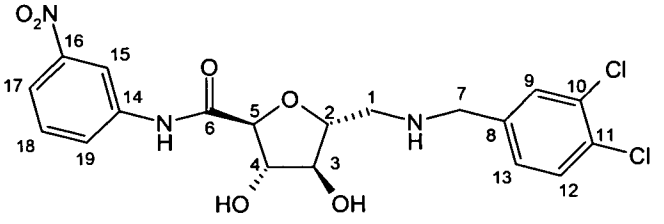

From **95**, yield = 15 mg, 23 %.

^{1}H NMR (250 MHz, CD_3OD), δ (ppm): 3.34 (1H, dd, 1 x H-1), 3.42 (1H, dd, 1 x H-1), 4.04 (1H, t, $J_{2,3} = J_{3,4} = 2.0$ Hz, H-3), 4.31 (1H, d, $J_{gem} = 13.5$ Hz, 1 x H-7), 4.28 (1H, d, $J_{gem} = 13.5$ Hz, 1 x H-7), 4.48 (1H, t, $J_{3,4} = J_{4,5} = 2.0$ Hz, H-4), 4.53 – 4.59 (1H, m, H-2), 4.62 (1H, d, $J_{4,5} = 2.0$ Hz, H-5), 7.28 (1H, dd, $J_{12,13} = 8.5$ Hz, $J_{9,13} = 2.0$ Hz, H-13), 7.58 (1H, t, $J_{17,18} = J_{18,19} = 8.0$ Hz, H-18), 7.66 (1H, d, $J_{17,18} = 8.5$ Hz, H-12), 7.77 (1H, d, $J_{9,13} = 2.0$ Hz, H-9), 7.95 – 7.99 (2H, m, H-17, H-19), 8.63 (1H, t, $J_{15,17} = J_{15,19} = 2.0$ Hz, H-15).

ESI$^+$: $[M + H]^+ = 456.1$ [^{35}Cl – ^{35}Cl].

6.4.11.3 2,5-Anhydro-1-deoxy-1-(3,4-dichlorobenzylamino)-D-4-nitrophenylmannonamide, 109.

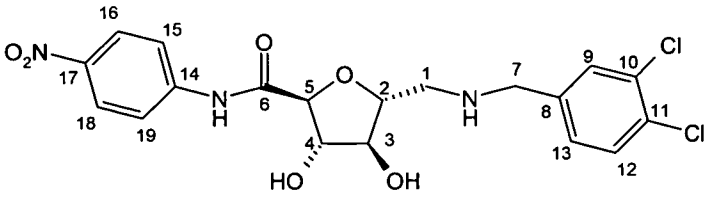

From **96**, yield = 5 mg, 20 %.

^{1}H NMR (360 MHz, CD_3OD), δ (ppm): 3.34 (1H, dd, J_{gem} = 13.0 Hz, $J_{1a,2}$ = 3.0 Hz, H-1a), 3.50 (1H, dd, J_{gem} = 13.0 Hz, $J_{1b,2}$ = 9.5 Hz, H-1b), 4.04 (1H, t, $J_{2,3} = J_{3,4}$ = 2.0 Hz, H-3), 4.32 (1H, d, J_{gem} = 13.0 Hz, 1 x H-7), 4.38 (1H, d, J_{gem} = 13.0 Hz, 1 x H-7), 4.49 (1H, t, $J_{3,4} = J_{4,5}$ 2.0 Hz, H-4), 4.54 – 4.59 (1H, m, H-2), 4.62 (1H, d, $J_{4,5}$ = 2.0 Hz, H-5), 7.47 – 7.91 (5H, m, H-9, H-12, H-13, H-15, H-19), 8.23 – 8.57 (2H, m, H-16, H-18).

ESI$^+$: $[M + H]^+$ = 456.0 [^{35}Cl – ^{35}Cl], 458.0 [^{35}Cl – ^{37}Cl], 460.0 [^{37}Cl – ^{37}Cl] (exp. 456.1, 458.1, 460.1).

6.4.11.4 2,5-Anhydro-1-deoxy-1-(3,4-dichlorobenzylamino)-D-3,4-dichlorobenzylmannonamide, 110.

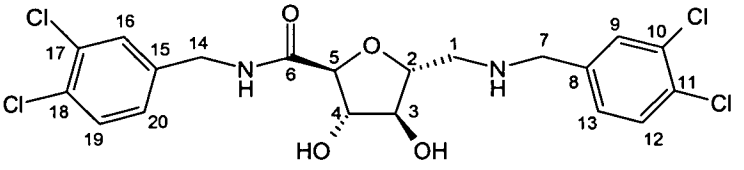

From **97**, yield = 16 mg, 58 %.

^{1}H NMR (360 MHz, CD_3OD), δ (ppm): 3.28 (1H, dd, J_{gem} = 13.0 Hz, $J_{1a,2}$ = 3.0 Hz, H-1a), 3.46 (1H, dd, J_{gem} = 13.0 Hz, $J_{1b,2}$ = 9.5 Hz, H-1b), 4.01 (1H, t, $J_{2,3} = J_{3,4}$ = 1.51 Hz, H-3), 4.24 – 4.34 (4H, m, 2 x H-7, 2 x H-14), 4.38 (1H, s, NH amine), 4.42 (1H, t, $J_{3,4} = J_{4,5}$ = 1.5 Hz, H-4), 4.44 – 4.48 (1H, m, H-2), 4.51 (1H, d, $J_{4,5}$ = 1.5 Hz, H-5), 7.19 – 7.27 (2H, m, H-13, H-20), 7.41 – 7.73 (4H, m, H-9, H12, H-16, H-19), 8.54 (1H, t, $J_{14,NH\text{-}amide}$ = 6.5 Hz, N**H**-amide).

ESI$^+$: $[M + H]^+$ = 493.1 [^{35}Cl – ^{35}Cl – ^{35}Cl – ^{35}Cl].

6.4.11.5 2,5-Anhydro-1-deoxy-1-(3,4-dichlorobenzylamino)-D-cycloheptylmannonamide, 111.

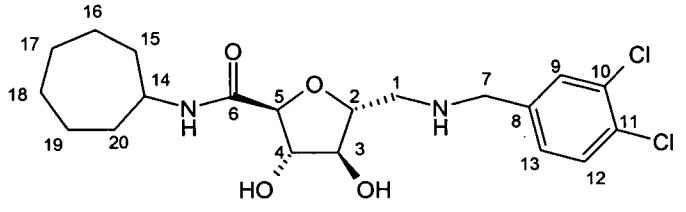

From **98**, yield = 11 mg, 48 %.

FTIR thin film (cm^{-1}): 3398 br (OH), 3074 (amide NH), 2965, 2935 and 2878 (CH), 1674 (amide I), 1541 (amide II).

$[\alpha]_D = 10.0^{\circ}$ (*c* 0.1, MeOH).

^1H NMR (250 MHz, CD_3OD), δ (ppm): 1.43 – 1.91 (12H, m, 6 x -CH_2- cycloheptane), 3.27 (1H, dd, J_{gem} = 13.0 Hz, $J_{1a,2}$ = 3.5 Hz, H-1a), 3.43 (1H, dd, J_{gem} = 13.0 Hz, $J_{1b,2}$ = 9.5 Hz, H-1b), 3.78 – 3.90 (1H, m, H-14), 3.94 (1H, t, $J_{2,3} = J_{3,4}$ = 2.0 Hz, H-3), 4.27 – 4.32 (3H, m, H-4, 2 x H-7), 4.36 – 4.42 (2H, m, H-2, H-5), 7.44 (1H, dd, $J_{12,13}$ = 8.5 Hz, $J_{9,13}$ = 2.0 Hz, H-13), 7.64 (1H, d, $J_{12,13}$ = 8.5 Hz, H-12), 7.73 (1H, d, $J_{9,13}$ = 2.0 Hz, H-9).

^{13}C NMR (63 MHz, CD_3OD), δ (ppm): 22.3 – 22.5 (2C, C16, C19), 27.1 – 27.4 (2C, C17, C18), 33.6 – 33.9 (2C, C15, C20), 48.1 (C1), 49.1 (C7), 49.9 (C14), 77.8 (C4), 79.5 (C3), 81.7 (C2), 85.2 (C5), 129.0 – 131.3 (3C, C9, C12, C13), 132.2 – 133.0 (2C, C10, C11), 138.0 (C8), 169.5 (C6).

ESI$^+$: $[M + H]^+$ = 431.2 [$^{35}Cl - ^{35}Cl$].

HRMS FAB (+ve) found m/z = 431.15032 and 431.14748 $[M + H]^+$, $C_{20}H_{29}N_2O_4Cl_2$ requires 431.15044 (2 x ^{35}Cl) and 433.14749 ($^{35}Cl + ^{37}Cl$).

6.4.11.6 2,5-Anhydro-1-deoxy-1-(3,4-dichlorobenzylamino)-D-phenylmannonamide, 112.

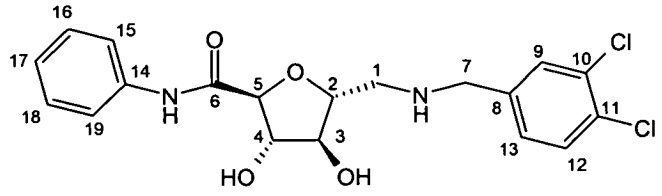

From **99**, yield = 10 mg, 50 %.

^{1}H NMR (250 MHz, CD_3OD), δ (ppm): 3.34 (1H, dd, J_{gem} = 13.0 Hz, $J_{1a,2}$ = 3.0 Hz, H-1a), 3.49 (1H, dd, J_{gem} = 13.0 Hz, $J_{1b,2}$ = 9.5 Hz, H-1b), 4.00 (1H, t, $J_{2,3} = J_{3,4}$ = 2.0 Hz, H-3), 4.27 (1H, d, J_{gem} = 11.5 Hz, 1 x H-7), 4.34 (1H, d, J_{gem} = 11.5 Hz, 1 x H-7), 4.44 (1H, t, $J_{3,4} = J_{4,5}$ = 2.0 Hz, H-4), 4.47 – 4.53 (1H, m, H-2), 4.56 (1H, d, $J_{4,5}$ = 2.0 Hz, H-5), 7.10 – 7.75 (8H, m, H-9, H-12, H-13, H-15 – H-19).

6.4.11.7 2,5-Anhydro-1-deoxy-1-(cycloheptylamino)-D-benzylmannonamide, 113.

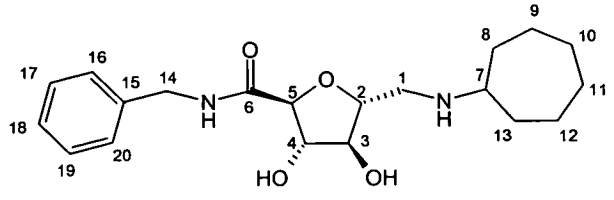

From **100**, yield = 17 mg, 60 %.

^{1}H NMR (250 MHz, CD_3OD), δ (ppm): 1.46 – 2.14 (12H, m, 6 x $-CH_2-$

cycloheptane), 3.22 – 3.43 (3H, m, 2 x H-1, H-7), 3.99 (1H, t, $J_{2,3} = J_{3,4} = 2.0$ Hz, H-3), 4.33 – 4.52 (5H, m, H-2, H-4, H-5, 2 x H-14), 7.19 – 7.33 (5H, m, 5 x Ar-H).

^{13}C NMR (63 MHz, CD_3OD), δ (ppm): 23.0 – 23.1 (2C, C9, C12), 27.7 (2C, C10, C11), 29.6 – 30.0 (2C, C8, C13), 41.7 (C14), 45.6 (C1), 58.9 (C7), 77.9 (C4), 79.6 (C3), 82.0 (C2), 85.4 (C5), 126.3 (C18), 126.5 (2C, C16, C20), 127.6 (C17, C19), 127.8 (C18), 171.0 (C6).

ESI$^+$: $[M + H]^+ = 363.1$.

6.4.11.8 2,5-Anhydro-1-deoxy-1-(cycloheptylamino)-D-allylmannonamide, 114.

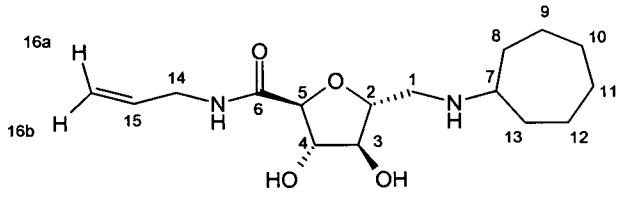

From **101**, yield = 10 mg, 43 %.

^{1}H NMR (250 MHz, CD_3OD), δ (ppm): 1.47 – 2.16 (12H, m, 6 x –$\mathbf{CH_2}$- cycloheptane), 3.22 – 3.44 (3H, m, 2 x H-1, H-7), 3.80 – 3.88 (2H, m, 2 x H-14), 3.97 (1H, t, $J_{2,3} = J_{3,4} = 2.0$ Hz, H-3), 4.31 – 4.38 (2H, m, H-2, H-4), 4.33 (1H, d, $J_{4,5} = 2.0$ Hz, H-5), 5.09 (1H, dq, $J_{15,16b} = 10.5$ Hz, $J_{14,16b} = J_{16a,16b} = 1.5$ Hz, H-16b), 5.24 (1H, dq, $J_{15,16a} = 17.0$ Hz, $J_{14,16b} = J_{16a,16b} = 1.5$ Hz, H-16a), 5.76 – 5.91 (1H, m, H-15).

ESI$^+$: $[M + H]^+ = 313.4$.

6.4.11.9 2,5-Anhydro-1-deoxy-1-(cycloheptylamino)-D-3-nitrophenylmannonamide, 115.

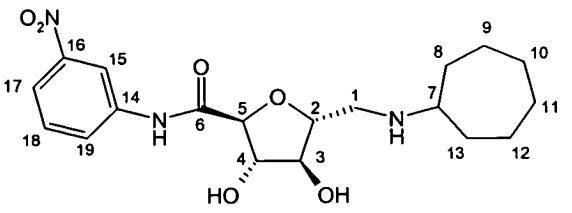

From **102**, yield = 9 mg, 36 %.

^{1}H NMR (250 MHz, CD_3OD), δ (ppm): 1.47 – 2.17 (12H, m, 6 x –C**H$_2$**-cycloheptane), 3.29 – 3.50 (3H, m, 2 x H-1, H-7), 4.05 (1H, t, $J_{2,3} = J_{3,4} = 2.0$ Hz, H-3), 4.43 – 4.52 (2H, m, H-2, H-4), 4.61 (1H, d, $J_{4,5} = 2.0$ Hz, H-5), 7.59 (1H, t, $J_{17,18} = J_{18,19} = 8.0$ Hz, H-18), 7.92 – 8.04 (2H, m, H-17, H-19), 8.64 (1H, t, $J_{15,17} = J_{15,19} = 2.0$ Hz, H-15).

^{13}C NMR (63 MHz, CD_3OD), δ (ppm): 23.0 – 23.1 (2C, C9, C12), 26.7 – 27.3 (2C, C10, C11), 29.7 – 30.3 (2C, C8, C13), 45.6 (C1), 58.9 C7), 77.6 (C4), 79.8 (C3), 82.1 (C2), 85.4 (C5), 114.4 (C15), 118.1 (C17), 125.5 (C19), 129.0 (C18), 138.4 (C14), 148.0 (C16), 169.9 (C6).

ESI$^+$: $[M + H]^+ = 394.3$.

6.4.11.10 2,5-Anhydro-1-deoxy-1-(cycloheptylamino)-D-4-nitrophenylmannonamide, 116.

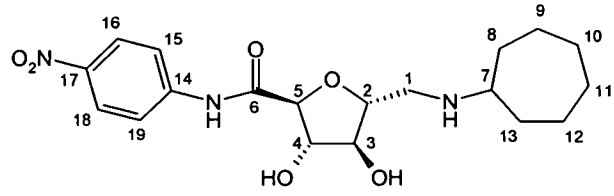

From **103**, yield = 12 mg, 50 %.

^{1}H NMR (250 MHz, CD_3OD), δ (ppm): 1.46 – 2.16 (12H, m, 6 x –CH_2- cycloheptane), 3.32 – 3.49 (3H, m, 2 x H-1, H-7), 403 (1H, t, $J_{2,3} = J_{3,4} = 2.0$ Hz, H-3), 4.45 – 4.50 (2H, m, H-2, H-4), 4.60 (1H, d, $J_{4,5} = 2.0$ Hz, H-5), 7.88 (2H, d, $J_{15,16} = J_{18,19} = 9.5$ Hz, H-15, H-19), 7.91 (1H, s, NH-amide), 8.13 (2H, d, $J_{15,16} = J_{18,19} = 9.5$ Hz, H-16, H-18).

ESI$^+$: $[M + H]^+ = 394.3$.

6.4.11.11 2,5-Anhydro-1-deoxy-1-(cycloheptylamino)-D-3,4-diclorobenzylmannonamide, 117.

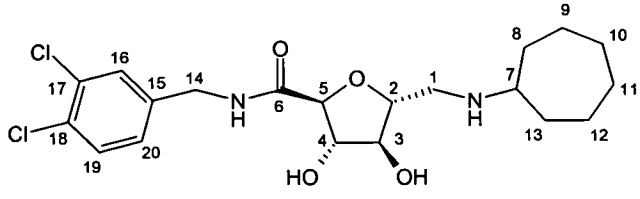

From **104**, yield = 10 mg, 77 %.

^{1}H NMR (250 MHz, CD_3OD), δ (ppm): 1.46 – 2.14 1.46 – 2.16 (12H, m, 6 x –CH_2-

cycloheptane), 3.22 – 3.45 (3H, m, 2 x H-1, H-7), 4.0 (1H, t, $J_{2,3} = J_{3,4} = 1.5$ Hz, H-3), 4.34 – 4.46 (5H, m, H-2, H-4, H-5, 2 x H-14), 7.19 – 7.53 (3H, m, H-16, H-19, H-20).

6.4.11.12 2,5-Anhydro-1-deoxy-1-(cycloheptylamino)-D-cycloheptylmannonamide, 118.

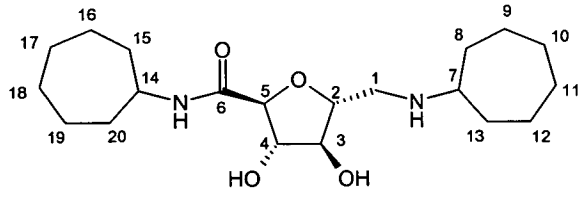

From **105**, yield = 11 mg, 99 %.

^{1}H NMR (250 MHz, CD_3OD), δ (ppm): 1.44 – 2.16 (24H, m, 12 x x –C**H**$_2$-cycloheptane), 3.19 – 3.42 (3H, m, 2 x H-1, H-7), 3.80 – 3.93 (2H, m, H-2, H-14), 3.95 (1H, t, $J_{2,3} = J_{3,4} = 2.0$ Hz, H-3), 4.32 (1H, t, $J_{3,4} = J_{4,5} = 2.0$ Hz, H-4), 4.37 (1H, d, $J_{4,5} = 2.0$ Hz, H-5).

ESI$^+$: $[M + H]^+ = 369.2$.

6.4.11.13 2,5-Anhydro-1-deoxy-1-(cycloheptylamino)-D-phenylmannonamide, 119.

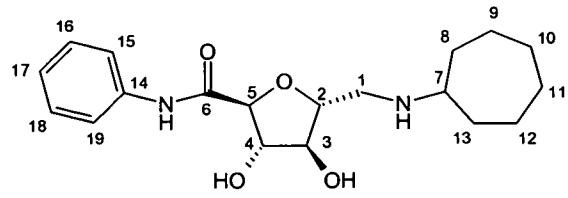

From **106**, yield = 5 mg, 50 %.

^{1}H NMR (250 MHz, CD_3OD), δ (ppm): 1.45 – 2.15 (12H, m, 6 x –C**H**$_2$-cycloheptane), 3.25 – 3.47 (3H, m, 2 x H-1, H-7), 4.01 (1H, t, $J_{2,3} = J_{3,4} = 2.5$ Hz, H-3), 4.40 – 4.47 (2H, m, H-2, H-4), 4.54 (1H, d, $J_{4,5} = 2.5$ Hz, H-5), 7.04 – 7.15 (1H, m, H-17), 7.23 – 7.37 (2H, m, H-16, H-18), 7.50 – 7.57 (2H, m, H-15, H-19).

ESI$^+$: $[M + H]^+ = 349.3$.

6.5 Non-Library Inhibitor Development.

6.5.1 Synthesis of 2,5-anhydro-1-deoxy-1-(3,4-dichlorobenzylamino)-D-mannonic acid (deprotection of 90), 120.

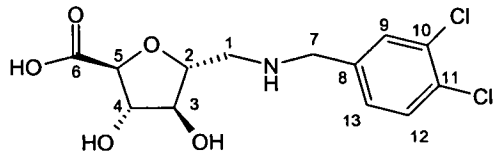

The *N*-BOC protected sugar amino acid **90** (54 mg) was dissolved in CH_2Cl_2 (1.5 ml). Trifluoroacetic acid (1 ml) was added and the reaction was stirred for 1 ½ hours.

The solvent was then removed and the residue dissolved in acetonitrile : water (1 : 1, 0.1 % acetic acid) and purified using mass directed purification (ZMD Method 2). Removal of the solvent by lyophilisation afforded the title compound as a white solid (17 mg, 34 %).

^{1}H NMR (250 MHz, CD_3OD), δ (ppm): 2.77 (1H, dd, J_{gem} = 12.5 Hz, $J_{1a,2}$ = 7.5 Hz, H-1a), 2.88 (1H, dd, J_{gem} = 12.5 Hz, $J_{1b,2}$ = 3.5 Hz, H-1b), 3.75 – 3.88 (3H, m, H-3, 2 x H-7), 4.08 – 4.22 (3H, m, H-2, H-4, H-5), 7.31 (1H, dd, $J_{12,13}$ = 8.5 Hz, $J_{9,13}$ = 2.0 Hz, H-13), 7.50 (1H, d, $J_{12,13}$ = 8.5 Hz, H-12), 7.55 (1H, d, $J_{9,13}$ = 2.0 Hz, H-9).

^{13}C NMR (63 MHz, CD_3OD), δ (ppm): 49.4 (C1), 50.9 (C7), 79.2 (C4), 80.2 (C3), 82.4 (C2), 84.3 (C5), 127.7 – 132.2 (5C, C9 – C13), 138.8 (C8), 171.8 (C6).

ESI$^+$: $[M + H]^+$ = 336.2 [^{35}Cl – ^{35}Cl].

6.5.2 Synthesis of 2,5-anhydro-1-deoxy-1-(cycloheptylamino)-D-mannonic acid (deprotection of 91), 121.

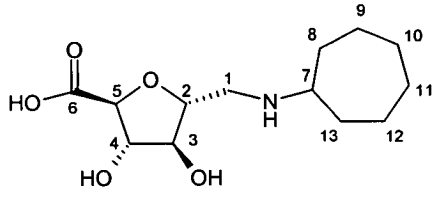

The *N*-BOC protected sugar amino acid **91** (31 mg) was dissolved in CH_2Cl_2 (1.5 ml). Trifluoroacetic acid (1 ml) was added and the reaction was stirred for 1 ½ hours. The solvent was then removed and the residue dissolved in acetonitrile : water (1 : 1, 0.1 % acetic acid) and purified using mass directed purification (ZMD Method 2).

Removal of the solvent by lyophilisation afforded the title compound as a white solid (13 mg, 57 %).

^{1}H NMR (250 MHz, CD_3OD), δ (ppm): 1.09 – 1.84 (12H, m, 6 x -CH_2- cycloheptane), 2.78 – 3.20 (3H, m, 2 x H-1, H-7), 3.63 – 4.03 (4H, m, H-2 – H-5).

ESI$^+$: $[M + H]^+ = 274.1$.

6.5.3 Synthesis of 2,5-anhydro-1-deoxy-1-(3,4-dichlorobenzylamino)-D-mannitol-6-phosphate, 122.

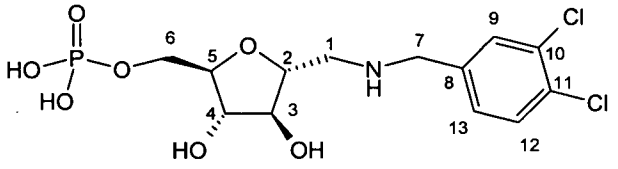

A stirring solution of phosphorous oxychloride (0.39 ml, 4.4 eq.) was cooled to O °C before addition of water (50 µl, 2.8 eq.), pyridine (0.37 ml, 4.8 eq.) and acetonitrile (0.5 ml). The *N*-BOC protected amine **88** (0.4 g, 1 eq.) was added and the reaction was stirred for 3 ¼ hours, maintaining the temperature between 0 and 2 °C. Crushed ice was then added and the reaction was allowed to stir for a further hour. CH_2Cl_2 (5 ml) was added and the two layers separated. The aqueous layer was washed with a further portion of CH_2Cl_2 (5 ml), neutralised by NaOH (0.5 M) and washed with Et_2O (2 x 5 ml) and CH_2Cl_2 (2 x 5 ml). The solution was then lyophilised to yield a pale yellow solid (0.40 g, 95 %). This was dissolved in acetonitrile : water (1 : 1, 0.1 % acetic acid) and purified using mass directed purification (ZMD Method 2). Removal of the solvent by lyophilisation yielded the title compound as a white solid

(18 mg, 5 %).

^{1}H NMR (250 MHz, D_2O), δ (ppm): 3.20 – 3.36 (2H, m, 2 x H-1), 3.87 (4H, m, H-3, H-4, 2 x H-6), 4.11 – 4.33 (4H, m, H-2, H-5, 2 x H-7), 7.37 (1H, dd, $J_{12,13}$ = 8.5 Hz, $J_{9,13}$ = 2.5 Hz, H-13), 7.59 (1H, d, $J_{12,13}$ = 8.5 Hz, H-12), 7.64 (1H, , $J_{9,13}$ = 2.5 Hz, H-9).

^{31}P NMR (101 MHz, D_2O), δ (ppm): 3.08.

ESI$^-$: $[M - H]^-$ = 399.7 [^{35}Cl – ^{35}Cl].

6.5.4 Synthesis of 2,5-anhydro-D-talose, 123.[110]

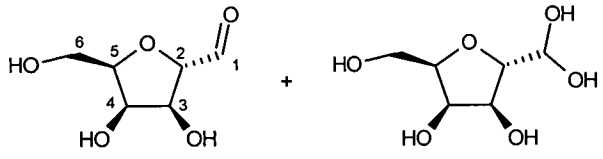

D-Galactosamine hydrochloride (1.00 g, 1 eq.) was dissolved in water (20 ml) and stirred at 0 °C for approximately 4 hours. Sodium nitrite (0.80 g, 2.5 eq.) was then added followed by cautious addition of Amberlite 120 H^+ resin (20 ml), maintaining the temperature between 0 – 5 °C. The reaction was then left to stir at 0 °C for 18 hours before the resin was removed by filtration. The solution was then neutralised by portion by portion addition of Dowex CO_3^{2-} resin. The resin was removed by filtration and the remaining solution was lyophilised to yield the title compound as a pale brown hygroscopic solid. (0.65 g, 87%).

^{1}H NMR (250 MHz, D_2O), δ (ppm): 3.48 – 3.64 (3H, m, H-2, 2 x H-6), 3.87 – 3.93

(1H, m, H-5), 4.02 – 4.10 (2H, m, H-3, H-4), 4.82 (1H, d, $J_{1,2}$ = 4.5 Hz, H-1 gem-diol).

^{13}C NMR (63 MHz, D_2O), δ (ppm): 60.6, (C6), 72.2 (C4), 37.1 (C3), 81.4 (C2), 83.4 (C5), 90.5 (C1 gem-diol).

6.5.5 Synthesis of 2,5-anhydro-1-deoxy-1-(3,4-dichlorobenzylamino)-D-talitol, 124.

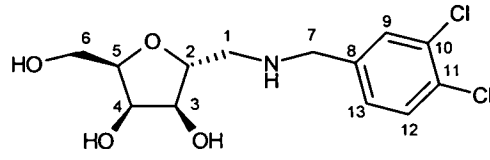

3,4-Dichlorobenzylamine (0.24 ml, 1 eq.) was added to a solution of aldehyde **123** (0.29 g) in methanol (10 ml) and was stirred for 1 hour. Sodium cyanoborohydride (0.11 g, 1 eq.) was added and the reaction was stirred for 30 minutes at pH 6, maintained by dropwise addition of HCl in methanol (0.5 M). The solvent was then removed under reduced pressure and the resulting residue was dissolved in acetonitrile : water (1 : 1, 0.1 % acetic acid) and purified using mass directed purification (ZMD Method 2). Removal of the solvent by lyophilisation afforded the title compound as a white solid (0.11 g, 19 %).

^{1}H NMR (250 MHz, CD_3OD), δ (ppm): 2.66 (1H, dd, J_{gem} = 12.5 Hz, $J_{1a,2}$ = 7.0 Hz, H-1a), 2.84 (1H, dd, J_{gem} = 12.5 Hz, $J_{1b,2}$ = 3.0 Hz, H-1b), 3.69 – 3.90 (4H, 2 x H-6, 2 x H-7), 3.92 – 4.06 (3H, m, H-2, H-3, H-5), 4.14 (1H, t, $J_{3,4}$ = $J_{4,5}$ = 4.0 Hz, H-4), 7.30 (1H, dd, $J_{12,13}$ = 8.0 Hz, $J_{9,13}$ = 2.0 Hz, H-13), 7.47 (1H, d, $J_{12,13}$ = 8.0 Hz, H-

12), 7.55 (1H, d, $J_{9,13}$ = 2.0 Hz, H-9).

^{13}C NMR (63 MHz, CD_3OD), δ (ppm): 50.5 (C1), 51.3 (C7), 60.4 (C6), 71.3 (C4), 74.1 (C3), 79.3 (C2), 80.3 (C5), 126.8 – 129.6 (3C, C9, C12, C13), 129.3 – 131.3 (2C, C10, C11), 139.8 (C8).

ESI$^+$: $[M + H]^+$ = 321.7 [^{35}Cl – ^{35}Cl].

6.5.6 Synthesis of 2,5-anhydro-1-deoxy-1-(benzhydrylamino)-D-talitol, 125.

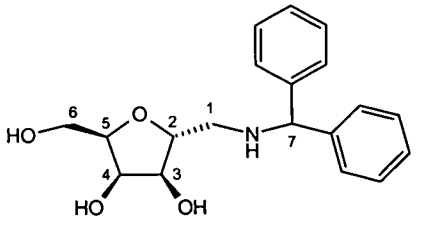

Aminodiphenylmethane (0.31 ml, 1 eq.) was added to a solution of aldehyde **123** (0.29 g) in methanol (10 ml) and was stirred for 1 hour. Sodium cyanoborohydride (0.11 g, 1 eq.) was added and the reaction was stirred for 4 hours, at pH 6, maintained by dropwise addition of HCl in methanol (0.5 M). The solvent was then removed under reduced pressure and the resulting residue was dissolved in acetonitrile : water (1 : 1, 0.1 % acetic acid) and purified using mass directed purification (ZMD Method 2). Removal of the solvent by lyophilisation afforded the title compound as a white solid (0.12 g, 20 %).

^{1}H NMR (250 MHz, CD_3OD), δ (ppm): 2.63 (1H, d, J_{gem} = 12.0 Hz, $J_{1a,2}$ = 7.0 Hz, H-1a), 2.80 (1H, dd, J_{gem} = 12.0 Hz, $J_{1b,2}$ = 3.5 Hz, H-1b), 3.70 – 3.82 (2H, m, 2 x H-

6), 3.92 – 4.05 (3H, m, H-2, H-3, H-5), 4.13 (1H, t, $J_{3,4} = J_{4,5} = 4.0$ Hz, H-4), 5.14 (1H, s, H-7), 7.10 – 7.42 (10H, m, 10 x Ar-H).

^{13}C NMR (63 MHz, CD_3OD), δ (ppm): 49.8 (C1), 60.4 (C6), 66.7 (C7), 71.3 (C4), 74.1 (C3), 79.6 (C2), 80.3 (C5), 126.1- 127.6 (10C, 10 x Ar-CH), 143.1 – 144.2 (2C, 2 x Ar**C**-CH-).

ESI$^+$: $[M + H]^+ = 330.1$.

6.5.7 Synthesis of *N*-methyl-2,5-anhydro-1-deoxy-(3,4-dichlorobenzylamino)-D-mannitol, 126.

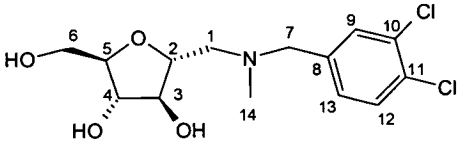

Amine **37** (0.31 g, 1 eq.) was dissolved in water (2.4 ml) and placed in a microwave tube. Formic acid (40 µl, 1.1 eq.) and formaldehyde solution (37 %, 88 µl, 1.1 eq.) were added and the tube was sealed. The tube was placed in a CEM discover microwave and heated for 5 minutes at 150 °C (120 W). The solvent was then removed under reduced pressure and the residue re-dissolved in water : acetonitrile (1 : 1, 0.1 % acetic acid) and purified using mass directed purification (ZMD Method 2). Removal of the solvent by lyophilisation yielded a pale brown oily solid (80 mg, 25 %).

^{1}H NMR (250 MHz, d^6-DMSO), δ (ppm): 2.06 (3H, s, 3 x H-14), 2.34 – 2.50 (2H, m, 2 x H-1), 3.30 – 3.48 (4H, m, 2 x H-6, 2 x H-7), 3.51 – 3.78 (4H, m, H-2, H-3, H-4,

H-5), 7.14 (1H, d, $J_{12,13}$ = 8.5 Hz, H-13), 7.40 – 7.46 (2H, m, H-9, H-13).

^{13}C NMR (63 MHz, d^6-DMSO), δ (ppm): 42.4 (C14), 59.3 (C1), 60.2 (C7), 61.6 (C6), 76.8 (C4), 79.4 (C3), 81.4 (C2), 83.7 (C5), 128.7 – 130.6 (5C, C9 – C13), 140.5 (C8).

ESI$^+$: $[M + H]^+$ = 336.1 [^{35}Cl – ^{35}Cl].

6.5.8 Synthesis of *N*-methyl-2,5-anhydro-1-deoxy-1-(cycloheptylamino)-D-mannitol, 127.

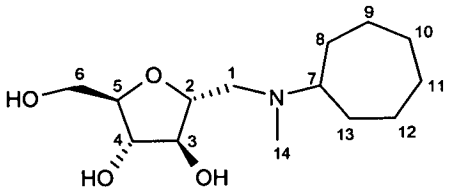

Amine **70** (50 mg, 1 eq.) was dissolved in water (0.5 ml) and placed in a microwave tube. Formic acid (9 µl, 11 eq.) and formaldehyde solution (37 %, 17 µl, 1.1 eq.) were added and the tube was sealed. The tube was placed in a CEM discover microwave and heated for 5 minutes at 150 °C (120 W). The resulting residue was dissolved in water : acetonitrile (1 : 1, 0.1 % acetic acid) and purified using mass directed purification (ZMD Method 2). Removal of the solvent by lyophilisation yielded a white solid (31 mg, 59 %).

^{1}H NMR (250 MHz, CD_3OD), δ (ppm): 1.45 – 2.04 (12H, m, 2 x –C**H$_2$**-cycloheptane), 2.53 (3H, s, 3 x H-14), 2.89 – 3.04 (3H, m, 2 x H-1, H-7), 3.67 (2H, 2dd, 2 x H-6), 3.81 – 4.05 (4H, m, H-2, H-3, H-4, H-5).

^{13}C NMR (63 MHz, CD_3OD), δ (ppm): 24.4 (2C, C9, C12), 26.6 – 26.7 (2C, C10, C11), 27.6 – 28.4 (2C, C8, C13), 36.8 (C14), 54.5 (C1), 61.1 (C1), 65.3 (C7), 76.4 (C4), 79.1 (C3), 80.0 (C2), 83.9 (C5).

ESI^+: $[M + H]^+ = 274.3$.

HRMS FAB (+ve) found m/z = 274.20177 $[M + H]^+$, $C_{14}H_{28}NO_4$ requires 274.20183.

6.5.9 Synthesis of *N*-ethyl-2,5-anhydro-1-deoxy-1-(3,4-dichlorobenzylamino)-D-mannitol, 128.

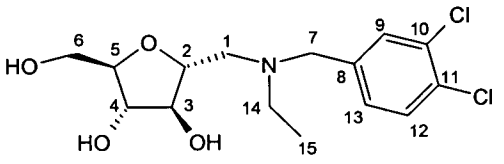

Amine **37** (50 mg, 1 eq.) was dissolved in water (0.4 ml) and placed in a microwave tube. Formic acid (6 µl, 1.1 eq.) and acetaldehyde (10 µl, 1.1 eq.) were added and the tube was sealed. The tube was placed in a CEM discover microwave and heated for 5 minutes at 150 °C (120 W). The solvent was then removed under reduced pressure and the residue re-dissolved in water : acetonitrile (1 : 1, 0.1 % acetic acid) and purified using mass directed purification (ZMD Method 2). Removal of the solvent by lyophilisation yielded a pale brown oily solid (34 mg, 63 %).

^1H NMR (250 MHz, CD_3OD), δ (ppm): 1.10 (3H, t, $J_{14,15}$ = 7.0 Hz, 3 x H-15), 2.58 – 2.81 (4H, m, 2 x H-1, 2 x H-14), 3.63 – 3.88 (6H, m, H-2, H-4, 2 x H-6, 2 x H-7),

3.97 – 4.06 (H, m, H-3, H-5), 7.34 (1H, dd, $J_{12,13}$ = 8.5 Hz, $J_{9,13}$ = 2.0 Hz, H-13), 7.50 (1H, d, $J_{12,13}$ = 8.5 Hz, H-12), 7.58 (1H, d, $J_{9,13}$ = 2.0 Hz, H-9).

^{13}C NMR (63 MHz, CD_3OD), δ (ppm): 9.62 (C15), 47.0 (C14), 54.3 (C1), 56.1 (C7), 61.0 (C6), 76.2 (C4), 79.1 (C3), 80.4 (C2), 82.8 (C5), 128.6, 129.4, 130.5 (3C, C9, C12, C13), 129.8, 130.9 (2C, C10, C11), 138.4 (C8).

ESI$^+$: $[M + H]^+$ = 350.3 [^{35}Cl – ^{35}Cl].

HRMS FAB (+ve) found m/z = 350.09290 and 452.08899 $[M + H]^+$, $C_{15}H_{22}NO_4Cl_2$ requires 350.09259 (2 x ^{35}Cl) and 452.08964 (^{35}Cl + ^{37}Cl).

References

1. R. B. Silverman, *The Organic Chemistry of Drug Design and Drug Action*; Academic Press, 1992.
2. A. Fleming, *Brit. J. Exp. Pathol.*, 1929, **10**, 226.
3. M. C. Wani, H. L. Taylor, M. E. Wall, P. Coggon, A. T. McPhail, *J. Am. Chem. Soc.*, 1971, **93**, 2325.
4. C. S. Swindell, N. E. Krauss, S. B. Horwitz, I. Ringel, *J. Med. Chem.*, 1991, **34**, 1176.
5. S. H. Chen, V. Farina, J. M. Wei, B. Long, C. Fairchild, S. W. Mamber, J. F. Kadow, D. Vyas, T. W. Doyle, *Bioorg. Med. Chem. Lett.*, 1994, **4**, 479.
6. F. Gueritte-Voegelein, D. Guenard, F. Lavelle, M. T. Le Goff, L. Mangatal, P. Potier, *J. Med. Chem.*, 1991, **34**, 992.
7. E. M. Gordon, M. A. Gallop, D. V. Patel, *Acc. Chem. Res.*, 1996, **29**, 144.
8. F. Balkenhohl, C. von dem Bussche-Huennefeld, A. Lansky, C. Zechel, *Angew. Chem. Int. Edn. Engl.*, 1996, **35**, 2288.
9. G. S. Sittampalam, S. D. Kahl, W. P. Janzen, *Curr. Opin. Chem. Biol.*, 1997, **1**, 384.
10. S. Wang, T. B. Sim, Y.-S. Kim, Y.-T. Chang, *Curr. Opin. Chem. Biol.*, 2004, **8**, 371.
11. M. A. Gallop, R. W. Barrett, W. J. Dower, S. P. A. Fodor, E. M. Gordon, *J. Med. Chem.*, 1994, **37**, 1233.
12. L. A. Thompson, J. A. Ellman, *Chem. Rev.*, 1996, **96**, 555.
13. A. Furka, F. Sebestyen, M. Asgedom, G. Dibo, *Int. J. Pept. Prot. Res.*, 1991,

37, 487.

14. M. P. Beavers, X. Chen, *J. Mol. Graph. Model.,* 2002, **20**, 463.

15. N. S. Gray, L. Wodicka, A. M. Thunnissen, T. C. Norman, S. Kwon, F. H. Espinoza, D. O. Morgan, G. Barnes, S. LeClerc, L. Meijer, S. H. Kim, D. J. Lockhart, P. G. Schultz, *Science,* 1998, **281**, 533.

16. R. N. Zuckermann, E. J. Martin, D. C. Spellmeyer, G. B. Stauber, K. R. Shoemaker, J. M. Kerr, G. M. Figliozzi, D. A. Goff, M. A. Siani, R. Simon, S. C. Banville, E. G. Brown, L. Wang, L. S. Richter, W. H. Moos, *J. Med. Chem.,* 1994, **37**, 2678.

17. P. R. Andrews, D. J. Craik, J. L. Martin, *J. Med. Chem.,* 1984, **27**, 1648.

18. T. J. A. Ewing, S. Makino, A. G. Skillman, I. D. Kuntz, *J. Comp-Aid. Mol. Des.,* 2001, **15**, 411.

19. C. A. Lipinski, F. Lombardo, B. W. Dominy, P. J. Feeney, *Adv. Drug Deliver. Rev.,* 1997, **23**, 3.

20. W. P. Walters, Ajay, M. A. Murcko, *Curr. Opin. Chem. Biol.,* 1999, **3**, 384.

21. T. I. Oprea, *J. Comp-Aid. Mol. Des.,* 2000, **14**, 251.

22. M. M. Hann, T. I. Oprea, *Curr. Opin. Chem. Biol.,* 2004, **8**, 255.

23. M. Vieth, M. G. Siegel, R. Higgs, I. Watson, D. Robertson, K. Savin, G. Durst, P. Hipskind, *J. Med. Chem.,* 2004, **47**, 224.

24. W. P. Walters, M. T. Stahl, M. A. Murcko, *Drug Discov. Today,* 1998, **3**, 160.

25. P. Kaellblad, N. P. Todorov, H. M. G. Willems, I. L. Alberts, *J. Med. Chem.,* 2004, **47**, 2761.

26. T. L. Blundell, S. Patel, *Curr. Opin. Pharmacol.,* 2004, **4**, 490.

27. T. L. Blundell, H. Jhoti, C. Abell, *Nat. Rev. Drug Discov.*, 2002, **1**, 45.

28. A. Sharff, H. Jhoti, *Curr. Opin. Chem. Biol.*, 2003, **7**, 340.

29. D. A. Erlanson, R. S. McDowell, T. O'Brien, *J. Med. Chem.*, 2004, **47**, 3463.

30. D. J. Maly, I. C. Choong, J. A. Ellman, *Proc. Natl. Acad. Sci. USA.*, 2000, **97**, 2419.

31. M. J. Hartshorn, C. W. Murray, A. Cleasby, M. Frederickson, I. J. Tickle, H. Jhoti, *J. Med. Chem.*, 2005, **48**, 403.

32. X. Wang, Y. Choe, C. S. Craik, J. A. Ellman, *Bioorg. Med. Chem. Lett.*, 2002, **12**, 2201.

33. S. B. Shuker, P. J. Hajduk, R. P. Meadows, S. W. Fesik, *Science,* 1996, **274**, 1531.

34. C. L. M. J. Verlinde, V. Hannaert, C. Blonski, M. Willson, J. J. Perie, L. A. Fothergill-Gilmore, F. R. Opperdoes, M. H. Gelb, W. G. J. Hol, P. A. M. Michels, *Drug Res. Updates,* 2001, **4**, 50.

35. J. Keiser, A. Stich, C. Burri, *Trends Parasitol.*, 2001, **17**, 42.

36. B. M. Bakker, H. V. Westerhoff, F. R. Opperdoes, P. A. M. Michels, *Mol. Biochem. Parasitol.* 2000, **106**, 1.

37. J. Atouguia, J. Costa, *Mem. I. Oswaldo Cruz,* 1999, **94**, 221.

38. M. P. Barrett, J. C. Mottram, G. H. Coombs, *Trends Microbiol.*, 1999, **7**, 82.

39. C. L. M. J. Verlinde, M. Callens, S. Van Calenbergh, A. Van Aerschot, P. Herdewijn, V. Hannaert, P. A. M. Michels, F. R. Opperdoes, W. G. J. Hol, *J. Med. Chem.*, 1994, **37**, 3605.

40. F. R. Opperdoes, *Annu. Rev. Microbiol.*, 1987, **41**, 127.

41. J. J. Cazzulo, *Faseb J.*, 1992, **6**, 3153.

42. C. E. Clayton, P. Michels, *Parasitol. Today,* 1996, **12**, 465.

43. A. G. M. Tielens, J. J. Van Hellemond, *Parasitol. Today,* 1998, **14**, 265.

44. A. P. Fernandes, K. Nelson, S. M. Beverley, *Proc. Natl. Acad. Sci. USA,* 1993, **90**, 11608.

45. F. R. Opperdoes, P. Borst, *FEBS Lett.* 1977, **80**, 360.

46. C. L. M. J. Verlinde, W. G. J. Hol, *Structure,* 1994, **2**, 577.

47. A. Seyfang, M. Duszenko, *Eur. J. Biochem.,* 1991, **202**, 191.

48. M. Duszenko, D. Mecke, *Mol. Biochem. Parasitol.,* 1986, **19**, 223.

49. J. P. Barnard, B. Reynafarje, P. L. Pedersen, *J. Biol. Chem.,* 1993, **268**, 3654.

50. E. A. C. Wiemer, P. A. M. Michels, F. R. Opperdoes, *Biochem. J.,* 1995, **312**, 479.

51. A. H. Fairlamb, F. R. Opperdoes, P. Borst, *Nature,* 1977, **265**, 270.

52. C. Van der Meer, J. A. M. Versluijs-Broers, F. R. Opperdoes, *Exp. Parasitol.,* 1979, **48**, 126.

53. N. Minagawa, Y. Yabu, K. Kita, K. Nagai, N. Ohta, K. Meguro, S. Sakajo, A. Yoshimoto, *Mol. Biochem. Parasitol.,* 1997, **84**, 271.

54. A. M. Aronov, S. Suresh, F. S. Buckner, W. C. Van Voorhis, C. L. M. J. Verlinde, F. R. Opperdoes, W. G. J. Hol, M. H. Gelb, *Proc. Natl. Acad. Sci. USA,* 1999, **96**, 4273.

55. M. L. Cardenas, A. Cornish-Bowden, T. Ureta, *Biochim. Biophys. Acta,* 1998, **1401**, 242.

56. F. R. Opperdoes, P. A. M. Michels, *Int. J. Parasitol.,* 2001, **31**, 482.

57. M. Nwagwu, F. R. Opperdoes, *Acta Trop.,* 1982, **39**, 61.

58. M. Willson, Y.-H. Sanejouand, J. Perie, V. Hannaert, F. Opperdoes, *Chem.*

Biol., 2002, **9**, 839.

59. M. Willson, I. Alric, J. Perie, Y. H. Sanejouand, *J. Enzyme Inhib.*, 1997, **12**, 101.

60. P. A. M. Michels, N. Chevalier, F. R. Opperdoes, M. H. Rider, D. J. Rigden, *Eur. J. Biochem.*, 1997, **250**, 698.

61. S. Claustre, F. Bringaud, L. Azema, R. Baron, J. Perie, M. Willson, *Carbohydr. Res.*, 1999, **315**, 339.

62. S. Claustre, C. Denier, F. Lakhdar-Ghazal, A. Lougare, C. Lopez, N. Chevalier, P. A. M. Michels, J. Perie, M. Willson, *Biochemistry,* 2002, **41**, 10183.

63. S. Claustre, *PhD Thesis*, Université Paul Sabatier, Toulouse, 2000.

64. D. M. Chudzik, P. A. Michels, S. de Walque, W. G. J. Hol, *J. Mol. Biol.*, 2000, **300**, 697.

65. W. D. Mercer, S. I. Winn, H. C. Watson, *J. Mol. Biol.*, 1976, **104**, 277.

66. B. M. Bakker, P. A. M. Michels, F. R. Opperdoes, H. V. Westerhoff, *J. Biol. Chem.*, 1997, **272**, 3207.

67. L. A. Fothergill-Gilmore, P. A. M. Michels, *Prog. Biophys. Mol. Biol.*, 1993, **59**, 105.

68. E. Van Schaftingen, F. R. Opperdoes, H. G. Hers, *Eur. J. Biochem.*, 1985, **153**, 403.

69. A. A.-H. Abdel-Rahman, E. S. H. El Ashry, R. R. Schmidt, *Carbohydr. Res.*, 1999, **315**, 106.

70. I. McCort, M. Saniere, Y. Le Merrer, *Tetrahedron,* 2003, **59**, 2693.

71. R. E. Lee, K. Mikusova, P. J. Brennan, G. S. Besra, *J. Am. Chem. Soc.*, 1995,

117, 11829.

72. R. C. Reynolds, N. Bansal, J. Rose, J. Friedrich, W. J. Suling, J. A. Maddry, *Carbohydr. Res.*, 1999, **317**, 164.

73. D. Horton, K. D. Philips, *Carbohydr. Res.*, 1973, **30**, 367.

74. J. Martinez, M. Brown, *Unpublished results*, University of Edinburgh, 2003.

75. J. Martinez, *Unpublished results*, University of Edinburgh, 2003.

76. M. Walkinshaw, *Unpublished results*, University of Edinburgh, 2004.

77. L. A. Fothergill-Gilmore, *Unpublished results*, University of Edinburgh, 2003.

78. N. Tranter, *Honours report: The identification of novel inhibitors of Leismania mexicana pyruvate kinase*, University of Edinburgh, 2004.

79. N. Tranter, *Unpublished results*, University of Edinburgh, 2004.

80. L. B. Tulloch, *PhD Thesis*, University of Edinburgh, Edinburgh, 2005.

81. V. Hannaert, C. Yernaux, D. J. Rigden, L. A. Fothergill-Gilmore, F. R. Opperdoes, P. A. M. Michels, *FEBS Lett.*, 2002, **514**, 255.

82. M. Navaro, *Unpublished results*, University of Edinburgh, 2004.

83. S.-Y. Han, Y.-A. Kim, *Tetrahedron,* 2004, **60**, 2447.

84. S. A. W. Gruner, E. Locardi, E. Lohof, H. Kessler, *Chem. Rev.*, 2002, **102**, 491.

85. H. Haruyama, T. Takayama, T. Kinoshita, M. Kondo, M. Nakajima, T. Haneishi, *J. Chem. Soc., Perkin Trans. 1,* 1991, **7**, 1637.

86. M. Nakajima, K. Itoi, Y. Takamatsu, T. Kinoshita, T. Okazaki, K. Kawakubu, M. Shindo, T. Honma, M. Tohjigamori, T. Haneishi, *J. Antibiot.*, 1991, **44**, 293.

87. D. Siehl, *Plant Physiol.*, 1996, **110**, 753.

88. H. Umezawa, T. Aoyagi, T. Komiyama, H. Morishima, M. Hamada, T. Takeuchi, *J. Antibiot.*, 1974, **27**, 963.

89. S. F. Oliver, C. Abell, *Curr. Opin. Chem. Biol.,* 1999, **3**, 299.

90. A. Kirschning, H. Monenschein, R. Wittenberg, *Angew. Chem., Int. Edn. Engl.,* 2001, **40**, 650.

91. S. W. Kaldor, M. G. Siegel, J. E. Fritz, B. A. Dressman, P. J. Hahn, *Tetrahedron Lett.,* 1996, **37**, 7193.

92. R. J. Booth, J. C. Hodges, *Acc. Chem. Res.,* 1999, **32**, 18.

93. R. J. Booth, J. C. Hodges, *J. Am. Chem. Soc.,* 1997, **119**, 4882.

94. P. H. J. Carlsen, T. Katsuki, V. S. Martin, K. B. Sharpless, *J. Org. Chem.,* 1981, **46**, 3936.

95. S. Carrettin, P. McMorn, P. Johnston, K. Griffin, G. J. Hutchings, *Chem. Commun.,* 2002, 696.

96. A. E. J. de Nooy, A. C. Besemer, H. van Bekkum, *Tetrahedron,* 1995, **51**, 8023.

97. A. E. J. De Nooy, A. C. Besemer, H. Van Bekkum, *Synthesis,* 1996, 1153.

98. R. Siedlecka, J. Skarzewski, J. Mlochowski, *Tetrahedron Lett.,* 1990, **31**, 2177.

99. A. E. J. de Nooy, A. C. Besemer, H. van Bekkum, *Carbohydr. Res.,* 1995, **29**, 89

100. N. J. Davis, S. L. Flitsch, *Tetrahedron Lett.,* 1993, **34**, 1181.

101. E. Graf von Roedern, H. Kessler, *Angew. Chem., Int. Edn. Engl.,* 1994, **33**, 667.

102. M. J. Sofia, R. Hunter, T. Y. Chan, A. Vaughan, R. Dulina, H. Wang, D. Gange, *J. Org. Chem.,* 1998, **63**, 2802.

103. R. M. van Well, M. E. A. Meijer, H. S. Overkleeft, J. H. van Boom, G. A. van der Marel, M. Overhand, *Tetrahedron,* 2003, **59**, 2423.

104. C. Bolm, A. S. Magnus, J. P. Hildebrand, *Org. Lett.,* 2000, **2**, 1173.

105. B. R. Travis, M. Sivakumar, G. O. Hollist, B. Borhan, *Org. Lett.,* 2003, **5**, 1031.

106. B. Tejo, *Unpublished results*, University of Edinburgh, 2005.

107. M. Walkinshaw, *Unpublished results*, University of Edinburgh, 2005.

108. J. W. Perich, R. B. Johns, *Synthesis,* 1988, 142.

109. T. Sowa, S. Ouchi, *Bull. Chem. Soc. Jpn.,* 1975, **48**, 2084.

110. W. L. Dills Jr, T. R. Covey, P. Singer, S. Neal, M. S. Rappaport, *Carbohydr. Res.,* 1982, **99**, 23.

111. W. Eschweiler, *Ber. Deut. Chem. Ges.,* 1905, **38**, 880.

112. H. T. Clarke, H. B. Gillespie, S. Z. Weisshaus, *J. Am. Chem. Soc.,* 1933, **55**, 4571.

113. P. Sahakitpichan, S. Ruchirawat, *Tetrahedron Lett.,* 2003, **44**, 5239.

114. G. Argouarch, G. Stones, C. L. Gibson, A. R. Kennedy, D. C. Sherrington, *Org. Biomol. Chem.,* 2003, **1**, 4408.

115. S. Torchy, D. Barbry, *J. Chem. Res., Synop.,* 2001, 292.

116. J. R. Harding, J. R. Jones, S.-Y. Lu, R. Wood, *Tetrahedron Lett.,* 2002, **43**, 9487.

117. V. Hannaert, *Unpublished results*, Université Catholique de Louvain, 2005.

Appendix 1

Lipinski Rule of 5 parameters for a selection of inhibitors.

(HBD = hydrogen bond donors, HBA = hydrogen bond acceptor.)

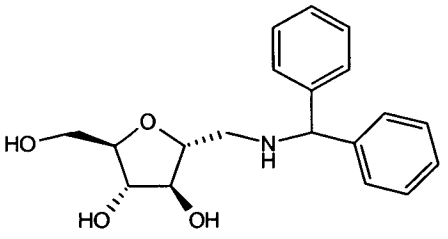

32, CLogP = 2.3,
MW = 329, HBD = 4, HBA = 5

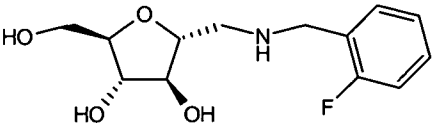

34, CLogP = 1.1,
MW = 271, HBD = 4, HBA = 5

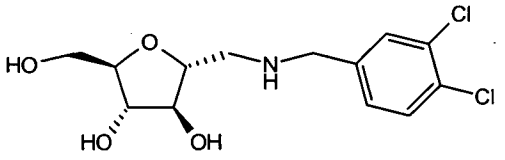

37, CLogP = 2.3,
MW = 322, HBD = 4, HBA = 5

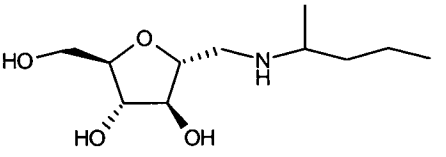

50, CLogP = 1.1,
MW = 233, HBD = 4, HBA = 5

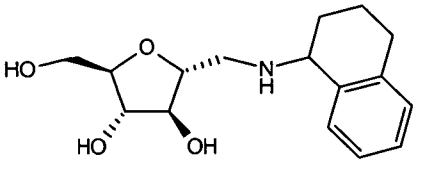

57, CLogP = 2.0,
MW = 293, HBD = 4, HDA = 5

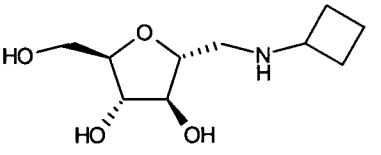

58, CLogP = 0.1,
MW = 217, HBD = 4, HBA = 5

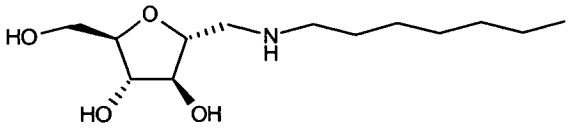

59, CLogP = 2.3,
MW = 261, HBD = 4, HBA = 5

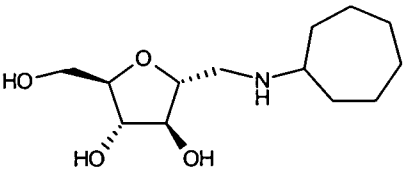

70, CLogP = 1.8,
MW = 259, HBD = 4, HBA = 5

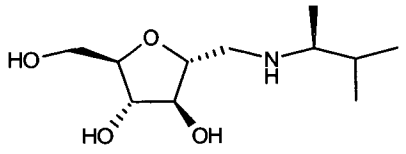

72, CLogP = 0.9,
MW = 233, HBD = 4, HBA = 5

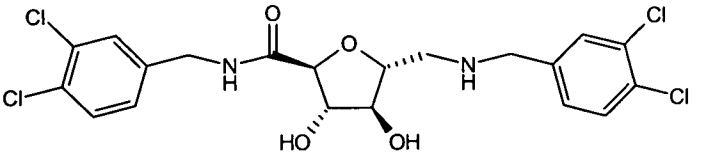

110, CLogP = 4.7,
MW = 492, HBD = 4, HBA = 6

Appendix 2

Dose-response curves for calculating IC_{50} values.

Determination of IC_{50} Values for **42**, **48**, **50** and **57**

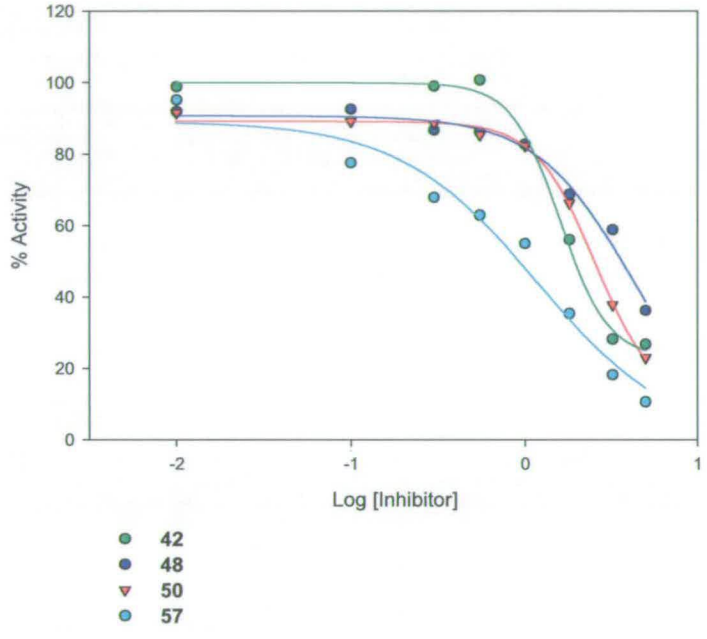

Determination of IC_{50} Values for **58**, **61** and **67**

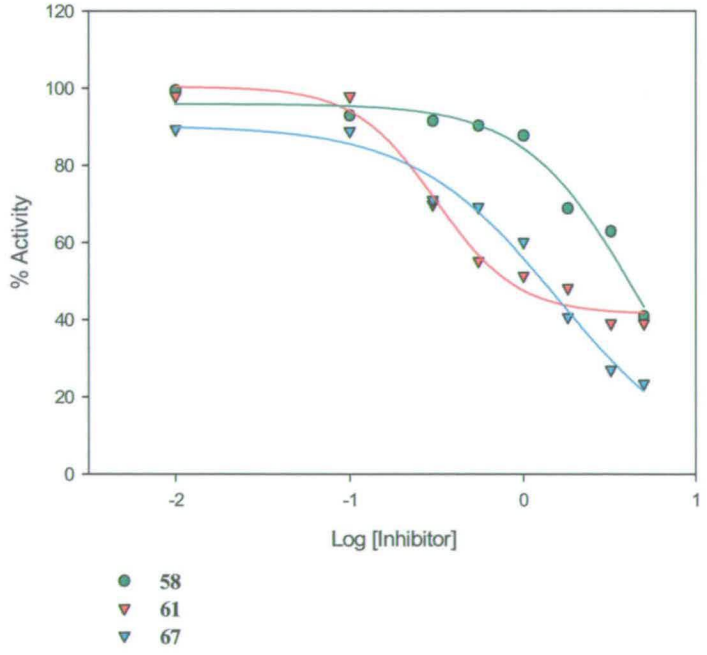

Determination of IC_{50} Values for **68**, **70**, **72** and **78**

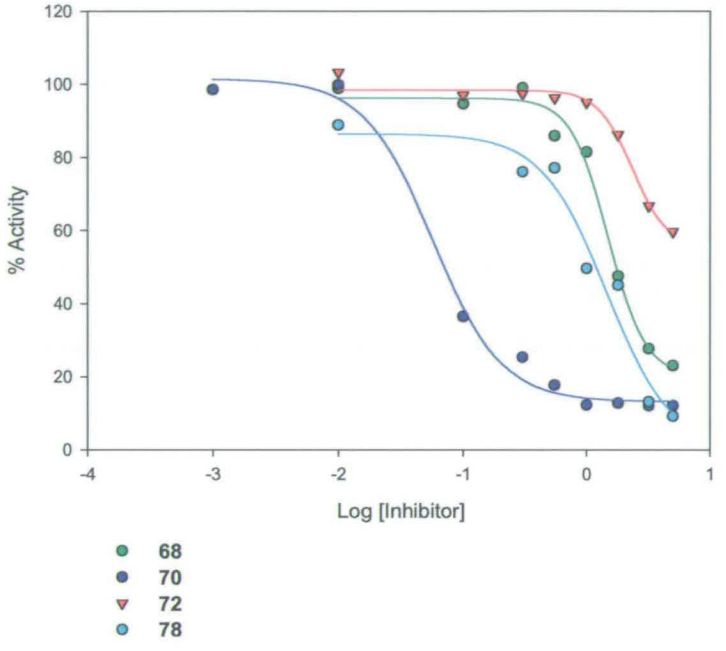

IC_{50} **107**

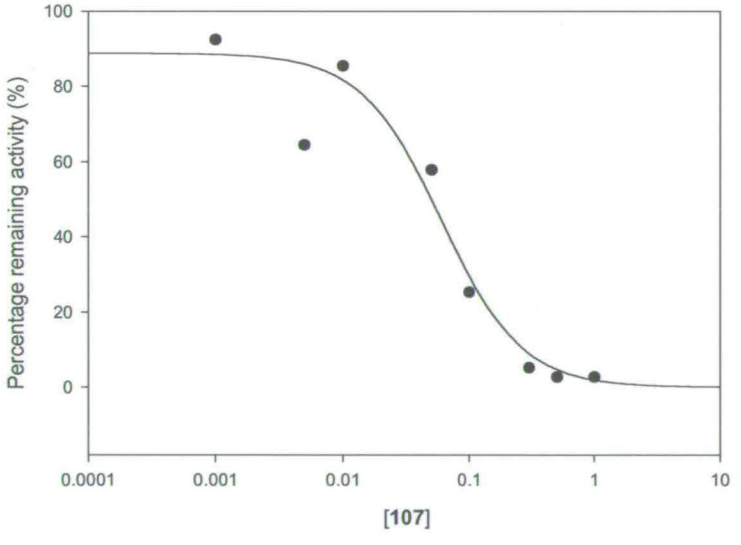

IC_{50} **110**

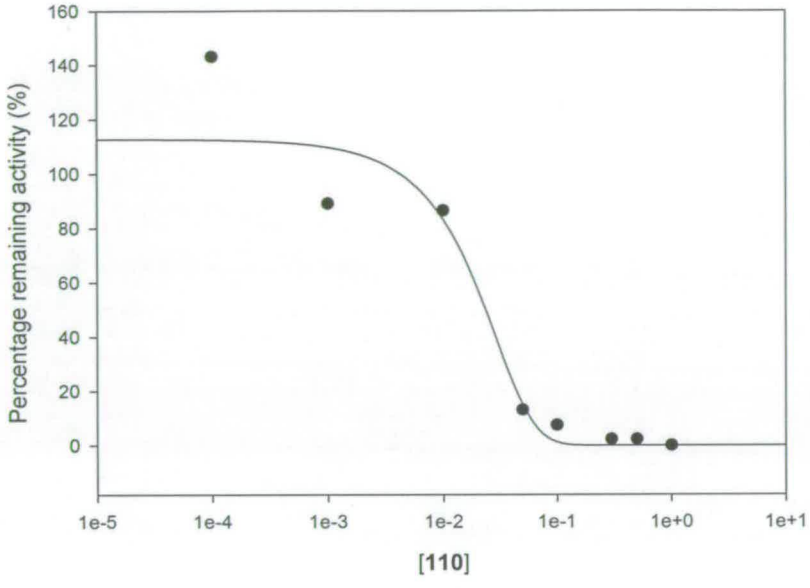

IC_{50} **111**

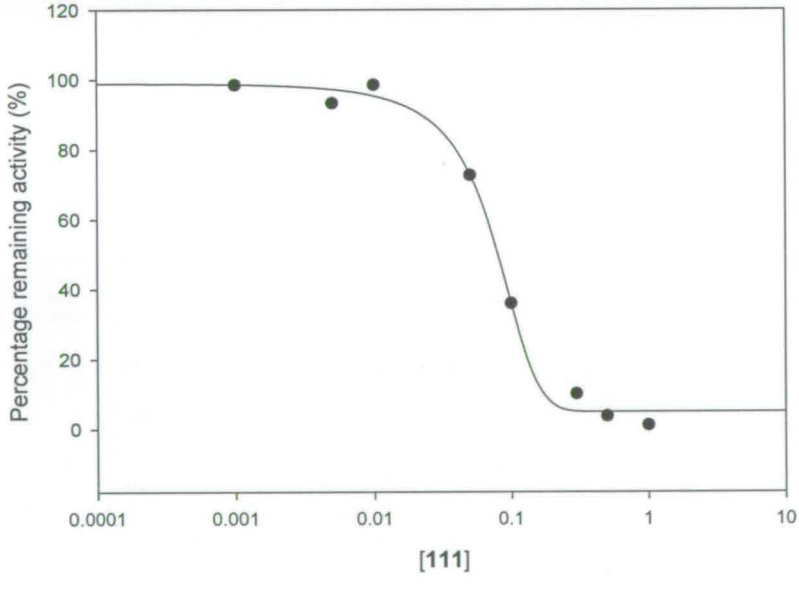

IC_{50} **117**

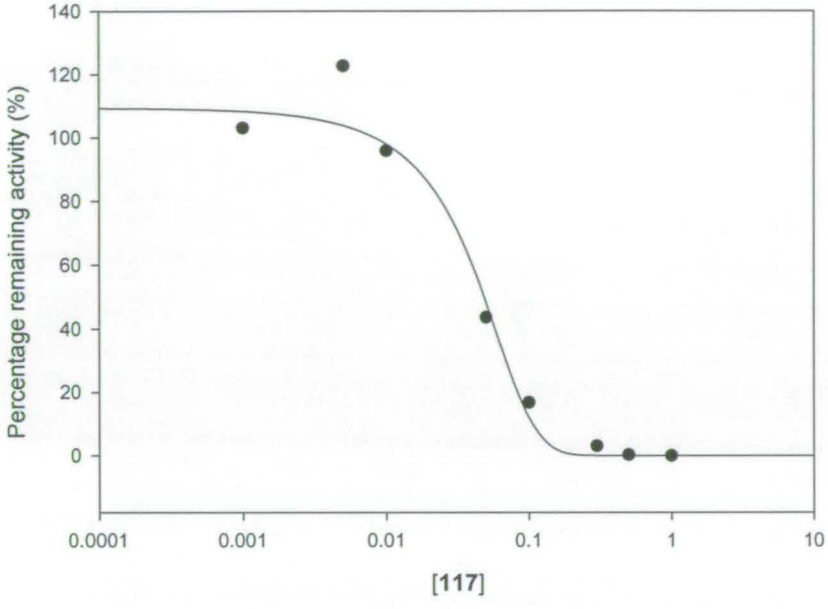
Percentage remaining activity (%)
140
120
100
80
60
40
20
0
0.0001
0.001
0.01
0.1
1
10
[117]

Appendix 3

Procedure for determining the molarity of reagent grade NaOCl.

NaOCl (10 ml) was diluted to 100 ml and 0.5 M potassium iodide solution (1 ml), 3 M H_2SO_4 and 3 % ammonium molybdate (3 drops) were added. 25 ml of the solution was titrated against 0.025 M $Na_2S_2O_4$.

Amount of $Na_2S_2O_4$ titrated = 17 ml.

Moles of $Na_2S_2O_4 = 4.25 \times 10^{-4}$

$OCl^- + 2I^- + 2H_3O^+ \rightarrow I_2 + Cl^- + 3H_2O$ and $I_2 + 2S_2O_3^{2-} \rightarrow 2I^- + S_4O_6^{2-}$

So, moles of $OCl^- = 2.125 \times 10^{-4}$

Moles in original 10 ml sample $= 8.5 \times 10^{-4}$

Therefore, concentration of NaOCl = 0.086 M.

Procedure for determining the molarity of commercial NaOCl.

Commercial NaOCl (1 ml) was diluted to 100 ml and 0.5 M potassium iodide solution (1 ml), 3 M H_2SO_4 and 3 % ammonium molybdate (3 drops) were added. 10 ml of the solution was titrated against 0.025 M $Na_2S_2O_4$.

Amount of $Na_2S_2O_4$ titrated = 13.5 ml.

Moles of $Na_2S_2O_4 = 3.375 \times 10^{-4}$

$OCl^- + 2I^- + 2H_3O^+ \rightarrow I_2 + Cl^- + 3H_2O$ and $I_2 + 2S_2O_3^{2-} \rightarrow 2I^- + S_4O_6^{2-}$

So, moles of $OCl^- = 1.6875 \times 10^{-4}$

Moles in original 1 ml sample $= 1.6875 \times 10^{-3}$

Therefore, concentration of commercial NaOCl = 1.69 M.